# Quantitative petroleum resource assessment in the Canada-Nova Scotia Offshore Area (Scotian Shelf, Scotian Slope, and Sydney Basin)

**Mark E. Deptuck*, Kristopher L. Kendell, Carl Makrides, and Brian Altheim**

Canada-Nova Scotia Offshore Petroleum Board, 27-201 Brownlow Avenue, Dartmouth, Nova Scotia, B3B 1W2

E-mail: mdeptuck@cnsopb.ns.ca*

## Executive Summary

A margin-wide quantitative petroleum resource assessment was carried out on the Scotian Shelf and Slope, focused mainly on the Scotian Basin, off mainland Nova Scotia, and the Sydney Basin, off Cape Breton Island (Figure 1). This offshore assessment was conducted using subsurface seismic mapping, geoscience/petrophysical interpretations, and available well data, in water depths ranging from a few tens of meters to roughly 4000 m.

The study area is separated into the following six geographic regions, based on geological criteria like sedimentation rates, depositional settings, and tectono-stratigraphic style (a combination of basement tectonics and salt-related deformation).

A. LaHave Platform (4 plays)
B. West Shelburne Corridor (7 plays)
C. Shelburne Corridor (7 plays)
D. Abenaki-Sable Corridor (12 plays)
E. Huron Corridor (11 plays)
F. Sydney Basin (3 plays)

Each geographic region contains between three and twelve play types, for a total of 44 plays. The total area for each of the 44 play types was determined using geological knowledge derived from well data and reflection seismic mapping, with the proportion of that area under trap determined primarily from cumulative lead mapping to estimate the total area of each play type under closure (generally with up to a +/-20% range depending on data density, mapping uncertainty, and accounting for potential velocity model errors). Other resource assessment input parameters such as net reservoir thickness, porosity, water saturation, etc. were derived from available and analogous Nova Scotia offshore wells and reservoirs, as applicable. Plays in each region were risked at both the play level and prospect level, with the risking in each region treated as separate assessments. As such, a successful proven play in one region (e.g. Cretaceous rollover traps in Abenaki-Sable Corridor, with a play-level chance of success/risk of 1.0), does not pre-suppose a zero play risk in another region (e.g. Cretaceous rollover traps in the West Shelburne Corridor, with untested potential, and hence lower play-level chance of success). This is necessary due to abrupt lateral variations in input parameters across different regions and resulting variations in play-level geological risk.

The above inputs and geological risk parameters were entered into the @Risk™ Monte Carlo style probabilistic simulation software to generate a series of risked and unrisked petroleum resource estimates for each play along with the overall probabilistic total volumes for the combined study area (Table 1). The CNSOPB's mean (expected value) resource estimate for the total risked recoverable natural gas across the study area is 48.1 Trillion cubic feet (Tcf). Of this volume, 2.1 Tcf were produced from the five gas fields in the Sable Offshore Energy Project (SOEP), 147 Billion cubic feet (Bcf) were produced from the Deep Panuke field (of the estimated 647 Bcf estimated to be in place) (Belghiszadeh et al. 2023), and another 2 Tcf of fully risked recoverable gas is estimated to be contained in undeveloped significant discoveries in the Sable Subbasin and eastern Scotian Shelf (Smith et al. 2014). The mean (expected value) resource estimate for the total risked recoverable oil across the study area is 1.3 billion barrels, of which 44.5 MMB was produced during the Cohasset-Panuke project, another 16.3 MMB is estimated to be recoverable from West Sable and Primrose significant discoveries, and 51.6 MMB of mean recoverable oil is contained in the undeveloped Penobscot discovery (Kendell et al. 2013; Smith et al. 2015).

**Table 1.** Petroleum Resource Estimates – Scotian Basin and Sydney Basin. Table shows Mean values, with P10 values in brackets.

| | **Natural Gas** | | **Natural Gas Liquids** | | **Oil** | | **Oil Equivalent** | |
|---|---|---|---|---|---|---|---|---|
| | **BCF** | **$10^9$ m$^3$** | **MMB** | **$10^6$ m$^3$** | **MMB** | **$10^6$ m$^3$** | **MMBOE** | **$10^6$ m$^3$** |
| **In-Place Unrisked** | **721,883** *(800,433)* | **20,441** *(22,666)* | **6,650** *(7,510)* | **1,057** *(1194)* | **81,836** *(97,133)* | **13,011** *(15,443)* | **232,707** *(259,058)* | **36,997** *(41,187)* |
| **In-Place Risked** | **70,424** *(139,593)* | **1,994** *(3,953)* | **669** *(1,344)* | **106** *(214)* | **4,356** *(9,963)* | **693** *(1,584)* | **17,962** *(35,344)* | **2,856** *(5,619)* |
| **Recoverable Unrisked** | **455,454** *(511,536)* | **12,897** *(14,485)* | **4,403** *(5,026)* | **700** *(799)* | **21,775** *(25,411)* | **3,462** *(4,040)* | **110,043** *(122,624)* | **17,495** *(19,496)* |
| **Recoverable Risked** | **48,097** *(98,011)* | **1,362** *(2775)* | **473** *(972)* | **75** *(155)* | **1,278** *(2,880)* | **203** *(458)* | **10,260** *(20,458)* | **1,631** *(3,253)* |

As such, this report indicates that the total mean recoverable hydrocarbon resource in the Scotian and Sydney basins is roughly ten times greater than the total volume of known recoverable and produced gas and oil to date. The mean overall petroleum resource estimates for natural gas, natural gas liquids, oil and oil equivalent volumes are tabulated above. For a detailed description of the results from the CNSOPB's petroleum resource assessment, please refer to the *Petroleum Resource Assessment* section of this report and Appendices 1 to 6.

Omissions from this resource assessment include the Fundy Basin and parts of the Maritimes Basin located west of Cape Breton Island, as well as areas beyond the 4000 m bathymetric contour where there is limited to no subsurface geophysical data (e.g. seismic). Likewise, a more fulsome geological evaluation of the Middle to Late Cenozoic succession (post-Eocene) has not been done beyond the work of Campbell et al. (2015), Campbell and Mosher (2015), and Deptuck and Kendell (2020). Shallow burial depths and erosion make this interval unlikely to have exploration potential on the continental shelf, but the more expanded and highly complex stratigraphic succession on the continental slope requires further study to evaluate its hydrocarbon resource potential (within interfingering turbidite, contourite, and mass transport deposits).

## Introduction

The oil and gas potential of the Scotian margin has been studied for more than six decades, resulting in the collection of widespread 2D and 3D multichannel seismic datasets and the drilling of 124 unique exploration wells that have tested Paleozoic, Mesozoic, and Cenozoic hydrocarbon targets. Twenty-three significant discoveries have been declared – all of which are located on the central to eastern Scotian Shelf – within 100 km of Sable Island (Figure 1 inset). Eight of these were developed into three separate commercial projects (Cohasset-Panuke, Sable Offshore Energy Project, and Deep Panuke), with production of natural gas, condensate, and oil from both siliciclastic and carbonate reservoirs (Smith et al. 2014; Belghiszadeh et al. 2023). Numerous other proven gas, condensate, and oil discoveries remain undeveloped on the continental shelf. However, with the decommissioning and abandonment of the above projects, there is no longer any hydrocarbon production on the Scotian Shelf. Likewise, the relatively small number of wells on the continental slope, to date, have failed to identify commercial volumes of hydrocarbons (Kidston et al. 2007; Deptuck and Kendell 2020, 2022), and all exploration licences have now expired, with land returned to crown.

The Canada-Nova Scotia Offshore Petroleum Board (CNSOPB) geophysical regulations require exploration companies to submit copies of collected seismic data to the CNSOPB for archiving (Figure 1a, b). Likewise, detailed well history reports describing drilling results are also archived at the CNSOPB (Figure 1c). As part of its resource management mandate, these datasets are used by CNSOPB geoscience staff to evaluate the geology and hydrocarbon potential of the Canada-Nova Scotia Offshore Area. The last exploration cycle (2012 to 2018) a)

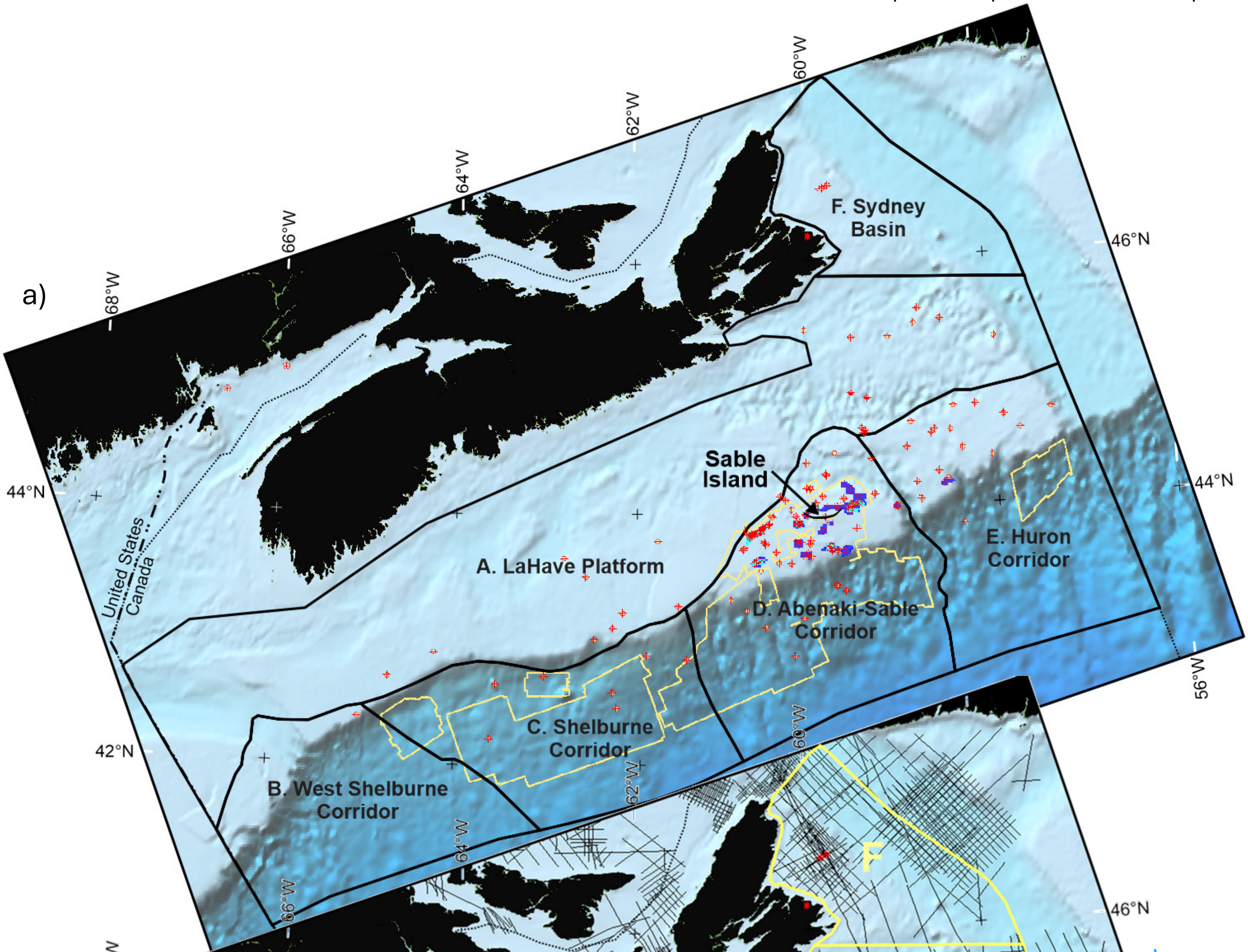

68°W
66°W
64°W
62°W
60°W
56°W
46°N
44°N
42°N
F. Sydney Basin
Sable Island
A. LaHave Platform
E. Huron Corridor
D. Abenaki-Sable Corridor
C. Shelburne Corridor
B. West Shelburne Corridor
United States
Canada


b)

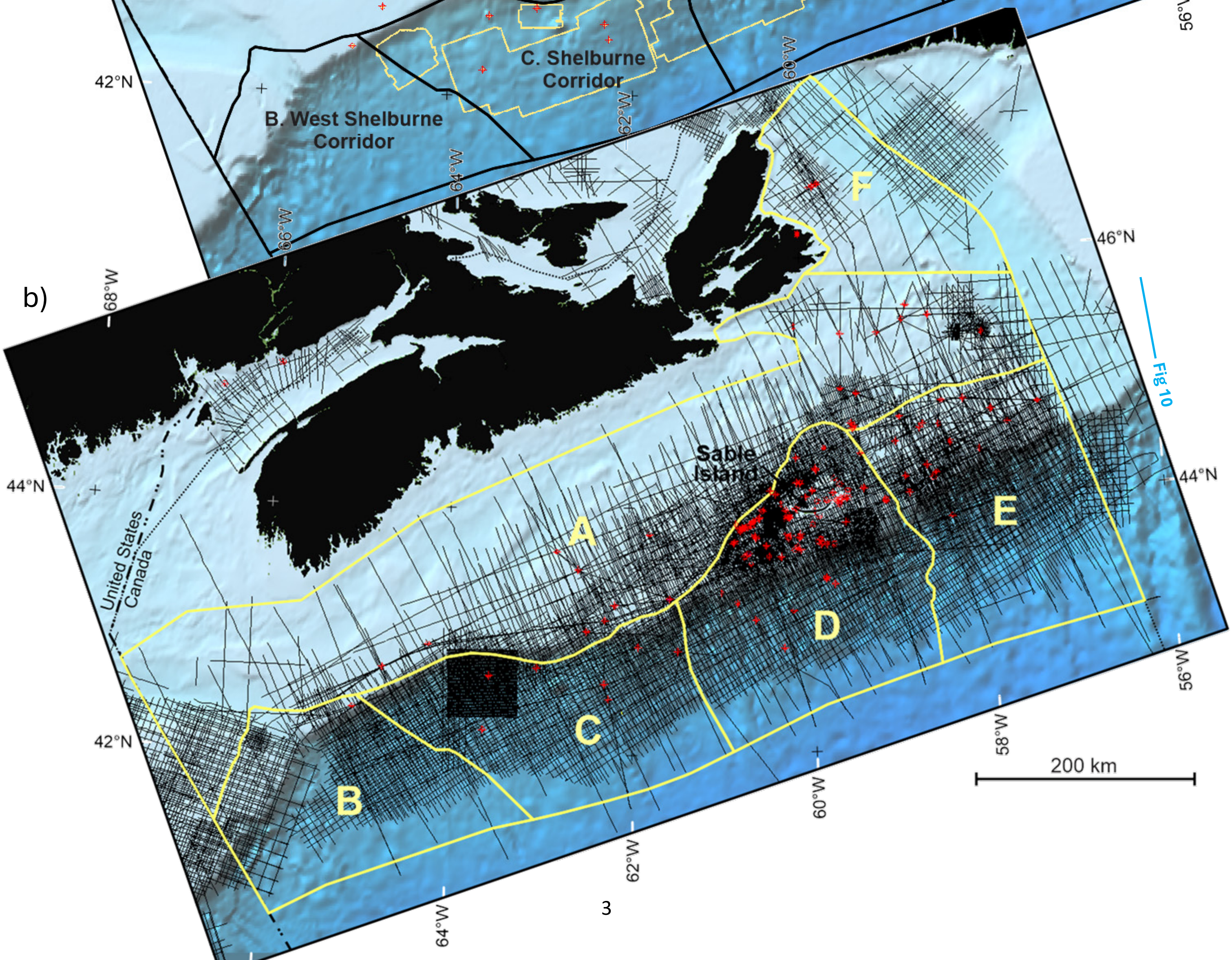

68°W
66°W
64°W
62°W
60°W
58°W
56°W
46°N
44°N
42°N
Sable Island
A
B
C
D
E
F
Fig 10
United States
Canada
200 km

**Figure 1** Bathymetry maps showing the location of the six geologically defined resource assessment regions, in relation to **(a)** 3D seismic data-sets (yellow), **(b)** 2D seismic profiles (black) and **(c)** well data.

c)

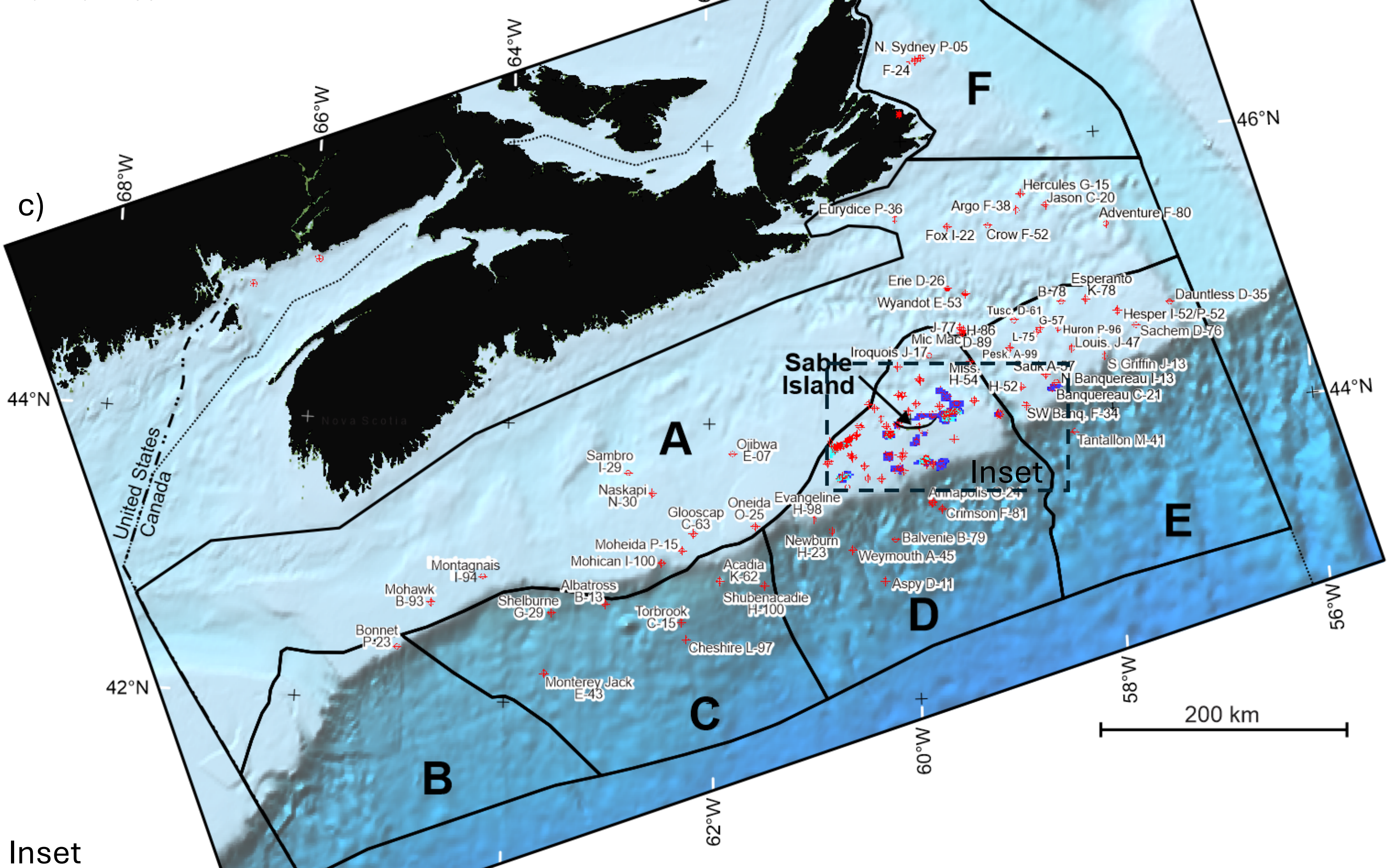


Inset

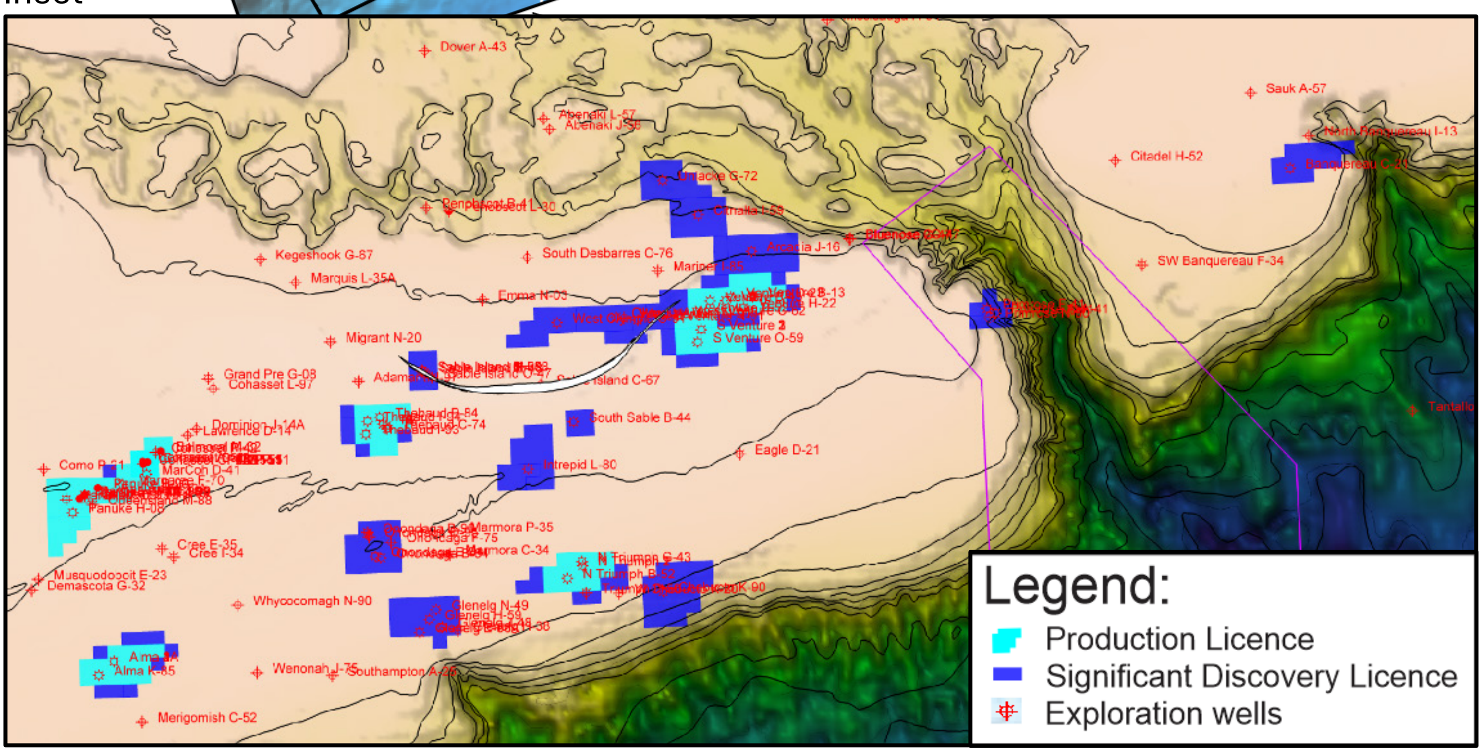


**Figure 1 continued…(Inset)** Closeup of the Sable Island area showing the distribution of former Production and current Significant Discovery licences.

resulted in the collection of two large wide-azimuth 3D seismic volumes on the central and western Scotian Slope (Shelburne and Tangier 3D volumes), and three wildcat exploration wells (Cheshire L-97/L-97A, Monterey Jack E-43/E-43A, and Aspy D-11/D-11A) (see Deptuck and Kendell 2020, 2022) (Figures 1, 2). Combined with historical archived data, interpretation of these datasets provides new insight into key elements of the petroleum system (trap, reservoir, seal, and source rock), how they vary across the study area, and their impacts of potential hydrocarbon resources.

### *Geographic subdivision of the study area*

This study provides an updated fully risked quantitative petroleum resource assessment of the Scotian Shelf (including the region east of Cape Breton Island) and the Scotian Slope stretching from the Canada-United States border to the Nova Scotia-Newfoundland-Labrador provincial boundary (Figure 1). Geological information presented in this report was derived from both unpublished work and several previously published CNSOPB reports that provide more in-depth geological information about the Scotian Shelf, Scotian Slope, and Sydney Basin (e.g. Kidston et al. 2007; Deptuck 2008, 2011, 2020; Deptuck and Kendell 2012, 2017, 2020, 2022; Kendell and Deptuck 2012; Kendell 2012; Smith et al. 2014, 2016, 2018; Kendell et al. 2013, 2016, 2017; Deptuck and Altheim 2018). The reader can access most of these reports here: Geoscience Publications | Canada-Nova Scotia Offshore Petroleum Board (CNSOPB). The reader is also referred to the collaborative *Scotian Basin Integration Atlas* (2023) for additional details about mapping deepwater architectural elements, sequence stratigraphy, lead high-grading, and petroleum system modelling (report can be accessed here: Scotian Basin Integration Atlas 2023 | Nova Scotia Offshore Energy Research Association (oera.ca)).

Seismic horizons were correlated through Upper Paleozoic, Mesozoic, and Lower Cenozoic strata variably distributed across the study area and calibrated to available well data. Seismic markers were then gridded and depth-converted using Petrel software and the velocity model described in Appendix 5 of Scotian Basin Integration Atlas (2023) that covers most of the Scotian Basin. For areas not covered by this model, an in-house layer-cake velocity model was used for depth conversions (e.g. for the Sydney Basin off Cape Breton Island; see Kendell et al. 2017). While depth-structure maps show the distribution, size, and style of potential hydrocarbon traps, isopach maps between key depth-structure surfaces provide important information about sediment dispersal through time. Using geological criteria like sedimentation rates (derived from isopach maps), dominant depositional environments, and the timing and style of salt expulsion (Shimeld 2004; Deptuck and Kendell 2017), the study area is separated into ***six*** geologically distinct geographic regions, each with a different suite of play types, geological risk parameters and resulting potential hydrocarbon resources (regions A through F). These regions are shown on Figure 1 and 2 and are described in more detail in the *Geological Setting* section. In addition to their geology, significant variations also exist in the extent and quality of reflection seismic coverage and the distribution of borehole information across each of these six regions.

### *Seismic data coverage*

Although 2D seismic coverage is extensive over most of the areas examined in this study, some seismic programs were acquired before 1980, and seismic image quality and resolution is highly variable. The continental slope of regions B, C, D, and E is generally covered by 3 to 6 km spaced 2D multichannel seismic profiles collected in the late 1990s to early 2000s, providing fair to good image quality and data density in most deepwater areas (Figure 1b). Exceptions do exist where salt overhangs or highly complex salt-related deformation degrades seismic imaging (e.g. areas below salt-stock canopies or flaring diapirs, in regions B, D, and parts of E), and out-of-plane artefacts can be severe. There is also generally poor data density seaward of the primary salt basin (areas B, C, D, E) and large swaths of the continental shelf lack modern data-sets, particularly in region A (LaHave Platform) and the landward parts of region B (Georges Bank). Most of the 2D seismic profiles in these areas were scanned and vectorized from paper copies or microfiche (e.g. see Deptuck and Altheim 2018), which strongly impacts interpretation confidence.

Since 1985, exploration companies have also amassed some 49 000 km$^2$ of 3D reflection seismic data across Nova Scotia's continental shelf and slope. Excluding overlap, these surveys provide very good to excellent subsurface imaging across an area of more than 39 700 km$^2$ (Figure 1a) The distribution of 3D seismic data, however, is sharply skewed towards region C (46%) and D (49%). All other areas have minimal or no 3D seismic coverage (less than 5% coverage; Table 2).

**Table 2.** Summary of 3D seismic coverage relative to each of the six regions examined in this study. Only two regions have more than 5% 3D seismic coverage (in bold). Also shown qualitatively is the relative coverage and quality of available 2D seismic programs on the shelf and slope in each region.

| Region | Area (km$^2$) | 3D seismic coverage (km$^2$) | % coverage by 3D seismic | 2D seismic coverage/overall quality (good, average, poor) |
|---|---|---|---|---|
| ***A. LaHave Platform*** | 109 013 | 212 | <<1 % | Shelf – poor/average to poor |
| ***B. West Shelburne Corridor*** | 31 767 | 518 | <2 % | Shelf – good/poor<br>Slope – average/average to poor |
| ***C. Shelburne Corridor*** | 34 733 | 15 996 | **46 %** | Shelf – average/poor<br>Slope – average/good to average |
| ***D. Sable-Abenaki Corridor*** | 42 852 | 21 057 | **49 %** | Shelf – good/average<br>Slope – average/average to poor |
| ***E. Huron Corridor*** | 40 894 | 1940 | 5 % | Shelf – poor/average to poor<br>Slope – good/average |
| ***F. Sydney Basin*** | 21 915 | 0 | 0 % | Shelf – poor/poor |

### *Well data and hydrocarbon occurrences*

Included within the perimeter of the study area are 122 exploration wells, distributed unevenly across the six defined regions (Table 3). In addition to providing direct calibration of rock types, petrophysical well logs and actual rock/fluid samples provide the clearest evidence for or against the existence of an active petroleum system.

*Region A* (LaHave Platform) is the largest area considered. With 22 wells, this region averages just one well for every 4955 sq km. Cretaceous fluvial-deltaic reservoirs in Erie D-26, Wyandot E-53, Mic Mac J-77, Mic Mac D-89 contain strong oil staining and several meters of reservoired oil that have been tied to an older, pre-Tithonian restricted marine, marly source rock (Kendell et al. 2013; Fowler 2020; Scotian Basin Integration Atlas 2023). Narrow rift basins underlie these well locations, which may have favoured late synrift or early post-rift accumulation of a restricted marine source rock. Aside from a minor gas show in unconsolidated Quaternary cover strata at Montagnais I-94 (377.6-383.7 m), no other hydrocarbon occurrences have been documented in the expansive area of region A.

*Region B* (West Shelburne Corridor) spans the shelf and slope off Georges Bank. With just one shelf well (Bonnet P-23) for an area covering 31 767 sq km, this region has the lowest well-density of the six regions examined in this study. Aside from minor gas shows in Bonnet P-23 (Deptuck et al. 2015), the dearth of wells and complete absence of deepwater wells, makes it difficult to evaluate its hydrocarbon potential. It is also noteworthy that an Early Eocene unconformity associated with the Montagnais bolide impact (Jansa and Pe-Piper 1987), coupled with older Cretaceous unconformities, cuts out much of the mid-Cretaceous succession (Deptuck and Campbell 2012), which remains largely untested in region B (discussed in more detail in the reservoir risking section).

*Region C* (Shelburne Corridor) contains seven wells, with a well-density of one well for every 4962 sq km. Two mud-gas peaks in Upper Jurassic carbonates on the shelf at the Albatross B-13 (3434-3440), and a minor mud-gas response from a thin Miocene siltstone on the slope at Torbrook C-15 (Kidston et al. 2007) provide the only borehole evidence of hydrocarbons in region C (Deptuck et al. 2015). Like Bonnet P-23, much of the Cretaceous succession in the two shelf wells in region C (Acadia K-62 and Albatross B-13) was eroded along Eocene and older unconformities or is condensed below seismic resolution. Five wells in region C are located on the slope (relative to Cretaceous paleogeography), with Shelburne G-29 (drilled in 1985), Monterey Jack E-43/E-43A and Cheshire L-97/97A (both drilled in 2016), providing the most complete stratigraphic calibration (and the *only* deepwater calibration of Jurassic strata anywhere in study area) (see Figure 2). None of these wells, however, encountered hydrocarbons, and likewise they found very

**Table 3.** Summary of exploration wells and hydrocarbon occurrences in each of the six areas examined in this study. References – 1. Kendell et al 2013; 2. Fowler 2019; 3. Smith et al. 2014; 4. Belghiszadeh et al. 2023; 5. Kendell et al. 2017; 6. Deptuck et al. 2015; 7. Smith et al. 2015

| Region | # of wells | Commercial and Significant Discoveries (hydrocarbon phase) | Other noteworthy hydrocarbon occurrences (hydrocarbon phase) | Ref. |
|---|---|---|---|---|
| ***A. LaHave Platform*** | 22 | - | Erie D-26, Wyandot E-53, Mic Mac J-77, Mic Mac D-89 (several meters of light reservoired oil, from pre-Tithonian source rock)<br>Mic Mac H-86 (minor oil staining) | 1, 2 |
| ***B. West Shelburne Corridor*** | 1 | - | Bonnet P-23 minor gas show | 6 |
| ***C. Shelburne Corridor*** | 7 | - | - | - |
| ***D. Sable-Abenaki Corridor*** | 71 | **Sable Offshore Energy Project** - Alma, North Triumph, Thebaud, Venture, South Venture (2.1 TCF gas produced)<br>**Cohasset-Panuke Field** (44.5 MMB oil produced)<br>**Deep Panuke Field** (147 Bcf gas produced of the 647 Bcf recoverable)<br>**Arcadia** (gas)<br>**Chebucto** (gas)<br>**Citnalta** (gas/condensate)<br>**Glenelg** (gas/condensate)<br>**Intrepid** (gas)<br>**Olympia** (gas/condensate)<br>**Onondaga** (gas/condensate)<br>**Primrose** (gas/oil)<br>**South Sable** (gas)<br>**Uniacke** (gas)<br>**West Olympia** (gas)<br>**West Sable** (gas/condensate/ oil)<br>**West Venture** C-62 (gas)<br>**West Venture** N-91 (gas) | Penobscot L-30 (light oil, 65-148 MMB in place)<br>Iroquois J-17 (oil staining)<br>Missisauga H-54 (minor oil staining)<br>Bluenose G-47 (gas show)<br>Eagle D-21 (gas, 1.27 Tcf in place)<br>Annapolis G-24 (gas/condensate)<br>Newburn H-23 (gas/condensate)<br>Aspy D-11 (gas/condensate) | 1, 3, 4, 7 |
| ***E. Huron Corridor*** | 19 | **Banquereau** (gas/condensate) | SW Banquereau F-34 (gas/condensate)<br>Louisbourg J-47 (gas/condensate)<br>Chippewa L-75, G-67 (minor oil staining) | 1, 3, |
| ***F. Sydney Basin*** | 2 | - | North Sydney P-05 (gas)<br>North Sydney F-24 (gas) | 5 |

little evidence for deepwater reservoir development (Deptuck and Kendell 2020).

*Region D* (Abenaki-Sable Corridor) contains 71 exploration wells, and a mean density of one well for every 604 sq km (Table 3). Well distribution in region D, however, is strongly skewed towards the continental shelf, with only six wells located on the continental slope where well density diminishes to just one well for every 4709 sq km. Nonetheless, there is widespread evidence for trapped hydrocarbons throughout region D. The continental shelf here is home to three former commercial developments (Cohasset-Panuke, Sable Offshore Energy Project, and Deep Panuke), with production of gas, condensate, and oil from both siliciclastic and carbonate reservoirs (Smith et al. 2014; Belghiszadeh et al. 2023). Likewise, several additional significant discoveries and other trapped hydrocarbons (both liquid and gas) demonstrate an effective hydrocarbon system is present in region D (Table 3). On the slope, three of the six exploration wells in region D (Newburn H-23; Aspy D-11/D-11A; and Annapolis G-24) encountered noteworthy gas-charged turbidite sandstones/siltstones, with minor gas shows also recorded in the reservoir-lean Balvenie B-79 and Weymouth A-45 wells (Kidston et al. 2007; Deptuck 2008; Deptuck and Kendell 2020).

*Region E* (Huron Corridor) contains 19 exploration wells, averaging one well for every 2131 sq km. The Banquereau significant discovery, located on the outer shelf of region E, consists of Cretaceous gas-charged fluvial-deltaic reservoirs in a fault rollover structure, similar to most of the significant discoveries in the Sable Subbasin (Smith et al. 2014). Significant gas shows were also documented at Southwest Banquereau F-34 and Louisbourg J-47, and minor oil staining is present in Chippewa L-75 and G-67, all located on the shelf (Kendell et al. 2013). Like region D, however, well control is strongly skewed towards the continental shelf, with only one well (Tantallon M-41) providing calibration of slope strata in an area of 24 259 sq km – the lowest well-density on the slope after region B. Tantallon M-41 well encountered a ~10 m interval of gas charged sands (Goodway et al., 2008), but very little reservoir-quality sandstone was encountered in the well. That the well did not reach earliest Cretaceous or Jurassic strata, means that the nearest calibration for such strata is Cheshire L-97, more than 350 km to the southwest, in an area with much slower sedimentation rates (region C - discussed in more detail in the reservoir risking section). Together, these hydrocarbon occurrences show that an active petroleum system is present in region E, but it is poorly calibrated on the slope.

*Region F* (offshore Sydney Basin) has just two wells in an area of 21915 sq km – North Sydney F-24 and North Sydney P-05 (Kendell et al. 2017). Both wells encountered gas in low porosity Pennsylvanian sandstone formations above the Horton Group. North Sydney F-24 was flow tested but was unable to flow gas to surface.

**Figure 2.** Bathymetric map of the Scotian Shelf and Slope, showing the location of the six geographic regions (yellow) relative to the perimeter of the Mesozoic primary salt basin (pink). The location of different basins and subbasins discussed in the report are labelled in black, with the three most recent exploration wells on the slope identified in red (in regions C and D).

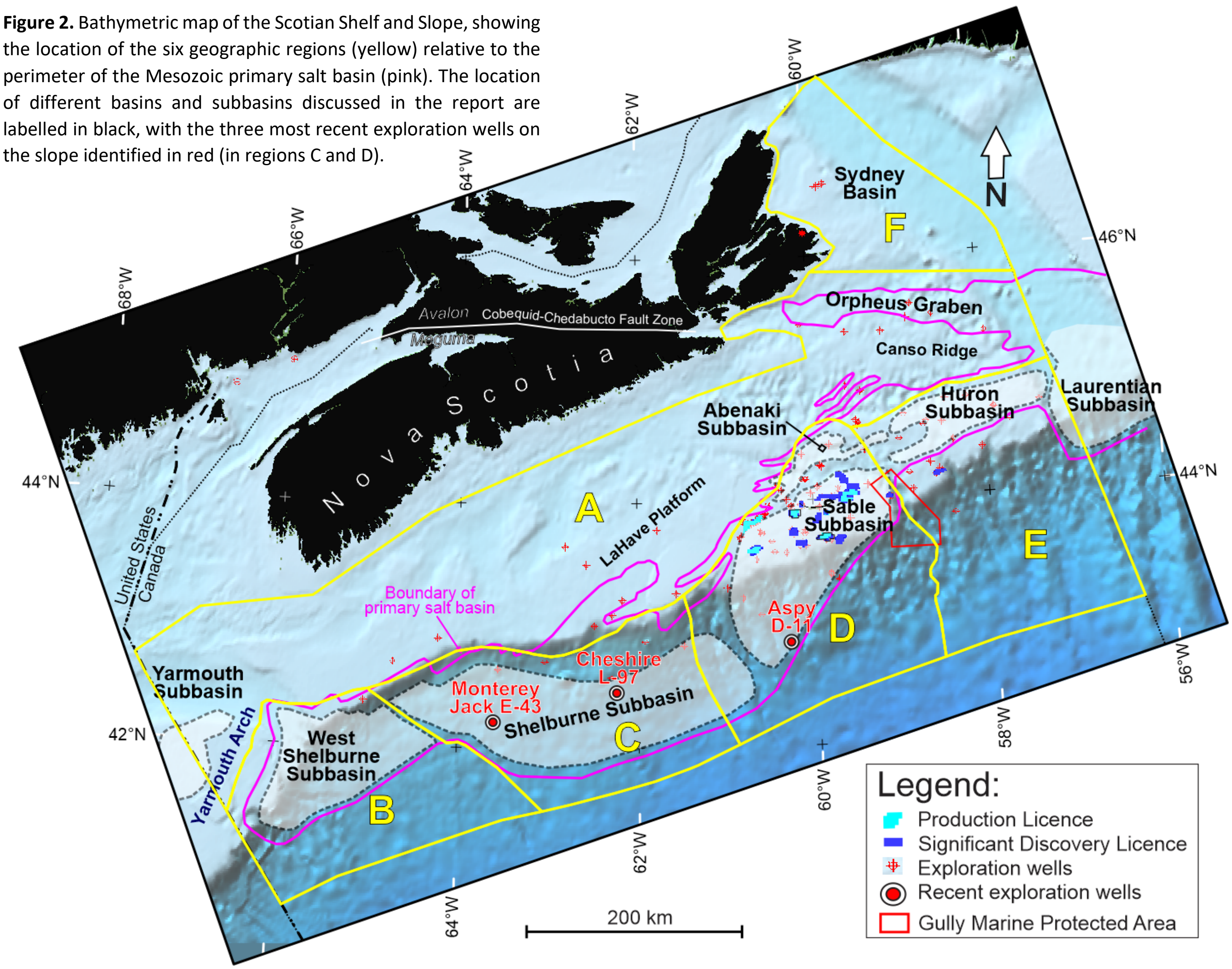

**Figure 3.** Top basement structure map of the Scotian margin (***top***) showing the location of important structural elements, including perimeter of primary salt basin (bold black dashed line); and (***bottom***) showing the distribution of expelled salt bodies (pink) that formed as Mesozoic sediments accumulated above the primary salt layer. SGR (South Griffin Ridge); SDRs (seaward dipping reflections). Line locations for Figure 6 shown in red. Modified from Deptuck and Kendell (2020).

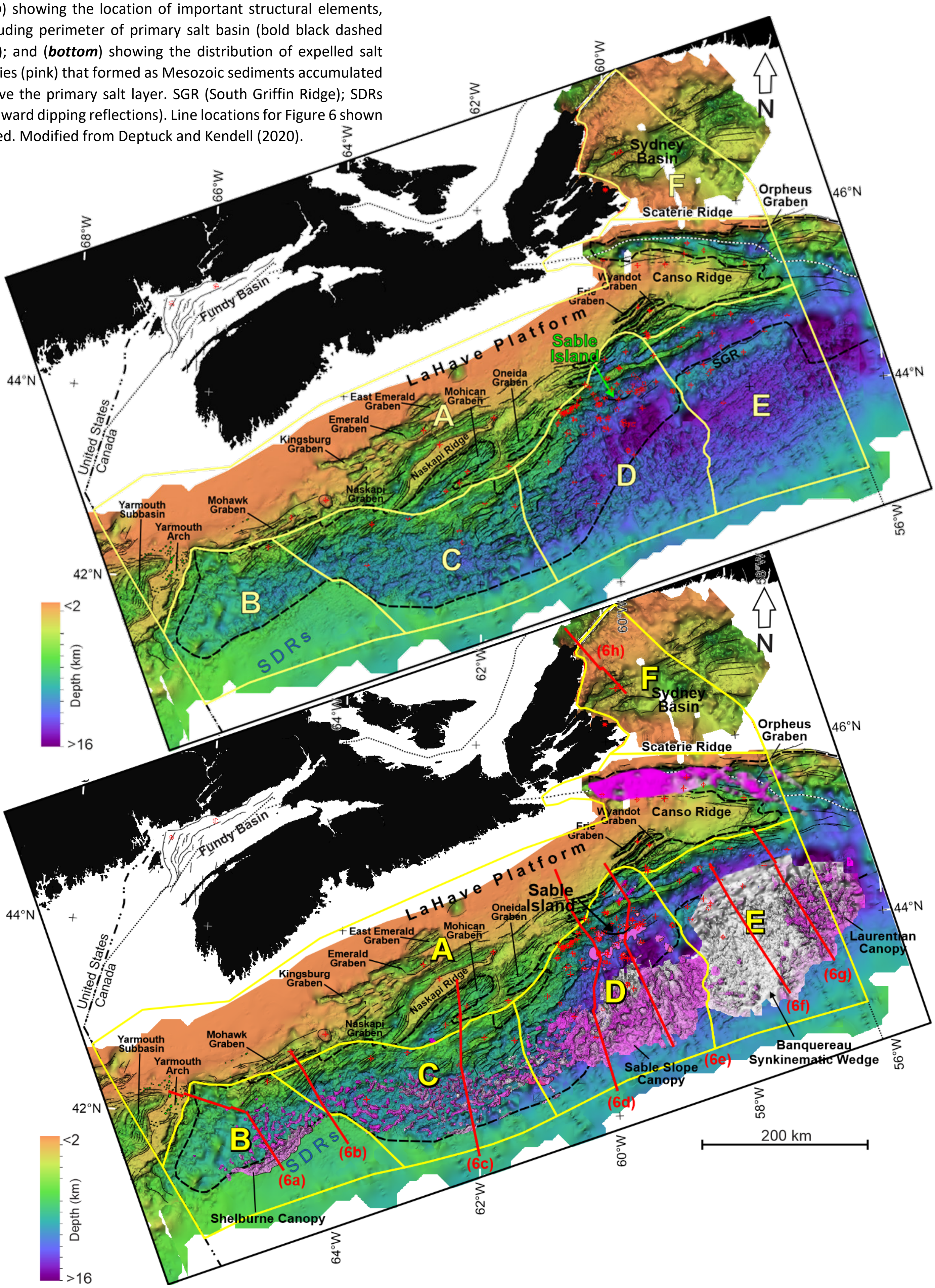

## Geologic Setting

The *six* geographic regions that make up the study area (Table 4) record important spatial variations in the tectonic setting, timing and amount of sediment supply, characteristics of the primary salt layer (age, location, thickness), and the magnitude of basement subsidence (combination of mechanical thinning of the crust, thermal subsidence, and isostatic loading). Regions A through E on the Scotian Shelf and Slope developed in the Mesozoic, during Triassic rifting, plate separation, and Early Jurassic break-up, with the eventual post-rift emplacement of oceanic crust between Nova Scotia and Morocco (e.g. McIver 1972; Jansa and Wade 1975; Given 1977; Holser et al. 1988; Welsink et al. 1989; Wade and MacLean 1990). In contrast, region F (Sydney Basin) located off Cape Breton Island, developed during an older Late Paleozoic period of tectonics involving oblique convergence as Pangea was assembled (Gibling et al. 2008; Waldron et al. 2015). Aside from the sharp truncation of folded Permian to Carboniferous strata along a prominent Quaternary unconformity, the Sydney Basin appears relatively unaffected by the younger Atlantic rift.

### *Mesozoic Atlantic margin*

In the early stages of Mesozoic rifting, Triassic sediments in region A accumulated in a complex network of rift basins that formed adjacent to the most prominent extensional basement border faults (Figures 3, 4). In some areas, like the Yarmouth Subbasin (Georges Bank; Deptuck et al. 2015) and Oneida Graben (central Scotian Shelf; Deptuck and Altheim 2018 – Figure 5), suspected intervals of pre-rift salt-bearing Carboniferous strata were variably overprinted by Mesozoic extensional tectonics (analogous to the situation along the southern Grand Banks, where several wells encountered pre-rift salt-bearing Carboniferous strata below Mesozoic salt-bearing syn-rift strata; Pascucci et al. 1999; McAlpine et al. 2004). The landward parts of the platform were heavily eroded, and as such both basement horst blocks and intervening rift basins are truncated along a prominent peneplain surface (Figure 5). Early fill, sourced locally from elevated pre- or syn-rift topography, is mainly made up of immature siliciclastics deposited in alluvial, fluvial, playa-lacustrine, or eolian environments (e.g. Wade et al. 1996; Olsen 1997; Leleu et al. 2009). Collectively referred to as Eurydice Formation (Jansa and Wade 1975), these syn-rift red beds pass up-section or laterally (moving further offshore) into evaporites (e.g. Holser et al. 1988; Wade and MacLean 1990; Deptuck and Kendell 2017; Deptuck and Altheim 2018).

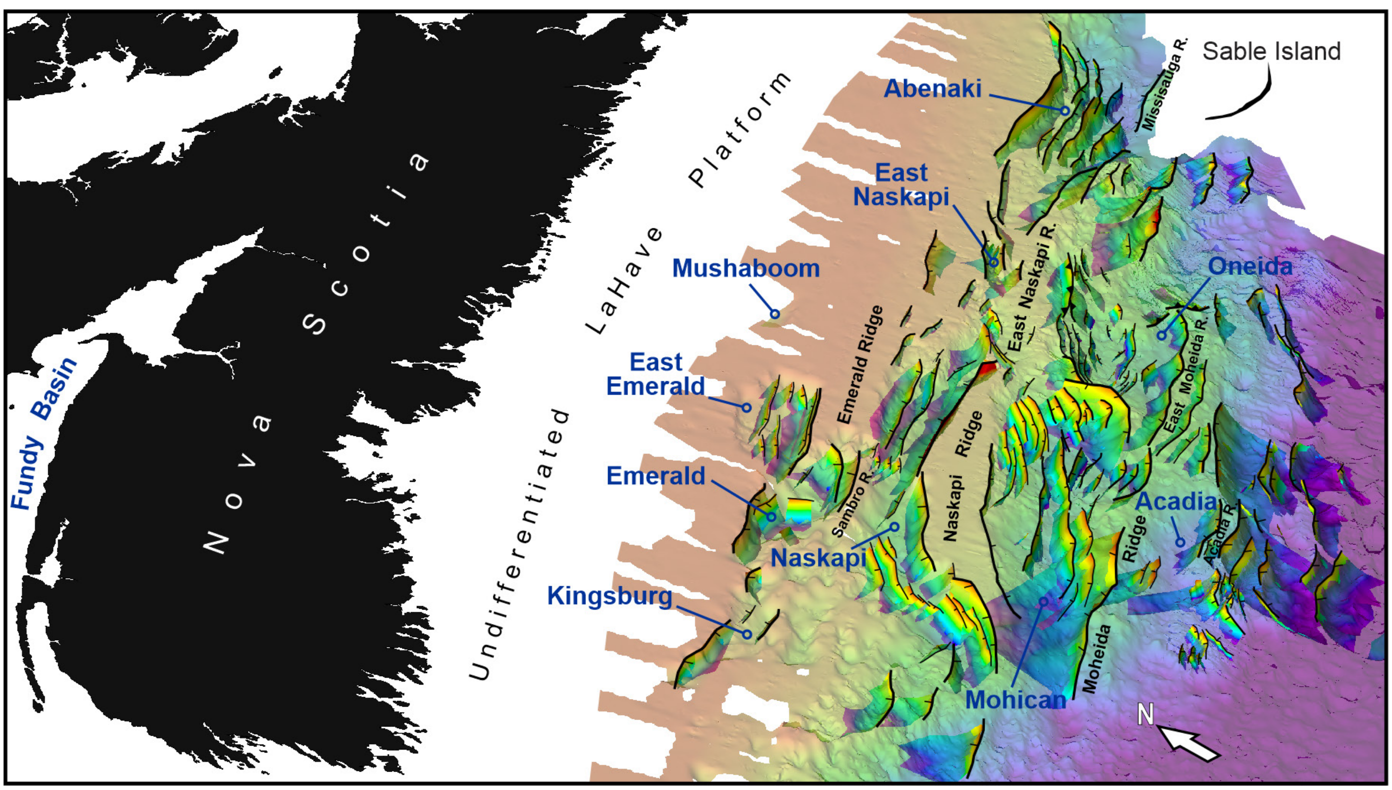


**Figure 4.** Perspective view from the southwest showing the semi-transparent top basement surface with basement-involved faults that were active during Mesozoic rifting along the Maritimes Atlantic margin (mainly on the LaHave Platform; from Deptuck and Altheim (2018).

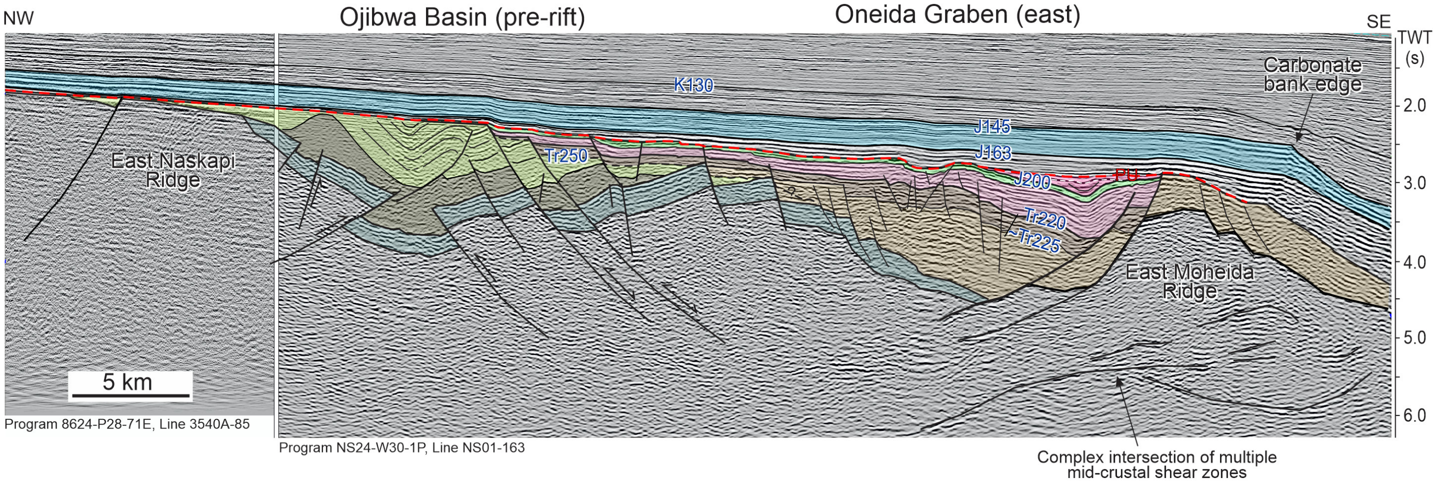


**Figure 5.** Composite seismic section across the Oneida Graben (region A), showing both folded/shortened pre-rift Carboniferous(?) strata (uncalibrated), and overlying Eurydice to Argo syn-tectonic succession. Note the bright green J200 marker was jump-correlated from Glooscap C-63 that encountered 152 m thick CAMP-related basalt in the Mohican Graben, southwest of the Oneida Graben; PU = post-rift unconformity. (from Deptuck and Altheim 2018).

### *Sedimentation and salt tectonics*

Widespread precipitation of Late Triassic and earliest Jurassic salt (mainly halite) took place during the latter stages of rifting between Nova Scotia and Morocco, resulting in two distinct periods of Mesozoic salt accumulation, separated by ~201 Ma basaltic lava flows associated with the Central Atlantic Magmatic Province (CAMP) (McHone 1996; Marzoli et al. 1999; MacRae and Pe-Piper 2022). Narrow folded or pillowed tongues of primary salt occupied the axes of numerous rift basins in region A, including the Orpheus, Mohican, Oneida (e.g. pink intervals in Figure 5), Acadia, Abenaki, Wyandot, and Erie grabens (Deptuck and Altheim 2018; Hanafi et al. 2022). Deformation of the primary salt layer took place mainly through sediment loading (e.g. mouth of the Orpheus Graben), though local basement inversion also played a role in some grabens (e.g. in the Mohican and Oneida grabens).

Both the primary salt layer and underlying syn-rift strata extend into areas seaward of the LaHave Platform, where post-rift mobilization of salt played a more important role in the structural and stratigraphic development of the slope. The boundaries between regions B, C, D, and E coincide with abrupt lateral changes in the timing and volume of sediment delivered to the margin and the resulting timing and style of salt expulsion (Table 4) (Shimeld 2004; Albertz et al. 2010; Deptuck and Kendell 2017).

Jurassic and Cretaceous seismic markers like J163, J145, K125, and K94 roughly match the top and base of major siliciclastic or carbonate lithostratigraphic units like the Mic Mac/Abenaki, Missisauga, and Logan Canyon formations that aggraded and prograded above the shelf (Welsink et al. 1989; Wade and MacLean 1990). Direct deepwater ties from Monterey Jack E-43 and Cheshire L-97 also make it possible to correlate the seismic stratigraphic framework onto the slope seaward of the salt basin, and ultimately towards the northeast. This provides an additional constraint on the age of seismic markers on the eastern Scotian Slope (where there is very little well calibration, and where correlations across the shelf are hindered by densely spaced listric faults and poor seismic imaging).

Middle Jurassic and Cretaceous thickness maps show the strong asymmetry in stratigraphic thickness, where along-strike sedimentation rates can vary by more than an order of magnitude (Figures 6, 7). In general, the western parts of the margin (regions B and C) were sediment-starved, with low sedimentation rates focused in numerous relatively stationary (vertically-subsiding) salt-withdrawal minibasins. Except for a small salt tongue canopy that extends ~25 km seaward of the primary salt basin off Georges Bank (associated with the 'Shelburne Delta'), most of the salt diapirs (stocks and walls) in regions B and C are located immediately above the primary salt basin from which they were expelled.

In contrast, the eastern parts of the margin (regions D and E) were sediment-rich, with an overall westward migration and seaward progradation of the thickest parts of the Mic Mac, Missisauga, and Logan Canyon formations (Figures 7, 8). Shifts in these major depocenters closely track the sequential development of laterally extensive "bands" of listric growth faults on the shelf (e.g. Figures 6d to g), and a wide spectrum of salt-related deformation styles on the slope, including seaward-leaning salt feeders and extensive amalgamated salt stock canopies or salt nappes that today are located up to 150 km seaward of the original primary salt layer (e.g. Figures 3, 6; Deptuck and Kendell 2020; 2022).

In Figure 9 - a compilation of six approximately strike-oriented seismic profiles across the middle slope - the asymmetry in sediment accumulation in clear, as is the westward migration of Jurassic and Cretaceous depocenters. Similarly, Figure 11 located seaward of the salt basin shows that the along-strike asymmetry in sedimentation continues even on the continental rise, ultimately reflecting broadscale shifts in depositional environments on the shelf.

**Table 4.** Summary of the tectonic setting, salt tectonic style, and dominant sedimentary setting in each of the six geographic regions evaluated in this study.

| *Region* | *Tectonic setting* | *Salt tectonic style* | *Sedimentation* |
|---|---|---|---|
| ***A. LaHave Platform*** | • Stable platform with thick continental crust<br>• Seaward half broken by 2-5 km deep Triassic extensional rift basins above mid-crustal shear zones<br>• Prominent eroded horst blocks separate some rift basins<br>• Slow post-rift subsidence | • Primary "syntectonic" salt was deposited in distal rift basins in the latter stages of rifting, probably continuing into the early postrift (e.g. Orpheus, Mohican, Oneida, Acadia grabens)<br>• Mainly salt pillows and folded interlayered salt and fine-grained dolomitic shale | • Rift basins containing immature siliciclastic sediment, with landward parts heavily eroded along post-rift unconformity<br>• Pass up-section into salt and interlayered salt and dolomitic shale<br>• Post-rift succession varies from carbonates to siliciclastics |
| ***B. West Shelburne Corridor*** | • Landward parts coincide with abruptly tapered 'necked' crust seaward of heavily eroded Yarmouth Arch<br>• Magmatic part of the margin, with SDRs seaward of salt basin | • Up-slope listric faults pass down-slope into thin-skinned shortening<br>• Small salt-tongue canopy expelled in Middle to Late Jurassic | • Region of the Middle Jurassic to Cretaceous 'Shelburne Delta'<br>• Volumetrically much smaller than Sable Island Delta, but strong indications of progradation |
| ***C. Shelburne Corridor*** | • Landward parts located above necked crust; seaward parts located above more rapidly subsiding hyperextended crust<br>• Good imaging of candidate reflection Moho ('M-marker')<br>• Outer band of ECMA coincides with outer edge of primary salt basin | • Up-slope thin-skinned gravity gliding above primary salt basin; downslope shortening and minibasin down-building into thicker primary salt<br>• Mainly vertical salt diapirism, with expelled salt bodies located immediately above primary salt layer | • Region generally sediment starved in Middle Jurassic through Cretaceous<br>• Aggradation of Jurassic carbonate bank (Abenaki Fm) with sharp bank edge and porous reef margin<br>• Generally condensed Lower Cretaceous strata ('Roseway unit') |
| ***D. Sable-Abenaki Corridor*** | • Landward parts located above necked crust; seaward parts located above hyperextended crust<br>• Abenaki and Sable depocenters separated by Missisauga Ridge, a prominent horst block<br>• Basement mapping beneath deepest parts of Sable Subbasin uncertain due to poor seismic imaging | • Jurassic salt loading, followed by Cretaceous progradation and emplacement of salt canopies on shelf and slope<br>• Amalgamated salt stock canopies in west, and salt nappe canopy in east<br>• Turtled minibasins both above primary salt and canopy salt<br>• along-strike alternation between roho-style salt-based detachments and expulsion rollovers | • Transition between sediment starved carbonate bank and voluminous Upper Jurassic mixed siliciclastics and carbonates<br>• Voluminous Lower to mid-Cretaceous sedimentation ('Sable Island Delta') after westward shift in sediment delivery (in response to Avalon Uplift)<br>• Primary reservoir interval for known discoveries on the shelf |
| ***E. Huron Corridor*** | • Landward parts located above abruptly necked crust<br>• Seaward boundary of salt basin corresponds to South Griffin Ridge, with hyper-extended crust further seaward still | • Most prominent salt tectonics took place in the Middle to Upper Jurassic on the slope, during emplacement of a large salt-based detachment (Banquereau Synkinematic Wedge; BSW) | • Voluminous Middle to Upper Jurassic sedimentation associated with "Mic Mac Delta"<br>• Westernmost Laurentian Subbasin included in this region where Mohican siliciclatics were thickest |
| ***F. Sydney Basin*** | • Basin perched above thick sutured crust cut by multiple oblique strike-slip reactivate terrane boundaries<br>• Unroofed Carboniferous/ Permian basin truncated along Quaternary Unconformity | • Windsor Group salt diapirs and folds; initial salt loading took place during Mabou deposition<br>• Salt distribution strongly impacted by Horton basement faulting<br>• Probable strike-slip deformation of salt bodies | Pre-salt Horton overlain by Windsor and variably loaded by post-Windsor siliciclastics (e.g. Mabou Group and younger Pennsylvanian strata) |

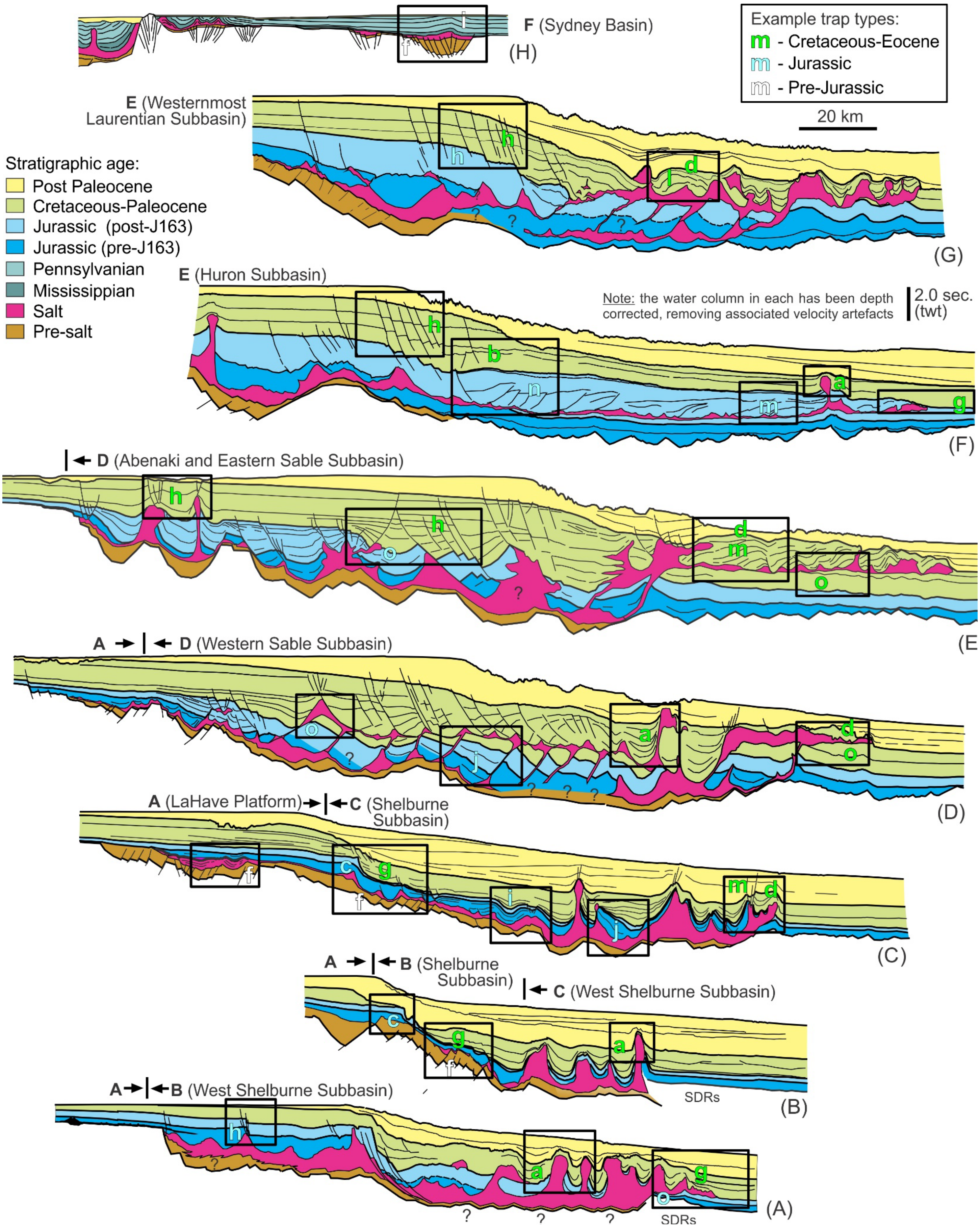


**Figure 6.** Line drawings of representative composite seismic sections across the study area. See table 4 for summary of tectonic setting, salt tectonic style and depositional environments. Line locations shown in figure 3. Adapted from Deptuck and Kendell (2017). Transect H is from Kendell et al. (2017). Black squares highlight different trapping styles described in this report; see letter key in Figure 19 for trap types.

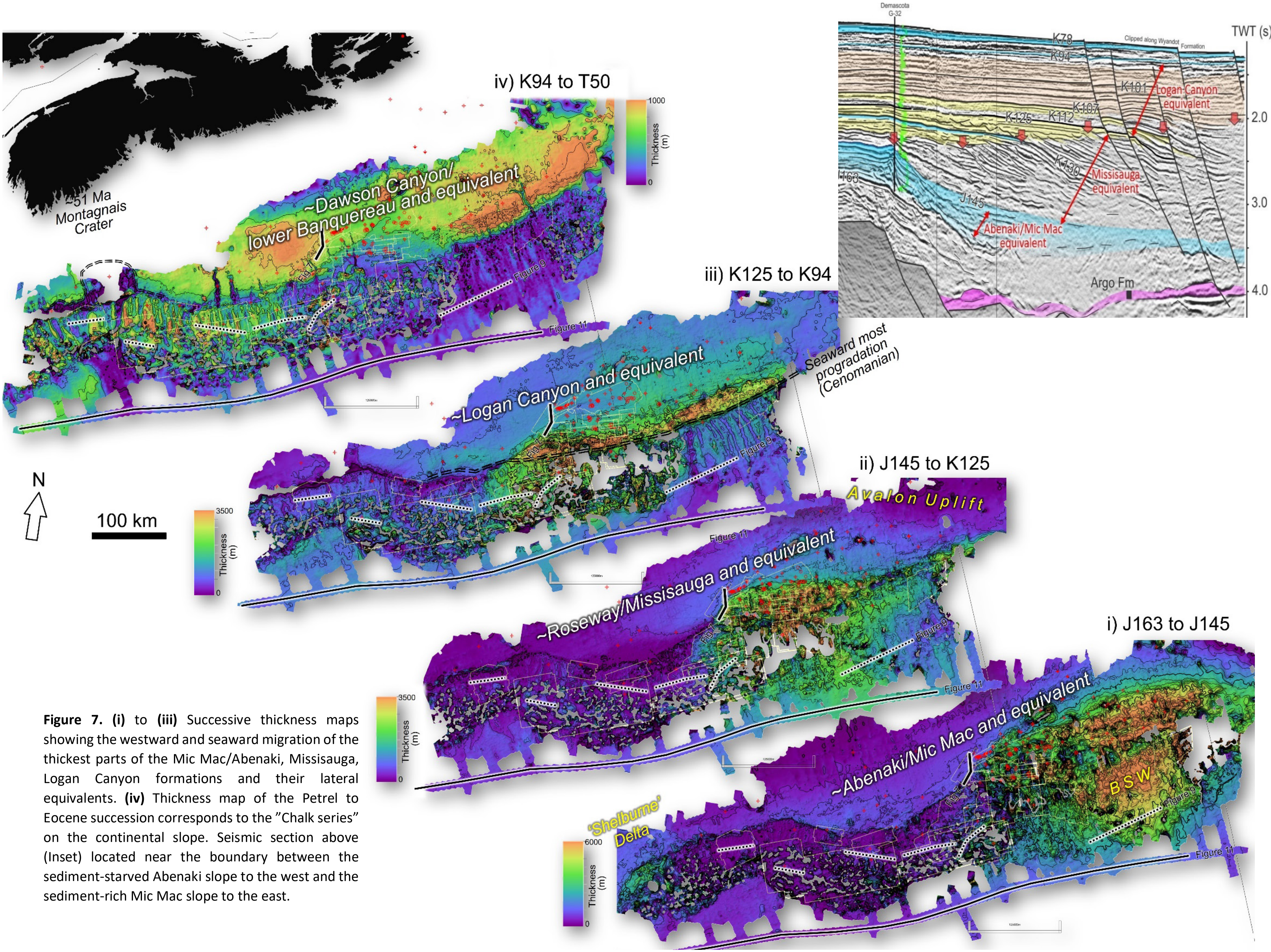


**Figure 7.** **(i)** to **(iii)** Successive thickness maps showing the westward and seaward migration of the thickest parts of the Mic Mac/Abenaki, Missisauga, Logan Canyon formations and their lateral equivalents. **(iv)** Thickness map of the Petrel to Eocene succession corresponds to the "Chalk series" on the continental slope. Seismic section above (Inset) located near the boundary between the sediment-starved Abenaki slope to the west and the sediment-rich Mic Mac slope to the east.

The sharp contrast in Middle-Late Jurassic sediment thickness in Figure 7i, 9i, and 11i reflects abrupt lateral changes in depositional environments. Carbonate-dominated sedimentation in region C took place as a rimmed carbonate platform aggraded (Abenaki Formation) on the shelf, versus ramp-style mixed carbonate-siliciclastic sedimentation in region E, where the much thicker Mic Mac Formation aggraded and prograded above the J163 marker (across the eastern Scotian Shelf; Wade and MacLean 1990). The sediment-starved carbonate foreslope in region C contrasts sharply with the 5 to 6 km of uncalibrated slope strata in region E where a large salt-based detachment formed (known as the Banquereau Synkinematic Wedge - BSW; Shimeld 2004; Ings and Shimeld 2006; Deptuck et al. 2014) (see Table 4). Several kilometers of Mic Mac-equivalent sediment also accumulated in the eastern reaches of region D at this time (in the Abenaki and Sable Subbasins), expelling vertical to seaward-leaning salt feeders that locally amalgamated into small salt-stock canopies before the end of the Jurassic.

The start of Cretaceous sedimentation is marked by an abrupt 125 km westward shift in the thickest parts of the Missisauga-equivalent isopach (Figures 7ii, 9ii). This shift probably reflects the development of the Avalon Uplift that took place near the end of the Jurassic in response to rejuvenated rifting between the Grand Banks and Iberia (Jansa and Wade 1975). Erosion of the Avalon Uplift produced a prominent angular unconformity on the eastern Scotian Shelf and southern Grand Banks (Figures 7, 10). Erosion and stratigraphic thinning imply that it remained a positive topographic element through at least the Early Cretaceous (Deptuck et al. 2014).

Whereas the primary salt budget was largely expended by the end of the Jurassic in the Huron Subbasin (that largely welded-out as the BSW formed), the primary salt layer in the Sable Subbasin had not yet been depleted. As such, progradation of the Sable Delta across the Sable Subbasin initiated a new generation of Cretaceous salt-related deformation that ultimately emplaced the younger 'Sable Slope Canopy' on the central Scotian Slope (Kendell 2012). Up to 3.5 km of siliciclastic-dominated fluvial-deltaic sediment of the Missisauga Formation (and its distal equivalents) accumulated in region D and the western parts of region E, as the Sable

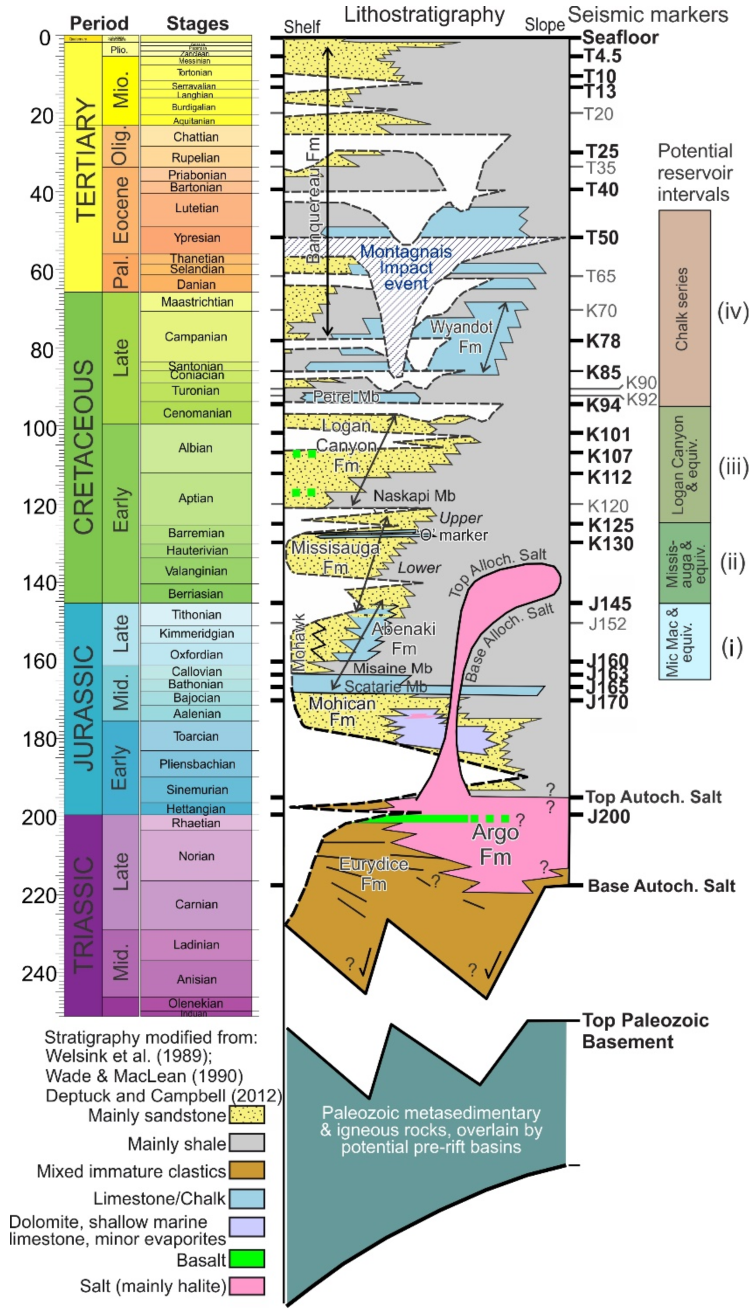


**Figure 8.** (above) General litho-chronostratigraphic chart for the Atlantic Scotian margin. Note that there are lateral variations in the thickness and lithology of several units. For example, the Abenaki Fm is replaced along the eastern parts of the margin by the Mic Mac Fm, composed of thicker mix intervals of carbonates and siliciclastics. Similarly, the Missisauga Fm passes towards the west into condensed carbonates with minor siliciclastics of the "Roseway Unit".

**Figure 9.** (next page) Composite transect compiled from six representative strike-oriented seismic profiles across the Scotian Slope. Note the overall westward migration of Mic Mac- to Missisauga- to Logan Canyon-equivalent slope successions. Also note that there is a ~125 km gap between the right two transects, where Jurassic and Cretaceous strata are complexly deformed above and below the allochthonous salt of the Sable Slope Canopy (Kendell 2012). Profile locations shown in Figures 7 and 28.

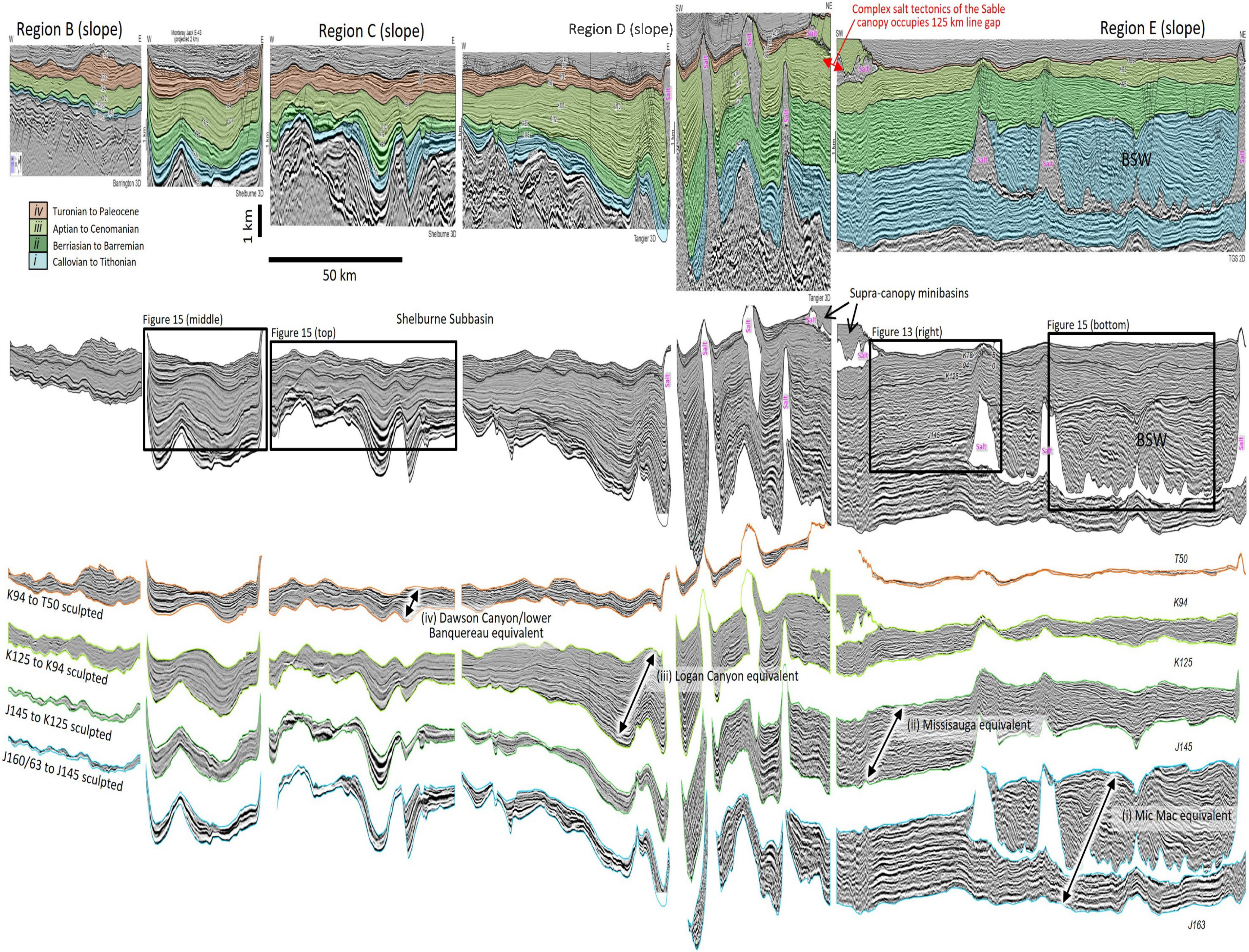
Region B (slope)
Region C (slope)
Region D (slope)
Region E (slope)
Complex salt tectonics of the Sable canopy occupies 125 km line gap
Monterey Jack E-43 (projected 2 km)
Barrington 3D
Shelburne 3D
Tangier 3D
TGS 2D
iv Turonian to Paleocene
iii Aptian to Cenomanian
ii Berriasian to Barremian
i Callovian to Tithonian
1 km
50 km
Salt
BSW
Supra-canopy minibasins
Shelburne Subbasin
Figure 15 (middle)
Figure 15 (top)
Figure 13 (right)
Figure 15 (bottom)
K78
94
K125
J145
T50
K94
K125
J145
J163
K94 to T50 sculpted
K125 to K94 sculpted
J145 to K125 sculpted
J160/63 to J145 sculpted
(iv) Dawson Canyon/lower Banquereau equivalent
(iii) Logan Canyon equivalent
(ii) Missisauga equivalent
(i) Mic Mac equivalent

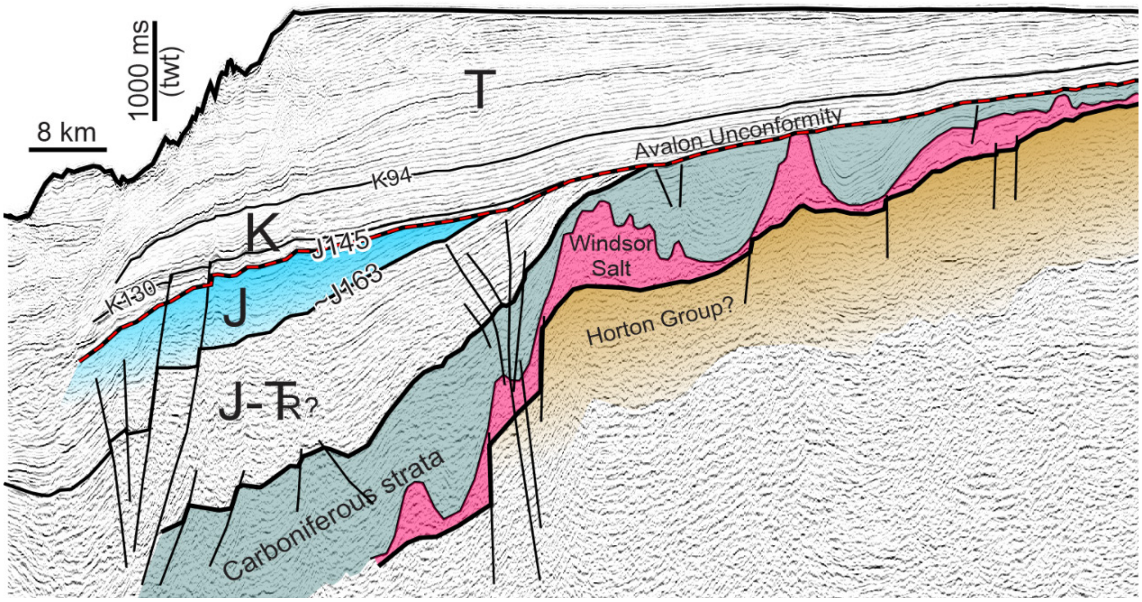


**Figure 10.** GSC multichannel seismic profile crossing the Avalon Unconformity on the southern Grand Banks (line location shown east of the map in Figure 1). Carboniferous, Triassic and Jurassic strata were eroded below the unconformity, with Mid to Late Cretaceous strata absent or thinning above it.

Island Delta prograded towards the south and west, driving salt-related deformation. In addition to diverting rivers towards the Sable Subbasin, the Avalon Uplift may also have shed sediment into deepwater (Jermannaud et al. 2023). Thick turbidite-successions accumulated on the slope in front of the early Sable Canopy, but also in front of the older BSW in region E, buttressing and stalling its seaward advance (Deptuck and Kendell 2017). At the same time, the pre-Albian western Scotian Shelf remained sediment-starved in the Early Cretaceous, with condensed platform carbonates and minor siliciclastics aggrading above the shelf ('Roseway Unit' of Wade and MacLean 1990; Moscardelli et al 2019) and slope of region C.

The westward and seaward march of the Sable Island Delta continued into the mid-Cretaceous, as up to 3.5 km of additional Logan Canyon-equivalent strata accumulating in region D (Figure 7iii). On the slope, expulsion rollovers and roho systems continued to grow as seaward-leaning salt tongues or amalgamated salt-stock canopies developed (e.g. Figure 6; Sable Slope Canopy of Kendell 2012). Further east in region E, where salt expulsion had already taken place in the Jurassic, the thickest parts of the Logan Canyon Formation reactivated the headward parts of the BSW. Up-slope thin-skinned extension across these listric faults drove down-slope shortening in the now-buttressed BSW, generating salt-cored buckle folds along its perimeter (forming the "Banquereau fold-belt" described later; Ings and Shimeld 2006; Deptuck et al. 2014).

The Logan Canyon Formation prograded as far west as the eastern parts of region C, where the delta built across the carbonate platform in the Late Albian, reaching its maximum regression sometime in the Cenomanian (Deptuck and Kendell 2020). Furthest west, in region B, a subtle increase in sediment thickness is detected in Late Jurassic and Cretaceous isopach maps in Figure 7, where several regressive-transgressive cycles record delta progradation across growth faults on Georges Bank. These are associated with progradation of the 'Shelburne Delta', that was intermittently active in the Middle to Late Jurassic and the Early to mid-Cretaceous (Beicip-Franlab et al. 2015).

The Upper Cretaceous to Early Eocene succession above the Logan Canyon Formation (and its equivalents) marks a general lithological change to pelagic chalks and marls of the Petrel Member, Wyandot Formation, and informal 'Ypresian Chalk' (Fensome et al. 2008; Weston et al., 2012) that accumulated on the shelf and slope between the K94 and T50 markers. Chalk facies pass landward into highstand deltas with clinoforms that first reached the continental shelf edge in the Maastrichtian landward of region C and in the Paleocene/Eocene along region E (Fensome et al. 2008).

The isopach map in Figure 7iv shows the southern and northern delta lobes on the shelf nicely. This situation is similar to equivalent strata in the Jeanne d'Arc Basin off Newfoundland where, despite the long period of mainly elevated eustatic sea level in the Late Cretaceous, landward clastic sediment sources eventually prograded

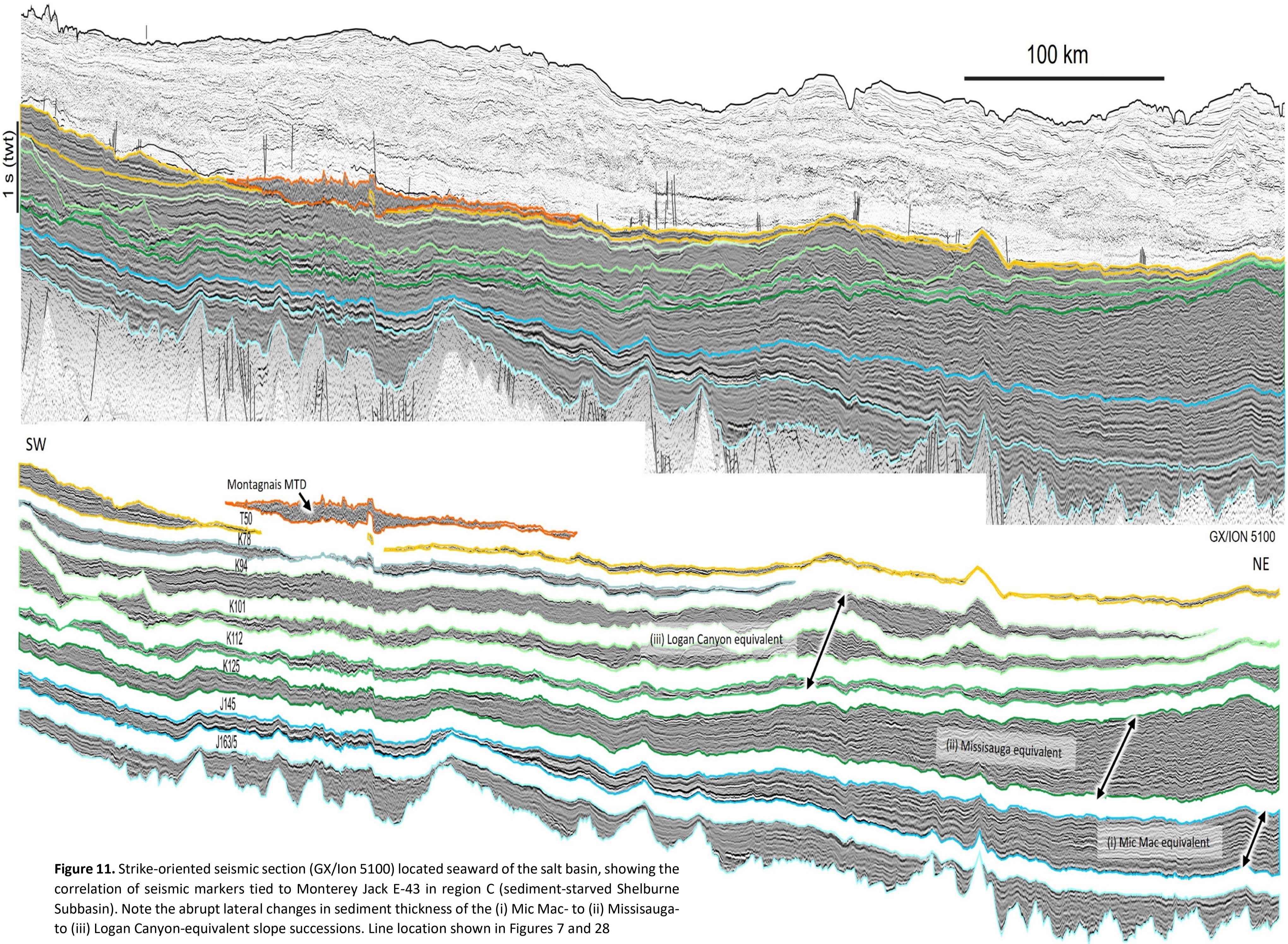


**Figure 11.** Strike-oriented seismic section (GX/Ion 5100) located seaward of the salt basin, showing the correlation of seismic markers tied to Monterey Jack E-43 in region C (sediment-starved Shelburne Subbasin). Note the abrupt lateral changes in sediment thickness of the (i) Mic Mac- to (ii) Missisauga- to (iii) Logan Canyon-equivalent slope successions. Line location shown in Figures 7 and 28

across older pelagic carbonates like the Petrel and Wyandot Formations (Deptuck et al. 2003). On the slope, the K94 to T50 chalk-bearing succession is thickest in areas C and D, where it is heavily dissected by Cenozoic younger canyon systems (Figures 7iv, 9iv, 11iv) (Deptuck and Campbell 2012).

### *Paleozoic Sydney Basin*

The Sydney Basin forms a depocenter between Cape Breton Island and Newfoundland where up to 7 km of mainly Carboniferous to Permian strata accumulated beneath the modern Laurentian Channel (Figure 12). Key seismic markers through the Syndey Basin were described in Kendell et al. (2017) and include top pre-Carboniferous basement, the Mississippian C352 (top Horton Group) and C325 (near top Windsor Group) markers, and the Pennsylvanian C308, C303, and C300 markers (within the Morien to Pictou Group). Although there is no well calibration for pre-C325 markers in the offshore Sydney Basin, marker age is inferred from onshore exposures of Carboniferous strata on Cape Breton Island and from studies in other parts of the Maritimes Basin (e.g. Durling and Marillier 1990; 1993).

The C352 marker is an unconformity that caps a faulted mixed-Horton Group succession deposited above rifted basement. Horton comprises mainly siliciclastics deposited in intermontane, alluvial to shoreline and lacustrine settings. They fill a series of isolated to interconnected northeast-trending rift basins that probably formed during or shortly after the middle-late Devonian Acadian orogeny (Pascucci et al., 2000) (Figure 6f). Rift basins pass up-section into a marine succession of mixed evaporites, limestones, dolomites, and finer-grained siliciclastics of the Windsor Group that accumulated in the remnant relief above Horton fault blocks. The near-top Windsor C325 maker, carried above salt diapirs in the Sydney basin, lies just below the deepest penetrated strata in the North Sydney wells. The C325 marker is overlain by a folded shallow-marine to continental-fluvial-lacustrine succession of the Mabou Group, accommodated in part through expulsion of underlying Windsor evaporites (see also Figure 10 for a similar situation on the southern Grand Banks). The succession passes upwards into Pennsylvanian strata that include braided to meandering fluvial sandstones in the Morien Group (that are gas-charged in the North Sydney wells), and alluvial deposits of red mudstones and sandstones of the late Pennsylvanian to early Permian Pictou Group that is capped by the C300 marker (Kendell et al. 2017, and references therein). Though Late Carboniferous loading of underlying Windsor units probably initiated salt expulsion, the east-west orientation of folds and lack of thinning above some fold crests, suggests some of these folds formed during inversion that took place in the Permian or later, in resp-

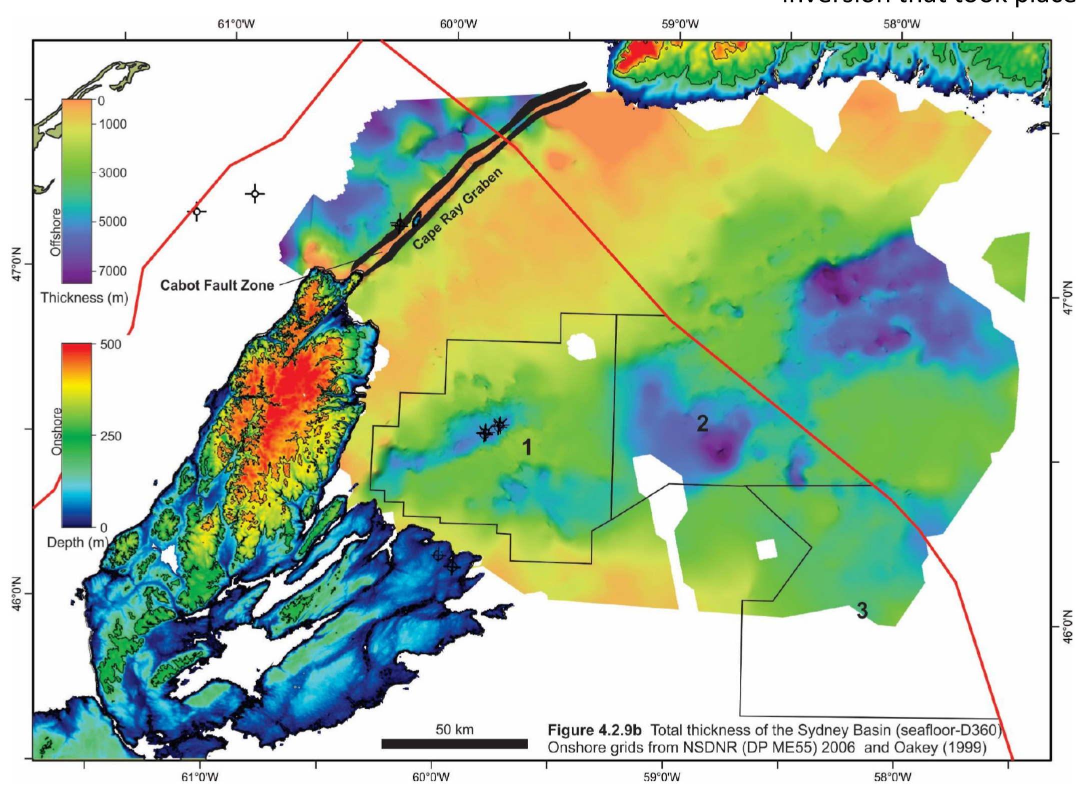


**Figure 12.** Total sediment thickness of the Sydney Basin (from seafloor to top Basement) (from Kendell et al. 2017)

onse to strike-slip and/or reverse reactivation along older Acadian faults (Kendell et al. 2017).

## Potential Reservoirs and Risking

Reservoir expectations in each of the six regions defined in this study vary both spatially and in different stratigraphic intervals. Four main potential reservoir intervals are discussed below: (i) Late Paleozoic clastics and carbonates; (ii) Middle to Upper Jurassic clastics and carbonates; (iii) Lower to middle Cretaceous clastics; and (iv) Upper Cretaceous to Paleogene chalks.

### *Late Paleozoic*

Reservoir distribution is poorly understood in region F. Both carbonates and siliciclastics could form viable reservoirs in Carboniferous strata, and in similar(?) successions in locally preserved remnants of Carboniferous basins in region A (e.g. Figure 5). Beneath Windsor Group rocks, sandstone units of the Horton Group are potential reservoirs, with Horton shales potentially serving as intra-formational seals for this play.

The Horton Group was not penetrated by the Sydney Basin wells but is a proven reservoir elsewhere in the Maritimes basin, often needing reservoir stimulation. There is onshore oil and gas production at the Stoney Creek field and gas production at the McCully field, both in New Brunswick. While the Horton sandstones have generally low to fair porosities they are able to achieve commercially viable production rates by reservoir stimulation.

The Windsor Group's Gays River Formation reefs may also be a potential reservoir for Horton generated hydrocarbons. These reefs would be localised, and potentially difficult to identify on the current seismic data. No carbonate reefs were encountered in the two wells but are inferred to be present in the basin. Onshore, these reefs are common where the Gays River Formation oversteps basin bounding topography.

Above Windsor and Horton group strata, both North Sydney wells have proven gas charge in Late Carboniferous fluvial sandstones. In the North Sydney F-24 well, two zones of the South Bar and Mabou formations were acidized and fractured in an attempt to flow gas to the surface. Porosity in the tested South Bar interval ranged of from 4 – 12%, with most values below 10%. Average porosity in a five meter sand in the Mabou Formation was 11%, but it did not flow when tested. The Sydney Mines, South Bar and Mabou formations appear to contain more porous sandstones in the P-05 well, though these intervals were not flow-tested. While gas-charge zones in the Sydney Basin wells appear to have poor reservoir properties (average net pay porosities all below 12%), the calculated net pay in these wells should be used with caution due the quality and vintage of available log data. The net pay assigned in this assessment allows for a somewhat more optimistic best case reservoir scenario (see Table 5), reflecting the potential for local reservoir improvements, sample bias, and uncertainties in data quality.

### *Mesozoic*

Reservoir distribution is better understood in the Scotian Basin, where regional seismic mapping, tied to wells, has shown clear patterns in the distribution and style of mid-Jurassic to Cretaceous shelf depositional systems and their linkage to sparsely calibrated deepwater strata (e.g. Cummings et al. 2005; 2006; Kendell and Deptuck 2012). We use the combination of sediment thickness (e.g. Figure 7), sharply contrasting seismic facies (e.g. Figures 9, 11, 13, 14), and limited well results, to help guide reservoir expectations and risking (Figure 17).

#### *Middle to Late Jurassic*

The most important Middle to Upper Jurassic reservoirs are likely to be associated with carbonates in region C and siliciclastics in regions B, D, and E. Of these areas, the thickest successions are found in the eastern parts of region D and throughout region E (Figures 7, 9, 10). Here, shelf wells encountered a complex mixture of silciclastics and shallow marine carbonates corresponding to the Mic Mac Formation (Wade and MacLean 1990). These sediments prograded across the continental shelf, starting in the Callovian, continuing intermittently through to the Tithonian (Deptuck et al. 2014). Calcite and/or silica cementation in some shelf wells has led to poor porosity preservation, increasing geological risk for potential Jurassic reservoirs in regions D and E.

There is no direct well calibration for Middle to Upper Jurassic strata on the slope in regions D and E, and reservoir expectations within the BSW on the slope are uncertain (Figures 6f, 9i). The only deepwater wells that calibrate the J163 to J145 interval are located on the sediment-starved slope of region C, more than 350 km to the southwest. Cheshire L-97/L-97A drilled by Shell in 2015 encountered mainly calcareous shales, marlstones, and limestone, on the slope seaward of the sediment-starved Jurassic carbonate bank (see Deptuck and Kendell 2020). As such, Cheshire is unlikely to be representative of the substantially thicker time-equivalent strata on the eastern Scotian Slope. For example, the long-term sedimentation rate for Callovian to Tithonian strata in Cheshire L-97/L-97A (~605 m section) is roughly 4 cm/ky, whereas the equivalent section beneath the Tantallon M-41 well (not penetrated, but nicely imaged on PSDM seismic profiles) is 4300 m thick, yielding a much higher sedimentation rate of ~28.7 cm/ky (without accounting for compaction). In fact, the eastern Scotian Slope records the thickest Middle to Upper Jurassic strata anywhere along the Scotian margin (Deptuck and Kendell 2017), and as such is likely to contain a significant siliciclastic component in region E and the eastern parts of region D (Figures 7, 9, 10).

Shallow marine carbonates may have preferentially accumulated on the shelf during periods of high sea level with siliciclastics and perhaps resedimented carbonates preferentially accumulating on the slope during periods of low sea level. The strong, continuous "hard" reflections (downward increase in impedance) within the BSW may correspond to impedance contrasts between thicker carbonates (pelagic or resedimented) and siliciclastics (Figures 7i, 9i, 11i). They could also correspond to calci-clastic submarine fans shed from the mixed clastic-carbonate systems on the shelf. Secondary porosity development could improve the reservoir potential of some deeply buried carbonates, but this too carries a high degree of uncertainty.

*Lower to middle Cretaceous*

The most prolific proven gas, condensate, and oil reservoirs in the Scotian Basin are Lower Cretaceous fluvial-deltaic to shoreface sandstones of the Missisauga and Logan Canyon formations, penetrated in numerous shelf wells in regions D and E (Cummings and Arnott 2005; Smith et al. 2014). The presence of fluvial-deltaic systems on the shelf, particularly those deposited during periods of forced regression, favour reservoir development on the slope (Jermannaud et al. 2023; Scotian Basin Integration Atlas 2023). The Crimson, Annapolis, Newburn, and Aspy wells in the distal Sable Subbasin (region D) all encountered turbidite reservoirs with average net pay porosity ranging from 14 to 19% (Kidston et al. 2007; Kendell et al. 2016; Kendell and Deptuck 2020). All but Crimson also encountered significant gas/condensate shows (Table 3). Likewise, the scarcity of reservoirs in the Cheshire and Monterey Jack wells in the Shelburne Subbasin (region C) is consistent with the absence of Lower Cretaceous fluvial-deltaic systems on the shelf (Figure 7ii). It is also consistent with the much thinner sediment accumulation on the shelf and slope in region C compared to regions D and E (Figure 9, 11, 13, 14), resulting in significant temporal and spatial variations in reservoir risking (see Figure 17).

The complicated salt tectonics in the Sable Slope Canopy of region D significantly hinders finer-scale seismic interpretation, especially for Cretaceous strata below salt. The absence of salt overhangs above Cretaceous slope strata in region E, however, makes more detailed

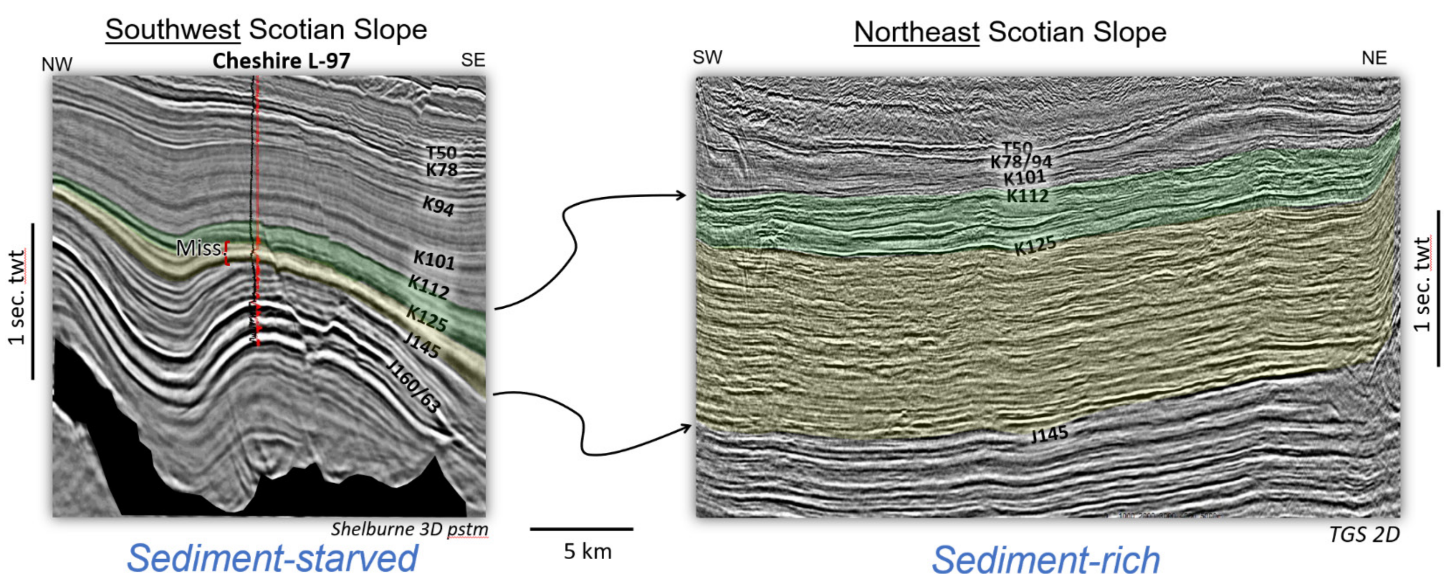


**Figure 13.** Comparison of Lower Cretaceous sediment thickness on the slope at Cheshire L-97 in region C and a representative seismic section from the slope in region E. See Figure 9 for line location.

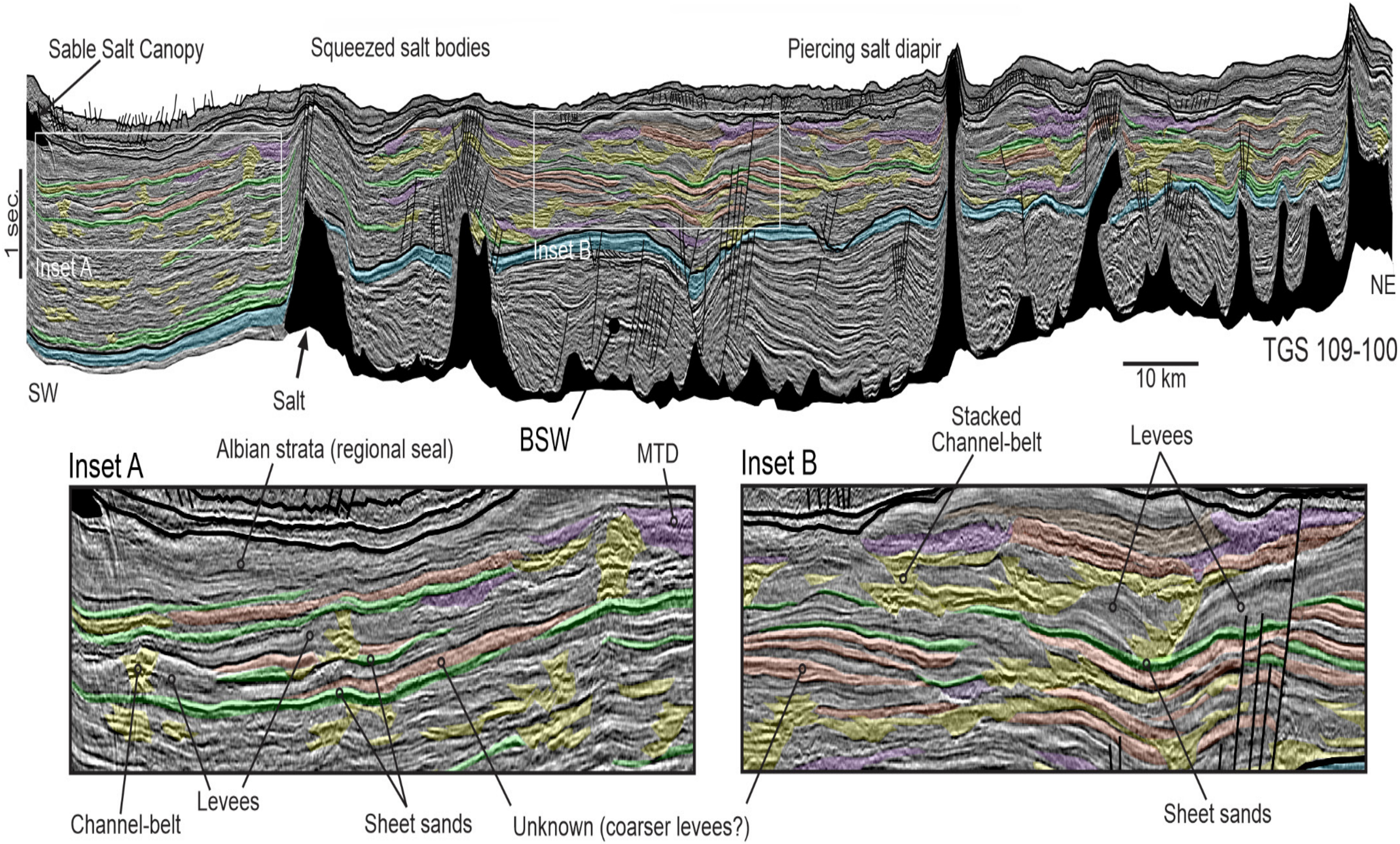


**Figure 14 (top)** Representative strike-oriented 2D seismic profile across the "Banquereau Synkinematic Wedge" (BSW), colour coded to show the different Cretaceous deepwater seismic facies recognized in region E. To a lesser extent these seismic facies can also be correlated under and above the Sable Slope Canopy in region D. Insets show close-up view of sand-prone channel-belts (yellow) flanked by levees, with potential sheet sands corresponding to lobe deposits identified in green. Orange identifies potential bottom-current reworked levee or lobe deposits, and blue identifies approximate Cretaceous-Jurassic boundary. See Figure 7 for line location (easternmost profile in Figure 9).

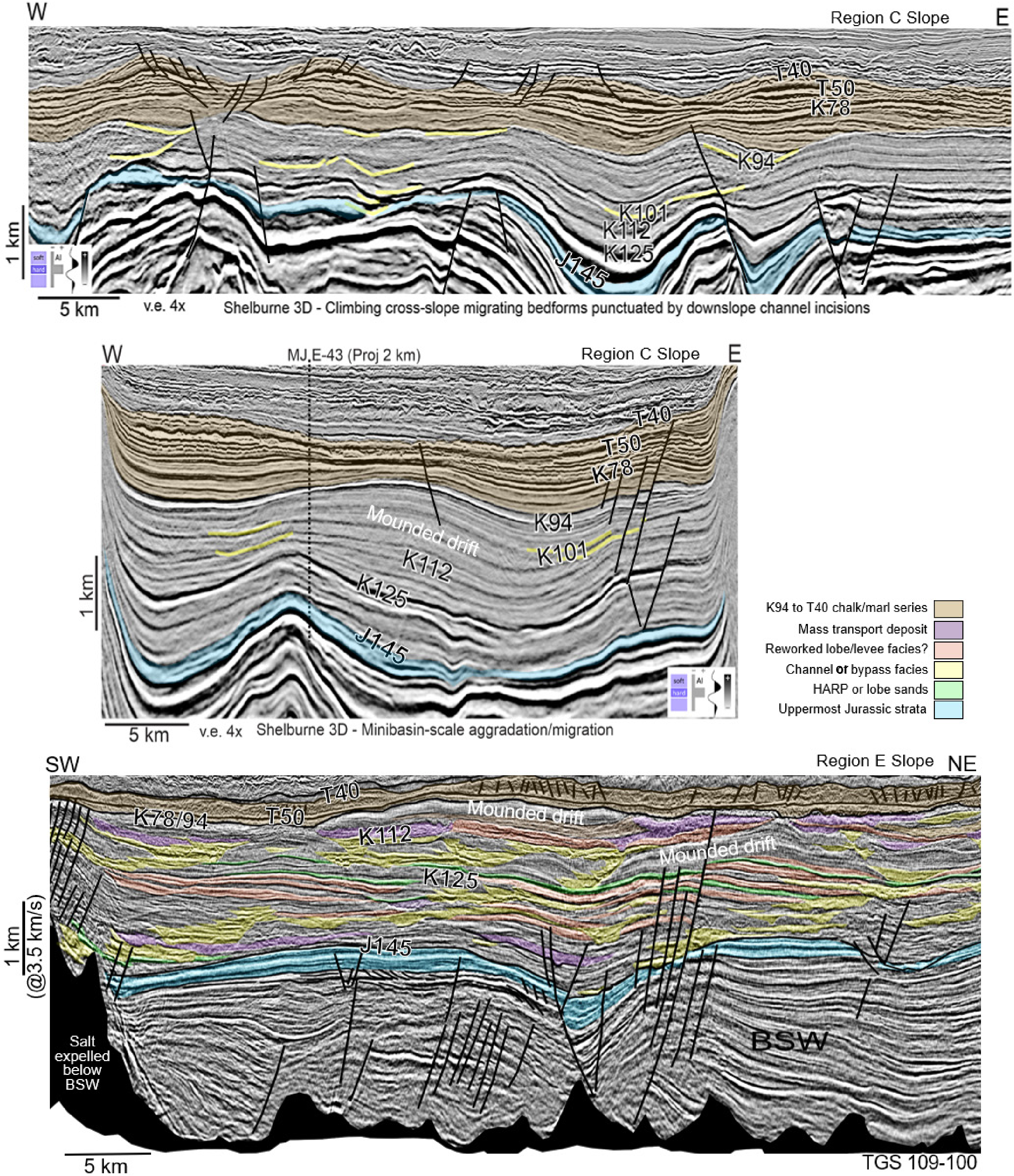


**Figure 15.** Stratal architectures associated with unidirectional migration of slope strata in both sediment-starved (top two images) and sediment-rich slope segments (bottom image). Condensed strata in region C (Shelburne Subbasin) are strongly influenced by bottom current reworking, with only minor indications that coarser clastics accumulated anywhere but along single-loop soft reflections along channel axes (yellow); (**upper image**) upper slope near Cheshire and (**middle image**) middle slope near the Monterey. **(bottom)** – Closeup of seismic profile across the middle slope in region E, where much more complex seismic facies are recognized, believed to be associated with bottom current reworking of a slope with frequent down-slope sediment transport. Location shown in Figure 9.

seismic facies analysis possible. Loop-scale interpretations reveal clear differences is seismic facies in region E compared to region C (Figures 13, 14, 15). Seismic facies are generally more complex on the eastern Scotian Slope, with laterally discontinuous clusters of bright and dim reflections. Some bright amplitude reflections can be correlated up to 70 km down the slope on 3 to 6 km spaced 2D seismic profiles, forming elongated curvilinear corridors. They are interpreted as 2 to 4 km wide sand-prone submarine channel-belts (yellow transparency in Figures 14) flanked by lower amplitude muddy wedge-shaped overbank deposits. Several of these channel-levee systems continue landward, beneath the Sable Slope Canopy in region D, where poor subsalt seismic imaging precludes mapping. They imply sediment was transported both through the Sable canopy system in region D and down the slope further east in region E.

Tantallon M-41 – the only well to sample slope strata in region E (and the only slope well east of Crimson) – encountered just ~10 m of gas charged sands in Lower Cretaceous slope strata (Goodway et al., 2008). Conventional cores from the well, however, show hundreds of stacked sharp-based thin-bedded turbidites composed of very fine-grained to medium-grained sandstone (Figure 16; see Piper et al. 2010). These sedimentary structures are consistent with fine-grained turbidites deposited on levees adjacent to submarine channels (e.g. Piper and Deptuck 1997). Likewise, more recently acquired 3D seismic data (Stonehouse 3D survey) shows that the upper slope immediately east of Tantallon consists of numerous narrower channel-belt corridors (see Goodway et al. 2008), rather than widespread sheet-sands. This may indicate that the limited reservoir development at Tantallon M-41 reflects poor well positioning relative to the location of sand-prone channel-belts, rather than the wholesale absence of deepwater reservoirs on the slope in region E.

Further seaward, channel-belts increasingly interfinger with more continuous bright amplitude, occasionally shingled, soft reflections (downward decrease in impedance), identified in green in Figures 14 and 15. They range from 10 to 15 km wide, up to 33 km long, and can cover areas up to 290 km$^2$. Their distribution and character are consistent with submarine lobe “sheet sands” deposited at the mouths of aggradational submarine channels or in response to channel-levee avulsions. Based on these observations, we anticipate some lateral confinement of turbidite channel corridors on the upper slope (i.e. where Tantallon M-41 was drilled), with a progressive downslope decrease in confinement where more laterally continuous turbidite sands were deposited in the deepwater parts of regions D and E (see also Piper and Normark 2001).

Some of the complicated stratigraphic architectures in Figures 14 and 15 are probably the consequence of synchronous bottom current reworking as Cretaceous sediment was exported from the shelf and down the slope (Deptuck and Kendell 2020; Rodriguez et al. 2022). Up-current, “unidirectional” migration of deepwater deposits are increasingly recognized as products of sustained bottom current reworking (e.g. Gong et al. 2013; Fonnesu et al. 2020). The stratigraphic architecture of sediment-starved slope segments (like region C) is dominated by condensed strata displaying unidirectional migration (Figures 13, 15). In contrast, the stratigraphic architecture of sediment-rich slope segments (like regions D and E), is more variable, with many channel-levee systems showing unilateral migration (on the upper slope; e.g. Inset B), and other’s not (e.g. inset A, Figure 14). This might reflect the increased terrigenous supply in regions D and E that can interrupt, mask, or bury geomorphic products associated with sustained bottom current reworking (see comparison in Figures 9, 13, 14). Whether such bottom current reworking ultimately degrades or improves reservoir properties is not yet clear, but they are a noteworthy complication compared to more traditional turbidite systems.

*Upper Cretaceous to Paleogene*

Like the Jeanne d’Arc Basin on the Grand Banks, and in the North Sea, Cenomanian to Eocene strata in the Scotian Basin include widespread pelagic chalk accumulations that have potential to form hydrocarbon reservoirs. For example, the Eagle gas discovery on the shelf of region D consists of 52 m of net gas pay in porous Upper Cretaceous chalks of the Wyandot Formation (in the Sable Subbasin). Likewise, 50 m of net gas pay was found in Wyandot chalks folded above a salt diapir in the Primrose Significant Discovery (Smith et al. 2014). Although neither of these were commercial developments, they demonstrate that chalks can form hydrocarbon reservoirs in Nova Scotia’s offshore. The chalk series is located mainly between the K94 and T40 markers. In deepwater, the succession is thickest along

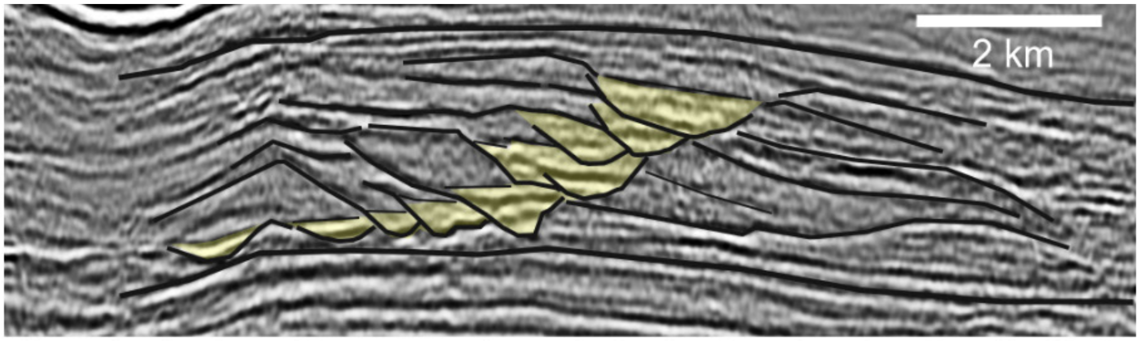


Example of a channel-levee system located a few km downslope from Tantallon M-41

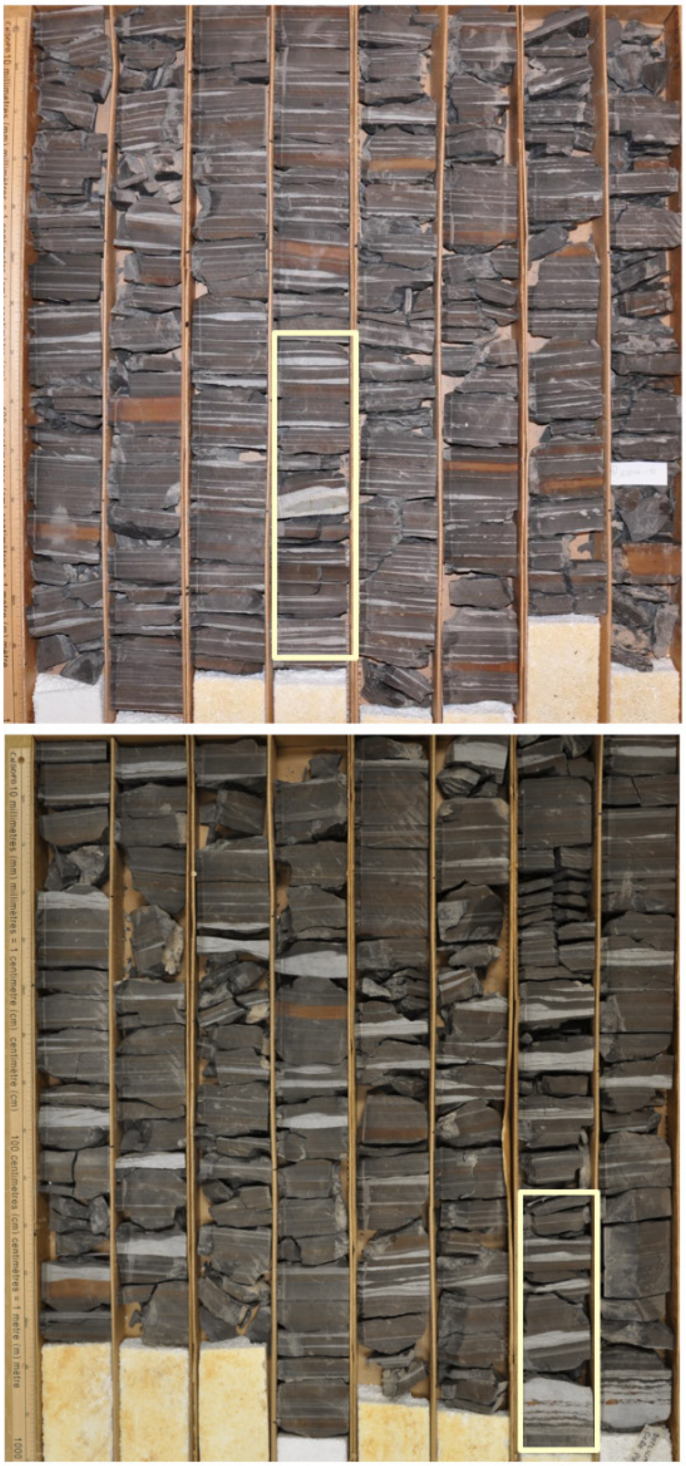

Fine grained, thin-bedded levee turbidites, capped by bottom current reworked starved ripples

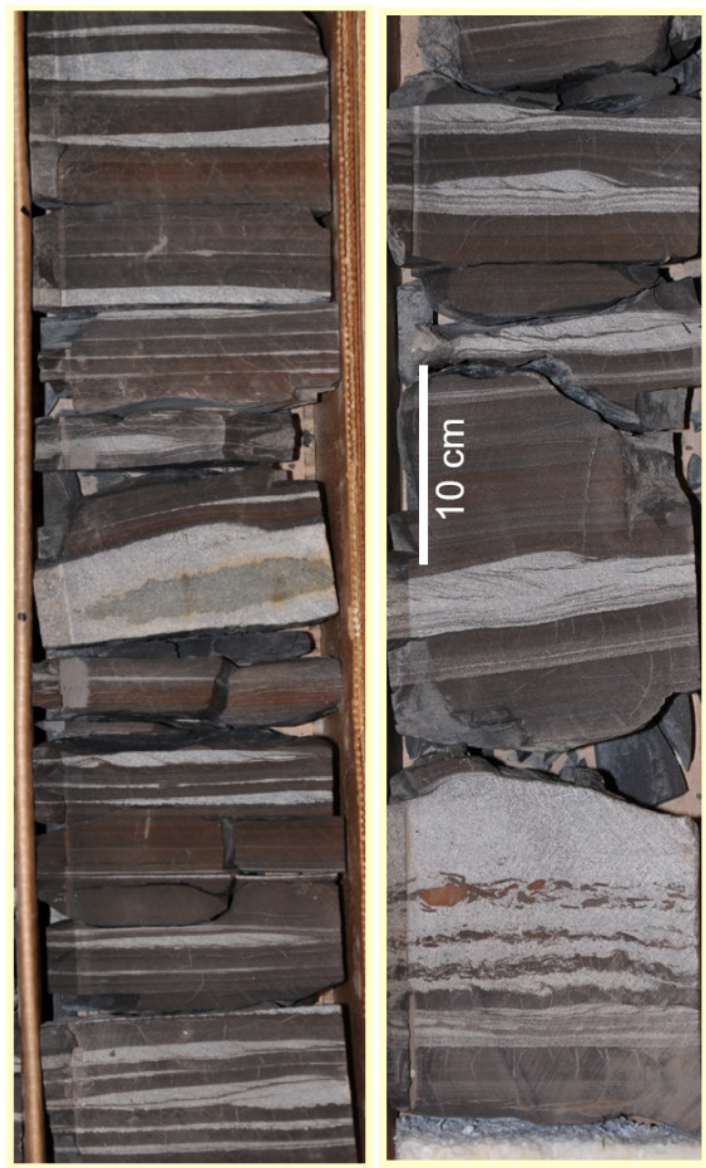


**Figure 16 (top)** Representative seismic profile across a unidirectionally migrated channel-levee system seaward of the Tantallon M-41 well location (seismic imaging is poor at the well location). We infer that the well missed the more sand-prone channel corridors, and instead sampled mainly inter-channel overbank deposits. Core photos (bottom) support this interpretation, showing hundreds of stacked fine-grained turbidites diagnostic of levee depositional settings.

the western parts of the margin (regions B and C), and comparatively thin in region E on the eastern Scotian Slope. On the shelf, the Wyandot Formation chalks are thickest in region E (see Figures 7iv, 9iv, 11iv). The generally low matrix permeability of chalk reservoirs remains a key risk element of Upper Cretaceous to Paleogene chalks, however these reservoirs may be able to achieve commercially viable production rates if stimulated by fracking. Resedimented chalks appear to form more favourable, higher permeability reservoirs, though many complex factors affect reservoir quality (Megson and Tygesen 2005). Although there is strong evidence for sediment failures involving chalks on the shelf where 3D seismic is available (in the Sable Subbasin; Smith et al. 2010), the associated mass transport deposits may be mixed with other sediment types (like shale from coeval prodelta clinoforms). This also applies to the widespread Montagnais mass transport deposit (see Figure 11) that was triggered by the Early Eocene Montagnais bolide impact on the western Scotian Shelf (Deptuck and Campbell 2012; Deptuck and Kendell 2020). It undoubtedly contains resedimented pelagic carbonates, but with significant uncertainty about its overall composition and viability as a hydrocarbon reservoir.

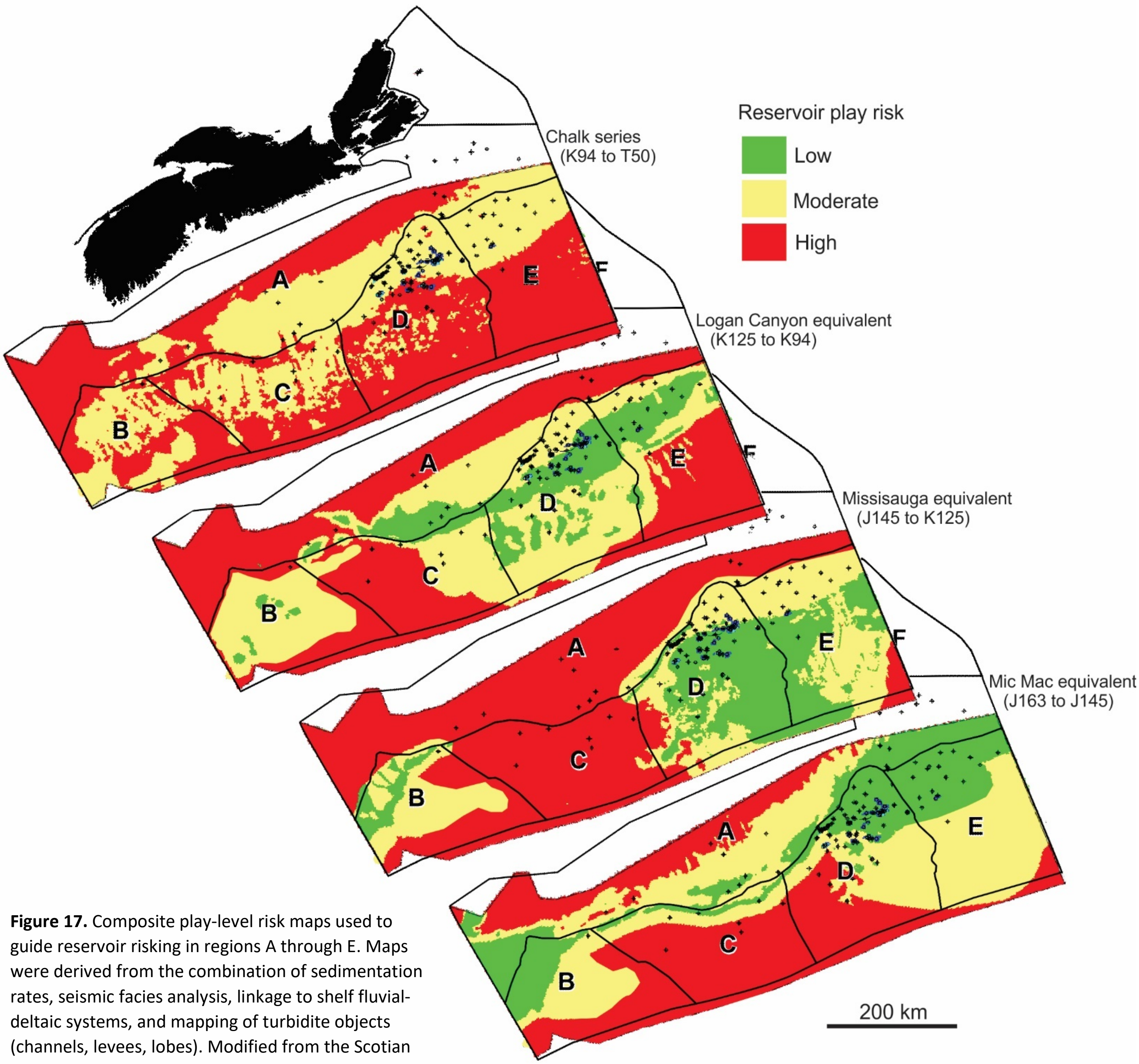


**Figure 17.** Composite play-level risk maps used to guide reservoir risking in regions A through E. Maps were derived from the combination of sedimentation rates, seismic facies analysis, linkage to shelf fluvial-deltaic systems, and mapping of turbidite objects (channels, levees, lobes). Modified from the Scotian Basin Integration Atlas (2023).

## Potential Source Rocks and Risking

### *Regions A to E*

Figure 18 shows the composite play-level risk map used to guide source rock risking in regions A to E. At the play level, risking considers both the presence and maturity of source rocks. One proven source rock interval (Tithonian) and one potential source rock (Pliensbachian) contribute to this map. Most of the discovered hydrocarbons along the Scotian margin have been tied to Tithonian-Kimmeridgian Mic Mac/Verrill Canyon Formation deltaic shales containing a mix of Type II to III organic matter (Fowler 2020). Up to 5% TOC type II to III source rocks were encountered in a 250 m thick interval of Tithonian strata at Louisbourg J-47 in region E (OETR 2011). They are interpreted to be linked to the ample supply of terrigenous material to the slope in the Upper Jurassic. As such, the Upper Jurassic thickness map was used as a guide, with green areas corresponding mainly to regions D and E where Upper Jurassic strata are thickest and petroleum system modelling shows it is mature. These are also areas where wells have encountered trapped gas, condensate, or oil.

There has also been speculation about a deeper oil-prone Lower Jurassic source rock along the Scotian margin (OETR 2011; Bishop 2020) and southern Grand Banks (Fowler 2019). Geochemical typing of oil samples in wells along the rift-shoulder (e.g. Mic Mac J-77) provide the closest evidence for a deeper (Lower Jurassic?) marly restricted-marine source rock (Fowler 2020), but it has not been demonstrated to extend onto the slope. Any leads on the slope in regions B or C require this older source rock because Tithonian strata are unlikely to be mature in these areas. If a Lower Jurassic source rock is present beneath the eastern Scotian Slope, its deep burial depth probably means it is overcooked and gas-prone. Yellow areas on the map (Figure 18) correspond to regions where the Tithonian source rock interval is only marginally mature, or where a deeper Lower Jurassic source rock, if present, is likely to be mature (see Scotian Basin Integration Atlas 2023). At the prospect level, source risking includes consideration of expulsion timing and charge access. For example, Lower Jurassic strata are absent in some areas, with thickness maps forming bulls-eye “pods” associated with sedimentation in early minibasins (see Deptuck 2020). Likewise, some plays lie above allochthonous salt, while the source rock lies below – both scenarios may create charge access challenges for traps above salt.

### *Other potential Mesozoic source rocks*

The deepwater equivalent of the Callovian shale-prone Misaine Member has also been proposed as a potential source rock (OETR 2011). A section with elevated TOC up to 1.24% was encountered at Cheshire L-97/L-97A – the only well to penetrate this interval on the Scotian Slope (SW of the Sable Subbasin) – but the interval is too thin to source significant volumes of hydrocarbons (Fowler 2019). Given that the BSW records the much higher Callovian to Tithonian sedimentation rates (605 m of strata at Cheshire L-97/L-97A versus > 4,000 m of strata in the BSW), a Callovian source rock with elevated intervals of terrestrial-derived organic matter is more likely to be present on the eastern Scotian Slope, if anywhere. The onset of the BSW on the slope has been linked to a period of hinterland erosion and abrupt seaward progradation above the Scatarie Member on the eastern Scotian Shelf (Deptuck et al. 2014), placing terrestrial-derived organic matter at deeper stratigraphic levels within the BSW. The dominance of terrestrial-derived organic matter in these potential clastic source rocks suggests they are likely to be gas- and condensate-prone throughout regions D and E.

Brown (2014; 2015) suggested that lacustrine oil-prone source rocks could also be present in the deeper, unsampled fill of Triassic rift basins off Nova Scotia. Similar lacustrine source rocks are known to be present in Mesozoic rift basins exposed on land in the northeastern United States. They formed at more humid paleo-latitudes that favoured the accumulation of lacustrine source rocks (Olsen 1985; Post and Coleman 2015). Off Nova Scotia, older Carnian strata may have accumulated at similar paleolatitudes, within or immediately adjacent to the tropic belt, in wet climatic conditions more favourable for the creation (and preservation) of organic matter in long lived lakes (Brown 2014).

The absence of source rock intervals in Sambro I-29 (the only well to test the pre-salt synrift succession west of Orpheus Graben), however, makes this interpretation challenging for the early synrift strata on the LaHave Platform, unless the red beds it encountered are not representative of basinal early syn-rift depositional environments (Deptuck and Altheim 2018). We should note that the well did not reach basement, so the composition of earliest syn-rift successions remain unknown. Other source rock intervals may be more likely. A number of oil, condensate, and gas discoveries have been made in similar rift basins in Morocco (e.g. Meskala field; Morabet et al. 1998; Mader et al. 2017), which was contiguous with the LaHave Platform before the Atlantic Ocean formed. In these basins, pre-rift successions (Silurian or Carboniferous) are the most likely source intervals for hydrocarbons in Triassic syn-rift fluvial reservoirs rotated above basement blocks, in turn sealed by late syn-rift salt (Tari et al. 2017).

### *Late Paleozoic source rocks*

Based on source rocks present in onshore areas of Nova Scotia and New Brunswick (see Langdon and Hall 1994, and Dietrich et al. 2011, and references therein), the offshore Sydney Basin (region F) also has numerous potential Carboniferous source rock intervals. The lowest source rock risk is found in areas where both Horton Group lacustrine source rocks and Windsor Group McCumber marine carbonate source rocks are possible (Figure 18; Kendell et al. 2017).

The lacustrine shales of the Horton Formation, as sampled from onshore Nova Scotia basins, are oil-prone with type I and type II signatures and TOC averaging 6%. (Fowler and Webb 2017). The lowermost section of the marine Windsor sequence contains organic-rich intervals of the McCumber Formation. Samples of this interval from onshore wells suggest TOC ranging from 1.2 to 2.6%. (Mossman 1992; Fowler and Webb 2017). Minor contributions may also be expected from the organic shales of the Mabou Group, and the widespread coal measures present in the Sydney Mines Formations penetrated in a number of offshore core holes (see Shimeld and Deptuck 1998). Table 5.1 of Kendell et al. 2017 provides a thorough summary of the potential source rock intervals, their thickness, depositional environment, TOC and hydrogen index within Sydney Basin.

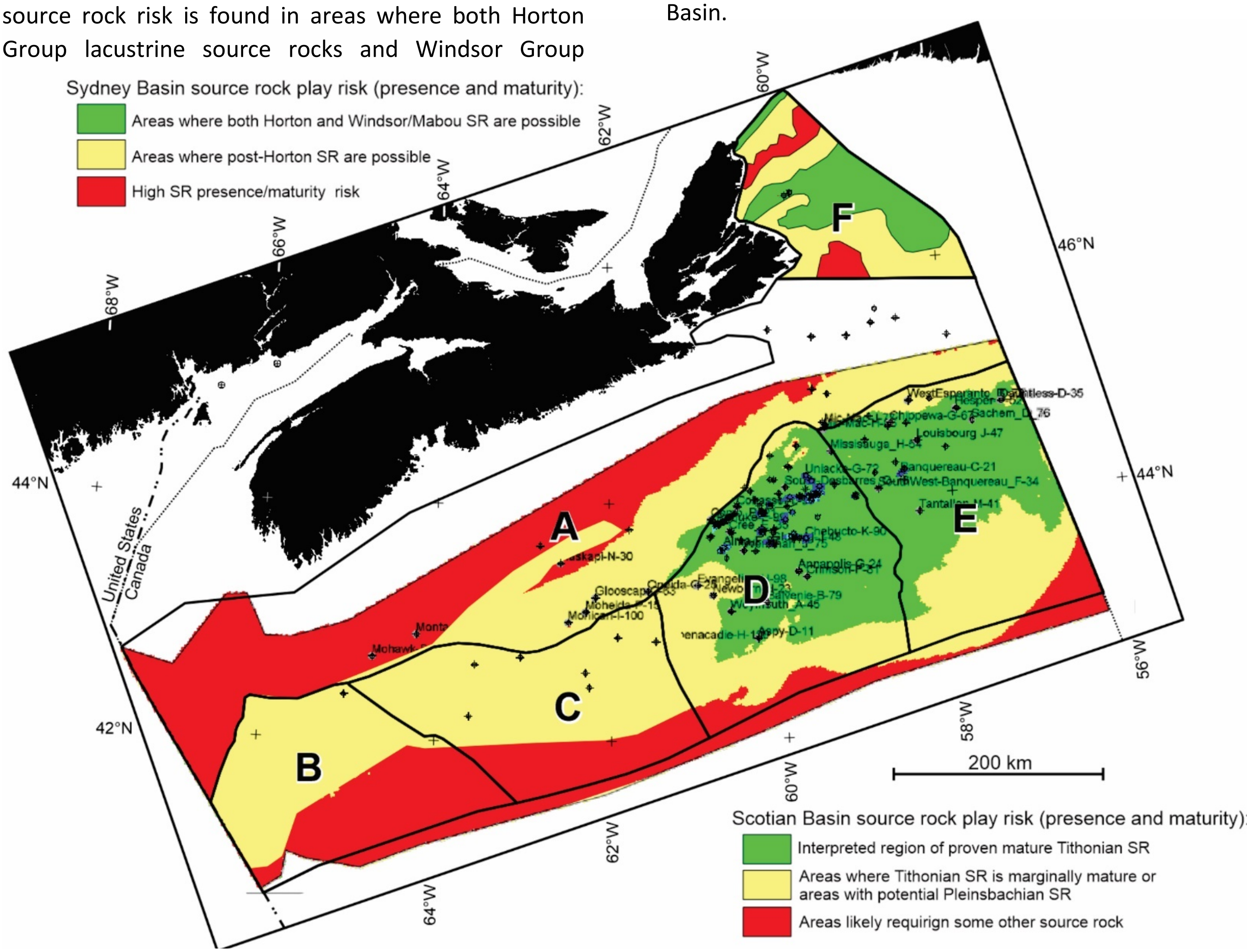


**Figure 18.** Composite play-level risk map used to guide source rock presence and maturity in regions A to E. At the prospect level, risking also includes consideration of hydrocarbon migration challenges (e.g. some plays lie above allochthonous salt, which could impede migration of hydrocarbons from sub-salt source rocks. Modified from the Scotian Basin Integration Atlas (2023).

## Play-type definition

Each geographic region contains between three and twelve play types, for a total of 44 plays (Table 5). The total area for each of the 44 play types was determined using geological knowledge derived from well data and regional reflection seismic mapping, to constrain areas where a specific play type could exist (for example, 'a supra-canopy turtle' can only exist where there are minibasins above salt canopies). Each play types may be present in more than one geographic area, though potentially with different associated play and prospect level geologic risk. The proportion of a given play area 'under trap' was determined individually for each play type in each geographic region, primarily from cumulative lead mapping on depth-converted regional seismic surfaces, then summing the areal trap coverage for a given play type in each region. Because there is some overlap in play types (e.g. a salt-cored fold trap that is also pierced by a salt diapir with potential three closure), a high degree of care was taken to avoid 'double-booking' any of the play types and associated area under trap. Seismic markers were gridded at 200 x 200 m spacing, and depth-converted using the velocity model in Appendix 5 of the Scotian Basin Integration Atlas (2023) for regions A to E, and the velocity model of Kendell et al. (2017) for region F. In most cases a +/-10 to 20% error bar was used to account for gaps in seismic data coverage or uncertainties associated with depth conversion. Larger error bars (up to 30%) were used for a small number of play types with larger trap size uncertainty, like sub-canopy cut-off traps or stratigraphic onlap traps that are more subtle in nature.

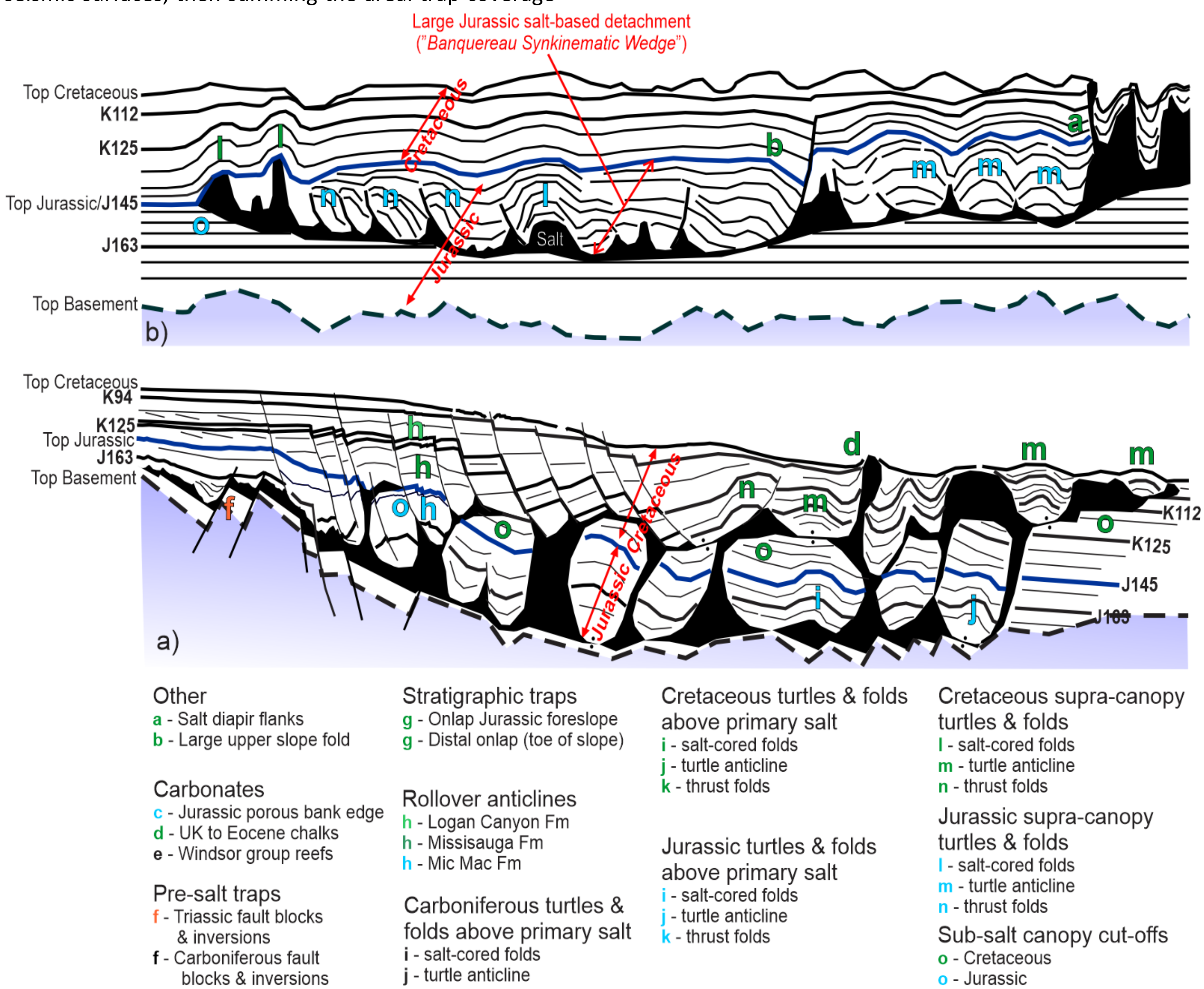


**Figure 19.** Schematic strike (top) and dip (bottom) sections showing examples of the range of potential traps on the Scotian shelf and slope. Green colours correspond to Cretaceous traps, blue to Jurassic traps, orange to Triassic traps, and black to Carboniferous traps.

**Table 5.** Key input parameters for each play type across the six geographic regions included in this study.

| | Discount Play Area (P100/P50/P0) | | | Net Reservoir (P100/P50/P0) | | | Porosity (P100/P50/P0) | | |
|---|---|---|---|---|---|---|---|---|---|
| **A. LaHave Platform** | | | | | | | | | |
| **a.** Pre-salt Triassic syntectonic rotated fault blocks & inversions | 506 | 625 | 756 | 10 | 15 | 30 | 0.1 | 0.18 | 0.22 |
| **b.** Carboniferous(?) post-Windsor turtles | 94 | 131 | 173 | 5 | 10 | 30 | 0.1 | 0.14 | 0.18 |
| **c.** Carboniferous(?) pre-Windsor fault blocks & inversions | 164 | 203 | 245 | 5 | 10 | 30 | 0.1 | 0.14 | 0.18 |
| **d.** Cretaceous fault rollovers and forced folds | 401 | 1002 | 1323 | 10 | 20 | 50 | 0.1 | 0.2 | 0.26 |
| **B. West Shelburne Corridor** | | | | | | | | | |
| **a.** Pre-salt Triassic syntectonic rotated fault blocks & inversions | 146 | 203 | 267 | 10 | 15 | 30 | 0.1 | 0.18 | 0.22 |
| **b.** Jurassic listric fault rollovers (shelf) | 329 | 514 | 740 | 10 | 20 | 60 | 0.08 | 0.14 | 0.18 |
| **c.** Cretaceous listric fault rollovers (shelf) | 235 | 367 | 529 | 10 | 20 | 60 | 0.1 | 0.18 | 0.22 |
| **d.** Upper Jurassic Subsalt canopy cutoff | 90 | 141 | 337 | 5 | 15 | 30 | 0.08 | 0.14 | 0.18 |
| **e.** Cretaceous stratigraphic onlap traps (landward & seaward) | 477 | 745 | 984 | 5 | 15 | 30 | 0.1 | 0.18 | 0.22 |
| **f.** Cretaceous three-way traps on diapirs flanks | 265 | 369 | 531 | 5 | 15 | 30 | 0.08 | 0.18 | 0.22 |
| **g.** Chalk Play - closures at T50 | 439 | 609 | 737 | 10 | 25 | 60 | 0.15 | 0.2 | 0.25 |
| **C. Shelburne Corridor** | | | | | | | | | |
| **a.** Pre-salt Triassic syntectonic rotated fault blocks & inversions | 201 | 279 | 369 | 10 | 15 | 30 | 0.1 | 0.18 | 0.22 |
| **b.** Jurassic porous carbonate bank edge ("Acadia segment") | 115 | 255 | 337 | 10 | 50 | 100 | 0.04 | 0.1 | 0.24 |
| **c.** Jurassic slope turtles & folds (above primary salt) | 244 | 509 | 672 | 5 | 10 | 30 | 0.08 | 0.14 | 0.18 |
| **d.** Cretaceous slope turtles & folds (above primary salt) | 407 | 637 | 840 | 5 | 15 | 20 | 0.1 | 0.18 | 0.22 |
| **e.** Cretaceous stratigraphic onlap traps (carbonate foreslope) | 312 | 488 | 751 | 5 | 15 | 20 | 0.1 | 0.18 | 0.22 |
| **f.** Cretaceous three-way traps on diapirs flanks | 504 | 700 | 924 | 5 | 15 | 20 | 0.1 | 0.18 | 0.22 |
| **g.** Chalk Play - closures at T50 | 1344 | 1867 | 2259 | 10 | 25 | 60 | 0.15 | 0.2 | 0.25 |
| **D. Abenaki-Sable Corridor** | | | | | | | | | |
| **a.** Pre-salt Triassic syntectonic rotated fault blocks & inversions | 171 | 238 | 393 | 10 | 15 | 30 | 0.1 | 0.2 | 0.24 |
| **b.** Upper Mic Mac to Missisauga listric fault rollovers & folds | 829 | 1295 | 1865 | 10 | 40 | 80 | 0.08 | 0.16 | 0.22 |
| **c.** Logan Canyon listric fault rollovers & folds | 657 | 1026 | 1477 | 10 | 30 | 60 | 0.14 | 0.2 | 0.26 |
| **d.** Jurassic porous carbonate bank edge ("Panuke segment") | 90 | 140 | 202 | 10 | 50 | 100 | 0.04 | 0.1 | 0.24 |
| **e.** Upper Jurassic to Cretaceous strat onlap traps (foreslope) | 31 | 125 | 280 | 10 | 15 | 30 | 0.08 | 0.16 | 0.22 |
| **f1.** Upper Jurassic subsalt canopy cut-off (shelf) | 95 | 148 | 267 | 10 | 15 | 30 | 0.08 | 0.14 | 0.18 |
| **f2.** Cretaceous subsalt canopy cut-off (slope) | 573 | 1432 | 2578 | 15 | 30 | 60 | 0.1 | 0.18 | 0.22 |
| **g.** Jurassic slope turtles & folds (above primary salt) | 536 | 837 | 1205 | 10 | 20 | 40 | 0.08 | 0.14 | 0.18 |
| **h.** Cretaceous slope turtles & folds (above primary salt) | 694 | 1085 | 1562 | 10 | 30 | 60 | 0.1 | 0.18 | 0.22 |
| **i.** Cretaceous supra-canopy turtles & folds | 954 | 1490 | 2146 | 10 | 30 | 60 | 0.1 | 0.18 | 0.22 |
| **j.** Cretaceous three-way traps on diapirs flanks | 423 | 660 | 951 | 10 | 20 | 40 | 0.1 | 0.18 | 0.22 |
| **k.** Chalk Play - closures at T50 | 561 | 876 | 1262 | 20 | 40 | 60 | 0.15 | 0.2 | 0.25 |
| **E. Huron Corridor** | | | | | | | | | |
| **a.** Upper Jurassic listric fault rollovers (shelf) | 472 | 655 | 855 | 10 | 15 | 30 | 0.08 | 0.14 | 0.18 |
| **b.** Missisauga listric fault rollovers & folds | 614 | 960 | 1382 | 15 | 25 | 50 | 0.1 | 0.18 | 0.22 |
| **c.** Logan Canyon listric fault rollovers & folds | 691 | 1080 | 1555 | 10 | 20 | 40 | 0.14 | 0.2 | 0.26 |
| **d.** Upper Jurassic large upper slope folds | 654 | 1023 | 1472 | 10 | 20 | 40 | 0.08 | 0.14 | 0.18 |
| **e.** Cretaceous large upper slope folds (Stonehouse trend) | 768 | 1200 | 1729 | 15 | 30 | 60 | 0.1 | 0.18 | 0.26 |
| **f.** Jurassic supra-canopy turtles & folds (within BSW) | 448 | 701 | 1009 | 10 | 20 | 40 | 0.08 | 0.14 | 0.18 |
| **g.** Cretaceous supra-canopy turtles & folds (W. Laurent. canopy) | 162 | 253 | 364 | 15 | 30 | 60 | 0.1 | 0.18 | 0.26 |
| **h.** Cretaceous fold-belt (Banquereau foldbelt) | 642 | 1003 | 1444 | 15 | 30 | 60 | 0.1 | 0.18 | 0.26 |
| **i.** Cretaceous subsalt canopy cuttoff (West Laurentian canopy) | 50 | 125 | 225 | 15 | 30 | 60 | 0.1 | 0.18 | 0.26 |
| **j.** Cretaceous stratigraphic onlap traps (seaward of BSW) | 73 | 183 | 329 | 15 | 30 | 60 | 0.1 | 0.18 | 0.22 |
| **k.** Three-way closures on diapir flanks | 405 | 562 | 810 | 10 | 30 | 50 | 0.1 | 0.18 | 0.26 |
| **F. Sydney Basin** | | | | | | | | | |
| **a.** Horton fault blocks | 789 | 1972 | 3550 | 10 | 20 | 40 | 0.1 | 0.14 | 0.18 |
| **b.** Carboniferous inversion folds | 394 | 986 | 1775 | 10 | 20 | 40 | 0.1 | 0.14 | 0.18 |
| **c.** Windsor Reefs | 438 | 1096 | 1972 | 10 | 20 | 60 | 0.04 | 0.1 | 0.24 |

Other resource assessment input parameters such as net reservoir, porosity, water saturation, etc. were derived from available and analogous Nova Scotia offshore wells and reservoirs, as applicable. Plays in each region were risked at both the play level and prospect level, with the risking in each region treated as separate assessments. As such, a successful play in one region does not remove the play level risk in another region. Examples of different play types are show in Figures 19, colour coded for age and described in more detail below, with accompanying representative seismic profiles across different play types.

*Rotated/inverted fault blocks below primary salt* – Traps in this play type consists of rotated or inverted syn-rift pre-salt reservoirs (mainly fluvial) encased and sealed above by primary salt. The play exists only where there are rift basins that pass up-section into salt, and this scenario takes place in both Late Paleozoic and Early Mesozoic successions (Figure 14). The first play of this trap category exists in both region A and F, involving fault-offset mixed Horton Group clastics passing up-section into Carboniferous Windsor Group salt or carbonates (e.g. see Kendell et al. 2017) (e.g. Figure 21d). The second play within this trap category involves Triassic fluvial reservoirs of the Eurydice Formation sealed above by the Osprey/Argo primary salt layer (Figures 21a to c). This play is mainly restricted to the distal parts of rift basins in region A (including Orpheus Graben), and the landward parts of regions B, C, and D. The Muskat lead in region C falls into this category (see Deptuck 2020).

For either play type to work, a source rock within the pre-salt succession is required. This requirement is most easily met for Carboniferous strata, where potential source rocks are known in both the Horton and Lower Windsor group (Kendell et al. 2017). No source rocks have been identified in the study area within the Triassic Eurydice Formation (see Deptuck et al. 2015; Deptuck and Altheim 2018).

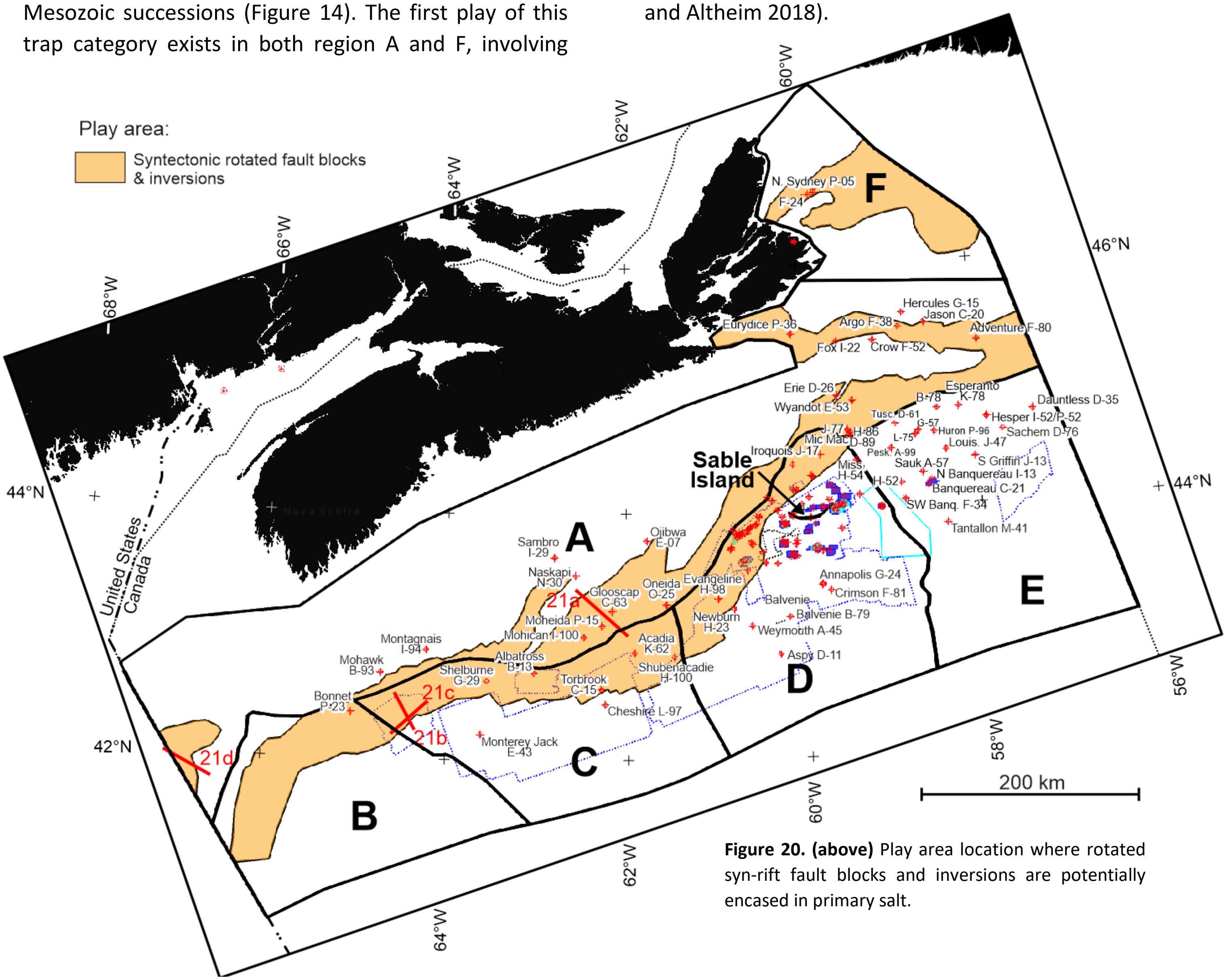


**Figure 20. (above)** Play area location where rotated syn-rift fault blocks and inversions are potentially encased in primary salt.

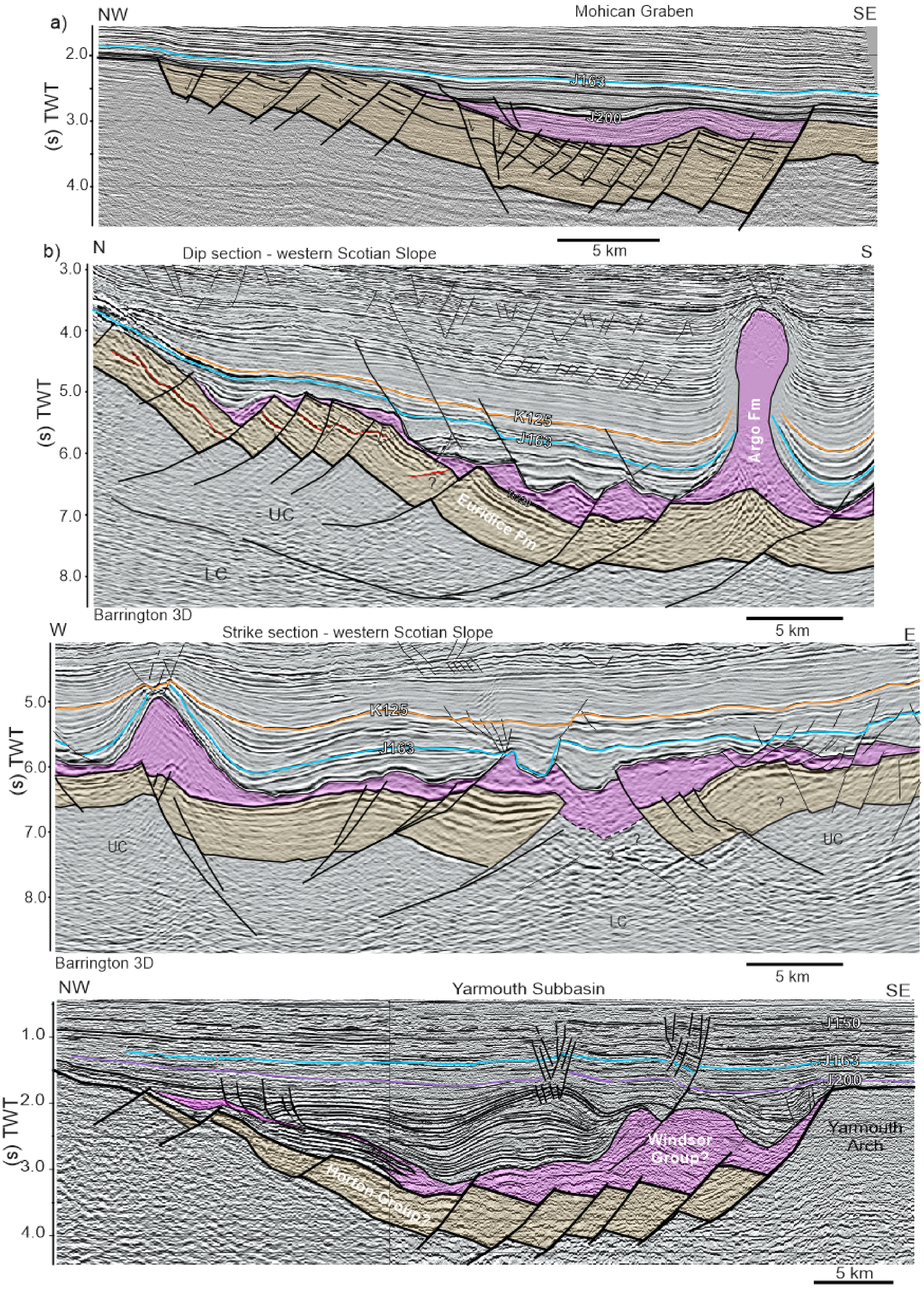
a)
NW
Mohican Graben
SE
2.0
3.0
4.0
(s) TWT
J163
J200
5 km
b)
N
Dip section - western Scotian Slope
S
3.0
4.0
5.0
6.0
7.0
8.0
(s) TWT
K125
J163
Argo Fm
UC
Euridice Fm
LC
?
Barrington 3D
5 km
W
Strike section - western Scotian Slope
E
5.0
6.0
7.0
8.0
(s) TWT
K125
J163
UC
LC
?
Barrington 3D
5 km
NW
Yarmouth Subbasin
SE
1.0
2.0
3.0
4.0
(s) TWT
J150
J163
J200
Windsor Group?
Horton Group?
Yarmouth Arch
5 km

**Figure 21. (previous page)** Representative seismic sections showing potential pre-salt trap configurations. (a) Layered primary salt layer in the Mohican Graben overlying more heavily faulted pre-salt (syn-rift) fluvial-lacustrine strata; (b) a dip-oriented section across the western Scotian Slope (region C) showing syn-rift strata offset along landward-dipping extensional basement faults, overlain by the primary salt layer (pink); c) strike-oriented section showing potential inversions-related folds beneath the primary salt layer; (d) Yarmouth Subbasin containing potential Horton Group fluvial-lacustrine strata, overlain by Windsor Group salt, and a potential Pennsylvanian turtle structure developed above the salt; Note that synrift or pre-rift source rocks are required for these play concepts to work - neither of which has been proven outside of region F (Sydney Basin). LC = lower crust; UC = upper crust; Line locations shown in Figure 20.

An analogue to this play is the Meskala field in Morocco, where oil, condensate, and gas are trapped in Triassic syn-rift fluvial reservoirs rotated above basement blocks, in turn sealed by late syn-rift salt (Morabet et al. 1998; Mader et al. 2017; Tari et al. 2017). Hydrocarbons in the Meskala field were likely sourced from pre-rift Silurian or Carboniferous organic-rich successions. This scenario could also exist, for example, in the Oneida Graben in region A where there are suspected remnants of a pre-rift Carboniferous basin with unknown source rock potential (e.g. Figure 5). Adequate source rock is perceived as the largest geological risk factor for this play type.

*Turtle anticlines and folds above primary salt* – These traps range from turtle anticlines to compressional folds located above either the Windsor Group or Argo/Osprey Formation primary salt (Figure 23). Carboniferous anticlinal structures are present in the Yarmouth Subbasin (region A) (see turtle structure in Figure 21d), in the Oneida Graben (see compressional folds (Figure 5), and in the Sydney Basin (region F), where there are supra-salt folds in the Carboniferous cover strata (Figure 22). This play type was tested in both of the North Sydney wells, with gas charge likely from Horton or lower Windsor source rocks. Reservoir quality is considered the primary risk element for the Carboniferous play.

Turtle anticlines and folds are also recognized above the Osprey/Argo primary salt layer, where both Jurassic and Cretaceous plays are present in regions C and D (Figure 23). Most traps correspond to either turtle/half turtle anticlines or compressional folds that involve the deepwater-equivalent of the Jurassic Mic Mac Formation and the Cretaceous Missisauga and Logan Canyon formations (Figure 24).

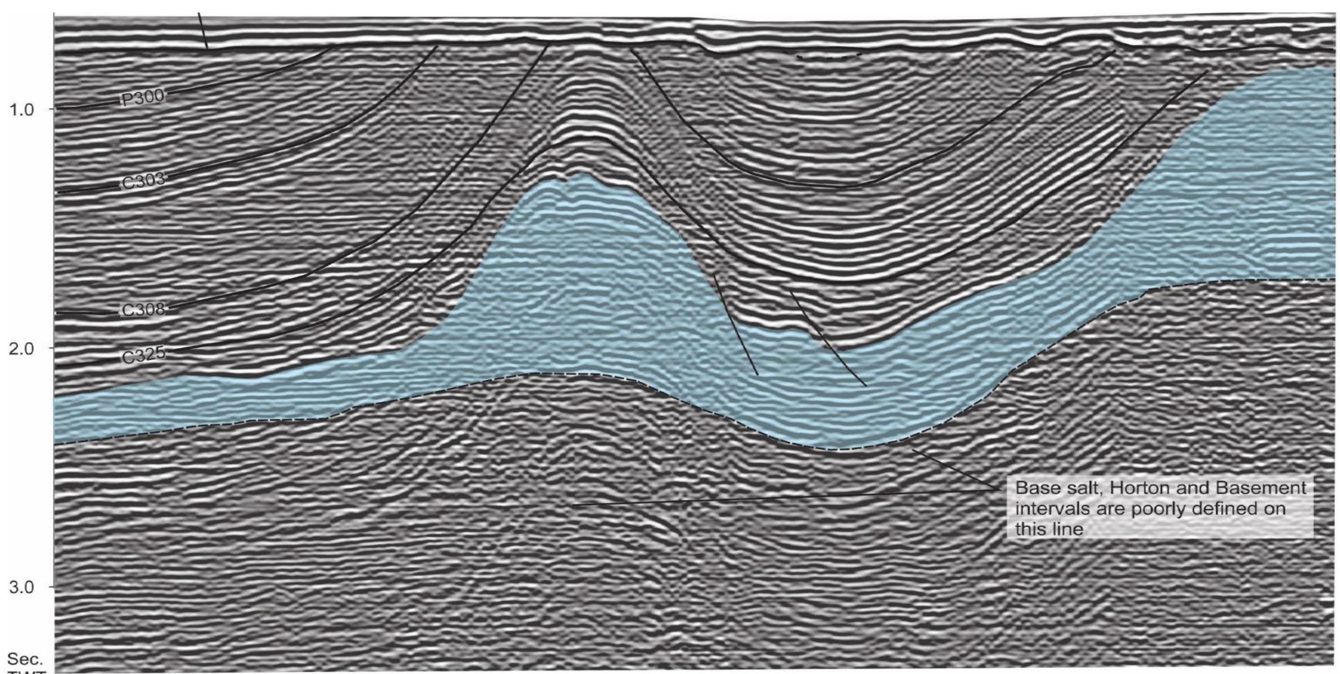


**Figure 22.** Seismic line from the Sydney Basin, showing the development of folds above the primary Windsor Group salt. From Kendell et al. (2017).

Potential traps are most evident beneath the Scotian Slope in the central parts of region C and D, where the original primary salt layer appears to have been thicker (Deptuck and Kendell 2020). The "Big Tancook" and "Big Thrum" leads (Deptuck 2008) fall into this play category. The Cretaceous turtles and folds play was tested at Newburn H-23 that encountered 7.5 m of gas pay in Cretaceous turbidites that were folded into thrust sheets immediately down-slope from a region of prominent growth and thin-skinned extension. The primary geological risk in these plays is reservoir presence and quality. In region C, source rock presence / maturity is also a primary geological risk.

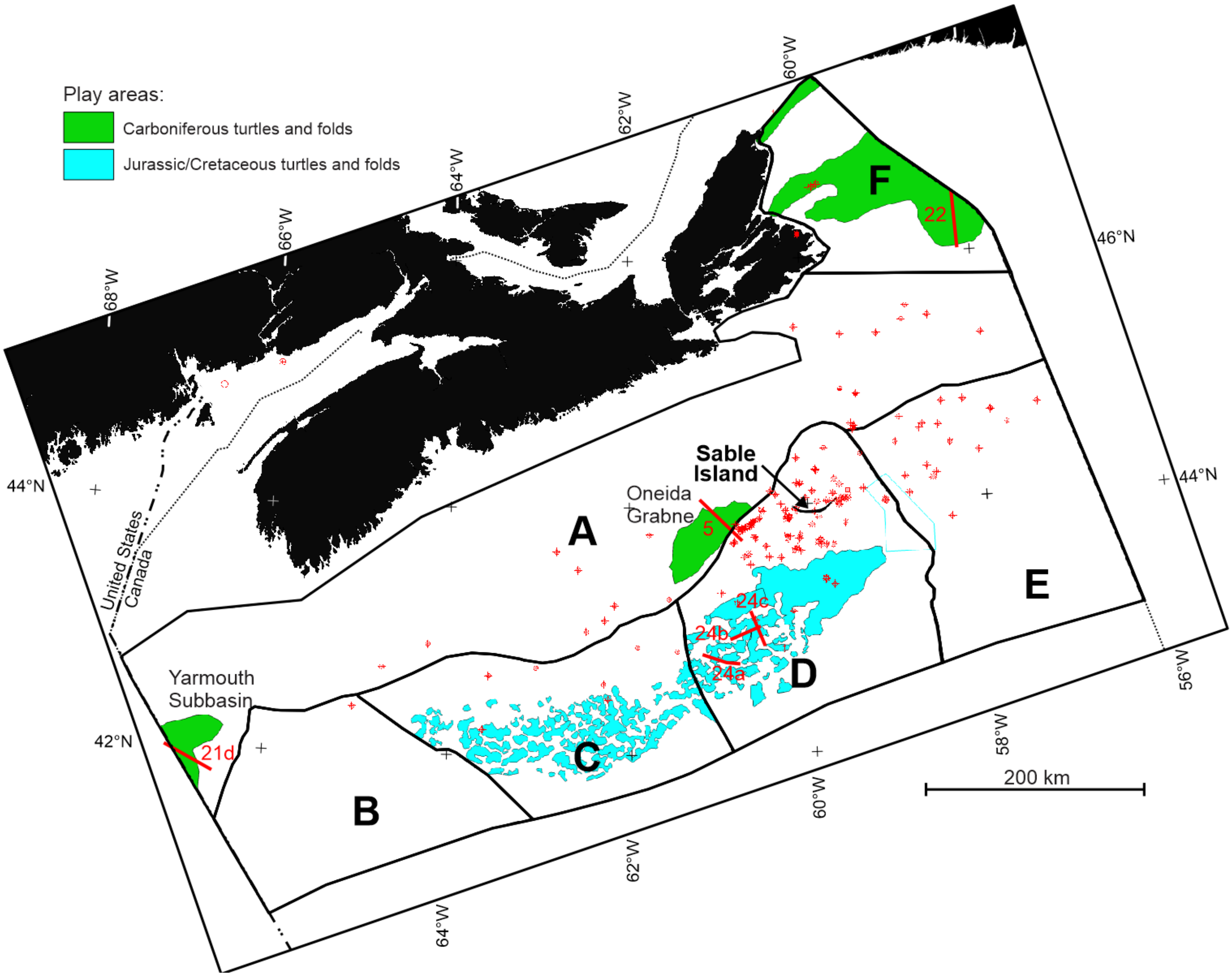


**Figure 23. (above)** Play area map for Carboniferous, Jurassic, and Cretaceous turtles and folds located above either Windsor Group primary salt (Late Paleozoic) or Osprey/Argo primary salt (early Mesozoic).

**Figure 24. (next page)** Several examples of turtles and folds above the primary salt layer in region D; (a) Big Thrum and Seawolf leads (Deptuck 2008); (b) Kinsac lead; (c) Liscom lead (see also the Scotian Basin Integration Atlas 2023). Line location shown on Figure 23.

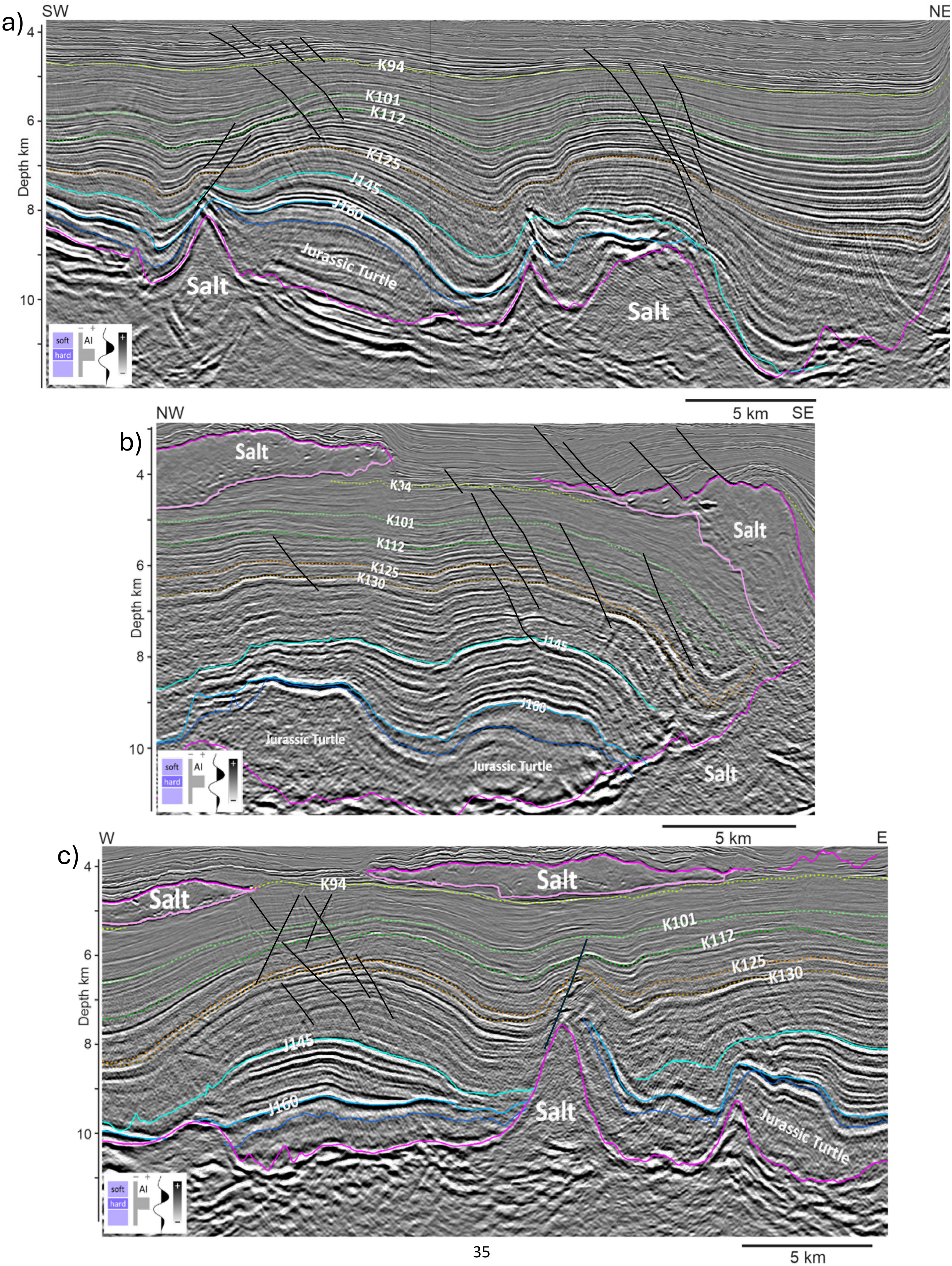
a)
SW
NE
K94
K101
K112
K125
J145
J160
Salt
Jurassic Turtle
Salt
Depth km
4
6
8
10
soft
hard
AI
5 km
b)
NW
SE
Salt
K94
K101
K112
K125
K130
J145
J160
Salt
Jurassic Turtle
Jurassic Turtle
Salt
Depth km
4
6
8
10
5 km
c)
W
E
Salt
K94
Salt
K101
K112
K125
K130
J145
J160
Salt
Jurassic Turtle
Depth km
4
6
8
10
5 km

*Listric rollover anticlines –* Rollover anticlines are found in the landward parts of region B, D, and E where they are associated with fluvial-deltaic environments that prograded above salt, with faults soling into both primary salt and above allochthonous salt bodies (Figures 6, 19a, 25). They are the dominant trapping style for gas- and condensate-bearing fluvial-deltaic reservoirs in the Sable Subbasin and are likewise the most common play type of the Significant Discovery Licences issued in the landward parts of regions D and E (Smith et al. 2014). On the eastern Scotian Shelf (region E), these structural traps are separated into three plays, corresponding to rollovers in the Middle to Upper Jurassic Mic Mac, Lower Cretaceous Missisauga and Lower to mid-Cretaceous Logan Canyon formations (Figures 8). Each successive play migrated further seaward as fluvial-deltaic to shoreface siliciclastics prograded south and west, periodically interrupted during periods of higher sea level that allowed shale to accumulate above the shelf.

In region D (Sable Subbasin), where Jurassic strata are more deeply buried, just two rollover plays are distinguished. The first includes the upper part of the Mic Mac and all the Missisauga formation, and the second corresponds to the Logan Canyon Formation. Forced folds that developed through differential compaction above basement highs or the carbonate bank are also grouped into this play (e.g. with Cretaceous reservoirs of the Cohasset-Panuke field corresponding to the latter). Rollover anticlines are also recognized in region B, where they are separated into a Middle to Upper Jurassic play and a Lower to mid-Cretaceous play (Figure 6a). Plays here are based mainly on seismic observations from vintage seismic profiles that show the development of growth faults, some with clear progradation recorded by clinoform packages (Deptuck et al. 2015).

**Figure 25.** Play area map of the Logan Canyon rollover anticline play, Cretaceous supra-canopy turtles and folds (located above the Sable and Laurentian salt canopies) and Jurassic turtles and folds (associated with the Banquereau Synkinematic Wedge).

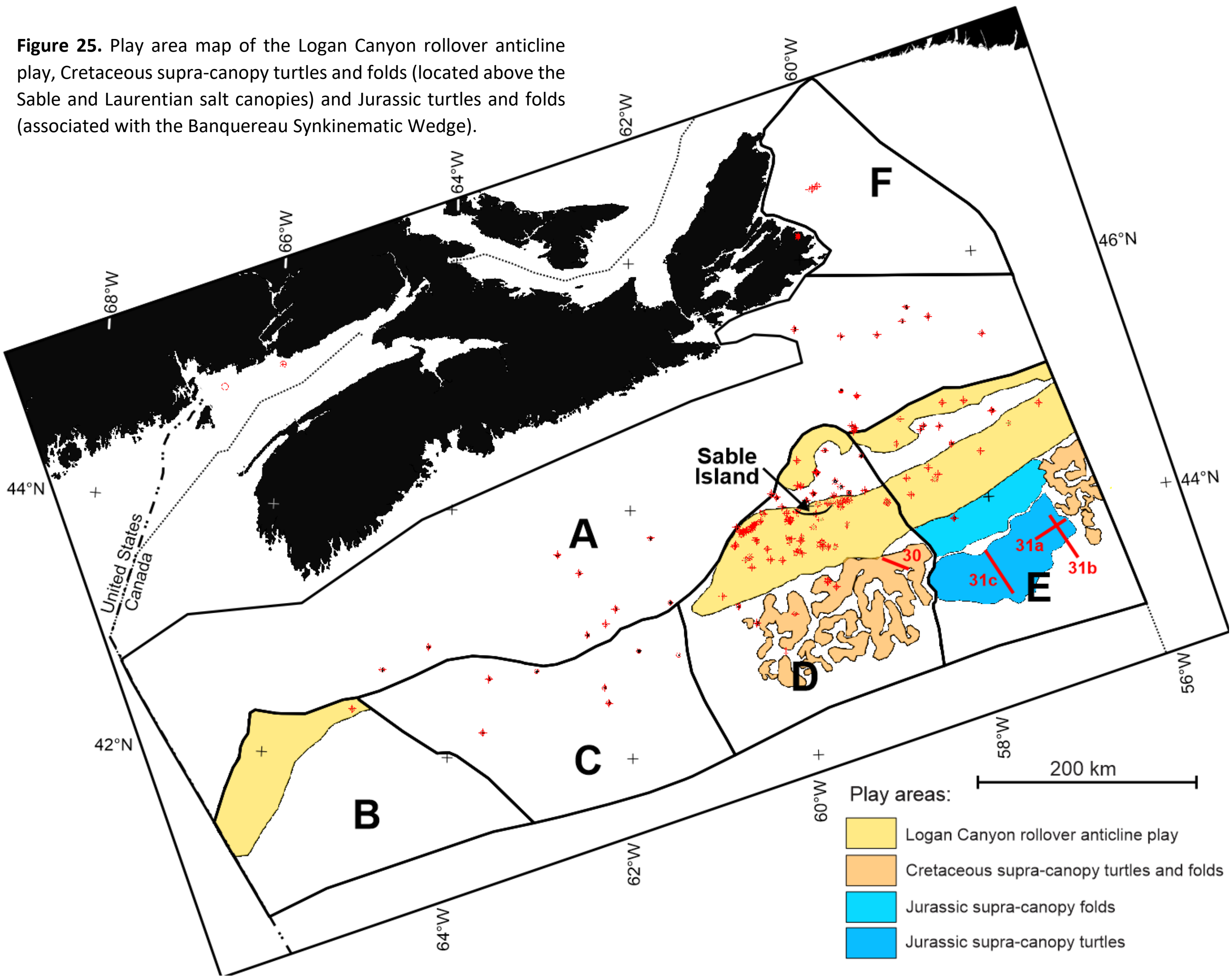

Both fault-seal dependent three-way traps and four-way dip closures are possible in regions D and E, with the former only being effective where there is sufficient shale in the succession (Smith et al. 2014). The Aptian Naskapi Member (shale) of the Logan Canyon Formation is the primary seal, with secondary seals corresponding to Albian to Cenomanian Sable Member (of the Logan Canyon Formation), and the Turonian to Santonian shale of the Dawson Canyon Formation. Numerous wells in region D and E have tested these traps, with water depths generally shallower than 100 m. Lack of fault seal associated with very high net:gross fluvial-deltaic successions appears to be the primary failure mechanism (Smith et al. 2014), with seal risk increasing in the landward direction and for reservoirs located above the Naskapi shale. Still, large swaths of the play areas lack 3D seismic coverage (Table 2; Fig 26), and most of the available shelf 3D data is more than two decades old.

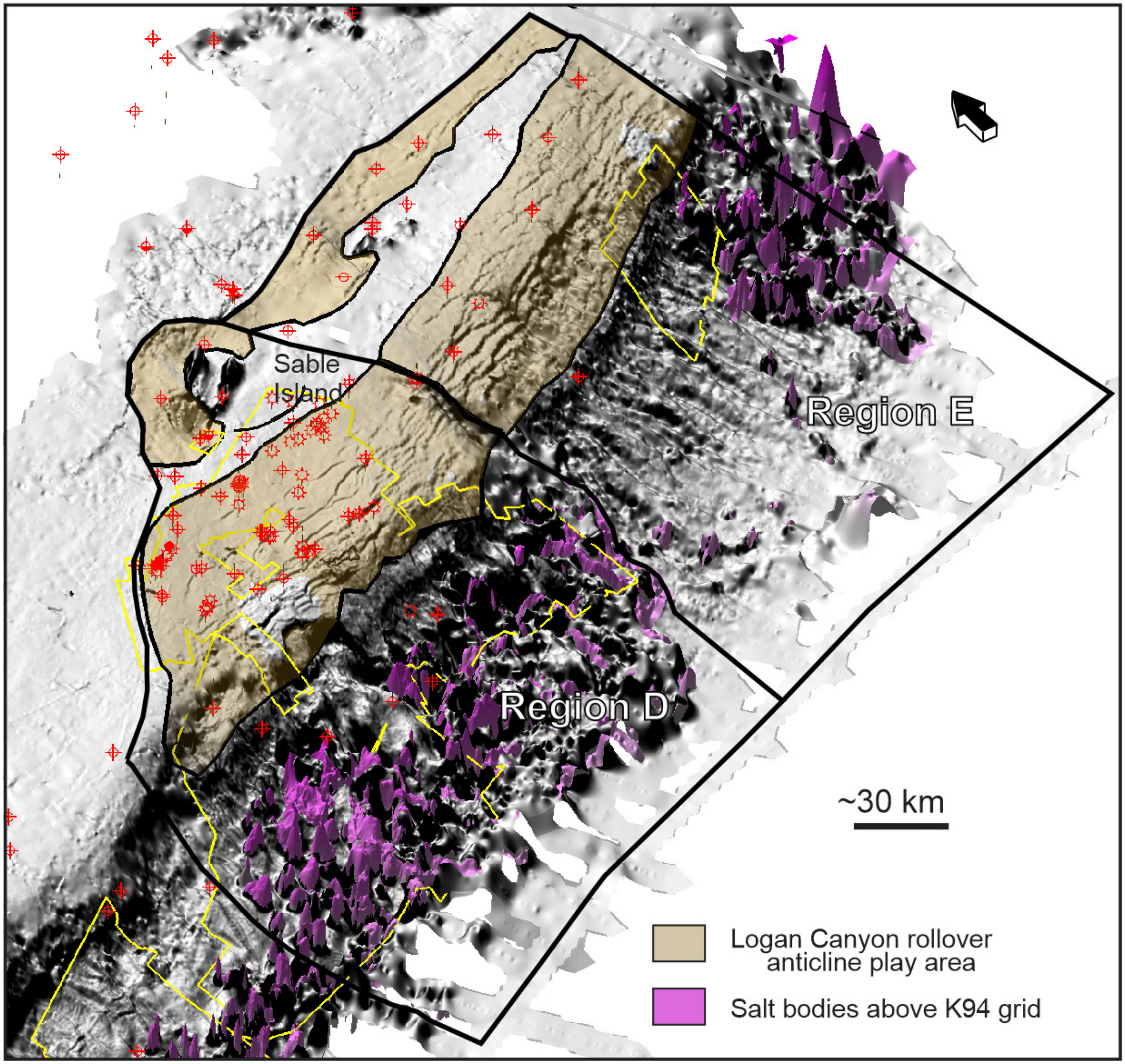


**Figure 26.** Perspective view from the southwest showing a dip map of the K94 marker in regions D and E (darker grey corresponds to steeper dips), with the top of expelled salt bodies posted in pink. Map shows the widespread listric faulting on the outer shelf, corresponding to the Logan Canyon rollover anticline play. The landward region of this play type corresponds to an area of listric faults that were reactivated in the Cenozoic. Yellow outline shows the perimeter around available 3D seismic data, and red symbols correspond to well locations that were draped on the K94 grid.

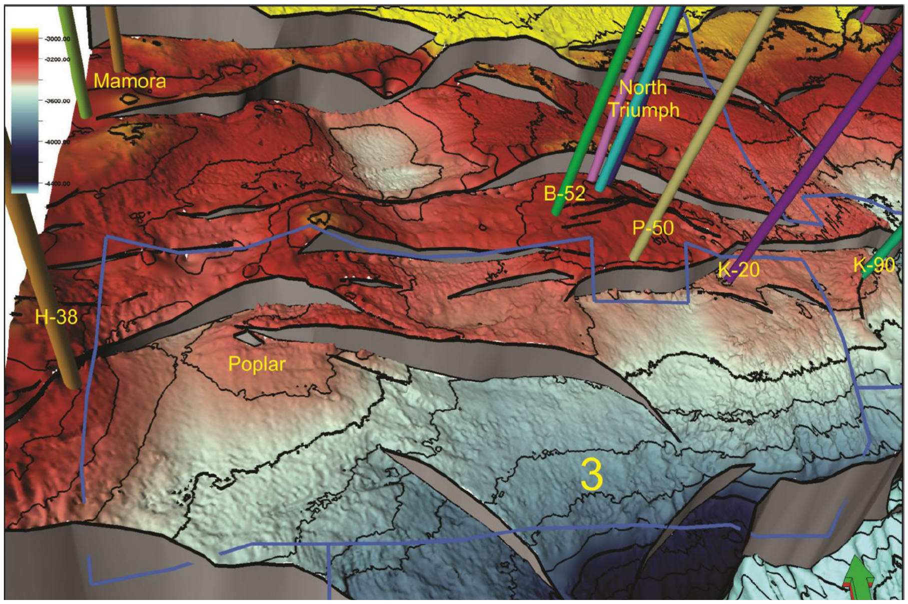


**Figure 27.** Perspective view from the south of the Hauterivian K130 time-structure map, showing an untested rollover anticline trap in the Sable Subbasin ("Poplar" lead from Smith et al. 2016).

**Figure 28.** (bottom) Play area map of the upper Mic Mac to Missisauga rollover anticline play, Cretaceous sub-canopy cut-off play (beneath the Sable and SW Laurentian salt canopies), Jurassic sub-canopy cut-off play (beneath the Shelburne Canopy), Cretaceous upper slope rollovers, and the Cretaceous salt-cored folds play.

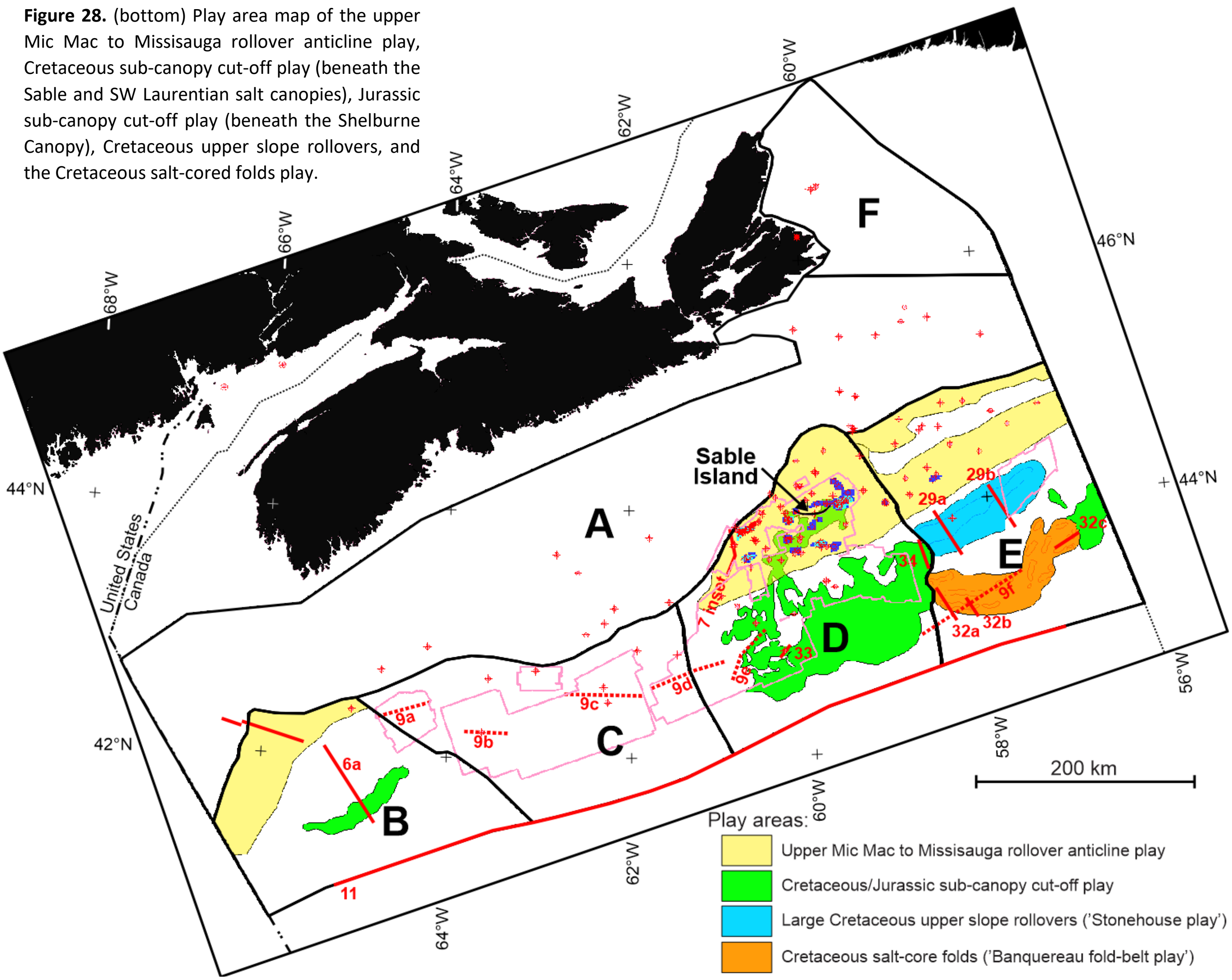

*Large upper slope rollover anticlines* - This trap style, a variation of a rollover anticline trap, is exclusively recognized on the upper slope in region E, where it corresponds to a long-wavelength and laterally continuous Cretaceous fold, referred to here as the "Stonehouse play". The main fold is a very large rollover anticline that formed in response to focused Albian to Cenomanian sedimentation above the headward/ landward parts of the buried Jurassic BSW. Its northeast-oriented fold crest stretches more than 120 km along the upper slope of region E. Water depths range from 1,500 to 2,500 m, with the primary reservoir interval located between the J145 to K112 markers (Lower to mid Cretaceous). Although the most optimistic closing contour defines a closure area exceeding 2,400 km$^2$, the location of Tantallon M-41 above the northern limb of the Stonehouse fold, indicates a shallower closing contour is more appropriate, covering about 1,200 km$^2$, which was used to define the P50 play area (Table 5). The presence of subtle saddles along the fold crest may further separate it into three or four smaller closures. Still, this play includes the largest individual structures in the study area.

Tantallon M-41 tested this play and encountered a ~10 m interval of gas charged sands (Goodway et al., 2008), but very little reservoir-quality sandstone was encountered in the well. Cores from the well sampled hundreds of stacked sharp-based thin-bedded turbidites composed of very fine-grained to medium-grained sandstone (see Piper et al. 2010), suggesting the well was positioned in a predominantly overbank settings adjacent to coarser grained sediment transport corridors

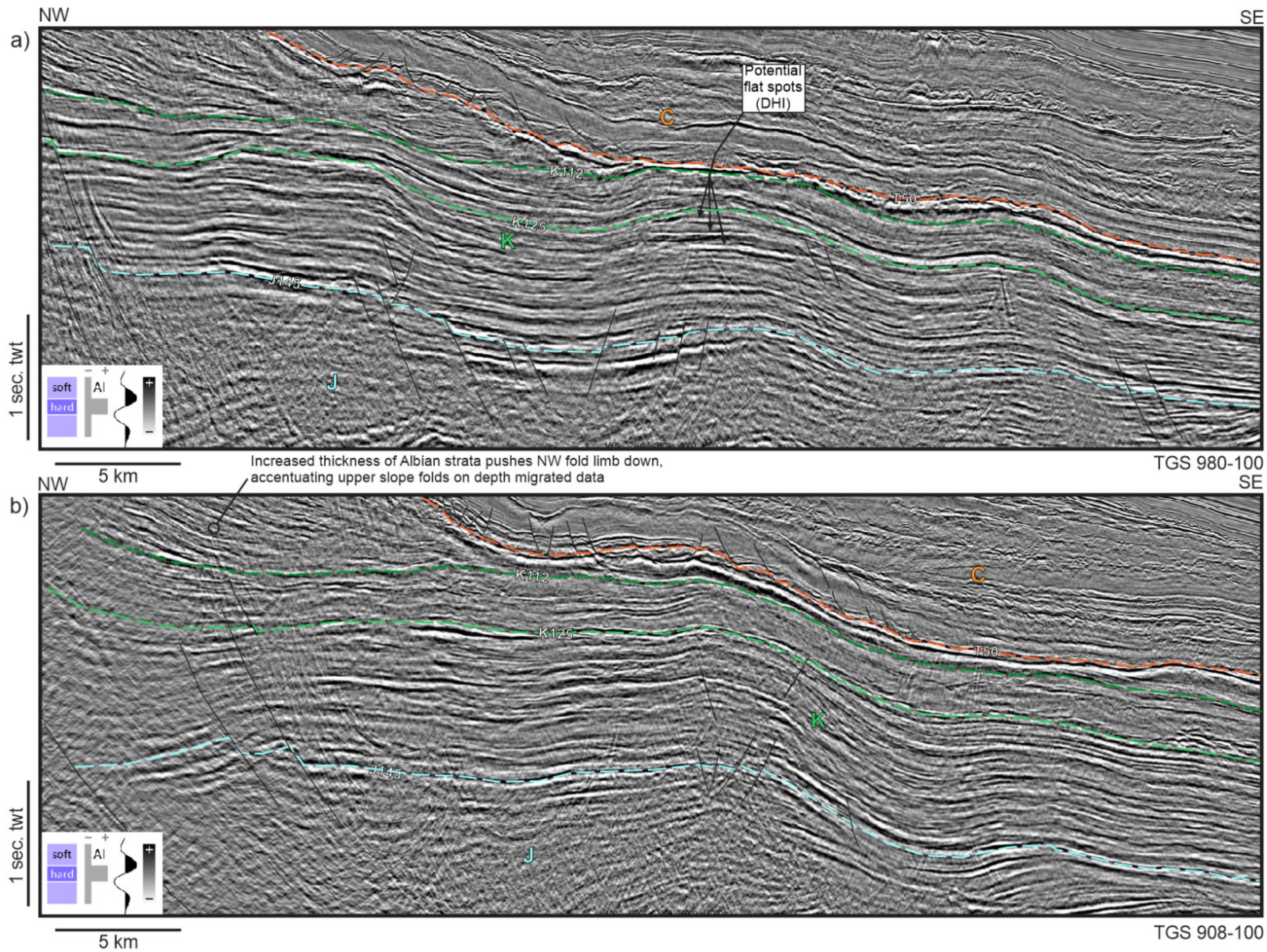


**Figure 29.** Example seismic profiles across long-wavelength rollover anticlines located on the upper slope in region E. Line locations shown in Figure 28. Note that the structures are much clearer in depth (see Deptuck et al. 2014).

(see Figure 16). If correct, much thicker reservoirs may be present along strike of the Stonehouse structure (see section on reservoir risking). A stratigraphic component (i.e. the lateral margins of one or more stacked channel-belts) may limit trap size. Adequate reservoir development and lateral reservoir extent are probably the largest geological risk factors for this upper slope play type.

*Supra-canopy turtles and folds –* Potential traps in this category correspond mainly to turtle structures, but also include other kinds of folds that develop above canopy salt (Figures 19, 25). They range in size from <10 to >170 km$^2$ and are found in water depths ranging from roughly 2,000 to 3,800 m. Traps are separated into a Cretaceous play and a Jurassic play. Numerous Cretaceous turtles and folds are present above the Sable Slope Canopy and SW Laurentian Canopy, located in regions D and E, respectively (e.g. Figure 23). These structures formed on the slope as the Missisauga and Logan Canyon formations prograded across the shelf. Complex slope morphology associated with the movement of salt and development of minibasins, enables turbidite sands to accumulate on the slope. Turtle anticlines form as the centers of some minibasins weld-out, and gradually inverted as minibasin flanks continued to deflate expelling salt laterally. Other minibasins experienced extension, rotation, and shortening, as canopy salt was mobilized seaward. This play type was tested by Annapolis B-24, which encountered 27 m of net gas and condensate pay within turbidite reservoirs (Kidston et al.2007; Kendell et al. 2012). In some situations, canopy salt may hinder hydrocarbon migration from both Tithonian and Pliensbachian source rocks located below the canopy. Charge access for traps located above the Sable Slope Canopy is an important geologic risk element for this play.

Numerous Middle to Upper Jurassic turtles and folds are also recognized. They are associated with Jurassic salt tectonics in region E, where voluminous Mic Mac-equivalent sediments were delivered to the slope. Four-way dip closures are associated with fault rollovers, turtles, half turtles, and thrust-related folds in the BSW (Figures 19b, 31). Reservoir quality in Jurassic turtles in region E is unknown, but the presence of carbonates in the Mic Mac Formation on the shelf is known to diminish reservoir porosity and permeability (Smith et al. 2014). The stratigraphic position of the Tithonian source rock interval relative to the Jurassic turtles and folds is also a key uncertainty for the viability of this play. Tithonian source rocks located above or adjacent to Jurassic leads, would require more complicated migration paths to charge these structures (including downward migration).

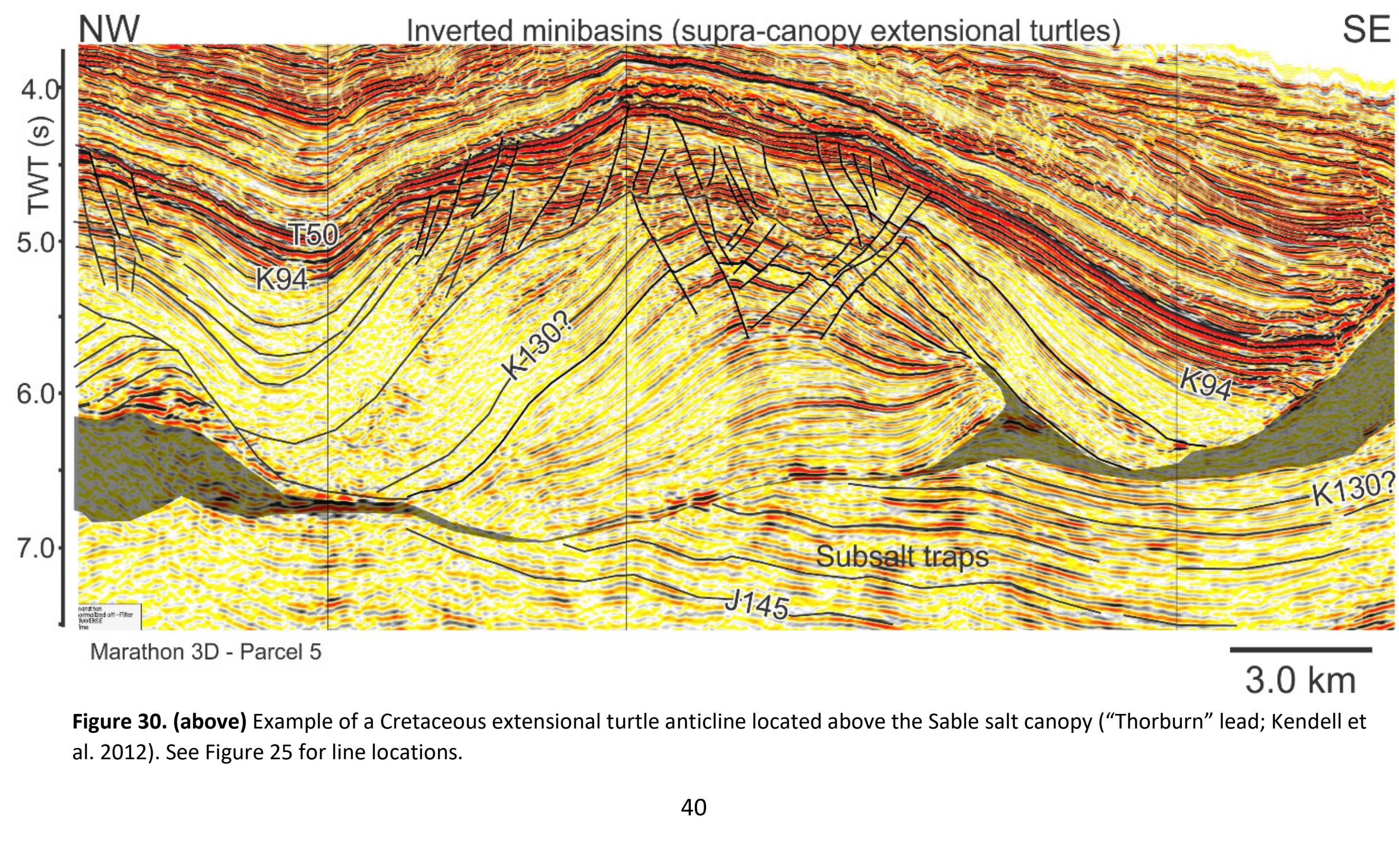


**Figure 30. (above)** Example of a Cretaceous extensional turtle anticline located above the Sable salt canopy (“Thorburn” lead; Kendell et al. 2012). See Figure 25 for line locations.

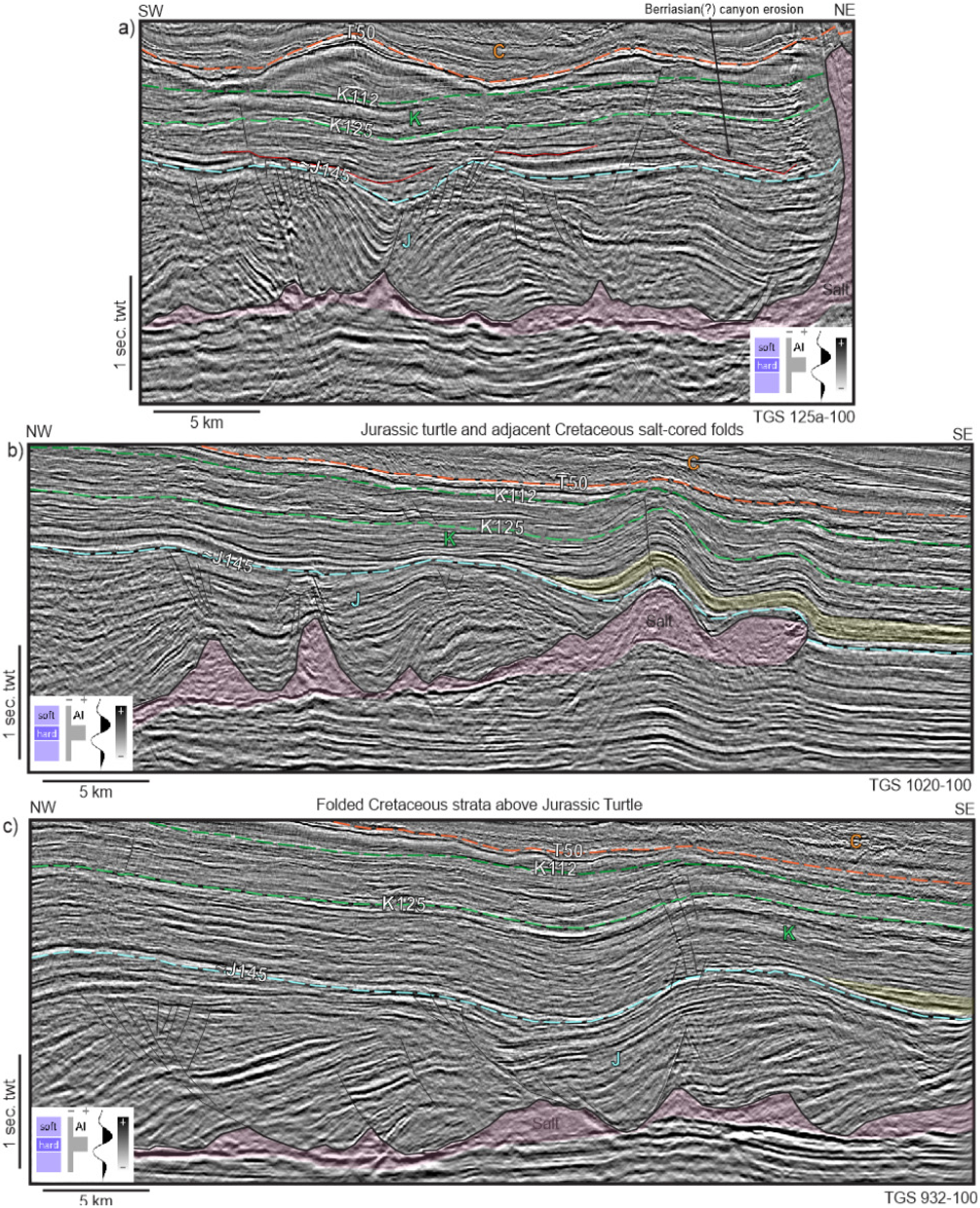


**Figure 31.** Several examples of Jurassic turtle anticlines within the Banquereau Synkinematic Wedge. See Figure 25 for line locations. Not the transparent yellow interval in (b) and (c) that pinches out above the BSW, interpreted as distal Lower Cretaceous turbidite packages.

*Salt-cored folds* – This play is a sub-set of the Cretaceous turtles and folds play. It is treated separately because the traps within it exist exclusively along the distal margins of the BSW in region E. Enhanced up-slope thin-skinned extension during the Albian-Cenomanian was balanced down-slope through shortening of pre-existing salt bodies, producing a series of salt-cored folds collectively referred to as the "Banquereau fold-belt". Folds are arranged in a 200 km long arch that mimics the shape of the underlying BSW (Figure 28). At least 15 four-way dip closures associated with these folds were identified on the K125 and K112 markers. Several examples of these folds are shown on the seismic profiles in Figure 32. They range in size from 31 to 180 km$^2$. Water depths generally range from 3,000 to 4,000 m. Traps are generally well-defined, comprising thick folded successions of Lower Cretaceous strata that accumulated above the seaward parts of the BSW. Folds are localized directly above mechanically weaker salt bodies that accommodated post-Aptian shortening. Their timing is similar to that of the Stonehouse play. Some localized syn-kinematic thinning of Aptian strata took place above the K125 marker, with more widespread and pronounced thinning taking place in the Albian, above the K112 marker, marking the most important period of fold growth. Albian strata provide a regional seal, while interlayered fine-grained sediment are also likely to provide local reservoir-seal pairs. Reservoirs are expected to be a combination of Valanginian to Aptian turbidite channel-belt sands and sheet-like lobe sands.

Some folds were pierced by salt diapirs, while others have a number of crestal faults that could affect trap integrity. The Late Miocene salt-cored Mississippi Fan fold-belt (Rowan and Peel 2005) is an excellent analogue for the Banquereau fold-belt.

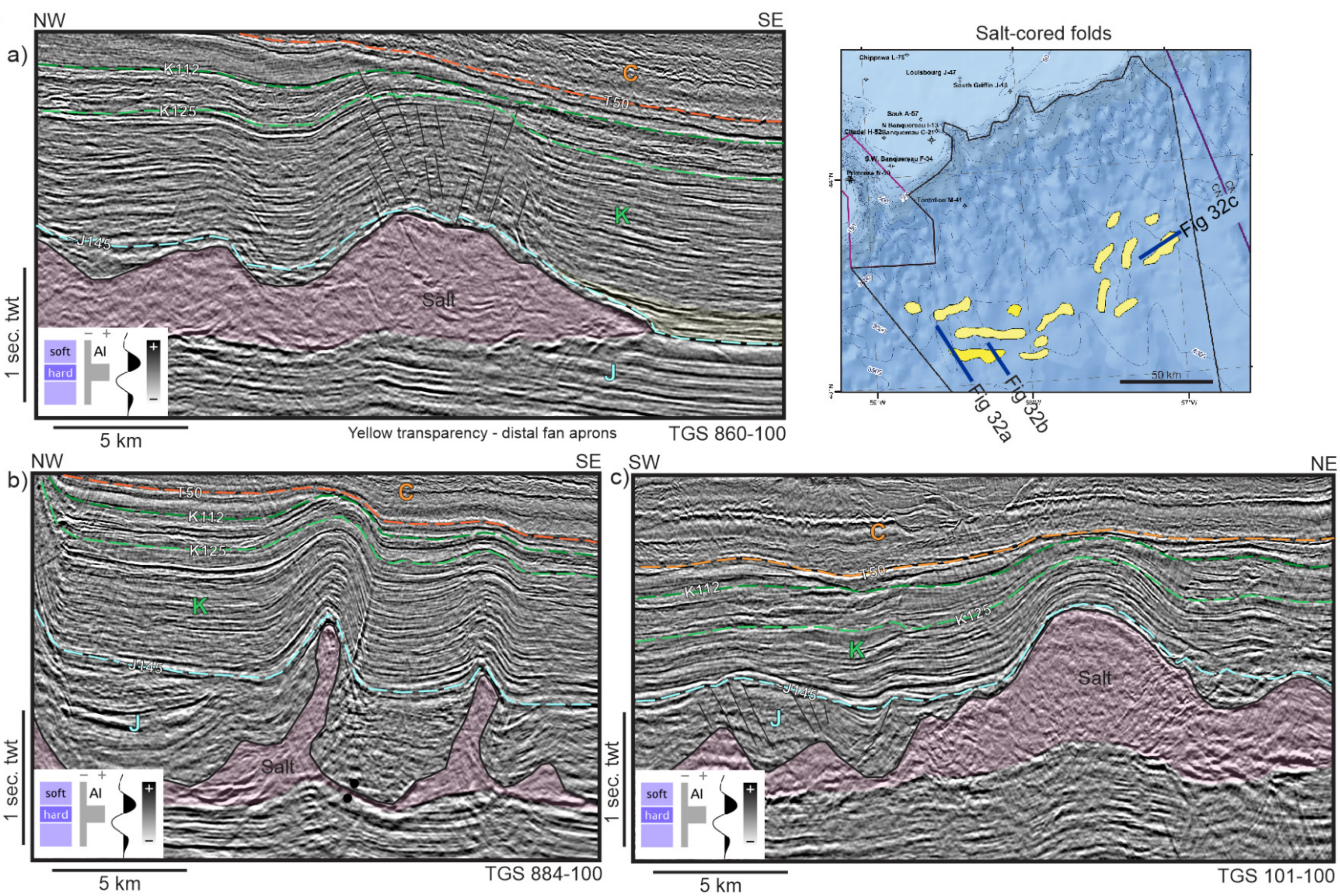


**Figure 32.** Seismic examples of salt-cored folds (D) above squeezed salt bodies in the BSW. Folds developed in the mid-Cretaceous in response to up-slope thin-skinned extension. Other examples are show in Figure 31b. Line locations shown in Figure 27.

*Sub-salt cut-off traps* – Potential sub-salt cut-off traps form as turbidite sands (or other reservoirs) are deposited in front of an advancing salt sheet, with potential reservoirs terminating up-dip along what ultimately becomes the base salt surface. They are recognized in four areas, forming four different plays (Figure 28). Beneath the Shelburne salt canopy in region B, and the "Sable Shelf Canopy" in region D, they correspond to potential Upper Jurassic reservoirs beneath more localized salt tongues expelled on the slope and the shelf, respectively. Beneath the "Sable Slope Canopy" in region D, and beneath the SW Laurentian canopy in region E, they correspond to potential Lower to mid-Cretaceous deepwater reservoirs deposited as the Missisauga and Logan Canyon formations prograded across the shelf, driving salt expulsion and turbidite sedimentation on the slope. Although such traps work in other settings (like the Gulf of Mexico), poor seismic imaging below salt canopies coupled with sparse line density make it challenging to map specific three-way closures.

Two deepwater wells have tested this play type – both in region D. Weymouth A-45 encountered no significant hydrocarbon shows and very little reservoir quality sandstone. Aspy D-11 targeted a narrow, east-west trending, sub-canopy trap, requiring three-way closure against a combination of overlying salt and a fault/salt-weld to its east (Figure 33). The subsalt reservoir intervals were interpreted to be Lower Cretaceous turbidite lobes and channel complexes age-equivalent to the widespread sandstone reservoirs on the shelf in the Missisauga and Logan Canyon formations. The well encountered a 130 m thick interval containing multiple Aptian aged siltstones with significantly elevated mud-gas readings and fluorescent cuttings. While reservoir quality sandstones were not encountered in this interval, there were clear indications of gas charge. Deeper in the well, two Barremian-Hauterivian aged sandstones were wet, probably because the lateral seal for this trap failed where the salt feed welded out (e.g. right side of Figure 33). The primary geologic risks associated with sub-salt traps is a combination of trap integrity and reservoir presence. Similar geologic risks apply to other sub-canopy cut-off traps like Brooklyn, which contains several stacked "hard-over-soft" reflections consistent with potential turbidite sands beneath the eastern parts of the Sable Slope Canopy (Figure 34).

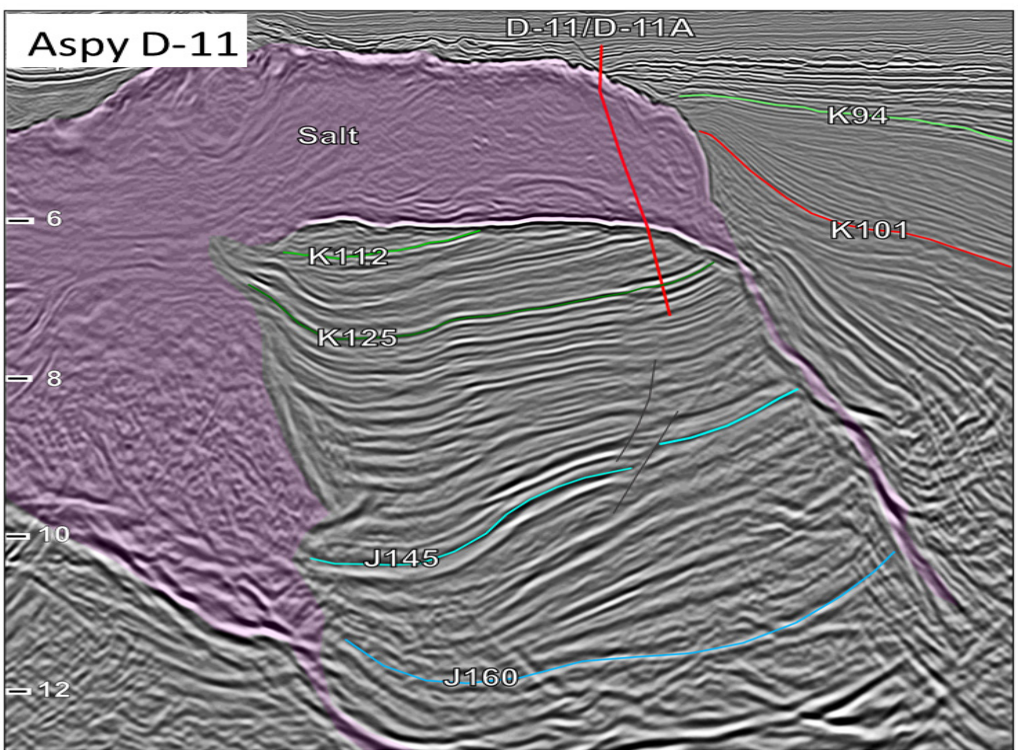


**Figure 33.** Dip-oriented depth profile along the Aspy D-11 deviated borehole. Line location shown in Figure 27.

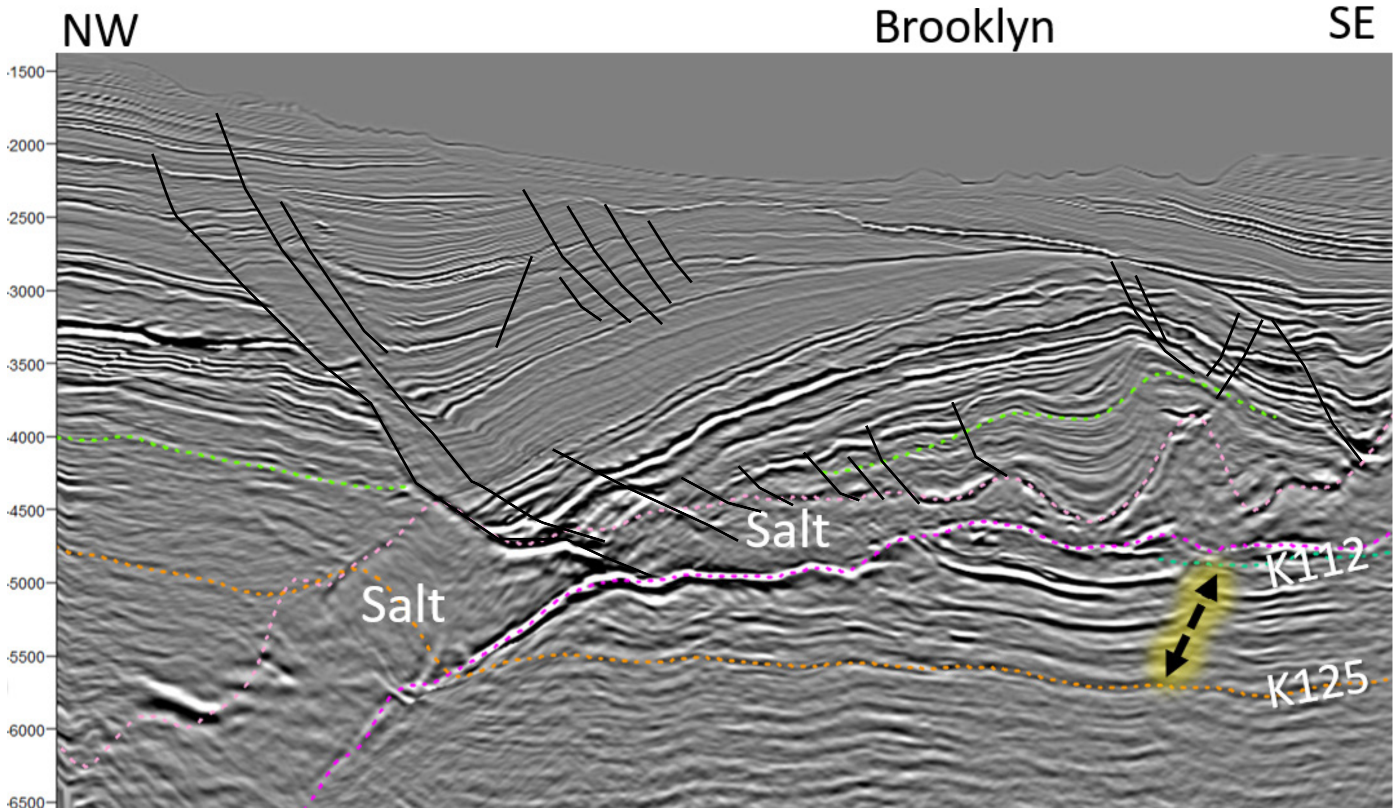


**Figure 34.** Dip-oriented seismic depth profile through the 'Brooklyn' lead where several bright "soft" reflections terminate along the base salt surface beneath the eastern part of the Sable Slope Canopy. Line location shown in Figure 28.

*Three-way closures on salt body flanks* – Several potential three-way and four-way traps are found above and along the flanks of salt diapirs in regions B, C, D, and E (Figures 35, 36). They are mainly located where Cretaceous strata is upturned along the flanks, or folded above the crests, of younger salt bodies (e.g. Figure 35). A number of potential salt flank traps are also present where salt diapirs pierced the salt-cored folds in the "Banquereau Foldbelt", generating additional trap geometries.

Trap definition with existing 2D seismic profiles is complicated by the small size of some potential leads, and the complexity of salt tectonics, especially above the Sable and SW Laurentian canopies. Likewise, the young timing of salt diapirism – in some cases continuing into the Paleogene – may increase risk of breaching trap integrity. Trap integrity, reservoir presence, and adequate trap size are considered the highest risk elements for this play type.

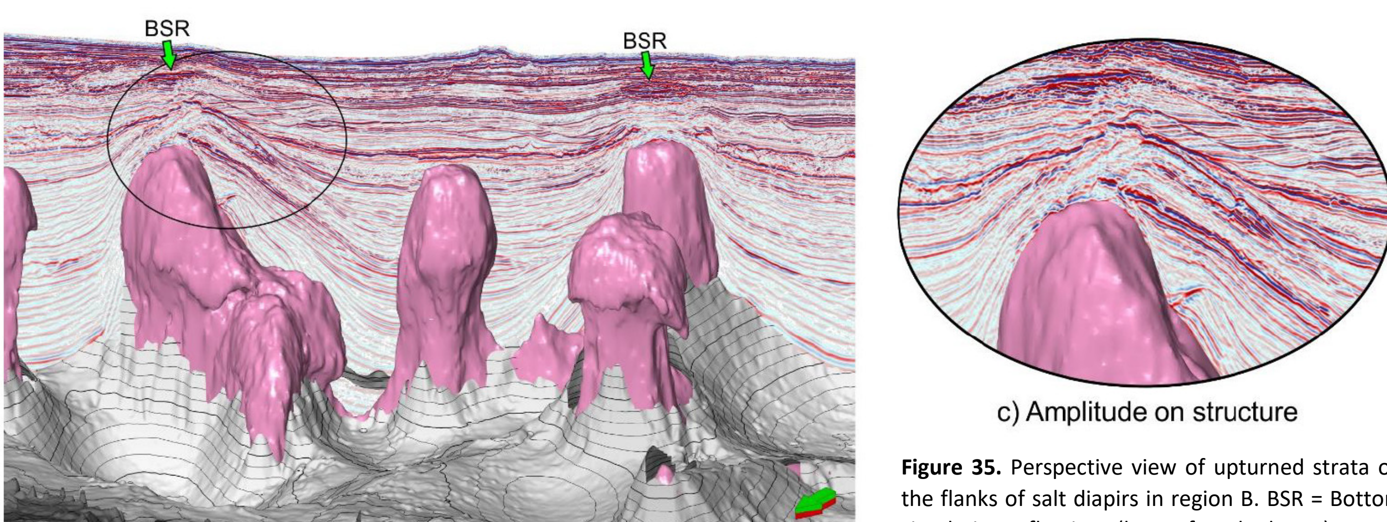


**Figure 35.** Perspective view of upturned strata on the flanks of salt diapirs in region B. BSR = Bottom simulating reflections (base of gas hydrates)

**Figure 36.** Play area map for the Cretaceous stratigraphic onlap play, with components in the deep water areas of regions B and E, and a shallower component where Cretaceous (and to a lesser extent Jurassic) strata onlap the carbonate foreslope. Also shown is the location of the carbonate bank edge, where potential hydrocarbons are trapped within porous carbonates along the bank edge. Salt bodies (pink), show where three-way dip closures are possible along salt flanks (e.g. see Figure 37).

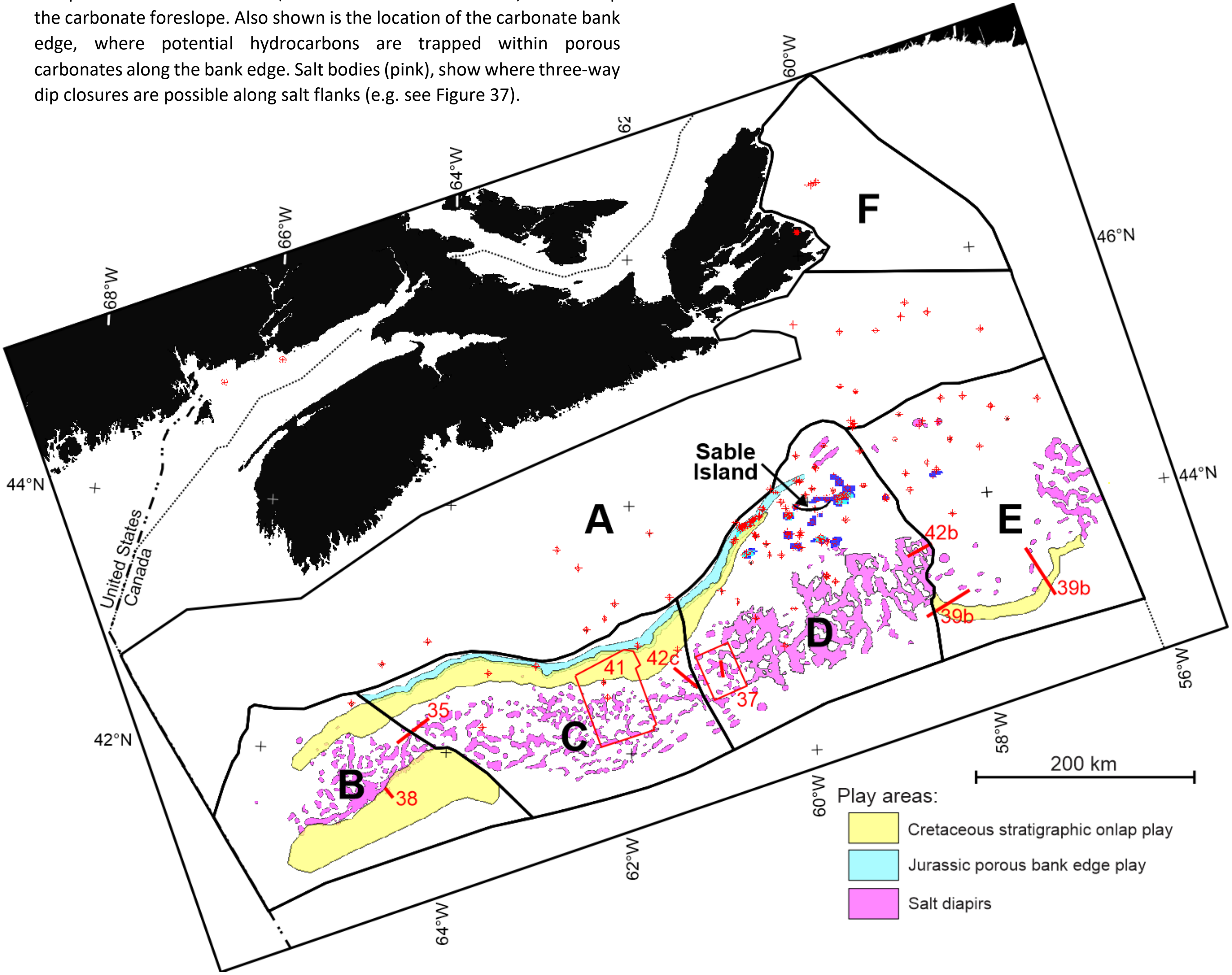


*Stratigraphic traps –* Stratigraphic traps fall into two categories, those generated by up-dip stratigraphic pinch-out/onlap onto the Jurassic carbonate foreslope, and those located further seaward, near the termination of deepwater turbidite systems on the lower slope or rise. The Cayuga lead is an example of the former, corresponding to mid-Cretaceous turbidite channels that onlap onto the carbonate foreslope and show abrupt amplitude cut-off down slope (Figure 38). Similar onlap traps are present in regions B, C, and D (Figure 36).

Potential deeper-water stratigraphic traps are present in regions B and E (Figure 36). Examples include the distal pinch-out of earliest Cretaceous aprons in Figure 39, consisting of stacked intervals of bright-amplitude soft reflections that onlap and pinch-out against the distal perimeter of the BSW. They are believed to have been supplied during erosion of the Avalon Uplift. Potential analogues for the pinch-out traps along the distal margins of the BSW include the Buzzard field in the North Sea, which contains 400 million barrels of oil in Late Jurassic turbidite reservoirs that form a wedge-shaped stratigraphic trap thinning onto the slope, sourced by Late Jurassic source rocks (Dore and Robbins 2005).

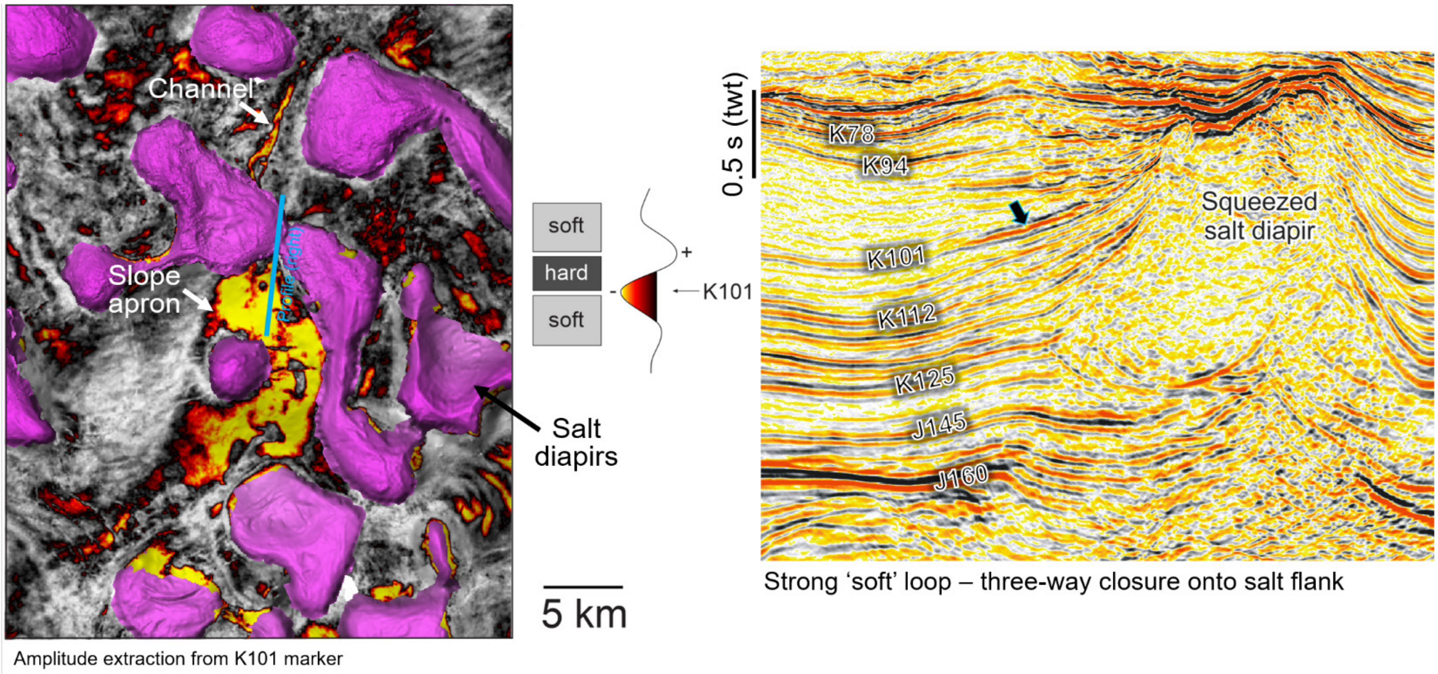


**Figure 37.** Amplitude extraction from the K101 marker, showing a strong negative reflection interpreted as a turbidite apron supplied by a narrow submarine channel. On the right side, is a seismic profile showing the potential three-way trap on the flank of the diapir (line identified in blue on the amplitude extraction.

Other examples are present in region B, where broad bottom-current reworked channel corridors pinch-out above the Shelburne salt canopy or the positive relief generated by Cretaceous contourite drifts (e.g. the Petite Pearl lead; Deptuck 2020) (Figure 38). Water depths for these distal examples generally range from 3,000 to 4,500 m.

Although many stratigraphic plays are very large, they also carry a higher risk. Trap presence and integrity are considered the highest risk factor for this play. Sparse line density along the seaward parts of the BSW, preclude mapping specific three-way closures with the data available for this study. Likewise, such traps can be very subtle, requiring a higher confidence velocity model than the one used in this study.

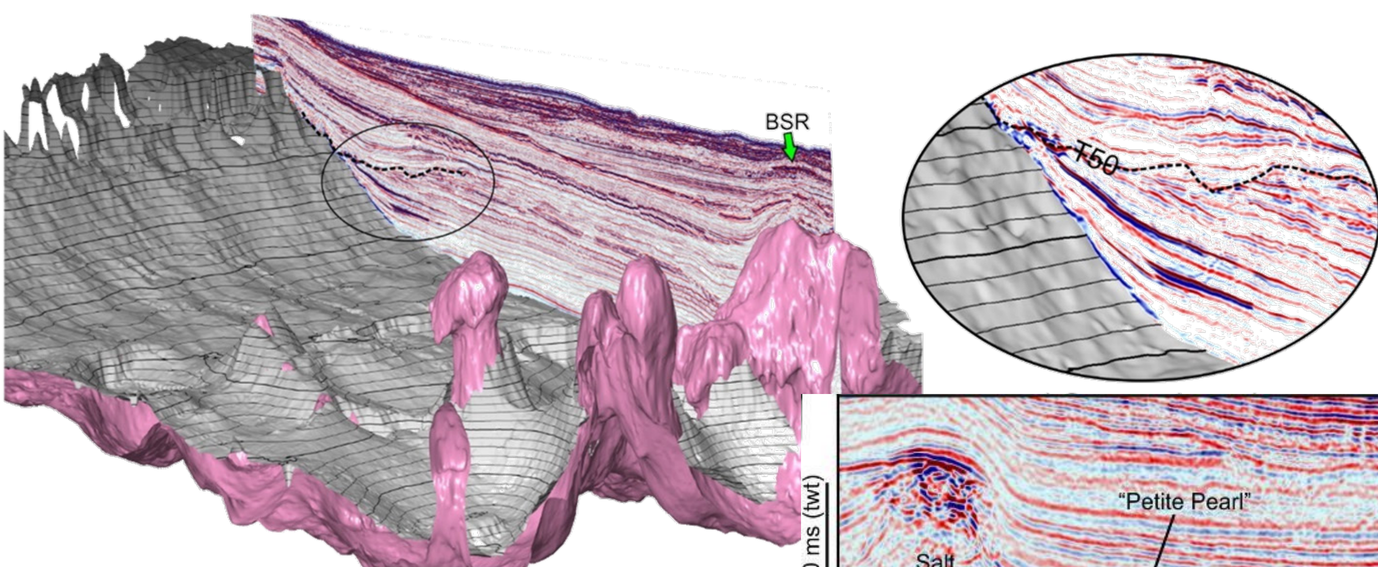


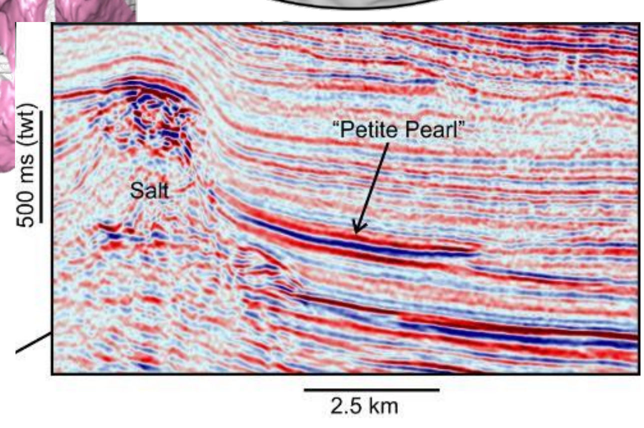


**Figure 38.** Examples of potential up-dip pinch-out traps in regions B and C. Oval identifies the "Cayuga" lead corresponding to mid-Cretaceous turbidites that onlap the carbonate foreslope; rectangle identifies the "Petite Pearl" lead corresponding to a broad 3.5 to 8 km wide bottom-current reworked 'channel' that onlaps the Shelburne salt tongue canopy (see Deptuck 2020).

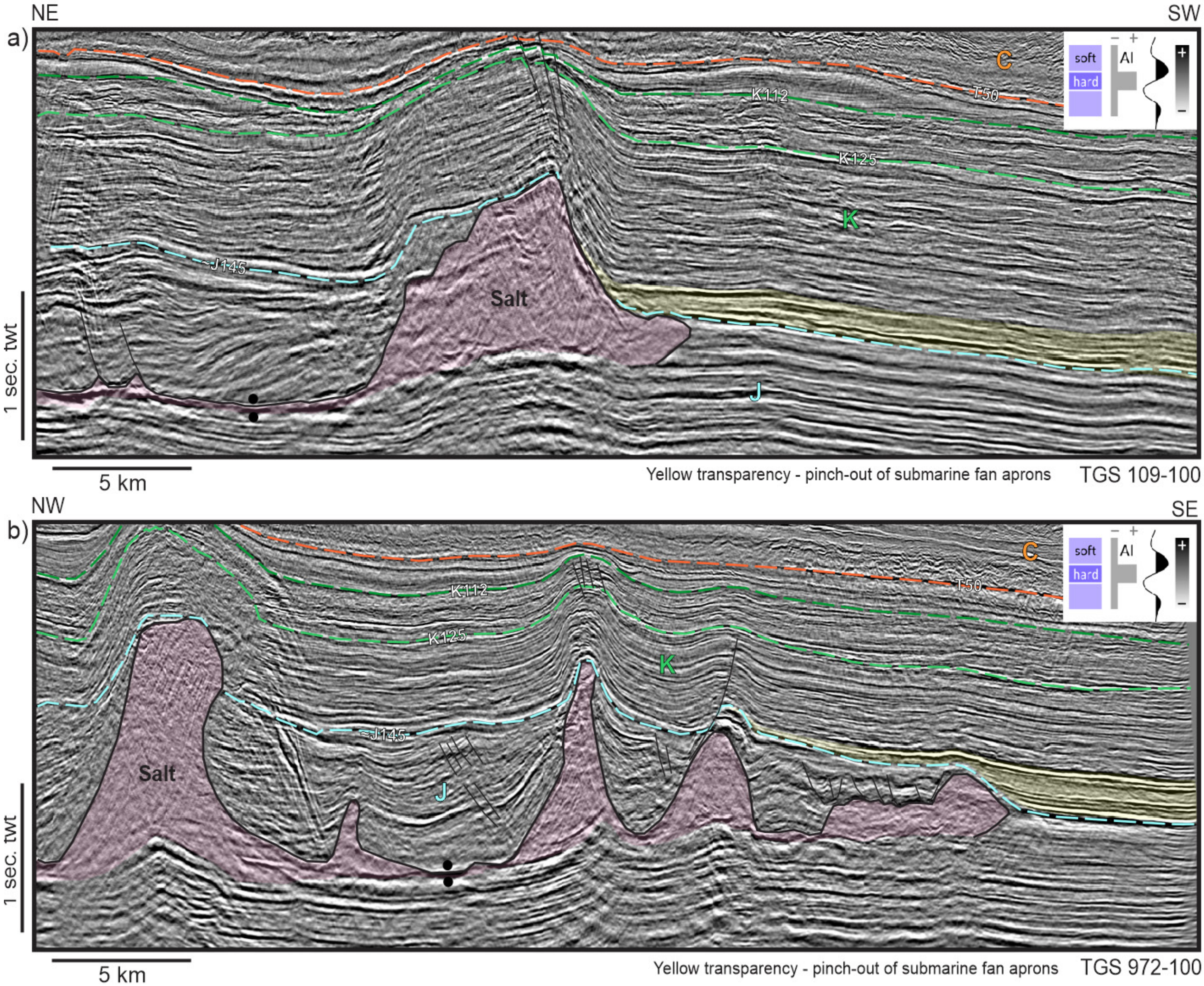


**Figure 39.** Two seismic profiles crossing the toe of the Banquereau Synkinematic Wedge, showing to up-dip pinch-out/onlap of bright amplitude hard-over-soft reflections interpreted as turbidite sheet sands supplied in the earliest Cretaceous. These profiles also show the salt-cored folds of the "Banquereau fold-belt" that reactivated the buried salt bodies along the seaward perimeter of the BSW.

*Porous bank edge/carbonate build-ups –* Two play types involve higher energy carbonate buildups in the study area. The first – a Windsor reef play (Table 2) - is present in region F, where local Gays River Formation dolomitized reef buildups may be present along the margins of the Early Carboniferous Windsor Sea (Savard 1996; Kendell et al. 2017). These reefs would be localised and potentially difficult to identify on the current seismic data but are a potential reservoir for hydrocarbons generated from Horton or even lower Windsor group source rocks. Onshore, these reefs are common where the Gays River Formation oversteps basin bounding topography (Ryan et al. 1991).

The second play is younger, corresponding to an Upper Jurassic carbonate bank-edge with potential for porous reef margin reservoirs in regions C and parts of D (Figure 36). The play area is narrow (~ 5 km wide) and roughly 250 km, where it parallels the modern shelf edge. Jurassic reefal buildups developed as the Abenaki Formation aggraded above the slowly subsiding LaHave Platform (Eliuk 1978; Wade and MacLean 1990; Figure 8).

**Figure 40.** Depth structure map of the J145 marker, showing the scalloped carbonate bank edge along regions C and D (light blue shading), as well as salt bodies (pink) that pierce overlying Cretaceous strata. Seismic sections crossing the bank edge shown in red (see Figure 6). The transition to a ramp-style, prograded carbonate margin begins near Figure 6d. (Contour interval is 500 m).

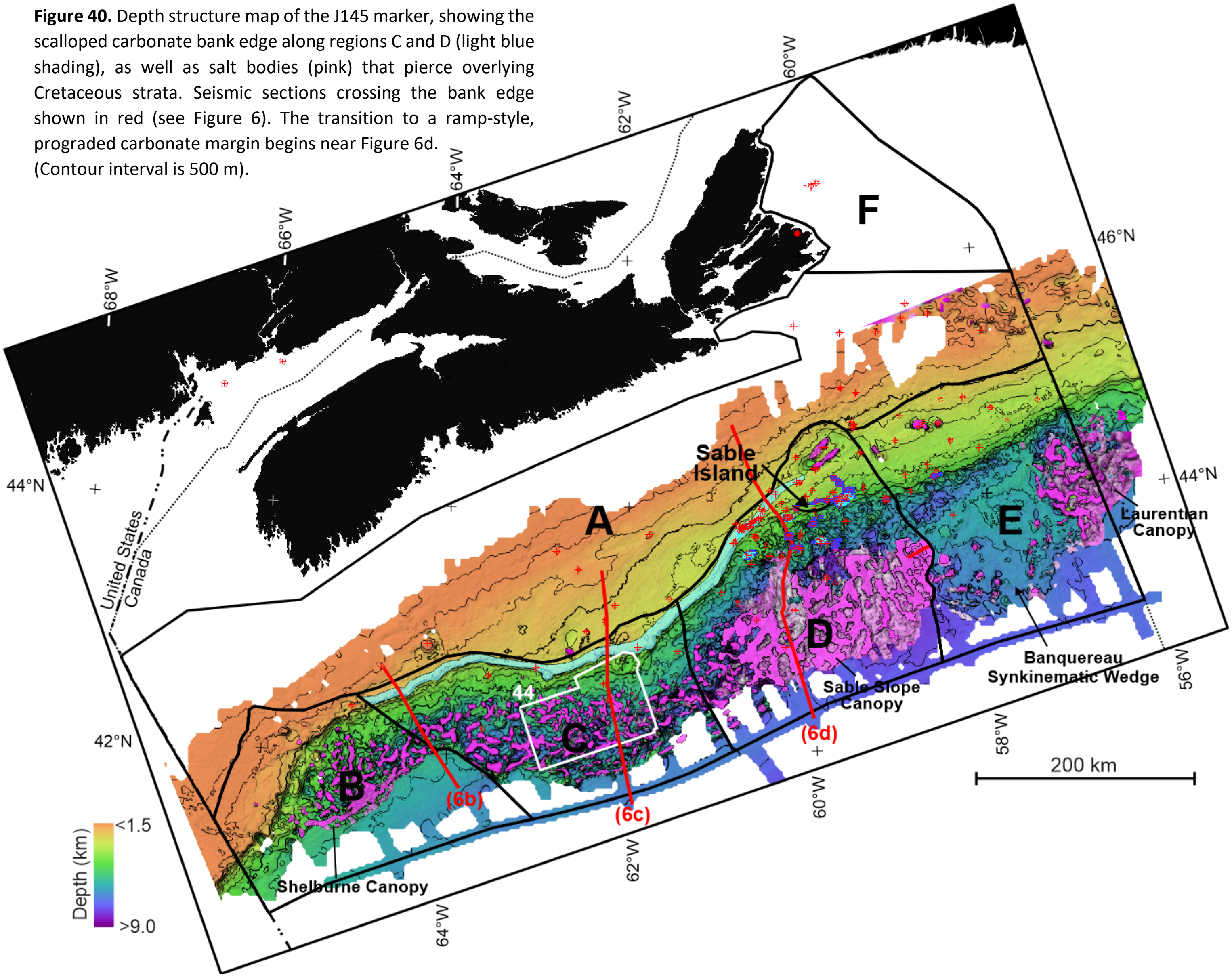


The Deep Panuke gas field, discovered in 1998, shows that the porous reefal facies of the Abenaki Formation can form effective reservoirs. Much of the vuggy or cavernous porosity was created through leaching and secondary dolomitization, with a top seal generated by tight limestones (Kidston et al. 2005). Although production of gas proved challenging from the Deep Panuke carbonate reservoirs due to excessive water production, overall recovery of liquid hydrocarbons (oil), if discovered, may not be as adversely affected by these production issues from such reservoirs. Trap integrity is a primary geological risk, as several younger periods of erosion, including the Montagnais marine impact event, have focused erosion near the bank edge, potentially breaching some traps or removing the porous reef margin.

*Chalk Play –* The chalk play includes a broad spectrum of potential anticlinal traps on the slope that involve either in-situ or resedimented chalk reservoirs. The Eagle gas discovery on the shelf of region D consists of 52 m of net gas pay in porous Upper Cretaceous chalks of the Wyandot Formation (1.27 Tcf gas in place, Sable Subbasin), while the Primrose Significant Discovery further east consists of 50 m of net gas pay in Wyandot chalks folded above a salt diapir (Smith et al. 2014; 2018). Chalk in both locations is likely in-situ (see Ings et al. 2005); it accumulated during periods of high eustatic sea level that drowned the shelf starting in the Late Cretaceous.

Resedimented chalks are likely to form higher permeability reservoirs (Brasher and Vagle 1996; Megson and Tygesen 2005), but these may be more

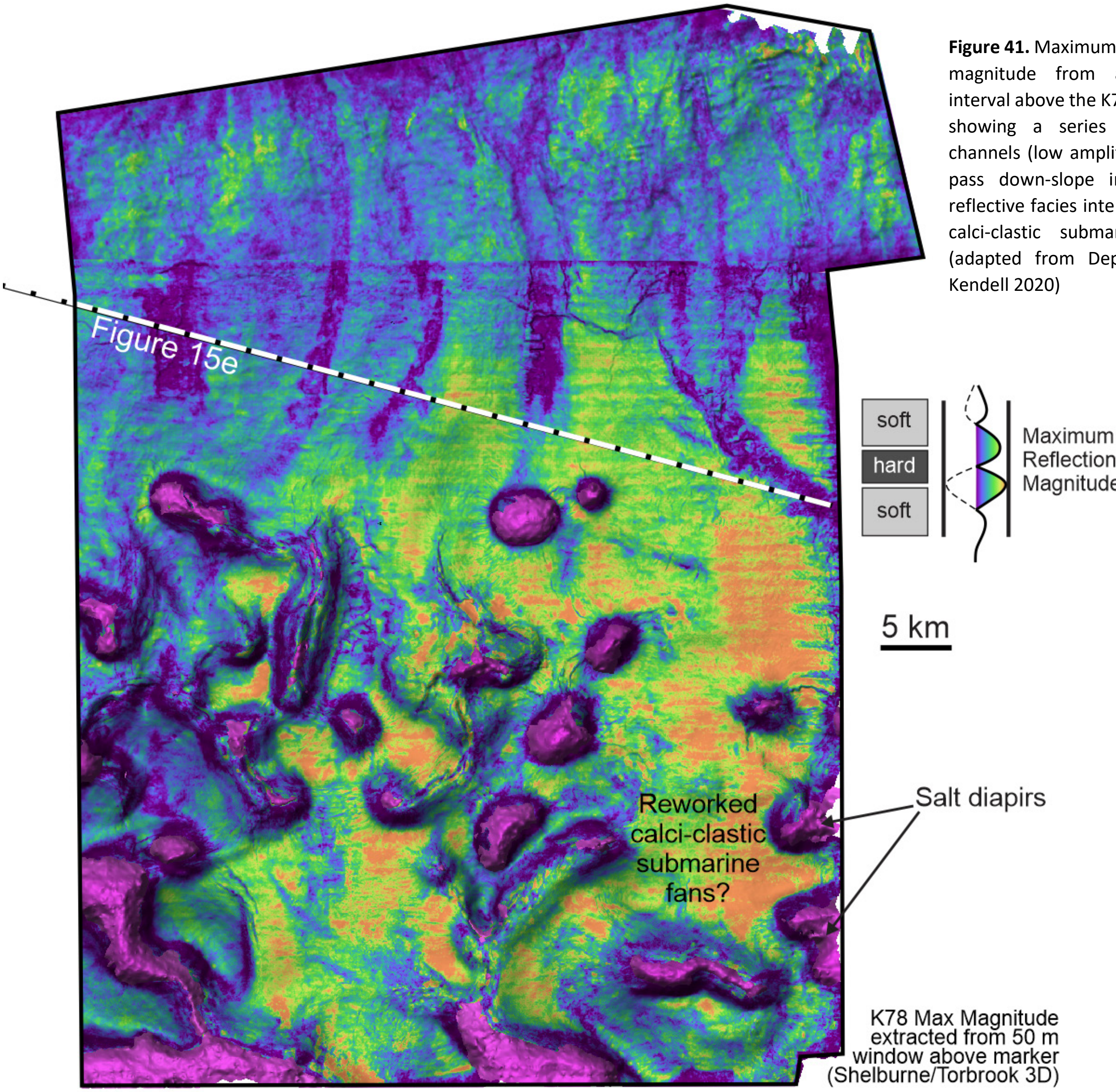


**Figure 41.** Maximum reflection magnitude from a 50 m interval above the K78 marker, showing a series of slope channels (low amplitude) that pass down-slope into more reflective facies interpreted as calci-clastic submarine fans (adapted from Deptuck and Kendell 2020)

common on the slope than on the shelf. For example, Figure 41 shows a series of broad erosive upper slope channels that pass down-slope into higher amplitude seismic facies interpreted as overlapping calci-clastic submarine fans composed of resedimented chalk. One interesting question is to what degree does bottom current reworking also impact the reservoir properties of chalks? Even if resedimented/re-worked chalk is prolific throughout the slope of regions B, C, and D, the generally low matrix permeability of chalk reservoirs remains a key risk element for the chalk play. Enhanced production techniques such as acidizing, hydraulic fracturing and multiple fracture horizontal wells are commonly required to improve production in chalk reservoirs in other jurisdictions (e.g. Ekofisk field in the North Sea).

Potential traps in the chalk play are widespread on the slope (Figures 36, 42). They include folded chalk intervals above numerous squeezed salt bodies in regions B and C (e.g. Figure 42 bottom) and turtle structures and folds above canopy salt in region D (e.g. Figure 41 middle). The burial depth of the chalk series and associated mechanical compaction and cementation remain key risk factors for reservoir quality in the chalk play (e.g. Brasher and Vagle 1996; Ings et al. 2005), though present-day burial depths above some salt crests and the distal parts of the Sable Slope Canopy are comparable to the shelf (see Deptuck and Kendell 2020).

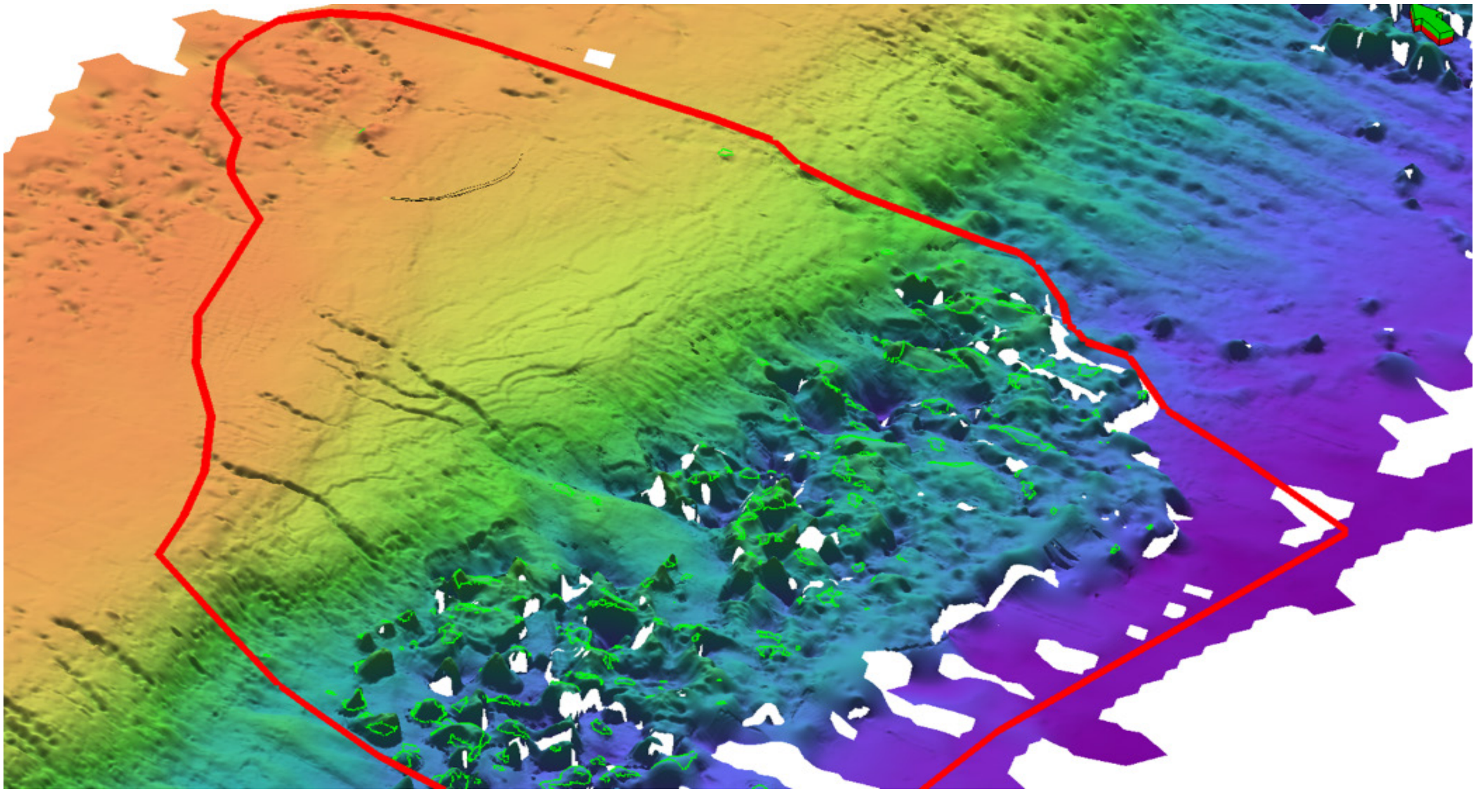

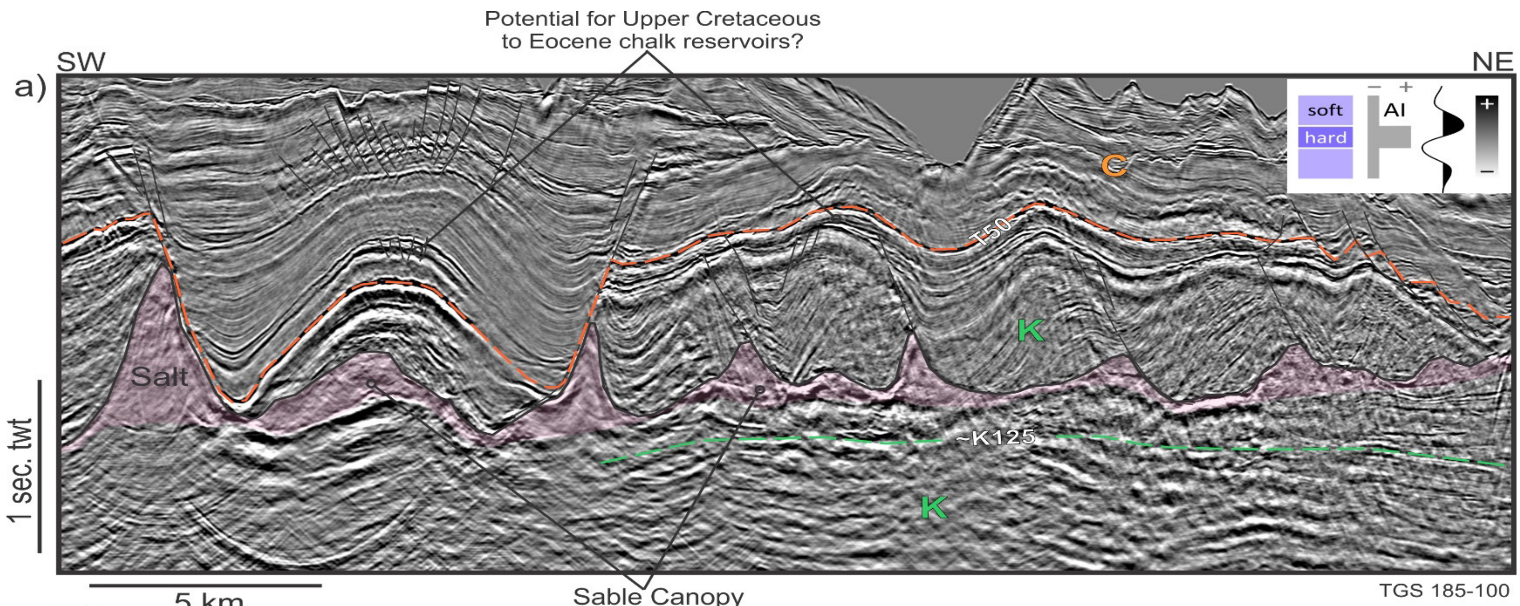


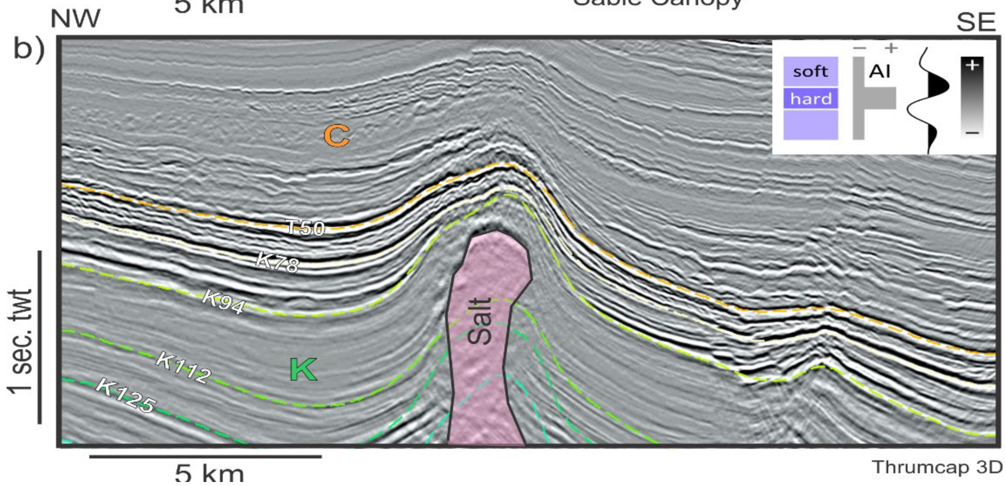


**Figure 42. (top)** Perspective view of the Early Eocene T50 marker in region D, draped by bright green polygons corresponding to four-way dip closures on the slope; **(a)** Strike seismic section (TGS 2D) across the eastern part of the Sable canopy; **(b)** Dip seismic section (Thrumcap 3D) across pre-kinematic chalk intervals folded above salt diapir (K94 to just above the T50 marker). Onlap of some bright markers implies that at least some chalks in deepwater were resedimented.

# Petroleum Resource Assessment

## *Inputs, Risking Parameters & Results*

Calculations of original hydrocarbon in place (OHIP) were conducted using the following standard volumetric equation, employed within a Monte Carlo style probabilistic simulation using the @Risk™ software:

$$OHIP = A * h * \Phi * (1-S_w) * FVF$$

| | |
|---|---|
| ***OHIP*** | = Original Hydrocarbons (Gas/Oil) in Place (m3) |
| ***A*** | = Areal extent of the accumulation ($km^2$ * 1,000,000) |
| ***h*** | = Average Net reservoir thickness for the reservoir zone (m) |
| ***Φ*** | = Average Porosity (Fraction) |
| ***$S_w$*** | = Average Water Saturation (Fraction) |
| ***FVF*** | = Formation Volume Factor (m3/m3) |

Each input variable (Table 5) was defined as triangular distributions based on minimum (P100), most likely (P50) and maximum (P00) interpreted values. The CNSOPB analysis of input parameters included a review of all available well, seismic and production data. The play areas, for each region, were based on the discounted play area method, but with areas under trap constrained, where possible, by the closure area of mapped leads in each region.

Average net reservoir thickness, average porosity and water saturation were based on the interpretation of analogous wells with values chosen accordingly (see Table 5). Where it was believed there was potential for the play to work at multiple stratigraphic intervals (e.g. stacked reservoirs) the net reservoir input parameters were selected accordingly. Formation Volume Factor was determined based on the interpreted depth and pressure of the reservoir interval(s) supported by data from analogous wells.

*Risking –* In addition to the volumetric inputs above, an evaluation of the risk in each of the key petroleum system elements (source, reservoir, trap and seal) was assigned at both the play and prospect level for each play type (Table 6). Play risk was determined by evaluating the risk of each petroleum system element (source, reservoir trap and seal) “working” at the play level. A second level of risk (Prospect risk) was applied to all the “successful” @Risk simulation runs. Prospect risk is applied on the assumption that the play is working geologically and is determined by considering source, reservoir, trap, and seal risk at the lead (prospect) level within a play. The play and prospect risks applied to each play type are shown in Table 6. Just eight of the 44 plays have a chance of success greater than 10%, all of which are found in regions D and E and include both proven plays like rollover anticlines on the shelf, and technically successful plays like Cretaceous turtles and folds above both primary and canopy salt (e.g. hydrocarbon charged reservoirs encountered at Newburn H-23 and Annapolis G-24; Figure 1c).

## *Petroleum Resource Estimates*

Petroleum resource estimates for the six geographic regions are presented in tables 9 to 14. Petroleum resource estimates for each of the 44 individual play types are presented in Appendices 1 to 6. All resource estimate tables include the P90, P50, P10 and mean calculated volumes for natural gas, natural gas liquids and barrels of oil equivalent. In addition to resource estimates, a probability curve for the mean fully risked recoverable volumes are shown beneath each table, in million barrels of oil equivalent (MMBOE). The total mean, fully risked recoverable petroleum resource estimate for the study area is ~48 Tcf or 10 260 MMBOE, with P10 (best case) values of ~98 Tcf or 20 458 MMBOE.

In regions with proximity to known oil shows or discoveries (see Table 3), or where the main source rock interval corresponds to the theoretically more oil-prone restricted marine Pliensbachian source rock, oil volumes were also calculated. This is mostly applicable to regions A, B and C where a Pliensbachian or older source rock is required for any play to work, but also for areas on the shelf where light oil has been encountered in region D. The total fully risked recoverable oil for the study area is 1.3 billion barrels (Mean/most likely case) to 2.9 billion barrels (P10/best case) (Table 1). The results of this study show that significant exploration potential remains along the eastern parts of the study area (regions D and E), while the high geological risk and relatively low chance of success along the western parts of the margin (regions B and C) and east of Cape Breton Island (region F) present significant exploration challenges (Figure 43).

**Figure 43.** Fully risked total <u>Mean</u> to <u>P10</u> range of the potential recoverable resource volumes for regions A through F. Note that no P10 volumes were calculated for region A (see Table 9).

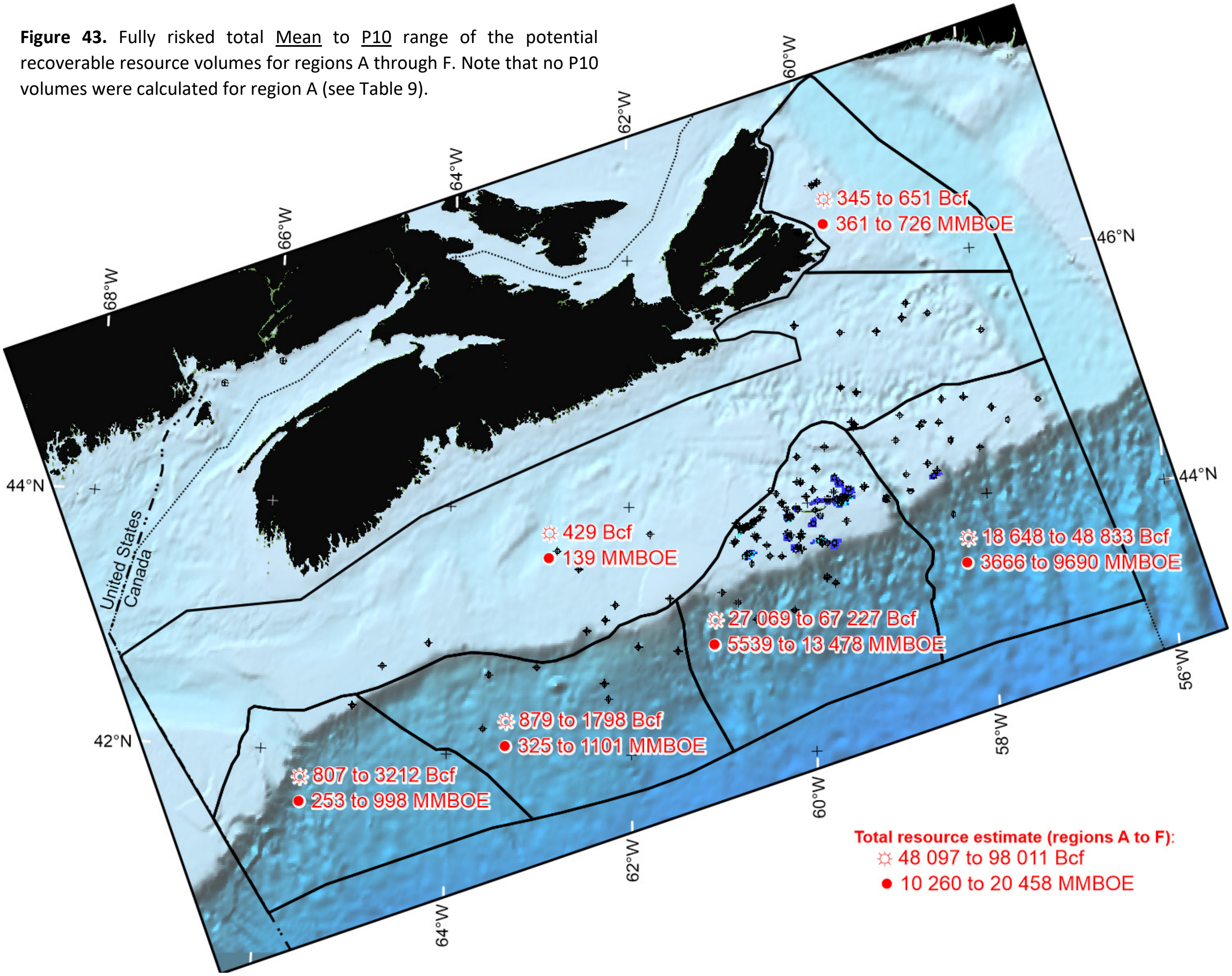


Regions D and E have the most favourable exploration potential and the lowest geological risk, accounting for 90% of the total estimated fully risked recoverable hydrocarbon volumes (based on MMBOE – see Figure 43). They also correspond to regions where oil and gas have already been discovered or produced (Figure 1 inset). Aside from the proven Jurassic and Cretaceous rollover anticline plays on the shelf, the most promissing play types in region D include Cretaceous slope turtles/folds (above primary salt), Cretaceous supra-canopy turtles/folds (above canopy salt), and Cretaceous subsalt canopy cut-offs (slope), with Mean recoverable gas of 5531, 4936, and 3763 BCF, respectively. The most promissing play types in region E include the salt-cored folds ("Banquereau fold-belt play") and the upper slope rollover anticlines ("Stonehouse play"), with Mean recoverable gas of 6355 and 3763 BCF, respectively.

Outside of regions D and E, the primary limiting factor on estimated hydrocarbon volumes is the risking profile, where some of the petroleum system elements are either missing, unclear, or reside in areas where there is an absence of good quality borehole and/or seismic data-sets. For example, listric growth faults beneath Georges Bank in region B are part of a gravity spreading system driven by progradation of the 'Shelburne Delta'. Up-slope extension above the primary salt layer was balanced down-slope by shortening, producing a variety of potential traps. Despite some similarities with the 'Sable Delta' in region D, the generally smaller aerial coverage of region B itself (31 767 km$^2$ versus 42 852 km$^2$; see Table 2), as well as individual plays within region B (e.g. P50 coverage of Cretaceous rollover anticlines is just7345 km$^2$ versus 13 929 km$^2$ in region D), coupled with the much thinner stratigraphic succession, and uncertainty about an unproven Lower Jurassic source rock, conspire to increase geological risk in region B compared to region D. As such, estimates of the unrisked recoverable mean hydrocarbon volumes in region B decrease from roughly 8.5 BBOE (Table 10) to a just 0.253 BBOE after risking (Figure 44). The lack of well control (Table 3) and generally poor seismic data quality in region B (Table 2) also increase geological uncertainty and add incremental exploration risk. It is noteworthy that one new exploration well encountering reservoir and/or hydrocarbons on the shelf or slope, would substantially improve the risk profile of region A, B, and perhaps even regions C, requiring an amendment to the reservoir and/or source rock play and prospect level risking that are likely to yield larger risked volumes. Likewise, while gas was encountered in low porosity sandstones in the Sydney Basin, if a well was drilled through higher porosity hydrocarbon charged sandstone or carbonates, geological risk in region F would show a marked decrease, with an increase in risked resource estimates. The same applies to the chalk play in regions B, C, and D, where the relatively small associated risked recoverable volumes would increase substantially with one successful slope well through higher porosity/permeability resedimented Upper Cretaceous to Eocene chalks on the slope.

Unlike region B where the absence of good quality seismic and borehole data contributed to its risk profile, region C has substantial 3D seismic coverage (see Tables 2) and was sparsely tested by seven wells, including two of the three most recent exploration wells (Monterey Jack E-43 and Cheshire L-97). Improved data quality and coverage reduce the geological uncertainty in region C, but bolsters the interpretation that reservoir presence is a key risk factor. Interpretation of 3D seismic volumes show little evidence for the accumulation of coarser grained Cretaceous turbidite reservoirs prior to the Late Albian, when fluvial-deltaic sediments in the westernmost Sable Delta had not yet reached the bank edge along the eastern reaches of the Shelburne Subbasin (Deptuck and Kendell 2020; 2022).

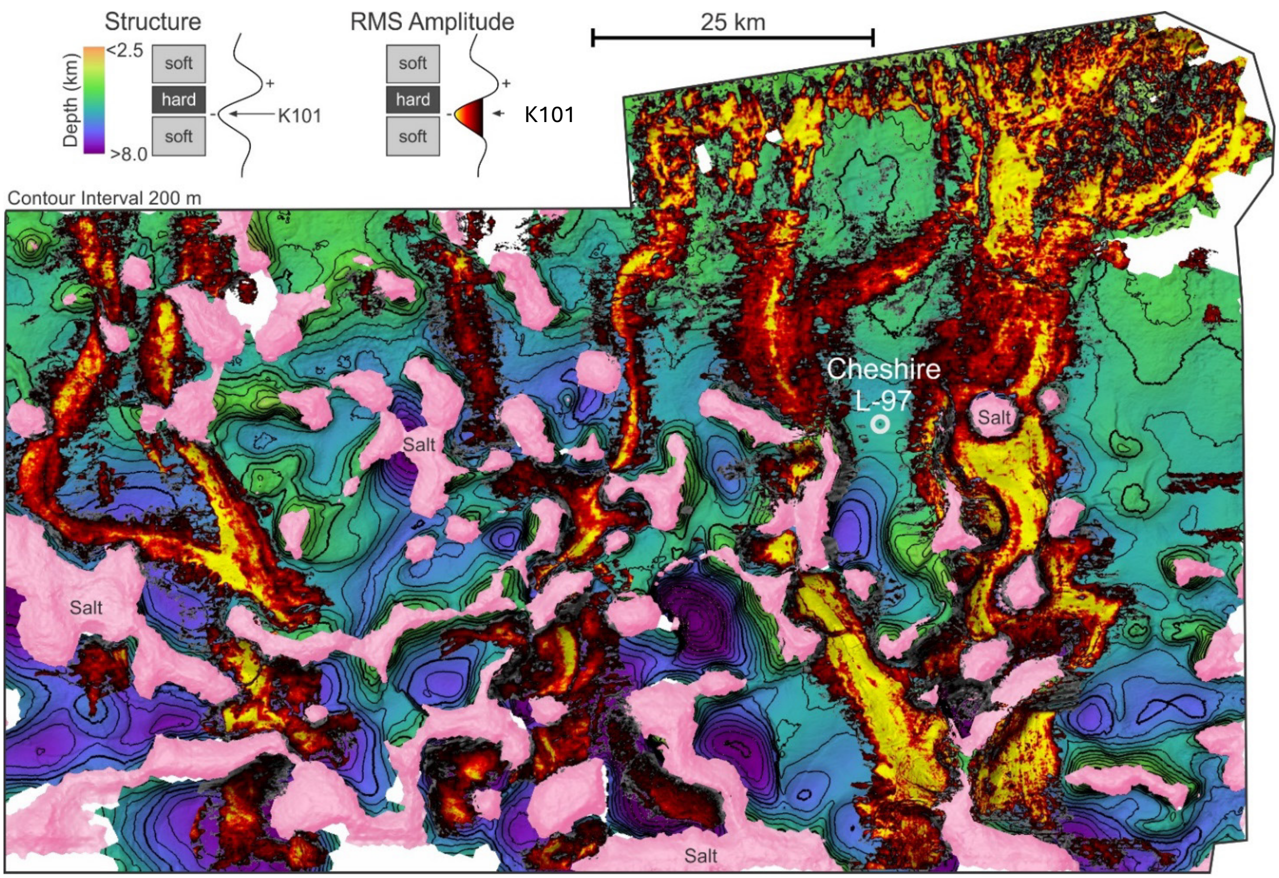


**Figure 44.** Depth-structure map of the Late Albian K101 marker in the eastern parts of region C, draped by an RMS amplitude extraction showing the elevated amplitudes along the axes of broad, bottom current reworked slope channels in the Shelburne and Torbrook 3D seismic volumes. Salt piercement through the K101 marker shown in pink. Note the position of Cheshire L-97 between two of these channels. See figure 40 for location (adapted from Deptuck and Kendell 2020).

Even still, most reservoirs are expected to be restricted to the axes of mainly non-aggradational slope channels rather than slope aprons (e.g. see the amplitude extraction from the Late Albian K101 marker in Figure 44), and the impact of bottom current reworking remains unclear.

**Table 6.** Summary of play and prospect risking used in regions A through F. Plays with total chance of success/risk higher than 10% are highlighted in red.

| | Play Risk | | | | | Prospect Risk | | | | | |
|---|---|---|---|---|---|---|---|---|---|---|---|
| | *Play Risk* | Reservoir | Source | Trap | Seal | *Prospect Risk* | Reservoir | Source | Trap | Seal | *Total Risk* |
| **A. LaHave Platform** | | | | | | | | | | | |
| **a.** Pre-salt Triassic syntectonic rotated fbs & inversions | ***0.06*** | 0.60 | 0.30 | 0.60 | 0.60 | ***0.04*** | 0.50 | 0.30 | 0.50 | 0.50 | ***0.002*** |
| **b.** Carboniferous(?) post-Windsor turtles | ***0.12*** | 0.50 | 0.50 | 0.80 | 0.60 | ***0.09*** | 0.50 | 0.50 | 0.70 | 0.50 | ***0.011*** |
| **c.** Carboniferous(?) pre-Windsor fault blocks & inversions | ***0.11*** | 0.50 | 0.50 | 0.70 | 0.60 | ***0.09*** | 0.50 | 0.50 | 0.60 | 0.60 | ***0.009*** |
| **d.** Cretaceous fault rollovers and forced folds | ***0.26*** | 1.00 | 0.75 | 0.70 | 0.50 | ***0.22*** | 0.90 | 0.70 | 0.70 | 0.50 | ***0.058*** |
| **B. West Shelburne Corridor** | | | | | | | | | | | |
| **a.** Pre-salt Triassic syntectonic rotated fbs & inversions | ***0.06*** | 0.60 | 0.30 | 0.60 | 0.60 | ***0.04*** | 0.50 | 0.30 | 0.50 | 0.50 | ***0.002*** |
| **b.** Jurassic listric fault rollovers (shelf) | ***0.26*** | 0.80 | 0.50 | 0.80 | 0.80 | ***0.17*** | 0.70 | 0.50 | 0.70 | 0.70 | ***0.044*** |
| **c.** Cretaceous listric fault rollovers (shelf) | ***0.26*** | 0.80 | 0.50 | 0.80 | 0.80 | ***0.18*** | 0.70 | 0.50 | 0.70 | 0.75 | ***0.047*** |
| **d.** Upper Jurassic Subsalt canopy cutoff | ***0.18*** | 0.65 | 0.50 | 0.70 | 0.80 | ***0.14*** | 0.60 | 0.50 | 0.60 | 0.80 | ***0.026*** |
| **e.** Cretaceous stratigraphic onlap traps | ***0.17*** | 0.80 | 0.50 | 0.70 | 0.60 | ***0.15*** | 0.70 | 0.50 | 0.70 | 0.60 | ***0.025*** |
| **f.** Cretaceous three-way traps on diapirs flanks | ***0.22*** | 0.80 | 0.50 | 0.80 | 0.70 | ***0.16*** | 0.70 | 0.50 | 0.70 | 0.65 | ***0.036*** |
| **g.** Chalk Play - closures at T50 | ***0.25*** | 0.80 | 0.50 | 0.90 | 0.70 | ***0.13*** | 0.60 | 0.50 | 0.70 | 0.60 | ***0.032*** |
| **C. Shelburne Corridor** | | | | | | | | | | | |
| **a.** Pre-salt Triassic syntectonic rotated fbs & inversions | ***0.06*** | 0.60 | 0.30 | 0.60 | 0.60 | ***0.04*** | 0.50 | 0.30 | 0.50 | 0.50 | ***0.002*** |
| **b.** Jurassic porous carbonate bank edge (Acadia) | ***0.44*** | 0.90 | 0.60 | 0.90 | 0.90 | ***0.22*** | 0.80 | 0.50 | 0.80 | 0.70 | ***0.098*** |
| **c.** Jurassic slope turtles & folds (above primary salt) | ***0.14*** | 0.40 | 0.55 | 0.80 | 0.80 | ***0.07*** | 0.30 | 0.50 | 0.70 | 0.70 | ***0.010*** |
| **d.** Cretaceous slope turtles & folds (above primary salt) | ***0.12*** | 0.40 | 0.55 | 0.70 | 0.80 | ***0.08*** | 0.40 | 0.50 | 0.60 | 0.70 | ***0.010*** |
| **e.** Cretaceous stratigraphic onlap traps (carb. foreslope) | ***0.16*** | 0.70 | 0.55 | 0.70 | 0.60 | ***0.11*** | 0.60 | 0.50 | 0.60 | 0.60 | ***0.017*** |
| **f.** Cretaceous three-way traps on diapirs flanks | ***0.09*** | 0.40 | 0.55 | 0.60 | 0.70 | ***0.06*** | 0.40 | 0.50 | 0.50 | 0.60 | ***0.006*** |
| **g.** Chalk Play - closures at T50 | ***0.28*** | 0.80 | 0.55 | 0.90 | 0.70 | ***0.14*** | 0.60 | 0.50 | 0.80 | 0.60 | ***0.040*** |
| **D. Abenaki-Sable Corridor** | | | | | | | | | | | |
| **a.** Pre-salt Triassic syntectonic rotated fb & inversions | ***0.06*** | 0.60 | 0.30 | 0.60 | 0.60 | ***0.04*** | 0.50 | 0.30 | 0.50 | 0.50 | ***0.002*** |
| **b.** Upper Mic Mac to Missisauga listric rollovers & folds | ***1.00*** | 1.00 | 1.00 | 1.00 | 1.00 | ***0.32*** | 0.90 | 1.00 | 0.70 | 0.50 | ***0.315*** |
| **c.** Logan Canyon listric fault rollovers & folds | ***1.00*** | 1.00 | 1.00 | 1.00 | 1.00 | ***0.18*** | 0.75 | 1.00 | 0.60 | 0.40 | ***0.180*** |
| **d.** Jurassic porous carbonate bank edge (Panuke) | ***1.00*** | 1.00 | 1.00 | 1.00 | 1.00 | ***0.26*** | 0.60 | 0.90 | 0.60 | 0.80 | ***0.259*** |
| **e.** Upper Jurassic to Cretaceous strat onlap traps | ***0.31*** | 0.80 | 0.80 | 0.70 | 0.70 | ***0.10*** | 0.60 | 0.80 | 0.40 | 0.50 | ***0.030*** |
| **f1.** Upper Jurassic subsalt canopy cut-off (shelf) | ***0.29*** | 0.60 | 0.90 | 0.60 | 0.90 | ***0.12*** | 0.40 | 0.75 | 0.60 | 0.65 | ***0.034*** |
| **f2.** Cretaceous subsalt canopy cut-off (slope) | ***0.36*** | 0.80 | 0.75 | 0.60 | 1.00 | ***0.20*** | 0.65 | 0.70 | 0.60 | 0.75 | ***0.074*** |
| **g.** Jurassic slope turtles & folds (above primary salt) | ***0.32*** | 0.50 | 0.80 | 0.90 | 0.90 | ***0.17*** | 0.50 | 0.70 | 0.80 | 0.60 | ***0.054*** |
| **h.** Cretaceous slope turtles & folds (above primary salt) | ***0.66*** | 0.90 | 0.90 | 0.90 | 0.90 | ***0.24*** | 0.60 | 0.80 | 0.70 | 0.70 | ***0.154*** |
| **i.** Cretaceous supra-canopy turtles & folds | ***0.58*** | 0.90 | 0.80 | 0.90 | 0.90 | ***0.21*** | 0.60 | 0.70 | 0.70 | 0.70 | ***0.120*** |
| **j.** Cretaceous three-way traps on diapirs flanks | ***0.34*** | 0.80 | 0.80 | 0.75 | 0.70 | ***0.08*** | 0.45 | 0.70 | 0.50 | 0.50 | ***0.026*** |
| **k.** Chalk Play - closures at T50 | ***0.42*** | 0.90 | 0.80 | 0.90 | 0.65 | ***0.19*** | 0.60 | 0.75 | 0.70 | 0.60 | ***0.080*** |
| **E. Huron Corridor** | | | | | | | | | | | |
| **a.** Upper Jurassic listric fault rollovers (shelf) | ***0.37*** | 0.80 | 0.90 | 0.80 | 0.65 | ***0.13*** | 0.80 | 0.80 | 0.60 | 0.35 | ***0.050*** |
| **b.** Missisauga listric fault rollovers & folds | ***1.00*** | 1.00 | 1.00 | 1.00 | 1.00 | ***0.24*** | 0.90 | 0.90 | 0.60 | 0.50 | ***0.243*** |
| **c.** Logan Canyon listric fault rollovers & folds | ***0.81*** | 0.95 | 0.95 | 0.95 | 0.95 | ***0.09*** | 0.70 | 0.90 | 0.50 | 0.30 | ***0.077*** |
| **d.** Upper Jurassic large upper slope folds | ***0.45*** | 0.70 | 0.80 | 0.90 | 0.90 | ***0.17*** | 0.50 | 0.70 | 0.80 | 0.60 | ***0.076*** |
| **e.** Cretaceous large upper slope folds (Stonehouse trend) | ***0.54*** | 0.75 | 0.90 | 1.00 | 0.80 | ***0.35*** | 0.60 | 0.80 | 0.90 | 0.80 | ***0.187*** |
| **f.** Jurassic supra-canopy turtles & folds (within BSW) | ***0.44*** | 0.70 | 0.70 | 1.00 | 0.90 | ***0.18*** | 0.55 | 0.70 | 0.80 | 0.60 | ***0.081*** |
| **g.** Cretaceous supra-canopy turtles & folds (W Laurent.) | ***0.40*** | 0.80 | 0.70 | 0.90 | 0.80 | ***0.21*** | 0.70 | 0.60 | 0.70 | 0.70 | ***0.083*** |
| **h.** Cretaceous fold-belt (Banquereau foldbelt) | ***0.48*** | 0.85 | 0.70 | 1.00 | 0.80 | ***0.25*** | 0.70 | 0.70 | 0.85 | 0.60 | ***0.119*** |
| **i.** Cretaceous subsalt canopy cuttoff (West Laurentian) | ***0.32*** | 0.70 | 0.90 | 0.50 | 1.00 | ***0.11*** | 0.60 | 0.60 | 0.40 | 0.75 | ***0.034*** |
| **j.** Cretaceous stratigraphic onlap traps (seaward of BSW) | ***0.33*** | 0.85 | 0.70 | 0.70 | 0.80 | ***0.12*** | 0.70 | 0.70 | 0.40 | 0.60 | ***0.039*** |
| **k.** Three-way closures on diapir flanks | ***0.31*** | 0.70 | 0.75 | 0.85 | 0.70 | ***0.13*** | 0.60 | 0.70 | 0.60 | 0.50 | ***0.039*** |
| **F. Sydney Basin** | | | | | | | | | | | |
| **a.** Horton fault blocks | ***0.20*** | 0.60 | 0.70 | 0.80 | 0.60 | ***0.15*** | 0.50 | 0.70 | 0.70 | 0.60 | ***0.030*** |
| **b.** Carboniferous inversion folds | ***0.36*** | 0.70 | 0.80 | 0.80 | 0.80 | ***0.24*** | 0.60 | 0.70 | 0.80 | 0.70 | ***0.084*** |
| **c.** Windsor Reefs | ***0.17*** | 0.60 | 0.80 | 0.50 | 0.70 | ***0.12*** | 0.50 | 0.80 | 0.50 | 0.60 | ***0.020*** |

**Table 7.** Summary of fully risked in place and recoverable gas and oil for each of the 44 play types (Mean).

| | Gas | | Oil | |
|---|---|---|---|---|
| | *Fully Risked GIP (BCF) Mean* | *Fully Risked Recov. (BCF) Mean* | *Fully Risked OIP (MMBbls) Mean* | *Fully Risked Recov. (MMBbls) Mean* |
| **A. LaHave Platform** | | | | |
| **a.** Pre-salt Triassic syntectonic rotated fbs & inversions | 21 | 16 | 7 | 2 |
| **b.** Carboniferous(?) post-Windsor turtles | 9 | 3 | 7 | 2 |
| **c.** Carboniferous(?) pre-Windsor fault blocks & inversions | 12 | 4 | 10 | 2 |
| **d.** Cretaceous fault rollovers and forced folds | 553 | 414 | 121 | 42 |
| **B. West Shelburne Corridor** | | | | |
| **a.** Pre-salt Triassic syntectonic rotated fbs & inversions | 7 | 5 | 2 | 1 |
| **b.** Jurassic listric fault rollovers (shelf) | 203 | 122 | 40 | 12 |
| **c.** Cretaceous listric fault rollovers (shelf) | 188 | 141 | 40 | 14 |
| **d.** Upper Jurassic Subsalt canopy cutoff | 70 | 42 | 8 | 2 |
| **e.** Cretaceous stratigraphic onlap traps | 253 | 190 | 67 | 23 |
| **f.** Cretaceous three-way traps on diapirs flanks | 168 | 126 | 46 | 16 |
| **g.** Chalk Play - closures at T50 | 531 | 144 | 65 | 13 |
| **C. Shelburne Corridor** | | | | |
| **a.** Pre-salt Triassic syntectonic rotated fbs & inversions | 7 | 5 | 2 | 1 |
| **b.** Jurassic porous carbonate bank edge (Acadia) | 516 | 140 | 187 | 65 |
| **c.** Jurassic slope turtles & folds (above primary salt) | 60 | 36 | 15 | 4 |
| **d.** Cretaceous slope turtles & folds (above primary salt) | 66 | 49 | 18 | 6 |
| **e.** Cretaceous stratigraphic onlap traps (carb. foreslope) | 96 | 72 | 26 | 9 |
| **f.** Cretaceous three-way traps on diapirs flanks | 46 | 35 | 12 | 4 |
| **g.** Chalk Play - closures at T50 | 2,076 | 561 | 206 | 52 |
| **D. Abenaki-Sable Corridor** | | | | |
| **a.** Pre-salt Triassic syntectonic rotated fb & inversions | 13 | 10 | 4 | 1 |
| **b.** Upper Mic Mac to Missisauga listric rollovers & folds | 10,669 | 8,004 | 802 | 281 |
| **c.** Logan Canyon listric fault rollovers & folds | 3,743 | 2,805 | 385 | 135 |
| **d.** Jurassic porous carbonate bank edge (Panuke) | 958 | 258 | 333 | 117 |
| **e.** Upper Jurassic to Cretaceous strat onlap traps | 66 | 49 | 0 | 0 |
| **f1.** Upper Jurassic subsalt canopy cut-off (shelf) | 89 | 53 | 0 | 0 |
| **f2.** Cretaceous subsalt canopy cut-off (slope) | 5,031 | 3,763 | 0 | 0 |
| **g.** Jurassic slope turtles & folds (above primary salt) | 1,024 | 615 | 0 | 0 |
| **h.** Cretaceous slope turtles & folds (above primary salt) | 7,093 | 5,331 | 0 | 0 |
| **i.** Cretaceous supra-canopy turtles & folds | 6,587 | 4,936 | 0 | 0 |
| **j.** Cretaceous three-way traps on diapirs flanks | 364 | 273 | 0 | 0 |
| **k.** Chalk Play - closures at T50 | 3,269 | 879 | 0 | 0 |
| **E. Huron Corridor** | | | | |
| **a.** Upper Jurassic listric fault rollovers (shelf) | 374 | 224 | 0 | 0 |
| **b.** Missisauga listric fault rollovers & folds | 4,852 | 3,637 | 0 | 0 |
| **c.** Logan Canyon listric fault rollovers & folds | 1,546 | 1,160 | 0 | 0 |
| **d.** Upper Jurassic large upper slope folds | 1,608 | 965 | 0 | 0 |
| **e.** Cretaceous large upper slope folds (Stonehouse trend) | 8,462 | 6,355 | 0 | 0 |
| **f.** Jurassic supra-canopy turtles & folds (within BSW) | 1,434 | 857 | 0 | 0 |
| **g.** Cretaceous supra-canopy turtles & folds (W Laurent.) | 868 | 652 | 0 | 0 |
| **h.** Cretaceous fold-belt (Banquereau foldbelt) | 5,012 | 3,763 | 527 | 185 |
| **i.** Cretaceous subsalt canopy cuttoff (West Laurentian) | 219 | 165 | 0 | 0 |
| **j.** Cretaceous stratigraphic onlap traps (seaward of BSW) | 337 | 253 | 36 | 13 |
| **k.** Three-way closures on diapir flanks | 769 | 579 | 87 | 30 |
| **F. Sydney Basin** | | | | |
| **a.** Horton fault blocks | 611 | 222 | 518 | 102 |
| **b.** Carboniferous inversion folds | 313 | 110 | 445 | 89 |
| **c.** Windsor Reefs | 264 | 70 | 240 | 48 |

**Table 8.** Cumulative results across the study area

| Offshore Nova Scotia - Regional Summary | | Natural Gas | | Natural Gas Liquids | | Oil Equivalent | |
|---|---|---|---|---|---|---|---|
| | | BCF | $10^9$ $m^3$ | MMB | $10^6$ $m^3$ | MMBOE | $10^6$ $m^3$ |
| In-Place Unrisked | P90 | 646,156 | 18,297 | 5,850 | 930 | 206,970 | 32,906 |
| | P50 | 717,673 | 20,322 | 6,601 | 1,049 | 231,430 | 36,794 |
| | P10 | 800,433 | 22,666 | 7,510 | 1,194 | 259,058 | 41,187 |
| | Mean | 721,883 | 20,441 | 6,650 | 1,057 | 232,707 | 36,997 |
| In-Place Fully Risked | P90 | 10,541 | 298 | 86.6 | 13.8 | 3,461 | 550 |
| | P50 | 62,169 | 1,760 | 587 | 93.3 | 15,573 | 2,476 |
| | P10 | 139,593 | 3,953 | 1,344 | 214 | 35,344 | 5,619 |
| | Mean | 70,424 | 1,994 | 669 | 106 | 17,962 | 2,856 |
| Recoverable Unrisked | P90 | 403,292 | 11,420 | 3,838 | 610 | 98,557 | 15,669 |
| | P50 | 452,503 | 12,813 | 4,360 | 693 | 109,454 | 17,402 |
| | P10 | 511,536 | 14,485 | 5,026 | 799 | 122,624 | 19,496 |
| | Mean | 455,454 | 12,897 | 4,403 | 700 | 110,043 | 17,495 |
| Recoverable Fully Risked | P90 | 6,050 | 171 | 54.8 | 8.71 | 1,707 | 271 |
| | P50 | 41,870 | 1,186 | 411 | 65.3 | 8,990 | 1,429 |
| | P10 | 98,011 | 2,775 | 972 | 155 | 20,458 | 3,253 |
| | Mean | 48,097 | 1,362 | 473 | 75.2 | 10,260 | 1,631 |

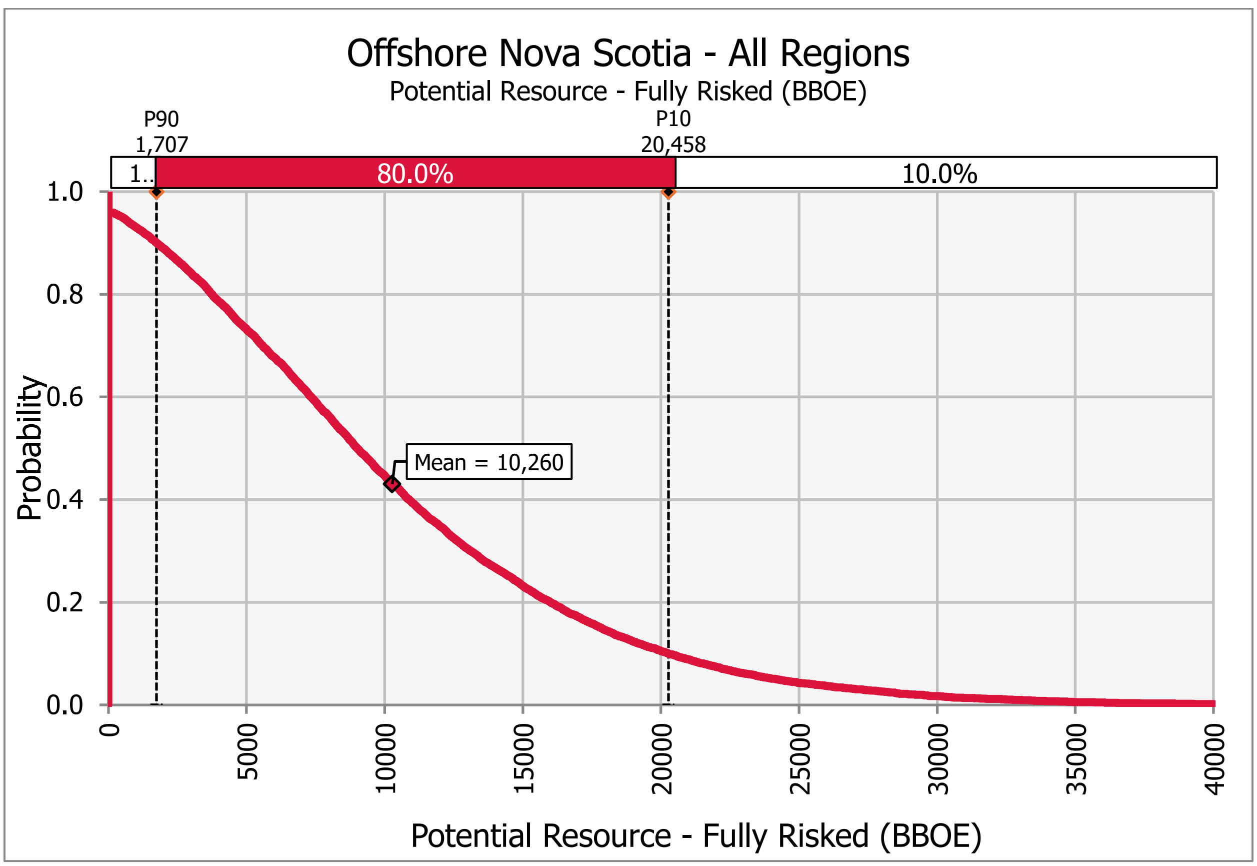

**Table 9.** Cumulative results across Region A.

| LaHave Platform Summary | | Natural Gas | | Natural Gas Liquids | | Oil Equivalent | |
|---|---|---|---|---|---|---|---|
| | | BCF | $10^9\ m^3$ | MMB | $10^6\ m^3$ | MMBOE | $10^6\ m^3$ |
| In-Place Unrisked | P90 | 14,174 | 401 | 136 | 21.6 | 8,685 | 1,381 |
| | P50 | 19,472 | 551 | 192 | 30.6 | 11,491 | 1,827 |
| | P10 | 27,311 | 773 | 280 | 44.4 | 15,308 | 2,434 |
| | Mean | 20,246 | 573 | 202 | 32.2 | 11,813 | 1,878 |
| In-Place Fully Risked | P90 | - | - | - | - | - | - |
| | P50 | - | - | - | - | - | - |
| | P10 | - | - | - | - | - | - |
| | Mean | 625 | 17.7 | 5.90 | 0.94 | 283 | 45.0 |
| Recoverable Unrisked | P90 | 9,817 | 278 | 93.3 | 14.8 | 3,622 | 576 |
| | P50 | 13,720 | 389 | 136 | 21.5 | 4,933 | 784 |
| | P10 | 19,466 | 551 | 202 | 32.2 | 6,764 | 1,075 |
| | Mean | 14,317 | 405 | 143 | 22.7 | 5,098 | 810 |
| Recoverable Fully Risked | P90 | - | - | - | - | - | - |
| | P50 | - | - | - | - | - | - |
| | P10 | - | - | - | - | - | - |
| | Mean | 429 | 12.1 | 4.43 | 0.70 | 139 | 22.1 |

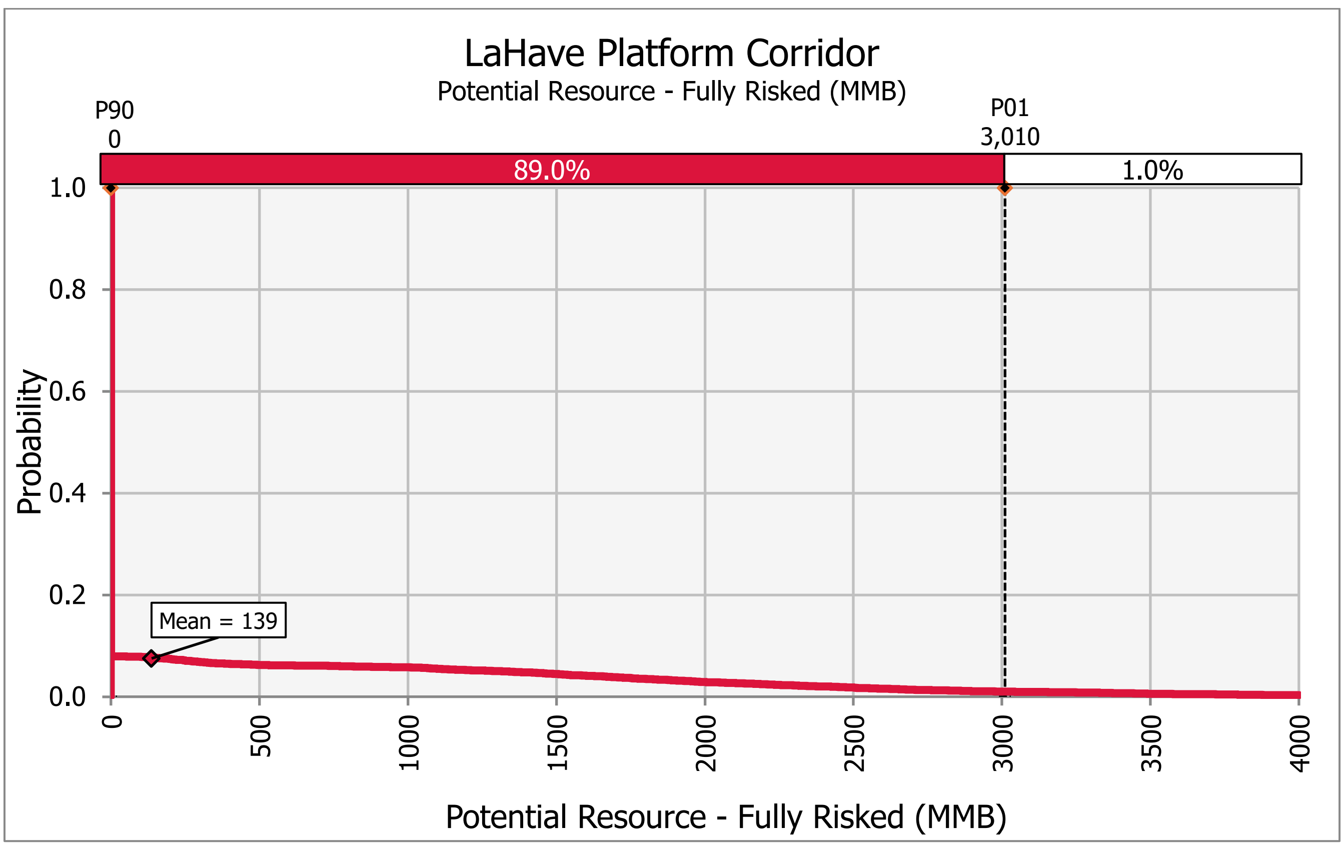

**Table 10.** Cumulative results across Region B.

| | | West Shelburne Summary | | | | | |
|---|---|---|---|---|---|---|---|
| | | Natural Gas | | Natural Gas Liquids | | Oil Equivalent | |
| | | BCF | $10^9$ $m^3$ | MMB | $10^6$ $m^3$ | MMBOE | $10^6$ $m^3$ |
| In-Place Unrisked | P90 | 37,865 | 1,072 | 237 | 37.7 | 16,093 | 2,559 |
| | P50 | 47,237 | 1,338 | 379 | 60.2 | 20,076 | 3,192 |
| | P10 | 59,783 | 1,693 | 632 | 100 | 25,359 | 4,032 |
| | Mean | 48,236 | 1,366 | 414 | 65.8 | 20,480 | 3,256 |
| In-Place Fully Risked | P90 | - | - | - | - | - | - |
| | P50 | - | - | - | - | - | - |
| | P10 | 5,025 | 142 | 39.6 | 6.29 | 2,269 | 361 |
| | Mean | 1,515 | 42.9 | 12.70 | 2.02 | 617 | 98.1 |
| Recoverable Unrisked | P90 | 20,898 | 592 | 143.1 | 22.7 | 6,650 | 1,057 |
| | P50 | 26,377 | 747 | 228 | 36.2 | 8,375 | 1,331 |
| | P10 | 33,468 | 948 | 380 | 60.4 | 10,614 | 1,687 |
| | Mean | 26,842 | 760 | 250 | 39.8 | 8,538 | 1,357 |
| Recoverable Fully Risked | P90 | - | - | - | - | - | - |
| | P50 | - | - | - | - | - | - |
| | P10 | 3,212 | 91.0 | 24.7 | 3.93 | 998 | 159 |
| | Mean | 807 | 22.9 | 8.11 | 1.29 | 253 | 40.3 |

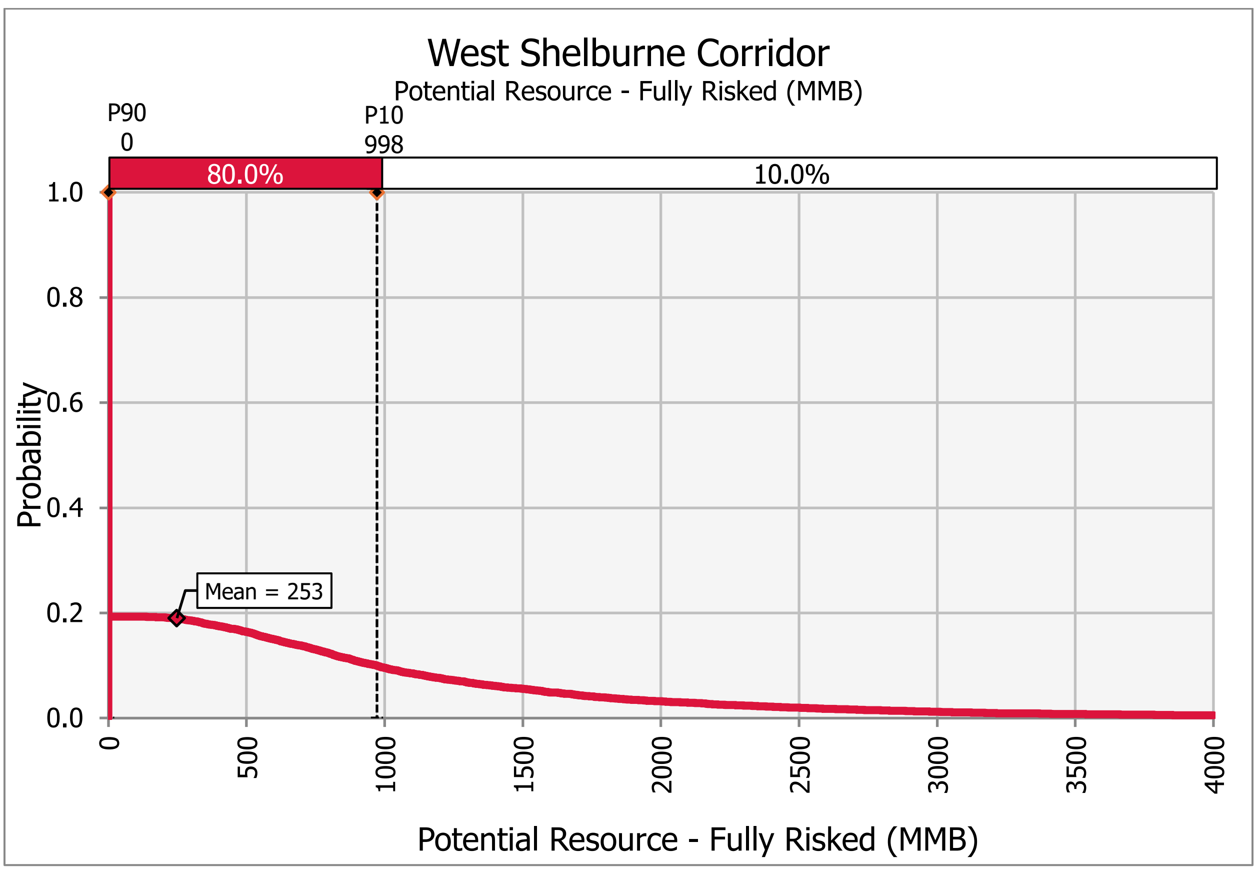

**Table 11.** Cumulative results across Region C.

| | | Shelburne Summary | | | | | |
|---|---|---|---|---|---|---|---|
| | | Natural Gas | | Natural Gas Liquids | | Oil Equivalent | |
| | | BCF | $10^9$ $m^3$ | MMB | $10^6$ $m^3$ | MMBOE | $10^6$ $m^3$ |
| In-Place Unrisked | P90 | 67,408 | 1,909 | 498 | 79.2 | 29,593 | 4,705 |
| | P50 | 87,794 | 2,486 | 645 | 103 | 37,278 | 5,927 |
| | P10 | 117,506 | 3,327 | 861 | 137 | 48,260 | 7,673 |
| | Mean | 90,658 | 2,567 | 666 | 106 | 38,274 | 6,085 |
| In-Place Fully Risked | P90 | - | - | - | - | - | - |
| | P50 | - | - | - | - | - | - |
| | P10 | 5,241 | 148 | 27.0 | 4.30 | 3,174 | 505 |
| | Mean | 2,848 | 80.6 | 18.2 | 2.90 | 1,201 | 191 |
| Recoverable Unrisked | P90 | 30,280 | 857 | 253 | 40.2 | 10,667 | 1,696 |
| | P50 | 38,228 | 1,083 | 323 | 51.3 | 13,153 | 2,091 |
| | P10 | 49,679 | 1,407 | 415 | 65.9 | 16,449 | 2,615 |
| | Mean | 39,409 | 1,116 | 330 | 52.5 | 13,404 | 2,131 |
| Recoverable Fully Risked | P90 | - | - | - | - | - | - |
| | P50 | - | - | - | - | - | - |
| | P10 | 1,798 | 50.9 | 8.06 | 1.28 | 1,101 | 175 |
| | Mean | 879 | 24.9 | 5.88 | 0.935 | 325 | 51.6 |

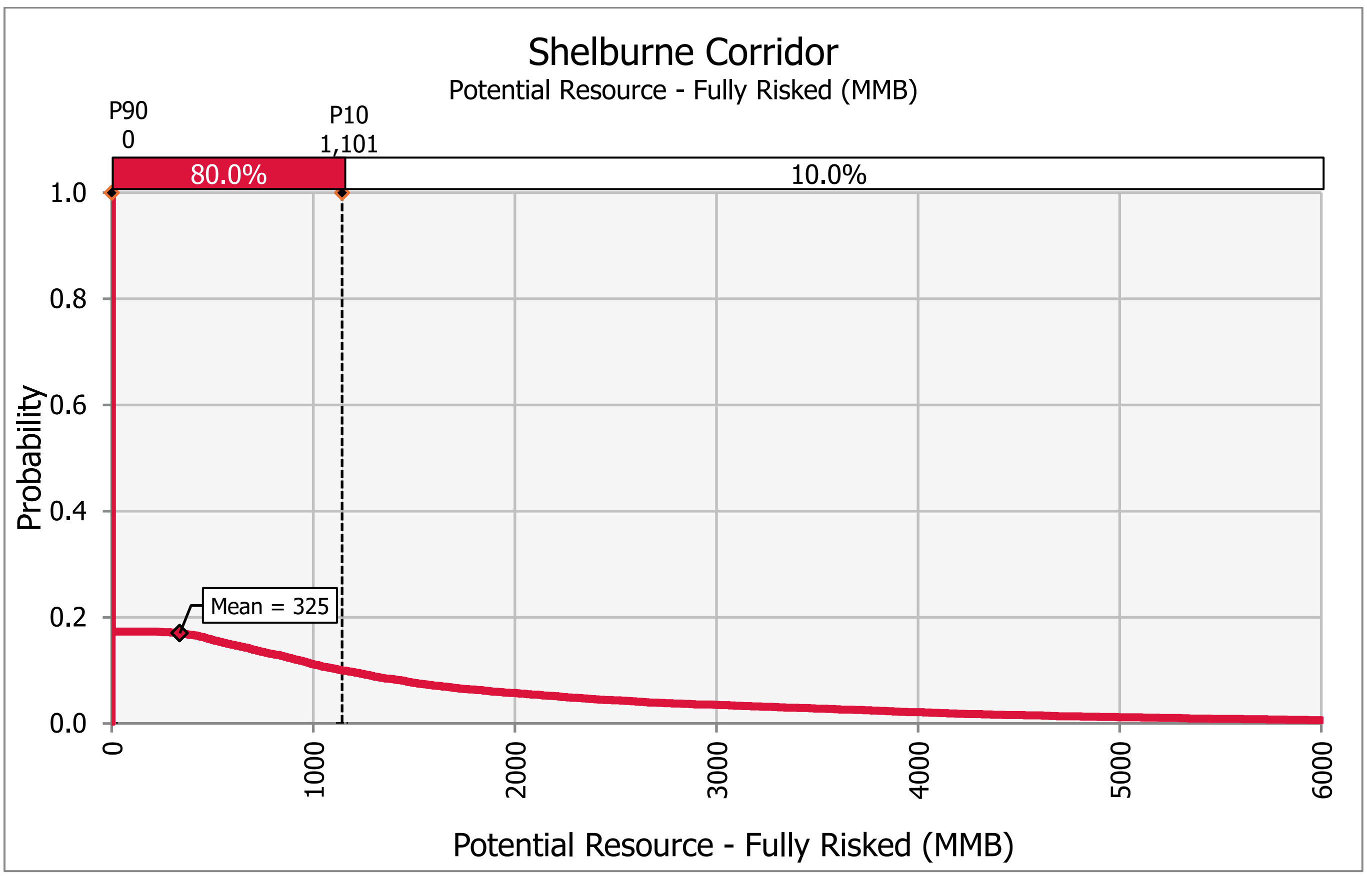

**Table 12.** Cumulative results across Region D.

| | | Abenaki-Sable Corridor Summary | | | | | |
|---|---|---|---|---|---|---|---|
| | | Natural Gas | | Natural Gas Liquids | | Oil Equivalent | |
| | | BCF | $10^9$ $m^3$ | MMB | $10^6$ $m^3$ | MMBOE | $10^6$ $m^3$ |
| In-Place Unrisked | P90 | 252,556 | 7,152 | 2,272 | 361 | 53,532 | 8,511 |
| | P50 | 304,762 | 8,630 | 2,851 | 453 | 64,009 | 10,177 |
| | P10 | 369,370 | 10,459 | 3,589 | 571 | 76,990 | 12,240 |
| | Mean | 309,049 | 8,751 | 2,905 | 462 | 64,769 | 10,297 |
| In-Place Fully Risked | P90 | - | - | - | - | - | - |
| | P50 | 29,190 | 827 | 271 | 43.1 | 7,363 | 1,171 |
| | P10 | 95,285 | 2,698 | 923 | 147 | 20,548 | 3,267 |
| | Mean | 38,778 | 1,098 | 374.00 | 59.5 | 8,886 | 1,413 |
| Recoverable Unrisked | P90 | 165,751 | 4,694 | 1,562 | 248 | 32,881 | 5,228 |
| | P50 | 203,746 | 5,769 | 1,972 | 313 | 40,053 | 6,368 |
| | P10 | 252,432 | 7,148 | 2,539 | 404 | 49,479 | 7,866 |
| | Mean | 206,920 | 5,859 | 2,020 | 321 | 40,700 | 6,471 |
| Recoverable Fully Risked | P90 | - | - | - | - | - | - |
| | P50 | 19,343 | 548 | 184 | 29.2 | 4,276 | 680 |
| | P10 | 67,227 | 1,904 | 667 | 106 | 13,478 | 2,143 |
| | Mean | 27,069 | 767 | 263 | 41.9 | 5,539 | 881 |

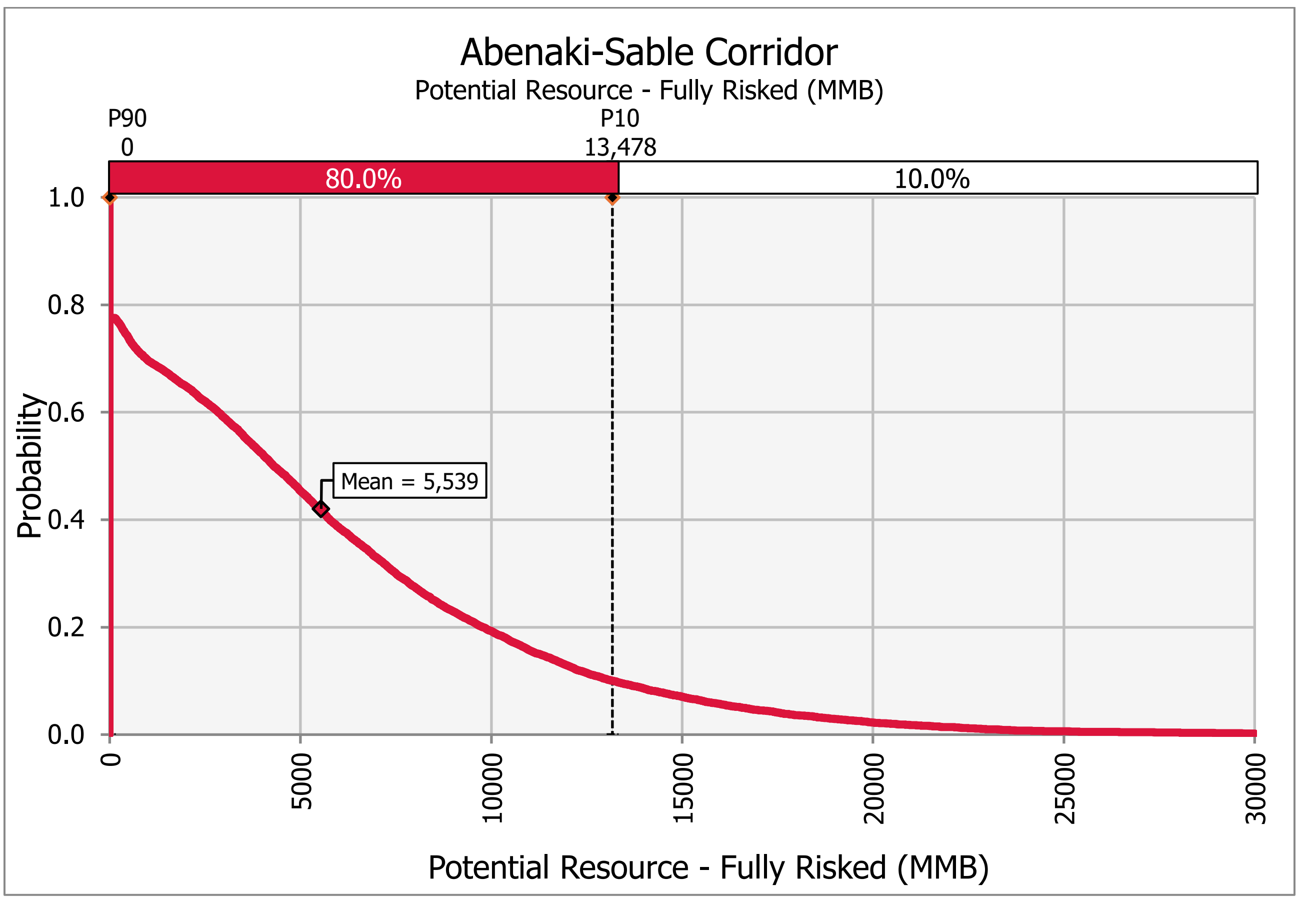

**Table 13.** Cumulative results across Region E.

| | | Huron Corridor Summary | | | | | |
|---|---|---|---|---|---|---|---|
| | | Natural Gas | | Natural Gas Liquids | | Oil Equivalent | |
| | | BCF | $10^9$ $m^3$ | MMB | $10^6$ $m^3$ | MMBOE | $10^6$ $m^3$ |
| In-Place Unrisked | P90 | 181,487 | 5,139 | 1,767 | 281 | 40,710 | 6,472 |
| | P50 | 215,339 | 6,098 | 2,142 | 341 | 48,750 | 7,751 |
| | P10 | 256,233 | 7,256 | 2,628 | 418 | 58,753 | 9,341 |
| | Mean | 217,616 | 6,162 | 2,176 | 346 | 49,400 | 7,854 |
| In-Place Fully Risked | P90 | - | - | - | - | - | - |
| | P50 | 17,550 | 497 | 174 | 27.6 | 3,325 | 529 |
| | P10 | 66,809 | 1,892 | 652 | 104 | 14,528 | 2,310 |
| | Mean | 25,596 | 725 | 253 | 40.3 | 5,465 | 868.8 |
| Recoverable Unrisked | P90 | 130,075 | 3,683 | 1,262 | 201 | 26,466 | 4,208 |
| | P50 | 154,474 | 4,374 | 1,538 | 245 | 31,455 | 5,001 |
| | P10 | 185,025 | 5,239 | 1,896 | 301 | 38,026 | 6,046 |
| | Mean | 156,383 | 4,428 | 1,563 | 249 | 31,921 | 5,075 |
| Recoverable Fully Risked | P90 | - | - | - | - | - | - |
| | P50 | 12,776 | 362 | 123 | 19.6 | 2,316 | 368 |
| | P10 | 48,833 | 1,383 | 484 | 76.9 | 9,690 | 1,541 |
| | Mean | 18,648 | 528 | 186 | 29.6 | 3,666 | 583 |

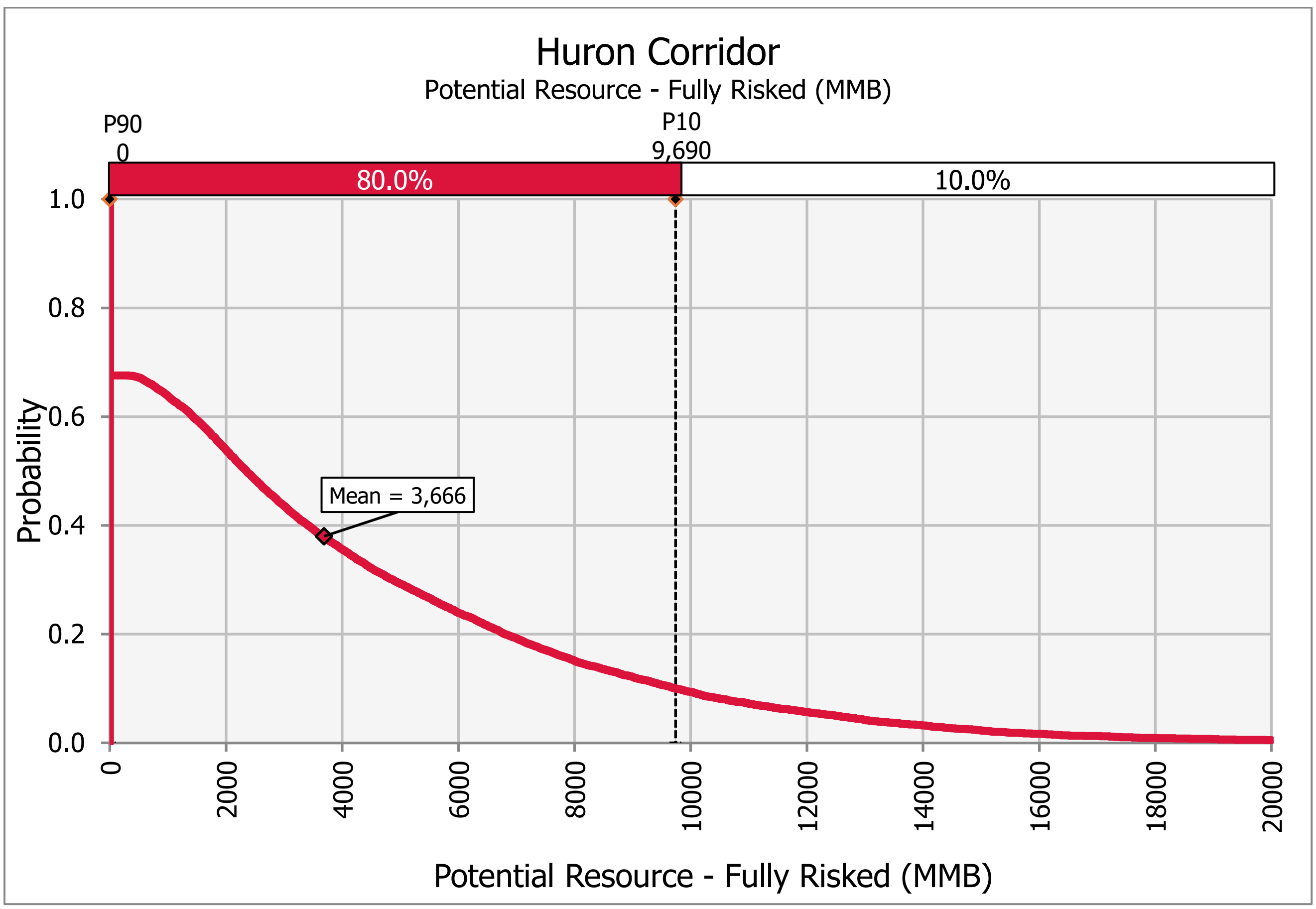

**Table 14.** Cumulative results across Region F.

| | | Sydney Basin Summary | | | | | |
|---|---|---|---|---|---|---|---|
| | | Natural Gas | | Natural Gas Liquids | | Oil Equivalent | |
| | | BCF | $10^9$ $m^3$ | MMB | $10^6$ $m^3$ | MMBOE | $10^6$ $m^3$ |
| In-Place Unrisked | P90 | 15,073 | 427 | 113 | 17.9 | 20,850 | 3,315 |
| | P50 | 30,215 | 856 | 232 | 36.8 | 40,596 | 6,454 |
| | P10 | 63,296 | 1,792 | 514 | 81.8 | 83,086 | 13,210 |
| | Mean | 36,070 | 1,021 | 286 | 45.4 | 47,968 | 7,626 |
| In-Place Fully Risked | P90 | - | - | - | - | - | - |
| | P50 | - | - | - | - | - | - |
| | P10 | 2,160 | 61.2 | 20.3 | 3.23 | 3,520 | 560 |
| | Mean | 1,211 | 34.3 | 11.0 | 1.75 | 1,729 | 275 |
| Recoverable Unrisked | P90 | 4,806 | 136 | 37.2 | 5.91 | 4,414 | 702 |
| | P50 | 9,700 | 275 | 76.6 | 12.2 | 8,752 | 1,392 |
| | P10 | 20,357 | 576 | 176 | 28.0 | 18,012 | 2,864 |
| | Mean | 11,591 | 328 | 95.9 | 15.2 | 10,387 | 1,651 |
| Recoverable Fully Risked | P90 | - | - | - | - | - | - |
| | P50 | - | - | - | - | - | - |
| | P10 | 651 | 18.4 | 6.26 | 1.00 | 726 | 115 |
| | Mean | 345 | 9.78 | 3.63 | 0.577 | 361 | 57.3 |

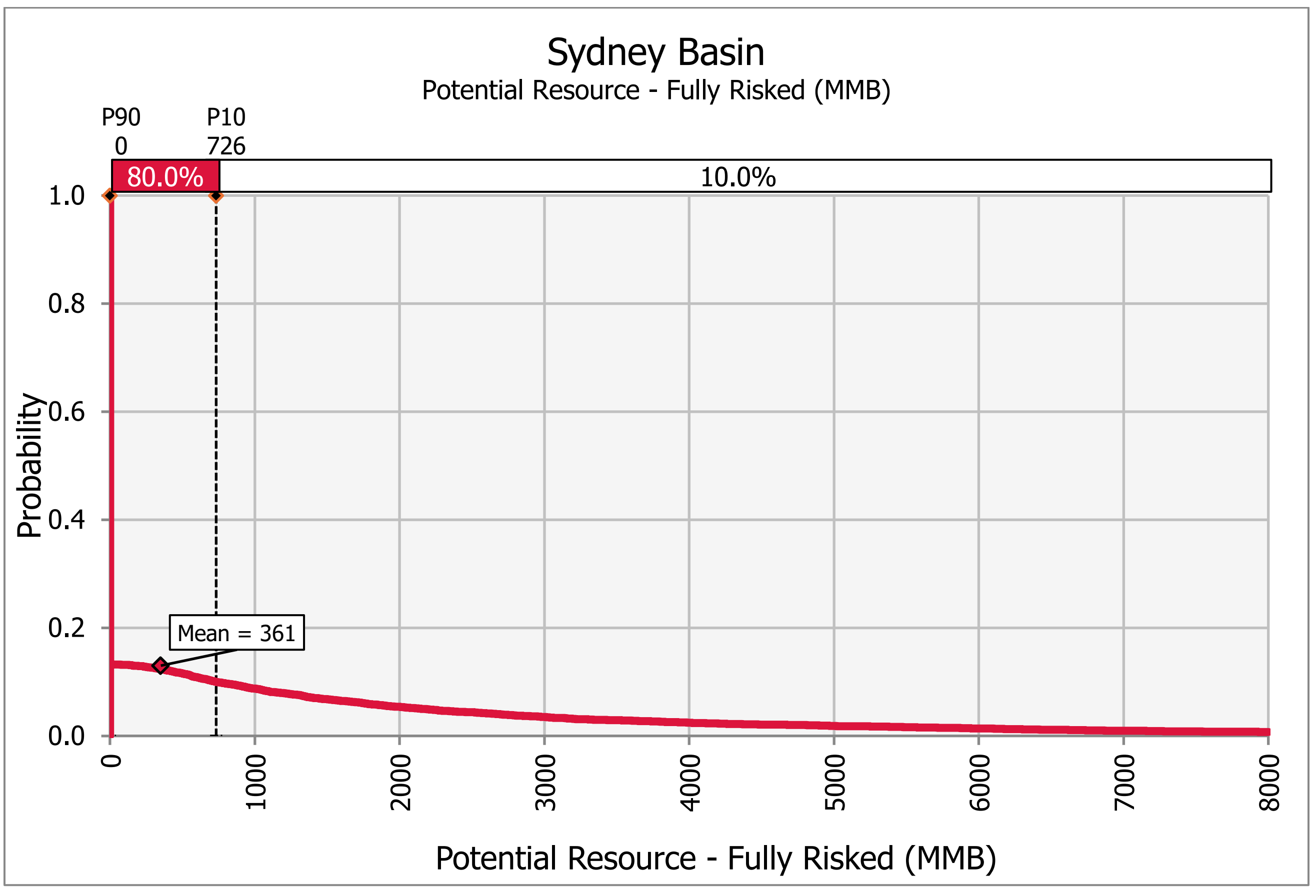

## Acknowledgements

This study benefitted from countless discussions over the past decade with former CNSOPB colleagues (Brent Smith, Dave Brown, Ehsan Belghiszadeh), numerous folks at NRCan (Calvin Campbell, Rob Fensome, Graham Williams, Sonya Dehler, David Piper, Keith Dewing, Elizabeth Atkinson, Ashley Krakowka, John Shimeld), NSDNRR (Fraser Keppie, Natasha MacAdam, Bill Richards, Sandy McMullin, Matt Luheshi), and local universities (Andrew MacRae, Vittorio Maselli, Chris Beaumont), as well as Beicip-Franlab. We also thank Matteo Niccoli for editorial feedback.

*Recommended citation:*

Deptuck, M.E., Kendell, K.L., Makrides, C., and Altheim, B. (2024) Quantitative petroleum resource assessment in the Canada-Nova Scotia Offshore Area (Scotian Shelf, Scotian Slope, and Sydney Basin), CNSOPB Geoscience Open File Report 2024-001MF, 111 p.

## References

Albertz, M., Beaumont, C., Shimeld, J. W., Ings, S. J. and Gradmann, S. (2010) An investigation of salt tectonic structural styles in the Scotian Basin, offshore Atlantic Canada: 1. Comparison of observations with geometrically simple numerical models. Tectonics, 29, TC4017. doi:10.1029/2009TC002539

Beicip-Franlab et al. (2015) South-West Nova Scotia Expansion: Georges Bank and Shelburne Subbasin Study. Nova Scotia Department of Energy Report. https://oera.ca/research/sw-nova-scotia-expansion-atlas-2015

Scotian Basin Integration Atlas (2023) A collaborative study of stratigraphy, architecture, evolution, and geological prospectivity; A technical collaboration with direct and indirect input provided by Canada-Nova Scotia Offshore Petroleum Board (CNSOPB), Leptis E&P, Stratum Reservoir, Weston Stratigraphic, APT (Canada) Ltd, Andrew MacRae, Bill Richards, and others. Atlas submitted to the Offshore Energy Research Association (OERA), and available online here: Scotian Basin Integration Atlas 2023 | Nova Scotia Offshore Energy Research Association (oera.ca)

Belghiszadeh, E. Kendell, K., Makrides, C., Rhyno, S. (2023) Sable Offshore Energy Project – Resource management study, CNSOPB Report, available at Geoscience Publications | Canada-Nova Scotia Offshore Petroleum Board (CNSOPB)

Bishop, A.N. (2020) Greater North Atlantic Liassic Petroleum Systems Synthesis, Technical Report OG-2020-01 https://oera.ca/research/greater-north-atlantic-liassic-petroleum-systems-synthesis (file downloaded in May 2020)

Brown, D.E. (2015) Lacustrine source rock potential in the Middle Triassic – Early Jurassic Chignecto Subbasin, offshore Eastern Canada. In: P.J. Post, J.L. Coleman Jr., N.C. Rosen, D.E. Brown, T. Roberts-Ashby, P. Kahn and M. Rowan (eds) Petroleum Systems in "Rift Basins", 34th Annual Gulf Coast Society – Society of Economic Paleontologists and Mineralogists Perkins-Rosen Research Conference, Houston Texas, December 13-16, 2015, p.8.

Brown, D.E. (2014) Lacustrine source rock potential in the Middle Triassic – Early Jurassic Chignecto Subbasin, offshore Eastern Canada. Geological Association of Canada/ Mineralogical Association of Canada Annual Meeting, University of New Brunswick, Fredericton, New Brunswick, May 21-23, 2014.

Campbell, D.C., Shimeld, J., Deptuck, M.E., Mosher, D.C. (2015) Seismic stratigraphic framework and depositional history of a large Upper Cretaceous and Cenozoic depocenter off southwest Nova Scotia, Canada. Marine and Petroleum Geology, 65: 22–42.

Campbell, D.C., and Mosher, D.C. (2015) Geophysical evidence for widespread Cenozoic bottom current activity from the continental margin of Nova Scotia, Canada, Marine Geology, 378: 237-260.

Cummings, D.C., and Arnott, R.W.C. (2005) Growth-faulted shelf-margin deltas: a new (but old) play type, offshore Nova Scotia. Bulletin of Canadian Petroleum Geology, 53: 211-236.

Cummings, D.C., Hart, B.S., and Arnott, R.W.C. (2006) Sedimentology and stratigraphy of a thick, areally extensive fluvial-marine transition, Missisauga Formation, offshore Nova Scotia and its correlation with shelf margin and slope strata. Bulletin of Canadian Petroleum Geology, 54: 152-174.

Deptuck, M.E. (2008) NS08-2 Call for Bids – Sub-regional geology and exploration potential for Parcels 1 and 2, Central Scotian Slope. 40 p. Geoscience Publications | Canada-Nova Scotia Offshore Petroleum Board (CNSOPB)

Deptuck, M.E. (2011) Proximal to distal postrift structural provinces on the western Scotian Margin, offshore Eastern Canada: Geological context and parcel prospectivity for Call-for-Bids NS11-1, Canada-Nova Scotia Offshore Petroleum Board, Geoscience Open File Report (GOFR) 2011-001MF, 42p. Geoscience Publications | Canada-Nova Scotia Offshore Petroleum Board (CNSOPB)

Deptuck, M.E (2020) Nova Scotia's volcanic passive margin - exploration history, geology, and play concepts off southwestern Nova Scotia. CNSOPB Geoscience Open File Report 2020-001MF, 32 p. Geoscience Publications | Canada-Nova Scotia Offshore Petroleum Board (CNSOPB)

Deptuck, M.E. and Altheim, B. (2018) Rift basins of the central LaHave Platform, offshore Nova Scotia. CNSOPB Geoscience Open File Report 2018-001MF, 54 p. Available here: Geoscience Publications | Canada-Nova Scotia Offshore Petroleum Board (CNSOPB)

Deptuck, M.E. and Campbell, D.C. (2012) Wide-spread erosion and mass failure from the ~51 Ma Montagnais marine bolide impact off southwestern Nova Scotia, Canada, Canadian Journal of Earth Sciences, 49: 1567-1594.

Deptuck, M.E. and Kendell, K. (2012) Contrasting salt tectonic styles on the western versus central parts of the Scotian Margin, offshore Nova Scotia, CNSOPB Geoscience Open File Poster 2012-001PF, 2 panels Geoscience Publications | Canada-Nova Scotia Offshore Petroleum Board (CNSOPB)

Deptuck, M.E. and Kendell, K.L. (2017) Chapter 13: A review of Mesozoic salt tectonics along the Scotian margin, eastern Canada, In: J. Soto, J. Flinch, and G. Tari, (Eds), Permo-Triassic Salt Provinces of Europe, North Africa and Central Atlantic: Tectonics and Hydrocarbon Potential, Elsevier, 287-312.

Deptuck, M.E. and Kendell, K.L. (2020) Atlas of 3D seismic surfaces and thickness maps, central and southwestern Scotian Slope. CNSOPB Geoscience Open File Report 2020-002MF – 2020-006MF, 59 panels Geoscience Publications | Canada-Nova Scotia Offshore Petroleum Board (CNSOPB)

Deptuck, M.E. and Kendell, K.L. (2022) Geology of the central Scotian Shelf and Slope - Call for Bids NS22-1. CNSOPB Geoscience Open File Report 2022-001MF, 24 p. Geoscience Publications | Canada-Nova Scotia Offshore Petroleum Board (CNSOPB)

Deptuck, M.E., MacRae, R.A., Shimeld, J.W., Williams, G., and Fensome, R. (2003) Revised Upper Cretaceous and lower Paleogene lithostratigraphy and depositional history of the Jeanne d'Arc Basin, offshore Newfoundland, Canada, AAPG Bulletin, 87: 1459-1483

Deptuck, M.E., Kendell, K. and Smith, B. (2009) Complex deepwater fold-belts in the SW Sable Subbasin, offshore Nova Scotia, Extended Abstract, 2009 CSPG CSEG CWLS Convention, Calgary, Alberta, 4 p. Geoscience Publications | Canada-Nova Scotia Offshore Petroleum Board (CNSOPB)

Deptuck, M.E., Kendell, K., Brown, D. and Smith, B. (2014) Seismic stratigraphic framework and structural evolution of the eastern Scotian Slope: geological context for the NS14-1 Call for Bids area, offshore Nova Scotia. CNSOPB Geoscience Open File Report 2014-001MF, 58 p. Geoscience Publications | Canada-Nova Scotia Offshore Petroleum Board (CNSOPB)

Deptuck, M.E., Brown, D.E. and Altheim, B. (2015). Call for Bids NS15-1 – Exploration history, geologic setting, and exploration potential: Western and Central regions. CNSOPB Geoscience Open File Report 2015-001MF, 49 p. Geoscience Publications | Canada-Nova Scotia Offshore Petroleum Board (CNSOPB)

Dore, G. and Robbins, J. (2005) The buzzard Field, In: A.G. Dore and B.A Vinning (Eds) Petroleum Geology: North-West Europe and Global Perspectives – Proceedings of the 6th Petroleum Geology Conference, 241-252.

Durling, P., and Marillier, F. (1990) Structural trends and basement rock subdivisions in the western Gulf of St. Lawrence, Northern Appalachians. Atlantic Geology, 26: 75-95.

Durling, P., and Marillier, F. (1993) Tectonic setting of Middle Devonian to Lower Carboniferous rocks in the Magdalen Basin. Atlantic Geology, 29: 199-217.

Eliuk, L.S. (1978) The Abenaki Formation, Nova Scotia Shelf, Canada - A depostional and diagenetic model for a Mesozoic carbonate platform. Bulletin of Canadian Petroleum Geology, 26: 424-514.

Fensome, R.A., Crux, J.A., Gard, I.G., MacRae, R.A., Williams, G.L., Thomas, F.C., Fiorini, F., and Wach, G. (2008) The last 100 million years on the Scotian Margin, offshore eastern Canada: an event-stratigraphic scheme emphasizing biostratigraphic data. Atlantic Geology, 44: 93-126.

Fowler, M. (2019) Jurassic oils and source rocks of Morocco – Part 1, OERA Report pp 67 (downloaded from OERA.ca in September 2021)

Fowler, M. (2020) Review of geochemical evidence for multiple source rocks on the Scotian Shelf, OERA Report pp 254 (downloaded from OERA.ca in September 2021)

Fowler, M. and Webb, J. (2016) Geochemistry Data Report for 2016 Scotian Slope Piston Coring Program, 620 p. (Report downloaded in April 2020 from https://oera.ca/research/piston-coring-geochemistry-program)

Fonnesu, M., Palermob, D., Galbiatia, M., Marchesinia, M., Bonaminia, E., and Bendiasc, D. (2019) A new world-class deep-water play-type, deposited by the syndepositional interaction of turbidity flows and bottom currents: The giant Eocene Coral Field in northern Mozambique, Marine Petroleum Geology, 111: 179-201.

Gibling, M.R., Culshaw, N., Rygel, M.C, and Pascucci, V. (2008) Chapter 6 - The Maritimes Basin of Atlantic Canada: Basin

Creation and Destruction in the Collisional Zone of Pangea In: A.D. Maill (Ed.), Sedimentary Basins of the World, Volume 5: The Sedimentary Basins of the United States and Canada, Elsevier, 211-244.

Given, M.M. (1977) Mesozoic and Early Cenozoic geology of offshore Nova Scotia, Bulletin of Canadian Petroleum Geology, 25: 63-91.

Gong, C., Wang, Y., Zhu, W., Li, W., Xu, Q. (2013) Upper miocene to quaternary unidirectionally migrating deep-water channels in the pearl river mouth basin, northern south China sea. AAPG Bull. 97, 285–308

Goodway, B., Szelewski, C., Overell, S., Corbett, N. and Skrypnek, T (2008) Calibrated AVO and LMR analysis using a new DHI flat-spot AVO class 6 fluid contact to mitigate reservoir risk at Stonehouse, offshore Nova Scotia, Canadian Society of Exploration Geophysicists Recorder, 22: 23-32.

Hanafi B.R., Withjack M.O,. Durcanin M.A., and Schlische R.W. (2022) The development of the eastern Orpheus rift basin, offshore eastern Canada: A case study of the interplay between rift related faulting and salt deposition and flow. Marine and Petroleum Geology, 139: 105629, doi:https://doi.org/10.1016/j.marpetgeo.2022.105629.

Holser, W. T., Clement, G. P., Jansa, L. F., & Wade, J. A. (1988). Evaporite deposits of the north Atlantic rift. In W. Manspeizer (Ed.), Triassic-Jurassic rifting: Continental breakup and the origin of the Atlantic Ocean and passive margins (part B), Amsterdam: Elsevier, 525–556.

Ings, S.J., and Shimeld, J.W. (2006) A new conceptual model for the structural evolution of a regional salt detachment on the northeast Scotian margin, offshore eastern Canada, AAPG Bulletin, 90: 1407-1423.

Ings, S.J., Shimeld, J.W., MacRae, R.A., and Pe-Piper, G. (2005) Diagenesis and porosity reduction in the Late Cretaceous Wyandot Formation, Offshore Nova Scotia: a comparison with Norwegian North Sea chalks. Bulletin of Canadian Petroleum Geology, 53: 237-249.

Jansa, L.F., and Pe-Piper, G. (1987) Identification of an underwater extraterrestrial impact crater. Nature, 327: 612-614.

Jansa, L.F., and Wade, J.A. (1975) Geology of the continental margin off Nova Scotia and Newfoundland. In W.J.M. Van Der Linden and J.A. Wade (eds), Offshore Geology of Eastern Canada, Geological Survey of Canada Paper 74-30, 2: 51-105.

Jermannaud, P., L. Gindre-Chanu, L., Deptuck, M.E., Kendell, K., Keppie, D.F., Cuilhe, L., Doublet, S. (2023) Detailed sequence stratigraphy and Gross Depositional Environment mapping of the offshore Nova Scotia Margin, European Association of Geoscientists & Engineers, 84th EAGE Annual Conference & Exhibition, Jun 2023, Volume 2023, 1 – 5 DOI: https://doi.org/10.3997/2214-4609.202310787

Kendell, K. and Deptuck, M.E. (2012) Lower Cretaceous shelf-edge trajectories, shelf-indenting canyons and the potential transfer of coarser clastics into deeper water, Sable Subbasin, offshore Nova Scotia, CNSOPB Geoscience Open File Poster 2012-002PF, 2 panels Geoscience Publications | Canada-Nova Scotia Offshore Petroleum Board (CNSOPB)

Kendell, K.L. (2012) Variations in salt expulsion style within the Sable Canopy Complex, central Scotian margin. Can. J. Earth Sci. 49(12), 1504–1522. https://doi.org/10.1139/e2012-069

Kendell, K.L., Smith, B.M. and Brown, D.E. (2013) Geological context and parcel prospectivity for Call for Bids NS13-1: Seismic interpretation, source rocks and maturation, exploration history and potential play types of the central and eastern Scotian Shelf. CNSOPB Call for Bids Summary Document, 64p. Geoscience Publications | Canada-Nova Scotia Offshore Petroleum Board (CNSOPB)

Kendell, K., Deptuck, M., Smith, B. and Brown, D. (2016) Call for Bids NS16-1 - Exploration history, geological setting and exploration potential of the central Scotian Slope. Geoscience Open File Report 2016-002MF, Canada-Nova Scotia Offshore Petroleum Board, 42 p. Geoscience Publications | Canada-Nova Scotia Offshore Petroleum Board (CNSOPB)

Kendell, K. L., Brown, D.E. and Rhyno, S. (2017) Call for Bids NS17-1 – Regional exploration history, geological setting, source rocks and exploration potential of Sydney Basin, offshore Nova Scotia. CNSOPB Geoscience Open File Report 2017-001MF, 50 p. Geoscience Publications | Canada-Nova Scotia Offshore Petroleum Board (CNSOPB)

Kidston, A.G., Brown, D.E., Smith, B.M., and Altheim, B. (2005) The Upper Jurassic Abenaki Formation, offshore Nova Scotia: A seismic and geologic perspective, Canada Nova Scotia Offshore Petroleum Board, Halifax, Nova Scotia, 168 p. Geoscience Publications | Canada-Nova Scotia Offshore Petroleum Board (CNSOPB)

Kidston, A.G., Smith, B.M., Brown, D.E., Makrides, C., Altheim, B. (2007) Nova Scotia deepwater post-drill analysis 1982-2004. Halifax, Nova Scotia, Canada, Canada-Nova Scotia Offshore Petroleum Board, 182 p. Geoscience Publications | Canada-Nova Scotia Offshore Petroleum Board (CNSOPB)

Leleu, S., Hartley, A.J. and Williams, B.P.J. (2009) Large-scale alluvial architecture and correlation in a Triassic pebbly braided river system, lower Wolfville Formation (Fundy Basin, Nova Scotia, Canada). Journal of Sedimentary Research, 79: 266-286.

MacRae, R.A., and Pe-Piper, G. (2022) Intra-salt palynology events in the Late Triassic-Early Jurassic of the southern Grand Banks: Implications for regional and trans-Atlantic correlation and paleoenvironments (Abstract). In Conjugate Margins Conference 2022. Marrakech, Morocco.

Mader, N.K., Redfern, J., and Ouataoui, M.U. (2017) Sedimentology of the Essaouira Basin (Meskala Field) in context of regional sediment distribution patterns during upper Triassic pluvial events. Journal of African Earth Sciences, 130: 293-318.

Marzoli, A., Renne, P.R., Piccirillo, E.M., Ernesto, M., Bellieni, G. & De Min, A. (1999) Extensive 200-million-year-old continental flood basalts of the Central Atlantic magmatic province. Science, 284: 616–618.

McHone, J. G. (1996) Broad-terrane Jurassic flood basalts across northeastern North America. Geology, 24: 319-322.

McAlpine, K.D., Deptuck, M.E., Wielens, J.B.W., Jauer, C.D., and Moir, P.N. (2004a) Lithostratigraphy I, Jeanne d'Arc Basin Cross Sections A-A' and B-B', In Moir, P.N., McAlpine, K.D., Edwards, A., Deptuck, M.E., Bell, J.S., Wielens, J.B.W., Wade, J.A., and Jauer, C.D. East Coast Basin Atlas Series: Grand Banks of Newfoundland – Lithostratigraphy. Geological Survey of Canada, Open File 4640; 4 sheets.

McIver, N.L., (1972) Cenozoic and Mesozoic Stratigraphy of the Nova Scotia Shelf. Canadian Journal of Earth Sciences, 9: 54-70

Megson, J. and Tygesen, T. (2005) The North Sea Chalk: an underexplored and underdeveloped play. In: DORE ´, A.G. and VINING, B. A. (eds) Petroleum Geology: North-West Europe and Global Perspectives—Proceedings of the 6th Petroleum Geology Conference, 159–168. Petroleum Geology Conferences Ltd. Published by the Geological Society, London.

Morabet, A.M., Bouchta, R. and Jabour, H. (1998) An overview the petroleum systems of Morocco. In: D.S. MacGregor, R.T.J. Moody, and D.D. Clark-Lowes (eds) Geological Society of London Special Publication, 132: 283-296.

Moscardelli, L. Ochoa, J., Lunt, I., and Zahm, L. (2019) Mixed siliciclastic–carbonate systems and their impact for the development of deep-water turbidites in continental margins: A case study from the Late Jurassic to Early Cretaceous Shelburne subbasin in offshore Nova Scotia, AAPG Bulletin, 103: 2487-2520.

Mossman, D.J. (1992) Carboniferous source rocks of the Canadian Atlantic Margin. Geological Society of London Sp. Pub. 62: 25-34.

Offshore Energy Technical Research Association (OETR) et al. (2011) Play Fairway Analysis Atlas - Offshore Nova Scotia, Nova Scotia Department of Energy Report, NSDOE Records Storage File No. 88-11-0004-01, 347p. Research Portal | Nova Scotia Offshore Energy Research Association (oera.ca)

Olsen, P.E. (1985) Distribution of organic-matter-rich lacustrine rocks in the early Mesozoic Newark Supergroup. In: G.R. Robinson Jr. and A.J. Froelich (eds), Proceedings of the 2nd USGS Workshop on the Early Mesozoic Basins of Eastern United States, United States Geological Survey, Bulletin 946: 61-64.

Olsen, P.E. (1997) Stratigraphic record of the early Mesozoic breakup of Pangea in the Laurasia-Gondwana rift system. Annual Reviews of Earth and Planetary Science, 25: 337-401.

Pascucci, V. Gilbing, M.R., and Williamson, M.A. (1999) Seismic stratigraphic analysis of Carboniferous strata on the Burin Platform, offshore Eastern Canada. Bulletin of Canadian Petroleum Geology, 47: 298-316.

Pascucci, P. Gibling, M.R. and Williamson, M.A. (2000) Late Paleozoic to Cenozoic history of the offshore Sydney Basin, Atlantic Canada. Canadian Journal of Earth Sciences, 37: 1165-1165.

Piper, D.J.W., and Deptuck, M. (1997) Fine-grain turbidites of the Amazon fan: facies characterization and interpretation, In: R.D. Flood, D.J.W. Piper, A. Klaus and L.C. Petersen (Eds), Proceedings of the Ocean Drilling Program - Scientific Results, 155: 109-146.

Piper, D.J.W., and Normark, W.R. (2001) Sandy fans: From Amazon to Hueneme and beyond, AAPG Bulletin, 85: 1407-1438.

Piper, D.J.W., Noftall, R. and Pe-Piper, G. (2010) Allochthonous prodeltaic sediment facies in the lower Cretaceous at the Tantallon M-41 well: Implications for the deep-water Scotian Basin, AAPG Bulletin, 94: 87-104.

Post, P. J. and Coleman, J.L. (2015) Mesozoic rift basins of the U.S. central Atlantic offshore: comparisons with onshore basins, analysis, and potential petroleum prospectivity, In: P.J. Post, J.L. Coleman, N.C. Rosen et al (Eds) Petroleum Systems in "Rift" Basins, 34th Annual GCSSEPM Foundation Perkins-Rosen Research Conference, p. 1-68.

Rodrigues, S., Deptuck, M.E., Kendell, K.L., Campbell, C., Hernandez-Molina, F.J. (2022) Cretaceous to Eocene mixed turbidite-contourite systems offshore Nova Scotia (Canada): Spatial and temporal variability of down- and along-slope processes. Mar. Pet. Geol. 138: 105572.

Ryan, R.J., Grist, A., and Zentilli, M. (1991) The thermal evolution of the Maritimes Basin: Evidence from apatite fission track analysis. In Nova Scotia Department of Mines and Energy, Report of Activities. Edited by D. MacDonald. Nova Scotia Department of Mines and Energy, Report 91-1, pp. 27-32.

Savard, M.M. (1996) Pre-ore burial dolomitization adjacent to the carbonate-hosted Gays River Zn -Pb deposit, Nova Scotia, Canadian Journal of Earth Sciences, 33: 303-315.

Shimeld, J., (2004) A comparison of salt tectonic sub-provinces beneath the Scotian slope and Laurentian Fan, in P.J. Post, D.L. Olson, K.T. Lyons, S.L. Palmes, P. F. Harrison, and N.C. Rosen, eds., Salt-sediment interactions and hydrocarbon prospectivity: Concepts, applications and case studies for the 21st century: 24th Annual Gulf Coast Section SEPM Foundation Bob F. Perkins Research Conference Proceedings, p. 291–306

Shimeld, J. and Deptuck, M. (1998) Lithostratigraphic correlation of the upper Sydney Mines Formation in the Sydney Basin (Donkin to Point Aconi), northeastern Nova Scotia. Geological Survey of Canada, Open File 3673, 1 Sheet https://doi.org/10.4095/210087

Smith, B.M., Deptuck, M.E., and Kendell, K.L. (2010) Upper Cretaceous mass transport systems above the Wyandot Formation chalk, offshore Nova Scotia. In: D. Mosher et al. (Eds.) Submarine Mass Movements and Their Consequences, Advances in Natural and Technological Hazards Research. Kluger-Springer Book Series, 28: 605-616. Geoscience Publications | Canada-Nova Scotia Offshore Petroleum Board (CNSOPB)

Smith, B., Makrides, C., Altheim B. and Kendell K.L. (2014). Resource Assessment of Undeveloped Significant Discoveries on the Scotian Shelf. Canada-Nova Scotia Offshore Petroleum Board, 182p. Geoscience Publications | Canada-Nova Scotia Offshore Petroleum Board (CNSOPB)

Smith, B.M., Kendell K., Makrides, C., Brown, D.E. (2016) Call for Bids NS16-1 – Exploration history, geologic setting, and exploration potential: Sable Subbasin Region. Geoscience Open File Report, 2016-001MF. Canada -Nova Scotia Offshore Petroleum Board, 19p. Geoscience Publications | Canada-Nova Scotia Offshore Petroleum Board (CNSOPB)

Smith, B.M., Kendell K., Makrides, C., Brown, D.E. (2018) Call for Bids NS18-3 – Seismic Interpretation, well summaries, source rock, and exploration leads in the Central Scotian Shelf, Sable Subbasin. CNSOPB Geoscience Open File Report 2018-002MF, 27 p. Geoscience Publications | Canada-Nova Scotia Offshore Petroleum Board (CNSOPB)

Swanson, M.T. (1986). Pre-existing fault control for Mesozoic basin formation in eastern North America. Geology, 14: 419–422.

Tari, G., Flinch, J.F., Soto, J.I. (2017) Chapter 6: Petroleum systems and play types associated with Permo-Triassic salt in Europe, North African, and the Atlantic region, In: J. Soto, J. Flinch, and G. Tari, (Eds), Permo-Triassic Salt Provinces of Europe, North Africa and Central Atlantic: Tectonics and Hydrocarbon Potential, Elsevier, p. 129-156.

Wade, J.A. and MacLean, B.C. (1990) The geology of the Southeastern Margin of Canada, Chapter 5, In: M.J. Keen and G.L. Williams (eds), Geology of the Continental Margin of Eastern Canada, Geological Survey of Canada, The Geology of Canada, p. 224-225.

Waldron, J.W.F., Barr, S.M., Park, A.F., White, C.E., and Hibbard, J. (2015) Late Paleozoic strike-slip faults in Maritime Canada and their role in the reconfiguration of the northern Appalachian orogen. Tectonics, vol. 34, no. 8, p.1661-1684, eological Society of America Bulletin, 125: 945-960.

Welsink., H.J., Dwyer, J.D. and Knight, R.J. (1989) Tectono-stratigraphy of the passive margin off Nova Scotia, Chapter 14, In: A.J. Tankard and H.R. Balkwill (eds) Extensional Tectonics and Stratigraphy of the North Atlantic Margins, AAPG Memoir 46: 215-231.

Weston, J.F., MacRae, R.A., Ascoli, P., Cooper, M.K.E., Fensome, R.A., Shaw, D. and Williams, G.L. (2012) A revised biostratigraphic and well-log sequence stratigraphic framework for the Scotian Margin, offshore eastern Canada, Canadian Journal of Earth Sciences, 49: 1417-1462.

## Appendix 1 – **A. LaHave Platform**

| | | LaHave Pre-salt Rotated Fault Blocks and Inversions | | | | | |
|---|---|---|---|---|---|---|---|
| | | Natural Gas | | Natural Gas Liquids | | Oil Equivalent | |
| | | BCF | $10^9$ $m^3$ | MMB | $10^6$ $m^3$ | MMBOE | $10^6$ $m^3$ |
| In-Place Unrisked | P90 | 5,157 | 146 | 46.4 | 7.38 | 2,956 | 470 |
| | P50 | 7,884 | 223 | 77.7 | 12.3 | 4,663 | 741 |
| | P10 | 11,965 | 339 | 126 | 20.0 | 7,179 | 1,141 |
| | Mean | 8,263 | 234 | 82.6 | 13.1 | 4,907 | 780 |
| In-Place Fully Risked | P90 | - | - | - | - | - | - |
| | P50 | - | - | - | - | - | - |
| | P10 | - | - | - | - | - | - |
| | Mean | 21.4 | 0.60 | 0.22 | 0.03 | 12.5 | 1.99 |
| Recoverable Unrisked | P90 | 3,839 | 109 | 34.4 | 5.48 | 1,416 | 225 |
| | P50 | 5,893 | 167 | 58.1 | 9.24 | 2,206 | 351 |
| | P10 | 9,068 | 257 | 94.5 | 15.0 | 3,369 | 536 |
| | Mean | 6,200 | 176 | 61.9 | 9.85 | 2,320 | 369 |
| Recoverable Fully Risked | P90 | - | - | - | - | - | - |
| | P50 | - | - | - | - | - | - |
| | P10 | - | - | - | - | - | - |
| | Mean | 15.9 | 0.451 | 0.160 | 0.025 | 5.82 | 0.925 |

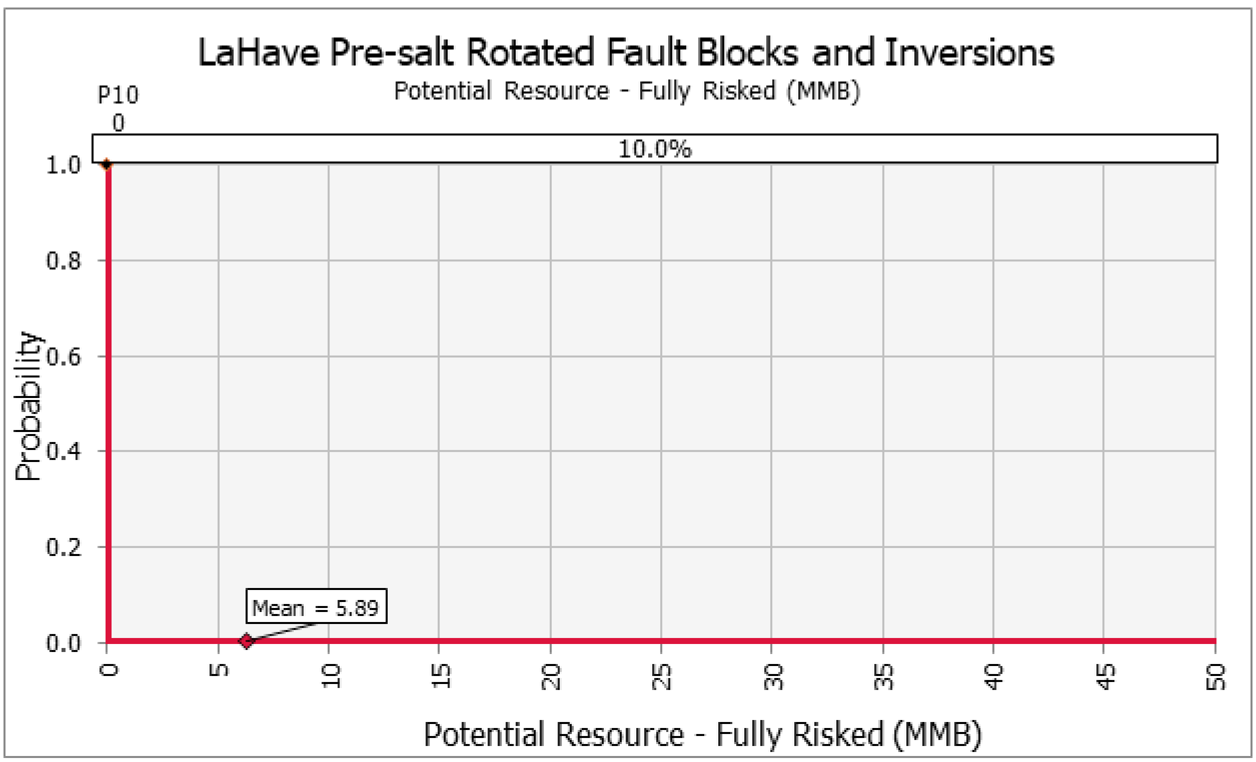

| | | LaHave Carboniferous Turtles (Yarmouth Basin) | | | | | |
|---|---|---|---|---|---|---|---|
| | | Natural Gas | | Natural Gas Liquids | | Oil Equivalent | |
| | | BCF | $10^9$ $m^3$ | MMB | $10^6$ $m^3$ | MMBOE | $10^6$ $m^3$ |
| In-Place Unrisked | P90 | 446 | 12.6 | 4.08 | 0.65 | 568 | 90.4 |
| | P50 | 795 | 22.5 | 7.76 | 1.23 | 1,009 | 160 |
| | P10 | 1,359 | 38.5 | 14.2 | 2.26 | 1,736 | 276 |
| | Mean | 856 | 24.2 | 8.57 | 1.36 | 1,090 | 173 |
| In-Place Fully Risked | P90 | - | - | - | - | - | - |
| | P50 | - | - | - | - | - | - |
| | P10 | - | - | - | - | - | - |
| | Mean | 8.93 | 0.25 | 0.09 | 0.01 | 11.3 | 1.80 |
| Recoverable Unrisked | P90 | 129 | 3.64 | 1.20 | 0.19 | 119 | 18.9 |
| | P50 | 267 | 7.57 | 2.61 | 0.41 | 220 | 35.0 |
| | P10 | 515 | 14.6 | 5.31 | 0.84 | 392 | 62.3 |
| | Mean | 300 | 8.48 | 3.00 | 0.48 | 241 | 38.4 |
| Recoverable Fully Risked | P90 | - | - | - | - | - | - |
| | P50 | - | - | - | - | - | - |
| | P10 | - | - | - | - | - | - |
| | Mean | 3.09 | 0.088 | 0.030 | 0.005 | 2.55 | 0.405 |

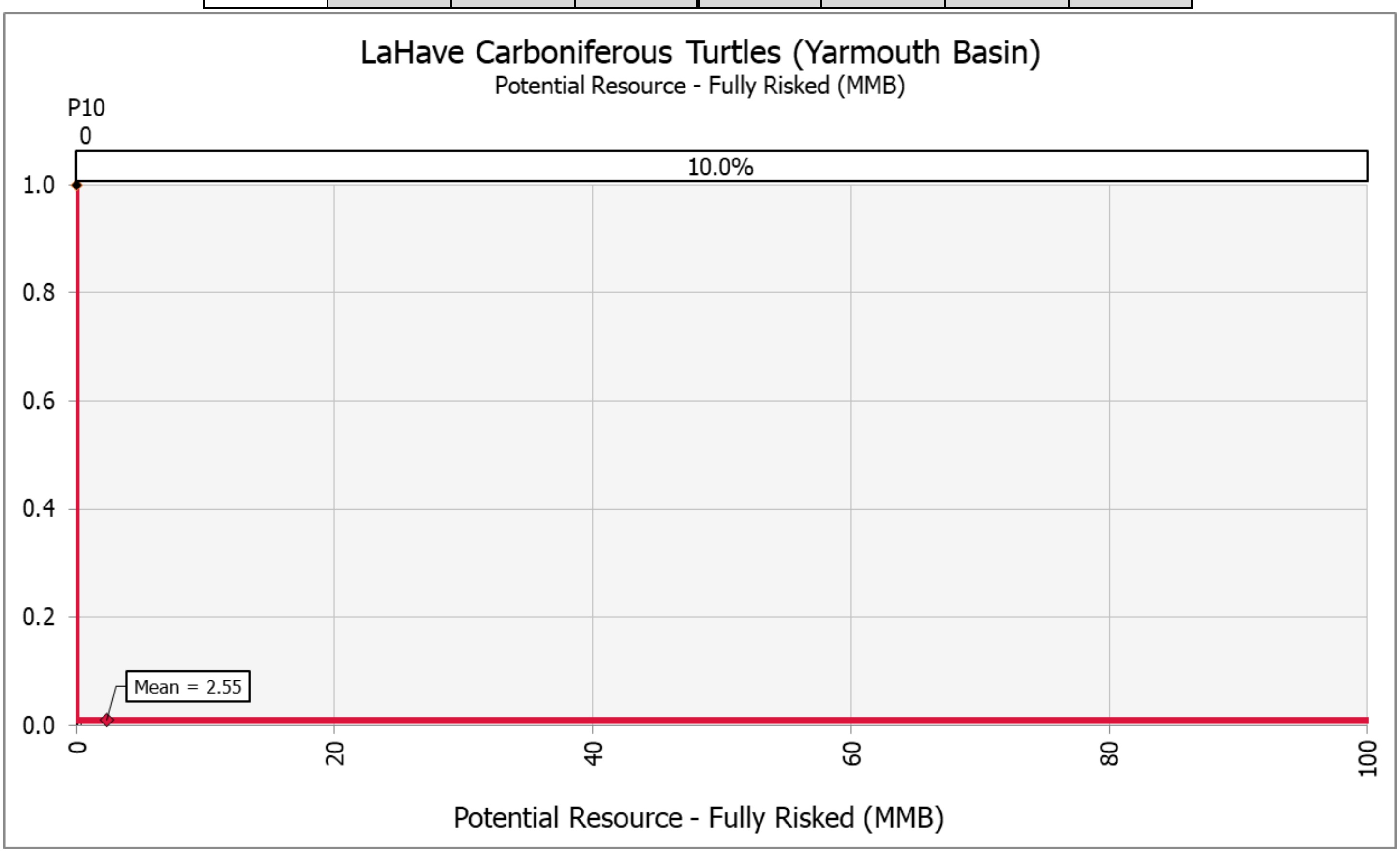

| | | Lahave Carboniferous Rotated Fault Blocks and Inversions | | | | | |
|---|---|---|---|---|---|---|---|
| | | Natural Gas | | Natural Gas Liquids | | Oil Equivalent | |
| | | BCF | $10^9$ $m^3$ | MMB | $10^6$ $m^3$ | MMBOE | $10^6$ $m^3$ |
| In-Place Unrisked | P90 | 697 | 19.7 | 6.44 | 1.02 | 887 | 141 |
| | P50 | 1,218 | 34.5 | 11.9 | 1.89 | 1,548 | 246 |
| | P10 | 2,059 | 58.3 | 21.4 | 3.41 | 2,632 | 418 |
| | Mean | 1,311 | 37.1 | 13.1 | 2.08 | 1,671 | 266 |
| In-Place Fully Risked | P90 | - | - | - | - | - | - |
| | P50 | - | - | - | - | - | - |
| | P10 | - | - | - | - | - | - |
| | Mean | 12.5 | 0.35 | 0.13 | 0.02 | 15.8 | 2.51 |
| Recoverable Unrisked | P90 | 202 | 5.71 | 1.87 | 0.30 | 187 | 29.8 |
| | P50 | 412 | 11.7 | 4.02 | 0.64 | 338 | 53.7 |
| | P10 | 779 | 22.0 | 8.05 | 1.28 | 599 | 95.2 |
| | Mean | 459 | 13.0 | 4.59 | 0.73 | 370 | 58.9 |
| Recoverable Fully Risked | P90 | - | - | - | - | - | - |
| | P50 | - | - | - | - | - | - |
| | P10 | - | - | - | - | - | - |
| | Mean | 4.42 | 0.125 | 0.045 | 0.007 | 3.50 | 0.556 |

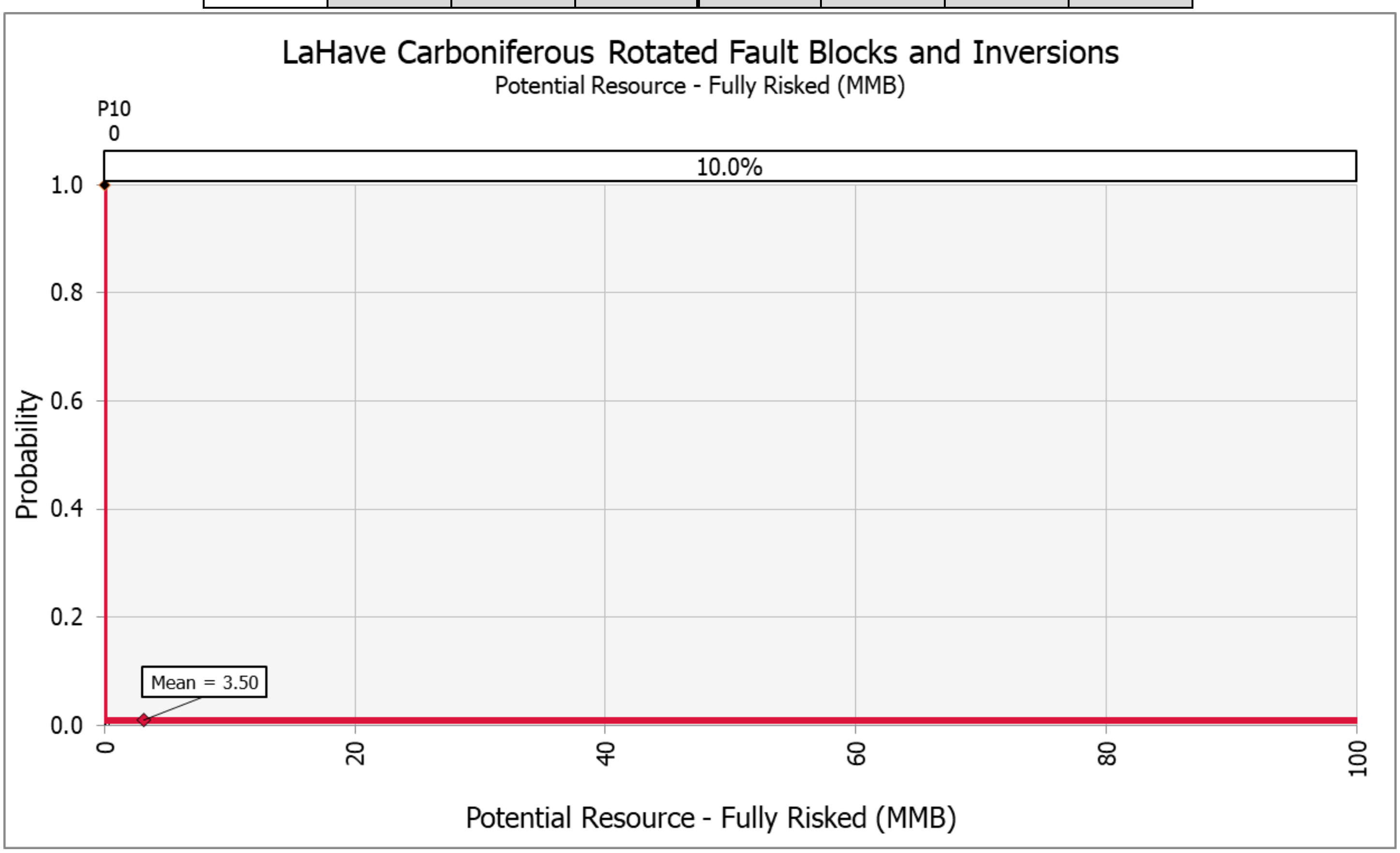

| | | Lahave Listric Fault Rollovers and Forced Folds | | | | | |
|---|---|---|---|---|---|---|---|
| | | Natural Gas | | Natural Gas Liquids | | Oil Equivalent | |
| | | BCF | $10^9$ $m^3$ | MMB | $10^6$ $m^3$ | MMBOE | $10^6$ $m^3$ |
| In-Place Unrisked | P90 | 4,691 | 133 | 43.8 | 6.96 | 1,994 | 317 |
| | P50 | 8,926 | 253 | 87.0 | 13.8 | 3,775 | 600 |
| | P10 | 16,166 | 458 | 168 | 26.7 | 6,843 | 1,088 |
| | Mean | 9,816 | 278 | 98.0 | 15.6 | 4,145 | 659 |
| In-Place Fully Risked | P90 | - | - | - | - | - | - |
| | P50 | - | - | - | - | - | - |
| | P10 | - | - | - | - | - | - |
| | Mean | 553 | 15.7 | 5.49 | 0.87 | 234 | 37.2 |
| Recoverable Unrisked | P90 | 3,499 | 99.1 | 32.7 | 5.19 | 1,044 | 166 |
| | P50 | 6,726 | 190 | 65.3 | 10.4 | 1,983 | 315 |
| | P10 | 12,083 | 342 | 126 | 20.0 | 3,557 | 566 |
| | Mean | 7,360 | 208 | 73.5 | 11.7 | 2,166 | 344 |
| Recoverable Fully Risked | P90 | - | - | - | - | - | - |
| | P50 | - | - | - | - | - | - |
| | P10 | - | - | - | - | - | - |
| | Mean | 414 | 11.7 | 4.11 | 0.653 | 122 | 19.3 |

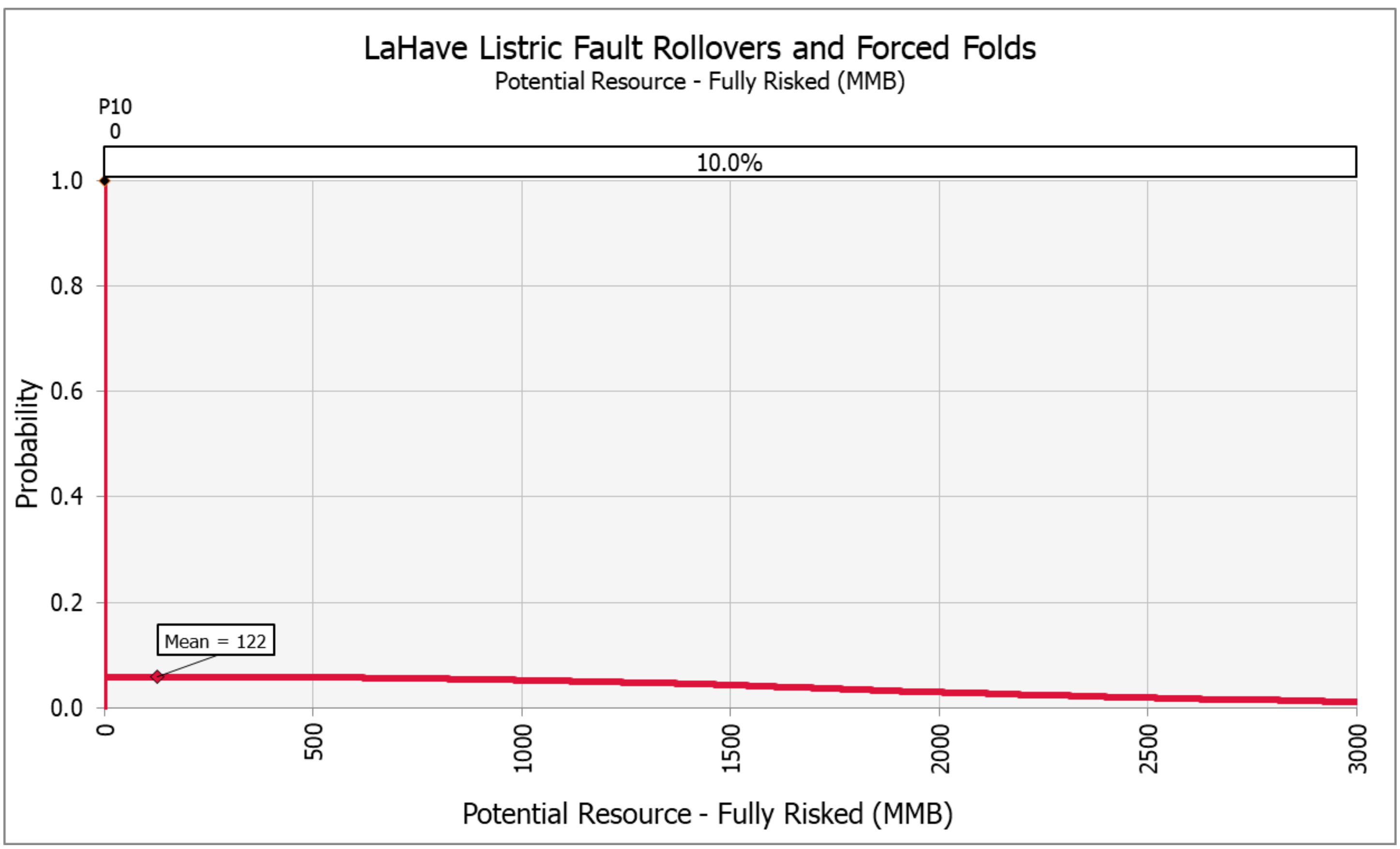

Appendix 2 – **B. West Shelburne Corridor**

| | | W Shelburne - Pre-salt rotated fault blocks | | | | | |
|---|---|---|---|---|---|---|---|
| | | Natural Gas | | Natural Gas Liquids | | Oil Equivalent | |
| | | BCF | $10^9$ $m^3$ | MMB | $10^6$ $m^3$ | MMBOE | $10^6$ $m^3$ |
| In-Place Unrisked | P90 | 2,077 | 58.8 | 18.7 | 2.98 | 1,127 | 179 |
| | P50 | 3,225 | 91.3 | 31.6 | 5.03 | 1,788 | 284 |
| | P10 | 4,908 | 139 | 52.0 | 8.27 | 2,792 | 444 |
| | Mean | 3,374 | 95.5 | 33.8 | 5.37 | 1,885 | 300 |
| In-Place Fully Risked | P90 | - | - | - | - | - | - |
| | P50 | - | - | - | - | - | - |
| | P10 | - | - | - | - | - | - |
| | Mean | 7.33 | 0.21 | 0.08 | 0.01 | 4.01 | 0.64 |
| Recoverable Unrisked | P90 | 1,545 | 43.8 | 13.9 | 2.21 | 547 | 87.0 |
| | P50 | 2,411 | 68.3 | 23.6 | 3.76 | 859 | 137 |
| | P10 | 3,695 | 105 | 39.1 | 6.21 | 1,334 | 212 |
| | Mean | 2,531 | 71.7 | 25.3 | 4.03 | 906 | 144 |
| Recoverable Fully Risked | P90 | - | - | - | - | - | - |
| | P50 | - | - | - | - | - | - |
| | P10 | - | - | - | - | - | - |
| | Mean | 5.45 | 0.154 | 0.056 | 0.009 | 1.94 | 0.308 |

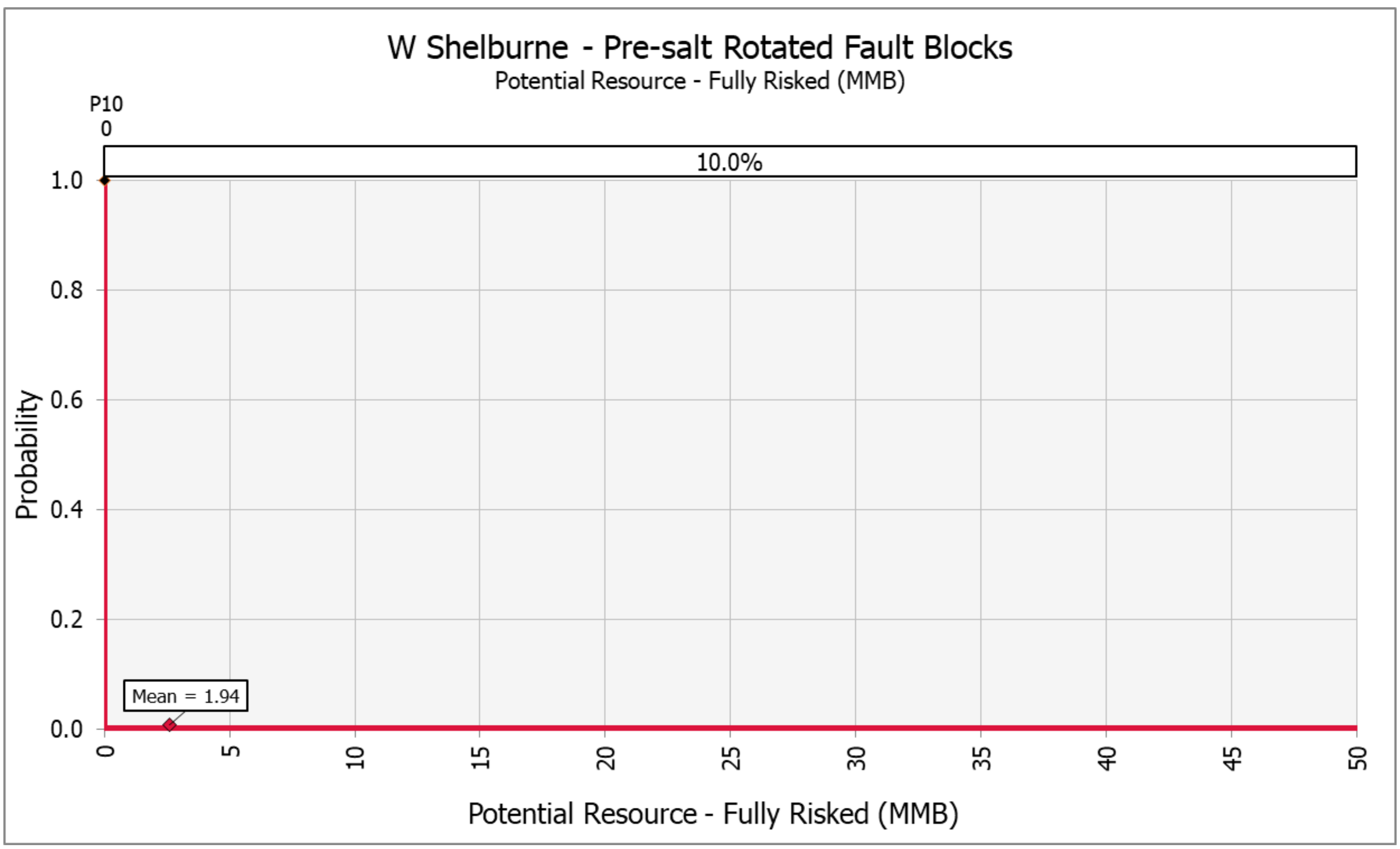

| | | W Shelburne Jurassic Listric Fault Rollovers - Shelf | | | | | |
|---|---|---|---|---|---|---|---|
| | | Natural Gas | | Natural Gas Liquids | | Oil Equivalent | |
| | | BCF | $10^9$ $m^3$ | MMB | $10^6$ $m^3$ | MMBOE | $10^6$ $m^3$ |
| In-Place Unrisked | P90 | 2,320 | 65.7 | 21.3 | 3.38 | 920 | 146 |
| | P50 | 4,207 | 119.1 | 41.1 | 6.54 | 1,695 | 269 |
| | P10 | 7,391 | 209 | 76.3 | 12.14 | 3,017 | 480 |
| | Mean | 4,585 | 129.8 | 45.9 | 7.30 | 1,851 | 294 |
| In-Place Fully Risked | P90 | - | - | - | - | - | - |
| | P50 | - | - | - | - | - | - |
| | P10 | - | - | - | - | - | - |
| | Mean | 203.32 | 5.76 | 2.04 | 0.32 | 81.2 | 12.9 |
| Recoverable Unrisked | P90 | 1,378 | 39.0 | 12.7 | 2.01 | 403 | 64.0 |
| | P50 | 2,516 | 71.3 | 24.6 | 3.90 | 736 | 117 |
| | P10 | 4,458 | 126 | 46.0 | 7.31 | 1,313 | 209 |
| | Mean | 2,751 | 77.9 | 27.6 | 4.38 | 806 | 128 |
| Recoverable Fully Risked | P90 | - | - | - | - | - | - |
| | P50 | - | - | - | - | - | - |
| | P10 | - | - | - | - | - | - |
| | Mean | 122 | 3.46 | 1.23 | 0.195 | 35.6 | 5.65 |

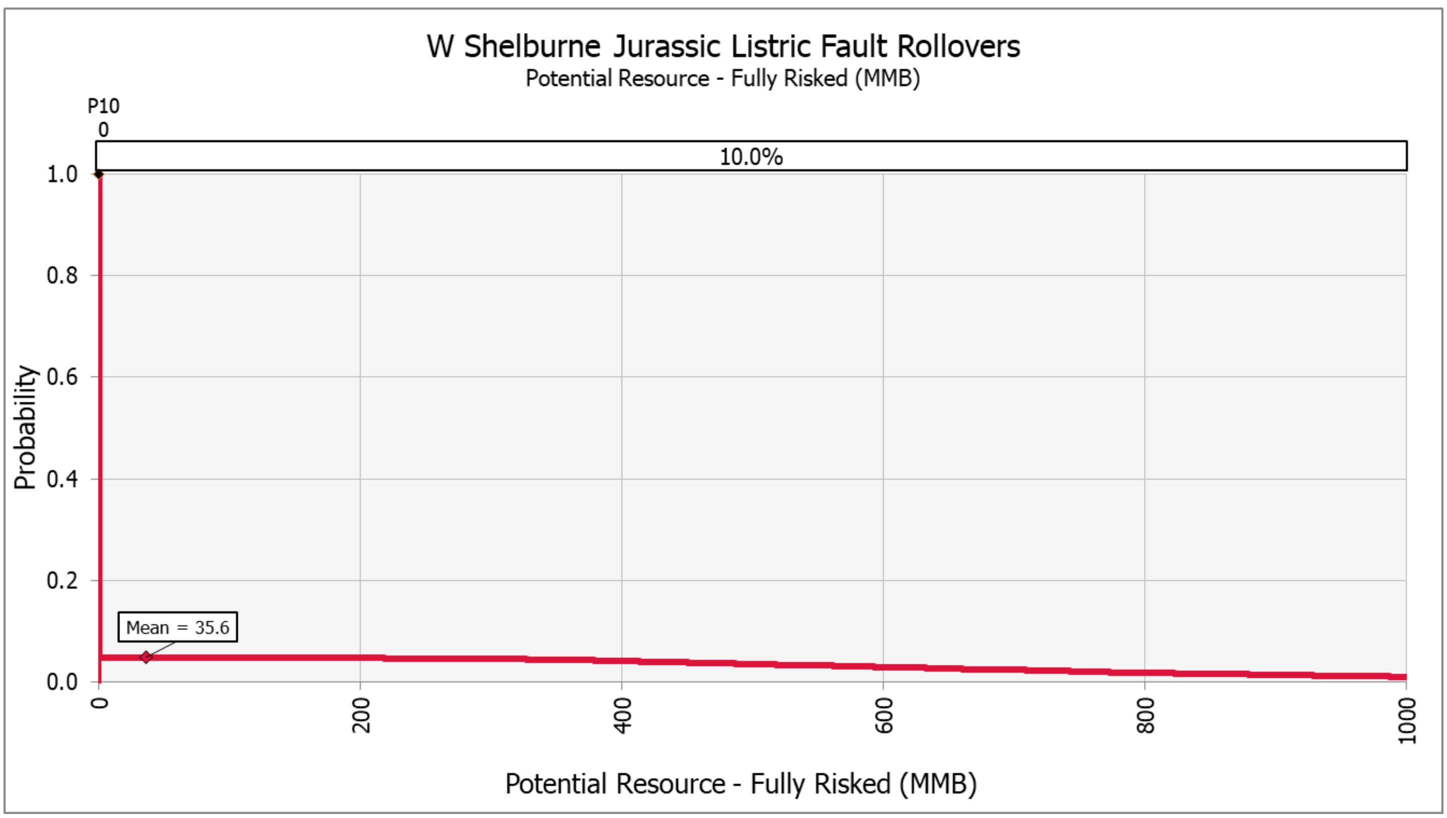

| | | W Shelburne Cretaceous Listric Fault Rollovers - Shelf | | | | | |
|---|---|---|---|---|---|---|---|
| | | Natural Gas | | Natural Gas Liquids | | Oil Equivalent | |
| | | BCF | $10^9$ $m^3$ | MMB | $10^6$ $m^3$ | MMBOE | $10^6$ $m^3$ |
| In-Place Unrisked | P90 | 2,101 | 59.5 | 19.3 | 3.06 | 864 | 137 |
| | P50 | 3,850 | 109 | 37.7 | 6.00 | 1,598 | 254 |
| | P10 | 6,914 | 196 | 71.3 | 11.3 | 2,875 | 457 |
| | Mean | 4,224 | 120 | 42.2 | 6.72 | 1,760 | 280 |
| In-Place Fully Risked | P90 | - | - | - | - | - | - |
| | P50 | - | - | - | - | - | - |
| | P10 | - | - | - | - | - | - |
| | Mean | 188 | 5.33 | 1.91 | 0.30 | 78.1 | 12.4 |
| Recoverable Unrisked | P90 | 1,567 | 44.4 | 14.3 | 2.28 | 457 | 72.7 |
| | P50 | 2,880 | 81.6 | 28.3 | 4.50 | 841 | 134 |
| | P10 | 5,207 | 147 | 53.6 | 8.53 | 1,512 | 240 |
| | Mean | 3,168 | 89.7 | 31.7 | 5.04 | 924 | 147 |
| Recoverable Fully Risked | P90 | - | - | - | - | - | - |
| | P50 | - | - | - | - | - | - |
| | P10 | - | - | - | - | - | - |
| | Mean | 141 | 3.98 | 1.43 | 0.227 | 40.9 | 6.51 |

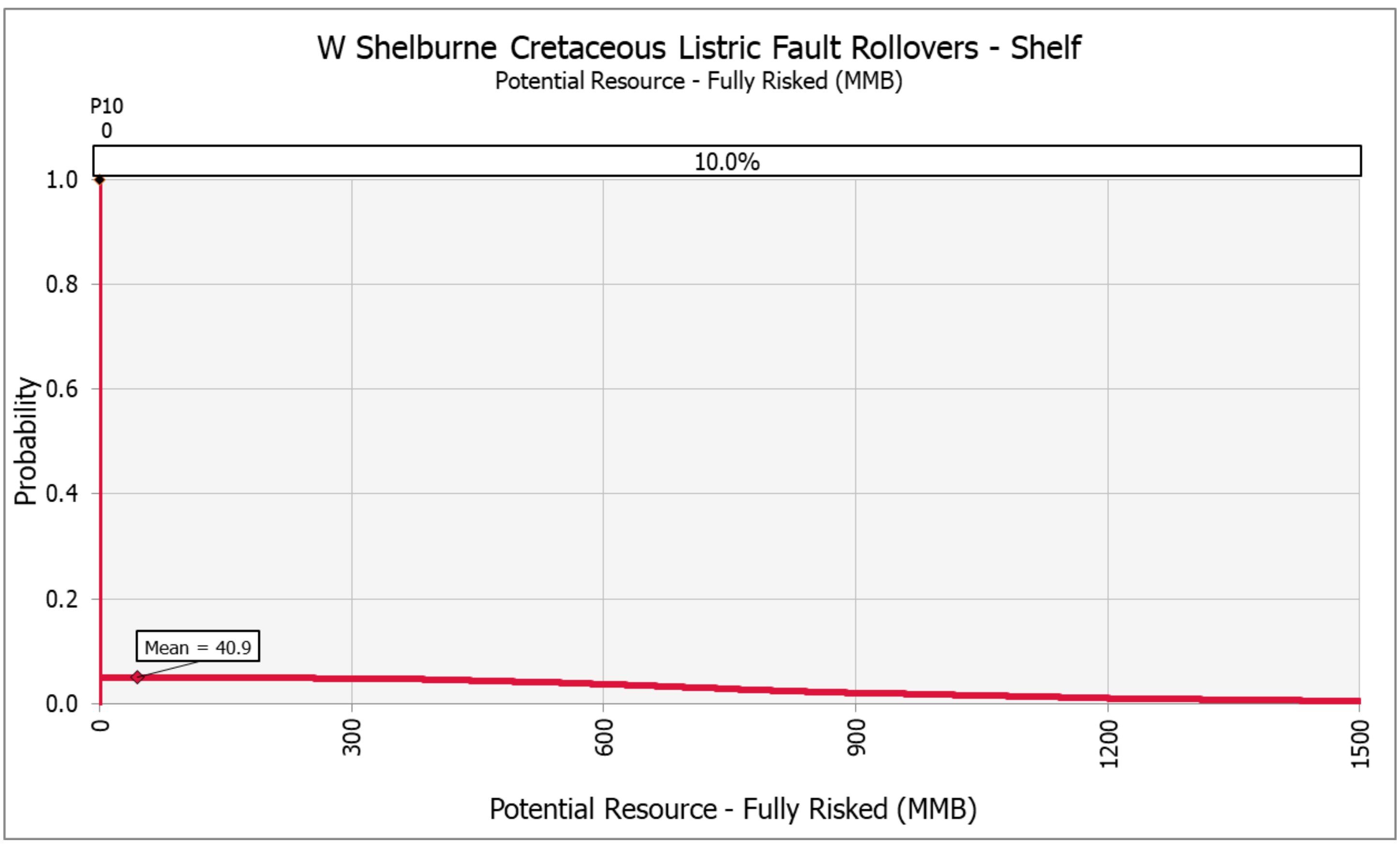

| | | W Shelburne Sub-Salt Canopy Cut-off (Slope) | | | | | |
|---|---|---|---|---|---|---|---|
| | | Natural Gas | | Natural Gas Liquids | | Oil Equivalent | |
| | | BCF | $10^9$ $m^3$ | MMB | $10^6$ $m^3$ | MMBOE | $10^6$ $m^3$ |
| In-Place Unrisked | P90 | 1,241 | 35.1 | 11.4 | 1.82 | 410 | 65.1 |
| | P50 | 2,347 | 66.5 | 23.1 | 3.67 | 779 | 124 |
| | P10 | 4,220 | 119 | 43.7 | 6.95 | 1,411 | 224 |
| | Mean | 2,574 | 72.9 | 25.8 | 4.10 | 858 | 136 |
| In-Place Fully Risked | P90 | - | - | - | - | - | - |
| | P50 | - | - | - | - | - | - |
| | P10 | - | - | - | - | - | - |
| | Mean | 70.0 | 1.98 | 0.71 | 0.11 | 23.5 | 3.74 |
| Recoverable Unrisked | P90 | 740 | 21.0 | 6.81 | 1.08 | 191 | 30.4 |
| | P50 | 1,405 | 39.8 | 13.8 | 2.20 | 361 | 57.3 |
| | P10 | 2,552 | 72.3 | 26.5 | 4.21 | 654 | 104 |
| | Mean | 1,544 | 43.7 | 15.5 | 2.46 | 398 | 63.3 |
| Recoverable Fully Risked | P90 | - | - | - | - | - | - |
| | P50 | - | - | - | - | - | - |
| | P10 | - | - | - | - | - | - |
| | Mean | 41.7 | 1.18 | 0.42 | 0.067 | 10.8 | 1.72 |

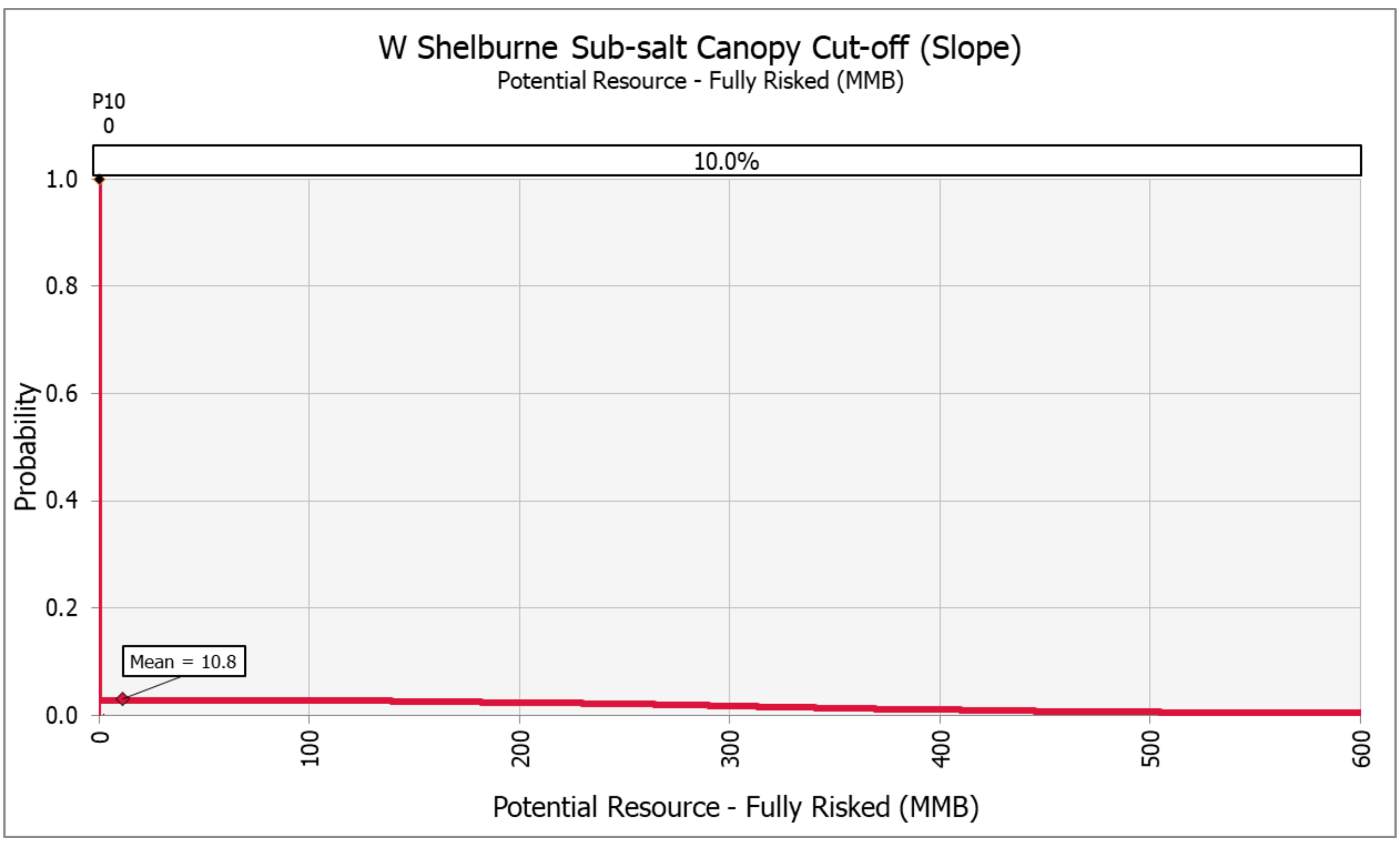

| | | W Shelburne - Cretaceous Stratigraphic Onlap | | | | | |
|---|---|---|---|---|---|---|---|
| | | Natural Gas | | Natural Gas Liquids | | Oil Equivalent | |
| | | BCF | $10^9$ $m^3$ | MMB | $10^6$ $m^3$ | MMBOE | $10^6$ $m^3$ |
| In-Place Unrisked | P90 | 5,759 | 163 | 53.1 | 8.45 | 2,909 | 462 |
| | P50 | 10,543 | 299 | 103 | 16.32 | 5,438 | 865 |
| | P10 | 17,434 | 494 | 183 | 29.12 | 9,226 | 1,467 |
| | Mean | 11,187 | 317 | 112 | 17.77 | 5,824 | 926 |
| In-Place Fully Risked | P90 | - | - | - | - | - | - |
| | P50 | - | - | - | - | - | - |
| | P10 | - | - | - | - | - | - |
| | Mean | 253 | 7.17 | 2.55 | 0.41 | 133 | 21.1 |
| Recoverable Unrisked | P90 | 4,293 | 122 | 39.7 | 6.31 | 1,446 | 230 |
| | P50 | 7,884 | 223 | 76.8 | 12.2 | 2,677 | 426 |
| | P10 | 13,176 | 373 | 137 | 21.8 | 4,490 | 714 |
| | Mean | 8,390 | 238 | 83.8 | 13.3 | 2,854 | 454 |
| Recoverable Fully Risked | P90 | - | - | - | - | - | - |
| | P50 | - | - | - | - | - | - |
| | P10 | - | - | - | - | - | - |
| | Mean | 190 | 5.38 | 1.92 | 0.305 | 64.8 | 10.3 |

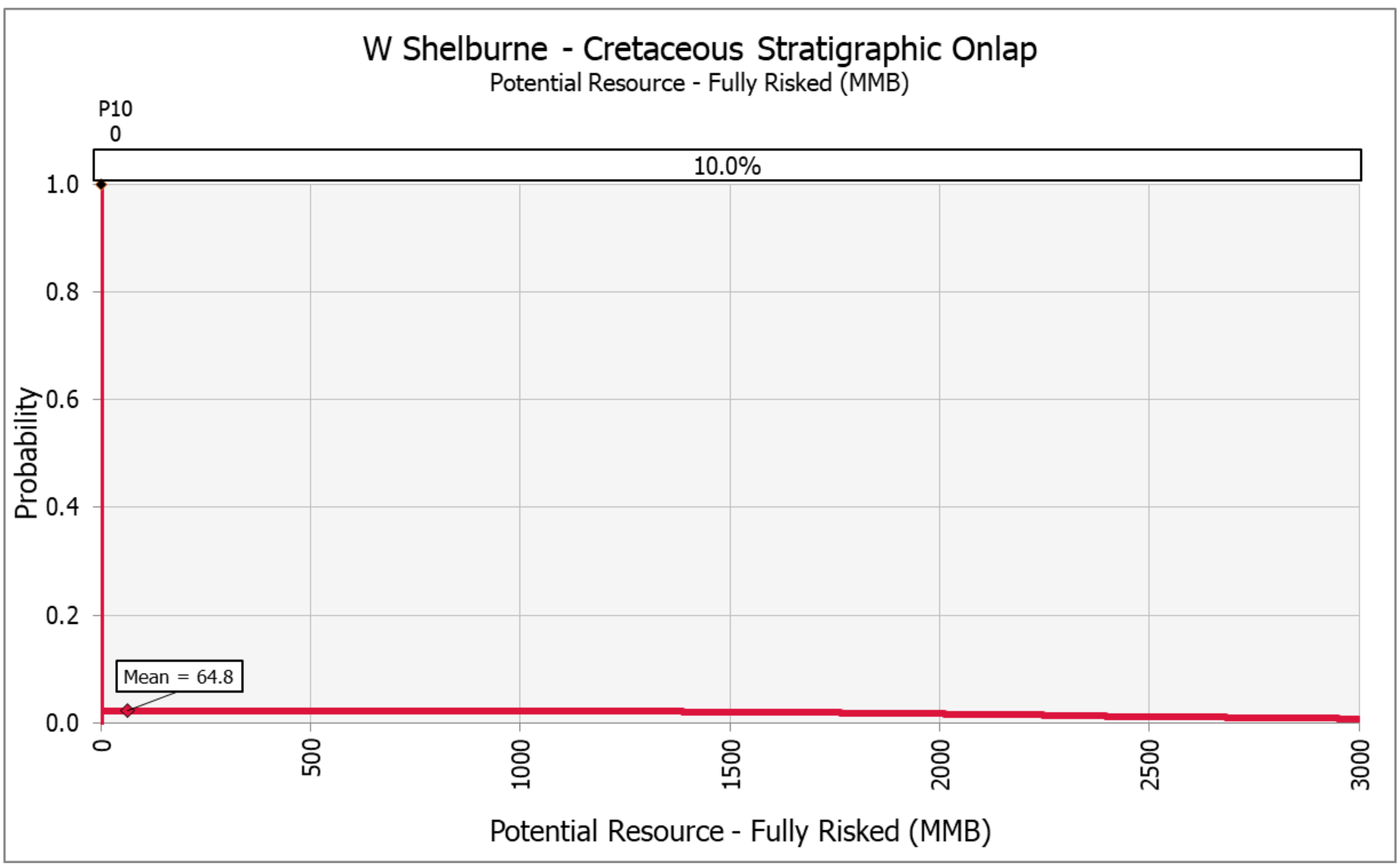

| | | W Shelburne - Cretaceous three way traps on salt flanks | | | | | |
|---|---|---|---|---|---|---|---|
| | | Natural Gas | | Natural Gas Liquids | | Oil Equivalent | |
| | | BCF | $10^9$ $m^3$ | MMB | $10^6$ $m^3$ | MMBOE | $10^6$ $m^3$ |
| In-Place Unrisked | P90 | 2,675 | 75.7 | 24.5 | 3.89 | 1,372 | 218 |
| | P50 | 4,875 | 138.0 | 47.7 | 7.59 | 2,530 | 402 |
| | P10 | 8,195 | 232 | 85.1 | 13.5 | 4,302 | 684 |
| | Mean | 5,200 | 147.2 | 52.0 | 8.27 | 2,714 | 431 |
| In-Place Fully Risked | P90 | - | - | - | - | - | - |
| | P50 | - | - | - | - | - | - |
| | P10 | - | - | - | - | - | - |
| | Mean | 168 | 4.76 | 1.65 | 0.26 | 89.1 | 14.2 |
| Recoverable Unrisked | P90 | 1,992 | 56.4 | 18.1 | 2.88 | 677 | 108 |
| | P50 | 3,645 | 103 | 35.7 | 5.68 | 1,241 | 197 |
| | P10 | 6,165 | 175 | 64.3 | 10.23 | 2,095 | 333 |
| | Mean | 3,901 | 110 | 39.0 | 6.20 | 1,329 | 211 |
| Recoverable Fully Risked | P90 | - | - | - | - | - | - |
| | P50 | - | - | - | - | - | - |
| | P10 | - | - | - | - | - | - |
| | Mean | 126 | 3.56 | 1.23 | 0.196 | 43.7 | 6.95 |

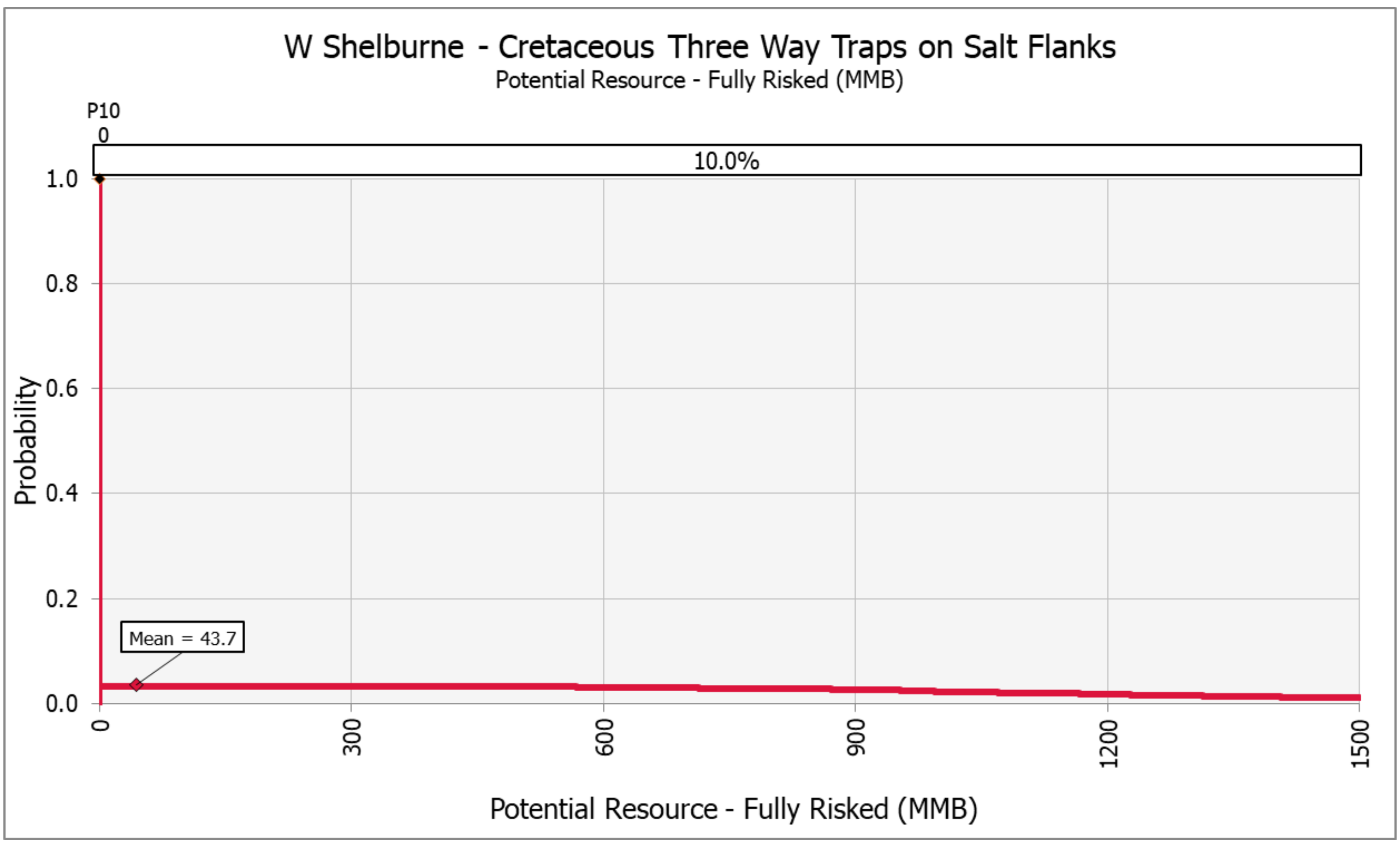

| | | W Shelburne - Chalk Play - T50 closures | | | | | |
|---|---|---|---|---|---|---|---|
| | | Natural Gas | | Natural Gas Liquids | | Oil Equivalent | |
| | | BCF | $10^9$ $m^3$ | MMB | $10^6$ $m^3$ | MMBOE | $10^6$ $m^3$ |
| In-Place Unrisked | P90 | 9,500 | 269 | 52.1 | 8.29 | 3,066 | 487 |
| | P50 | 16,152 | 457 | 95.2 | 15.1 | 5,275 | 839 |
| | P10 | 25,988 | 736 | 164 | 26.1 | 8,543 | 1,358 |
| | Mean | 17,093 | 484 | 103 | 16.3 | 5,589 | 889 |
| In-Place Fully Risked | P90 | - | - | - | - | - | - |
| | P50 | - | - | - | - | - | - |
| | P10 | - | - | - | - | - | - |
| | Mean | 531 | 15.0 | 3.17 | 0.50 | 174 | 27.7 |
| Recoverable Unrisked | P90 | 2,072 | 58.7 | 11.4 | 1.82 | 665 | 106 |
| | P50 | 4,098 | 116 | 24.2 | 3.85 | 1,227 | 195 |
| | P10 | 7,618 | 216 | 47.3 | 7.53 | 2,106 | 335 |
| | Mean | 4,556 | 129 | 27.3 | 4.35 | 1,321 | 210 |
| Recoverable Fully Risked | P90 | - | - | - | - | - | - |
| | P50 | - | - | - | - | - | - |
| | P10 | - | - | - | - | - | - |
| | Mean | 144 | 4.08 | 0.86 | 0.136 | 41.2 | 6.55 |

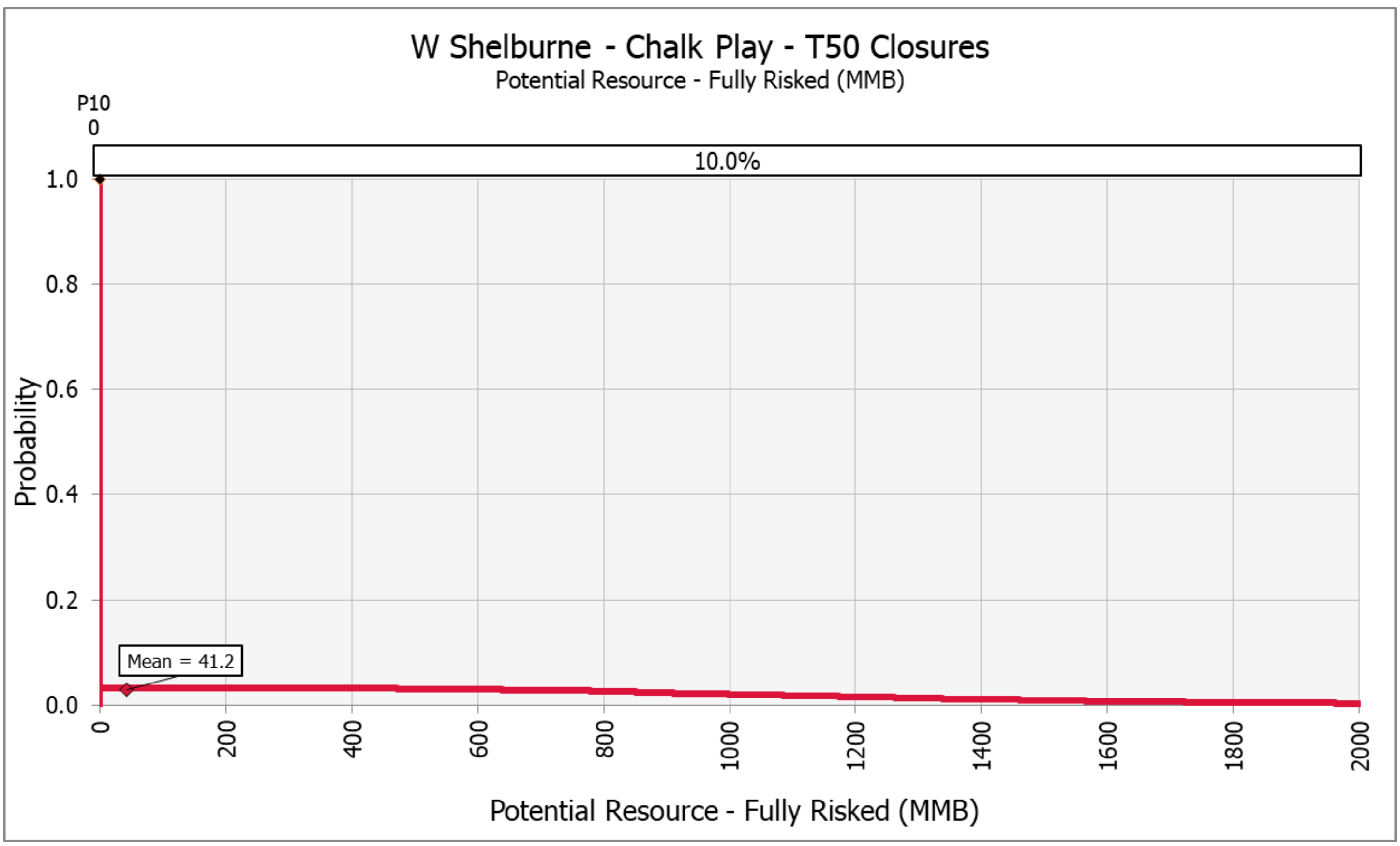

## Appendix 3 – **C. Shelburne Corridor**

| | | Shelburne - Pre-salt rotated fault blocks | | | | | |
|---|---|---|---|---|---|---|---|
| | | Natural Gas | | Natural Gas Liquids | | Oil Equivalent | |
| | | BCF | $10^9$ $m^3$ | MMB | $10^6$ $m^3$ | MMBOE | $10^6$ $m^3$ |
| In-Place Unrisked | P90 | 2,802 | 79.3 | 25.4 | 4.04 | 1,550 | 246 |
| | P50 | 4,330 | 123 | 42.5 | 6.76 | 2,450 | 390 |
| | P10 | 6,605 | 187 | 69.8 | 11.1 | 3,808 | 605 |
| | Mean | 4,559 | 129 | 45.6 | 7.25 | 2,583 | 411 |
| In-Place Fully Risked | P90 | - | - | - | - | - | - |
| | P50 | - | - | - | - | - | - |
| | P10 | - | - | - | - | - | - |
| | Mean | 6.92 | 0.20 | 0.07 | 0.01 | 4.07 | 0.65 |
| Recoverable Unrisked | P90 | 2,083 | 59.0 | 18.8 | 2.99 | 753 | 120 |
| | P50 | 3,240 | 91.7 | 31.9 | 5.07 | 1,172 | 186 |
| | P10 | 4,978 | 141 | 52.7 | 8.37 | 1,809 | 288 |
| | Mean | 3,419 | 96.8 | 34.2 | 5.44 | 1,237 | 197 |
| Recoverable Fully Risked | P90 | - | - | - | - | - | - |
| | P50 | - | - | - | - | - | - |
| | P10 | - | - | - | - | - | - |
| | Mean | 5.16 | 0.146 | 0.054 | 0.009 | 1.92 | 0.31 |

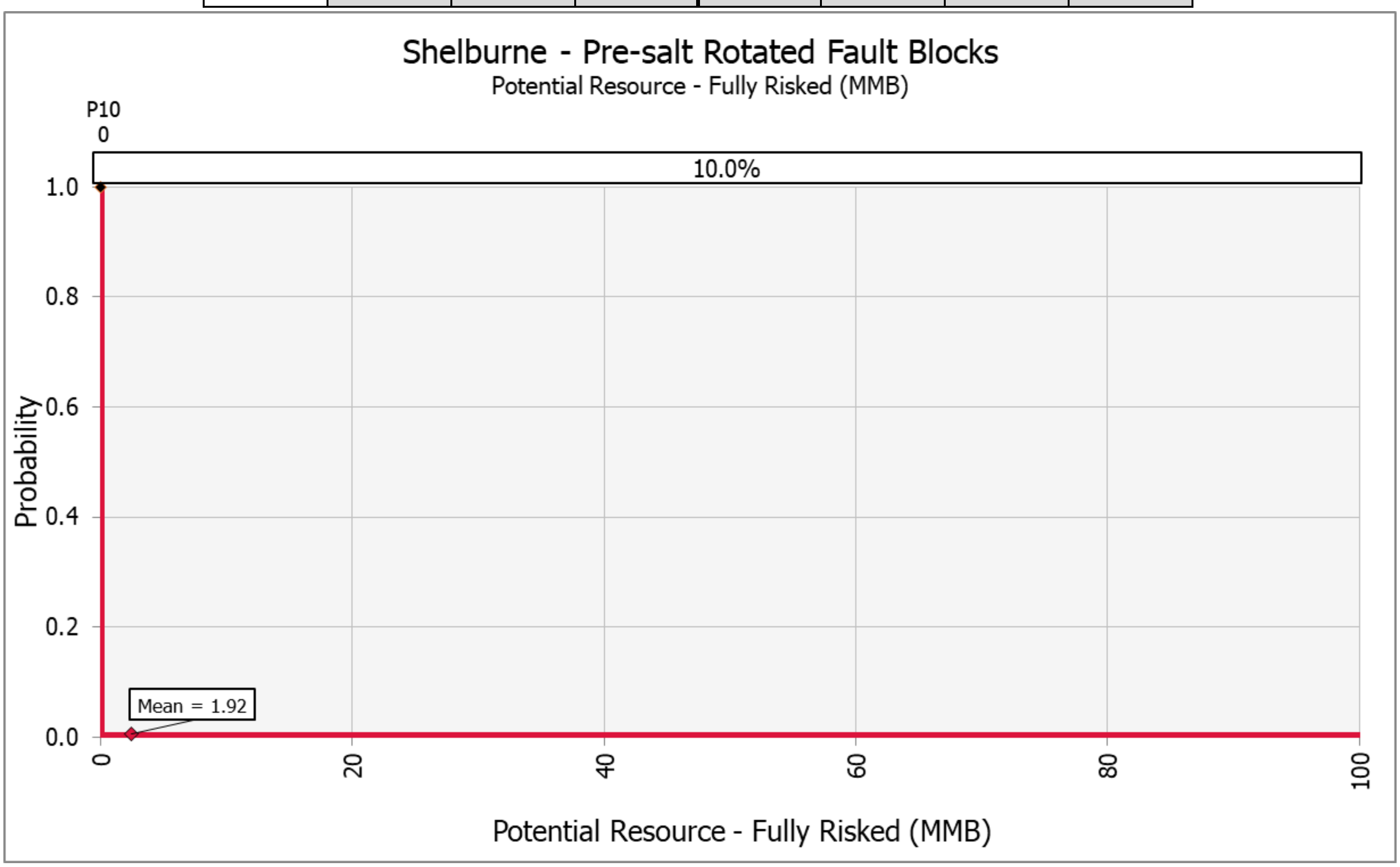

| | | Shelburne - Porous Carbonate Bank Edge | | | | | |
|---|---|---|---|---|---|---|---|
| | | Natural Gas | | Natural Gas Liquids | | Oil Equivalent | |
| | | BCF | $10^9$ m$^3$ | MMB | $10^6$ m$^3$ | MMBOE | $10^6$ m$^3$ |
| In-Place Unrisked | P90 | 2,084 | 59.0 | 7.80 | 1.24 | 1,220 | 194 |
| | P50 | 4,659 | 132 | 18.1 | 2.88 | 2,737 | 435 |
| | P10 | 9,324 | 264 | 38.5 | 6.12 | 5,596 | 890 |
| | Mean | 5,293 | 150 | 21.2 | 3.37 | 3,140 | 499 |
| In-Place Fully Risked | P90 | - | - | - | - | - | - |
| | P50 | - | - | - | - | - | - |
| | P10 | - | - | - | - | - | - |
| | Mean | 516 | 14.6 | 2.07 | 0.33 | 307 | 48.7 |
| Recoverable Unrisked | P90 | 477 | 13.5 | 1.81 | 0.29 | 388 | 61.6 |
| | P50 | 1,173 | 33.2 | 4.57 | 0.73 | 885 | 141 |
| | P10 | 2,651 | 75.1 | 10.8 | 1.71 | 1,832 | 291 |
| | Mean | 1,406 | 39.8 | 5.62 | 0.89 | 1,021 | 162 |
| Recoverable Fully Risked | P90 | - | - | - | - | - | - |
| | P50 | - | - | - | - | - | - |
| | P10 | - | - | - | - | - | - |
| | Mean | 140 | 3.96 | 0.559 | 0.089 | 100 | 15.9 |

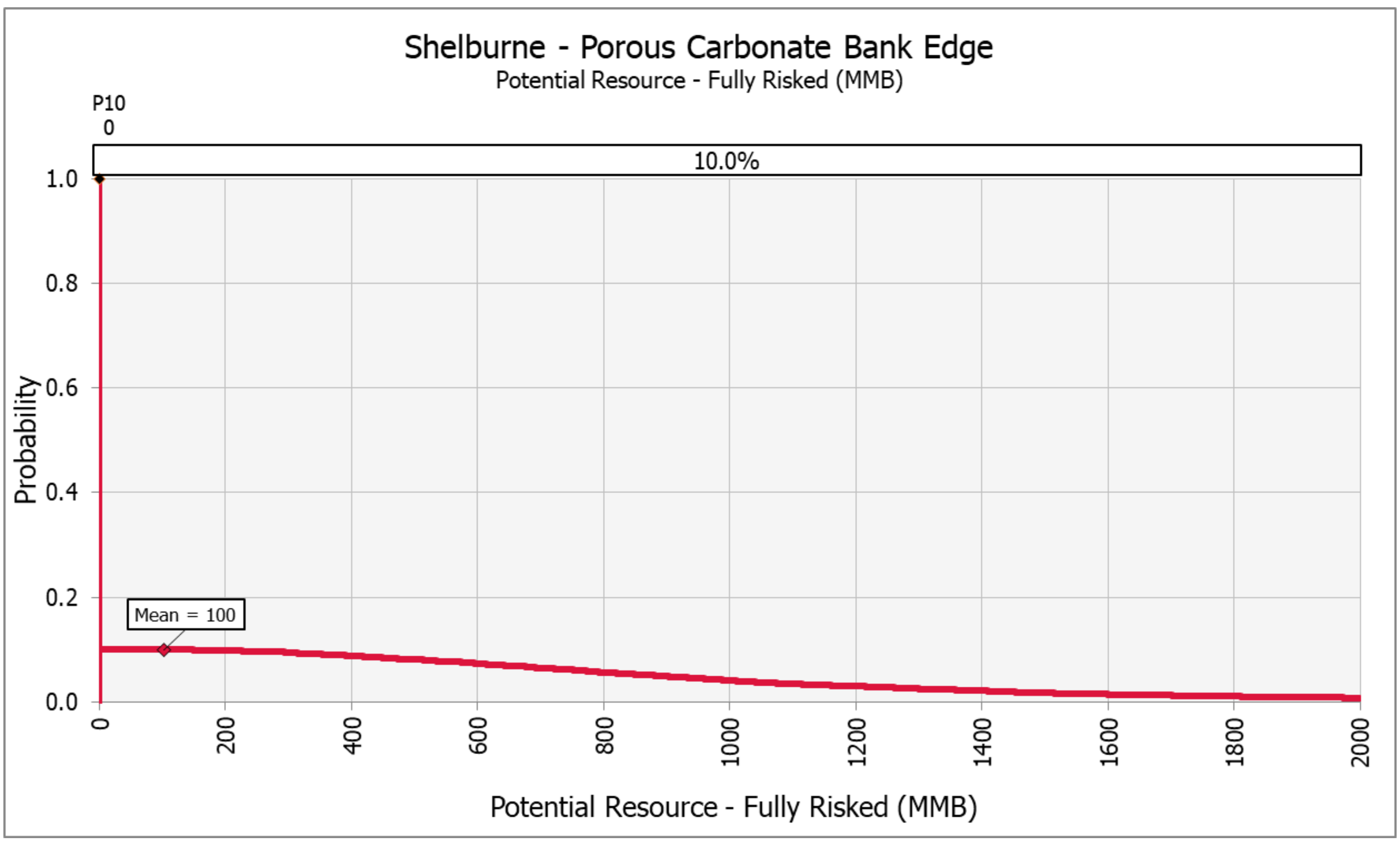

| | | Shelburne - Jurassic Turtles & Folds (primary salt) | | | | | |
|---|---|---|---|---|---|---|---|
| | | Natural Gas | | Natural Gas Liquids | | Oil Equivalent | |
| | | BCF | $10^9$ $m^3$ | MMB | $10^6$ $m^3$ | MMBOE | $10^6$ $m^3$ |
| In-Place Unrisked | P90 | 2,780 | 78.7 | 25.4 | 4.04 | 1,484 | 236 |
| | P50 | 5,156 | 146 | 50.5 | 8.03 | 2,793 | 444 |
| | P10 | 9,153 | 259 | 94.8 | 15.1 | 5,067 | 806 |
| | Mean | 5,645 | 160 | 56.4 | 8.97 | 3,072 | 488 |
| In-Place Fully Risked | P90 | - | - | - | - | - | - |
| | P50 | - | - | - | - | - | - |
| | P10 | - | - | - | - | - | - |
| | Mean | 60.2 | 1.70 | 0.62 | 0.10 | 32.4 | 5.14 |
| Recoverable Unrisked | P90 | 1,663 | 47.1 | 15.1 | 2.41 | 598 | 95.1 |
| | P50 | 3,080 | 87.2 | 30.3 | 4.82 | 1,121 | 178 |
| | P10 | 5,502 | 156 | 57.3 | 9.11 | 2,010 | 320 |
| | Mean | 3,387 | 95.9 | 33.9 | 5.39 | 1,230 | 196 |
| Recoverable Fully Risked | P90 | - | - | - | - | - | - |
| | P50 | - | - | - | - | - | - |
| | P10 | - | - | - | - | - | - |
| | Mean | 36.3 | 1.028 | 0.374 | 0.059 | 12.9 | 2.05 |

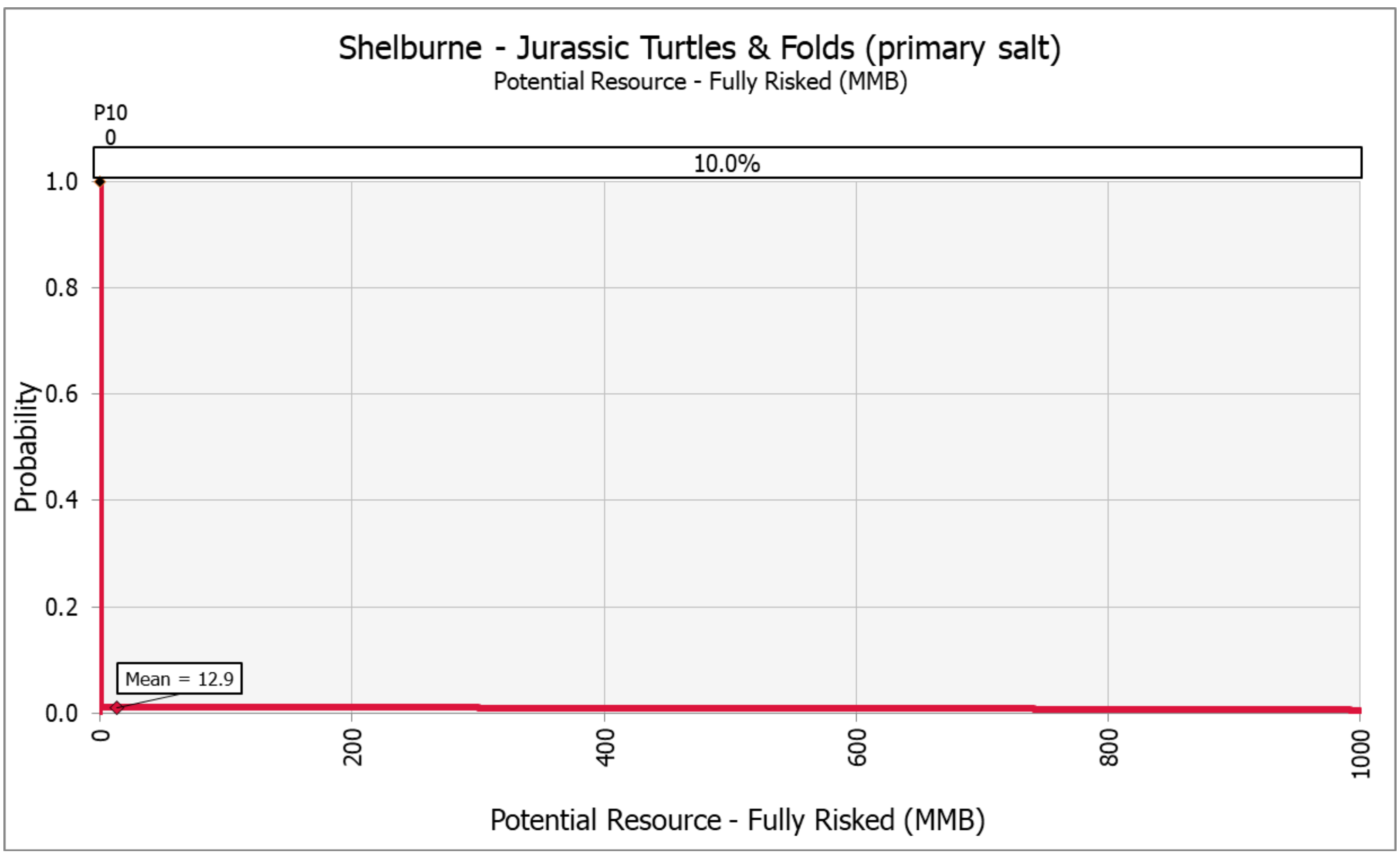

| | | Shelburne - Cretaceous Turtles & Folds (primary salt) | | | | | |
|---|---|---|---|---|---|---|---|
| | | Natural Gas | | Natural Gas Liquids | | Oil Equivalent | |
| | | BCF | $10^9$ $m^3$ | MMB | $10^6$ $m^3$ | MMBOE | $10^6$ $m^3$ |
| In-Place Unrisked | **P90** | 5,268 | 149 | 48.1 | 7.65 | 2,777 | 442 |
| | **P50** | 8,878 | 251 | 86.4 | 13.7 | 4,677 | 744 |
| | **P10** | 13,229 | 375 | 141 | 22.4 | 7,227 | 1,149 |
| | **Mean** | 9,094 | 258 | 91.0 | 14.5 | 4,865 | 773 |
| In-Place Fully Risked | **P90** | - | - | - | - | - | - |
| | **P50** | - | - | - | - | - | - |
| | **P10** | - | - | - | - | - | - |
| | **Mean** | 66.1 | 1.87 | 0.66 | 0.10 | 37.0 | 5.89 |
| Recoverable Unrisked | **P90** | 3,911 | 111 | 35.7 | 5.68 | 1,303 | 207 |
| | **P50** | 6,638 | 188 | 64.5 | 10.3 | 2,185 | 347 |
| | **P10** | 9,954 | 282 | 106 | 16.8 | 3,315 | 527 |
| | **Mean** | 6,821 | 193 | 68.3 | 10.9 | 2,259 | 359 |
| Recoverable Fully Risked | **P90** | - | - | - | - | - | - |
| | **P50** | - | - | - | - | - | - |
| | **P10** | - | - | - | - | - | - |
| | **Mean** | 49.2 | 1.39 | 0.487 | 0.077 | 16.9 | 2.68 |

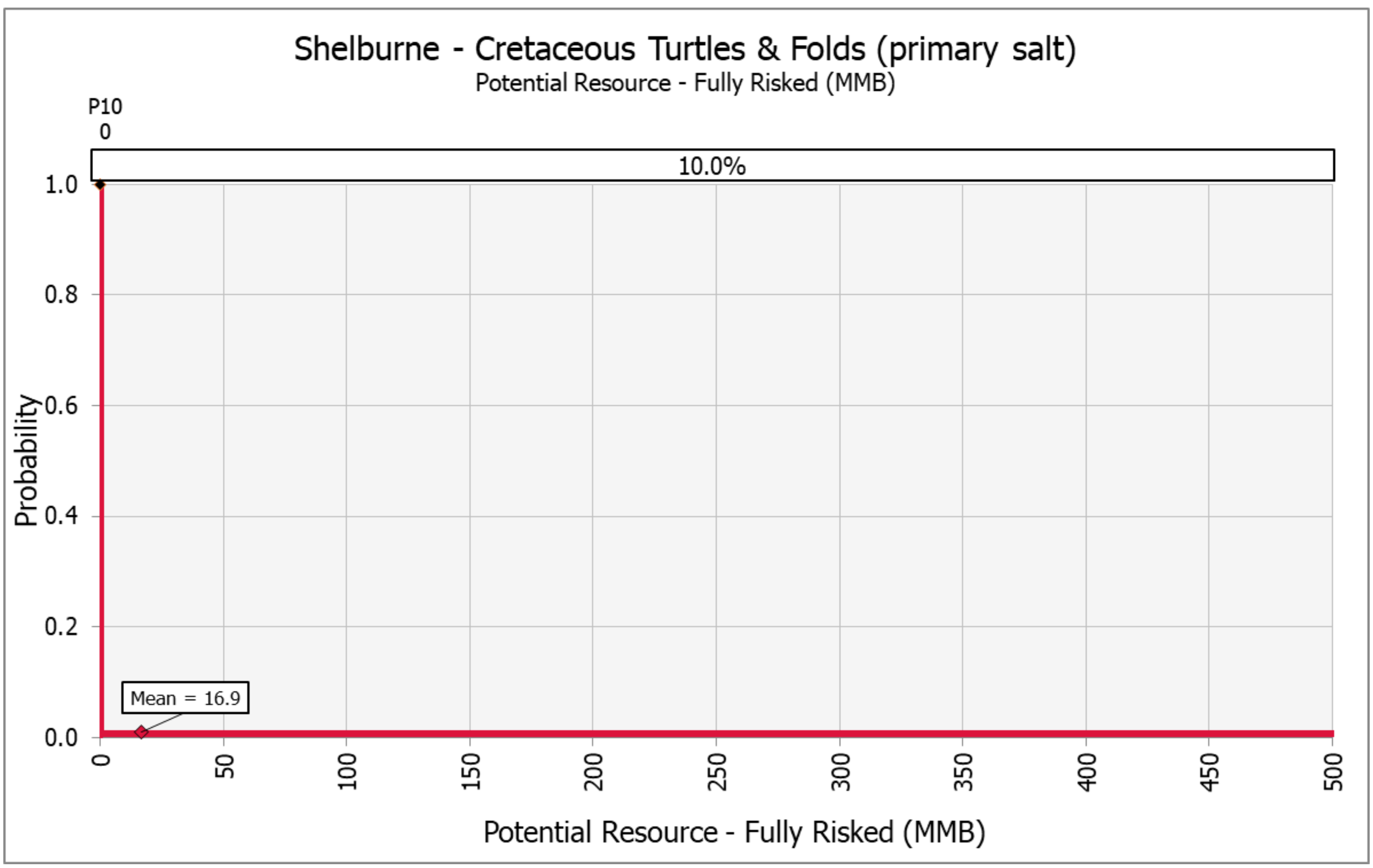

| | | Shelburne - Cretaceous Stratigraphic Onlap | | | | | |
|---|---|---|---|---|---|---|---|
| | | Natural Gas | | Natural Gas Liquids | | Oil Equivalent | |
| | | BCF | $10^9$ $m^3$ | MMB | $10^6$ $m^3$ | MMBOE | $10^6$ $m^3$ |
| In-Place Unrisked | P90 | 3,046 | 86.2 | 28.2 | 4.48 | 1,550 | 246 |
| | P50 | 5,096 | 144 | 49.6 | 7.9 | 2,605 | 414 |
| | P10 | 7,616 | 216 | 80.8 | 12.8 | 4,019 | 639 |
| | Mean | 5,254 | 149 | 52.5 | 8.3 | 2,717 | 432 |
| In-Place Fully Risked | P90 | - | - | - | - | - | - |
| | P50 | - | - | - | - | - | - |
| | P10 | - | - | - | - | - | - |
| | Mean | 96.0 | 2.72 | 1.00 | 0.16 | 50.6 | 8.05 |
| Recoverable Unrisked | P90 | 2,268 | 64 | 20.9 | 3.33 | 767 | 122 |
| | P50 | 3,814 | 108 | 37.0 | 5.89 | 1,286 | 204 |
| | P10 | 5,751 | 163 | 60.8 | 9.67 | 1,959 | 311 |
| | Mean | 3,940 | 112 | 39.4 | 6.26 | 1,334 | 212 |
| Recoverable Fully Risked | P90 | - | - | - | - | - | - |
| | P50 | - | - | - | - | - | - |
| | P10 | - | - | - | - | - | - |
| | Mean | 72.1 | 2.04 | 0.749 | 0.119 | 24.8 | 3.94 |

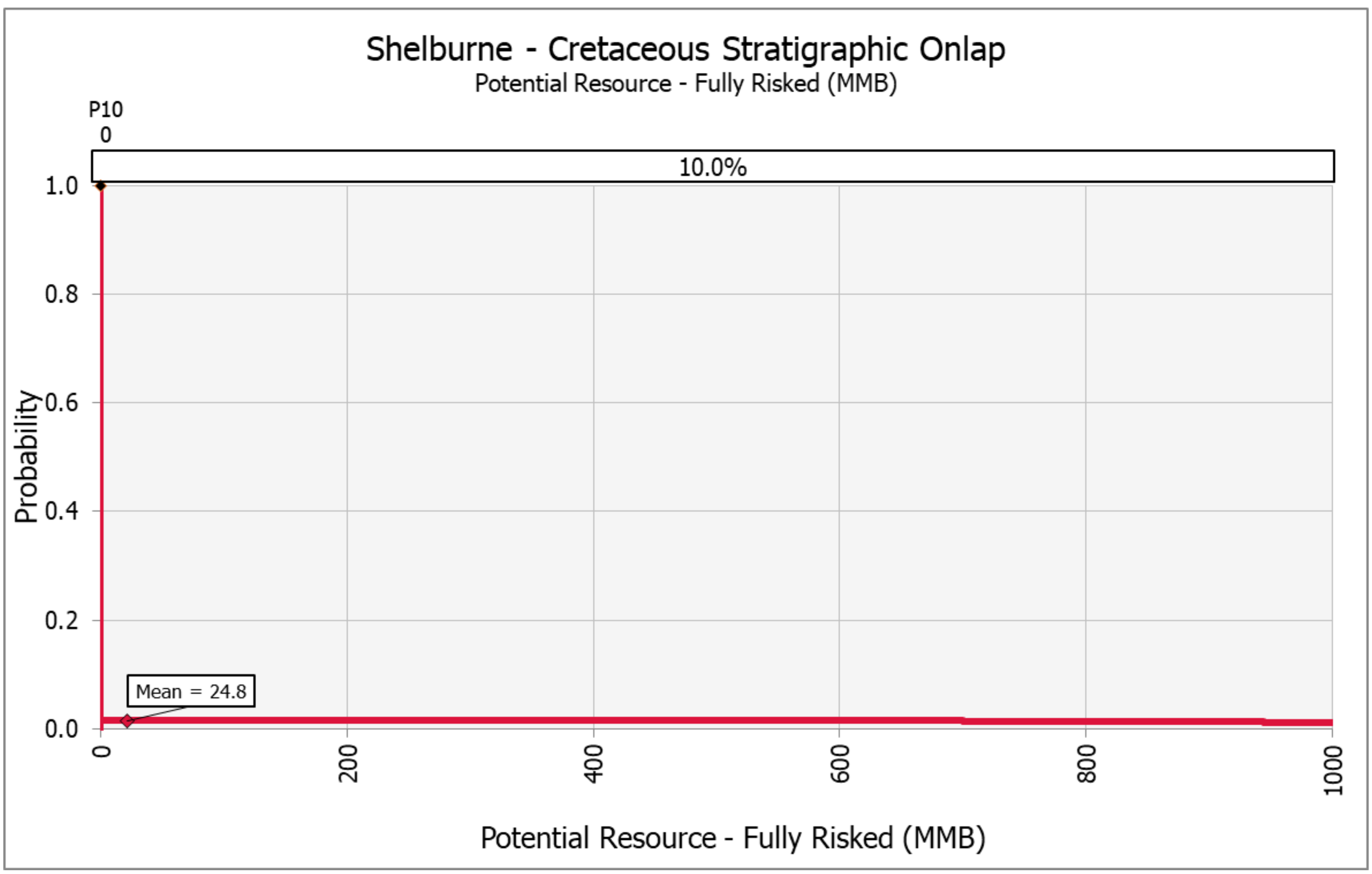

| | | Shelburne - Cretaceous three way traps on salt flanks | | | | | |
|---|---|---|---|---|---|---|---|
| | | Natural Gas | | Natural Gas Liquids | | Oil Equivalent | |
| | | BCF | $10^9$ $m^3$ | MMB | $10^6$ $m^3$ | MMBOE | $10^6$ $m^3$ |
| In-Place Unrisked | P90 | 5,097 | 144 | 46.6 | 7.41 | 2,610 | 415 |
| | P50 | 8,471 | 240 | 82.6 | 13.1 | 4,412 | 701 |
| | P10 | 12,562 | 356 | 134 | 21.3 | 6,747 | 1,073 |
| | Mean | 8,701 | 246 | 87.0 | 13.8 | 4,578 | 728 |
| In-Place Fully Risked | P90 | - | - | - | - | - | - |
| | P50 | - | - | - | - | - | - |
| | P10 | - | - | - | - | - | - |
| | Mean | 46.4 | 1.31 | 0.47 | 0.075 | 24.2 | 3.85 |
| Recoverable Unrisked | P90 | 3,813 | 108 | 34.6 | 5.49 | 1,296 | 206 |
| | P50 | 6,323 | 179 | 61.6 | 9.80 | 2,162 | 344 |
| | P10 | 9,457 | 268 | 101 | 16.0 | 3,266 | 519 |
| | Mean | 6,527 | 185 | 65.3 | 10.4 | 2,237 | 356 |
| Recoverable Fully Risked | P90 | - | - | - | - | - | - |
| | P50 | - | - | - | - | - | - |
| | P10 | - | - | - | - | - | - |
| | Mean | 34.7 | 0.983 | 0.351 | 0.056 | 11.7 | 1.86 |

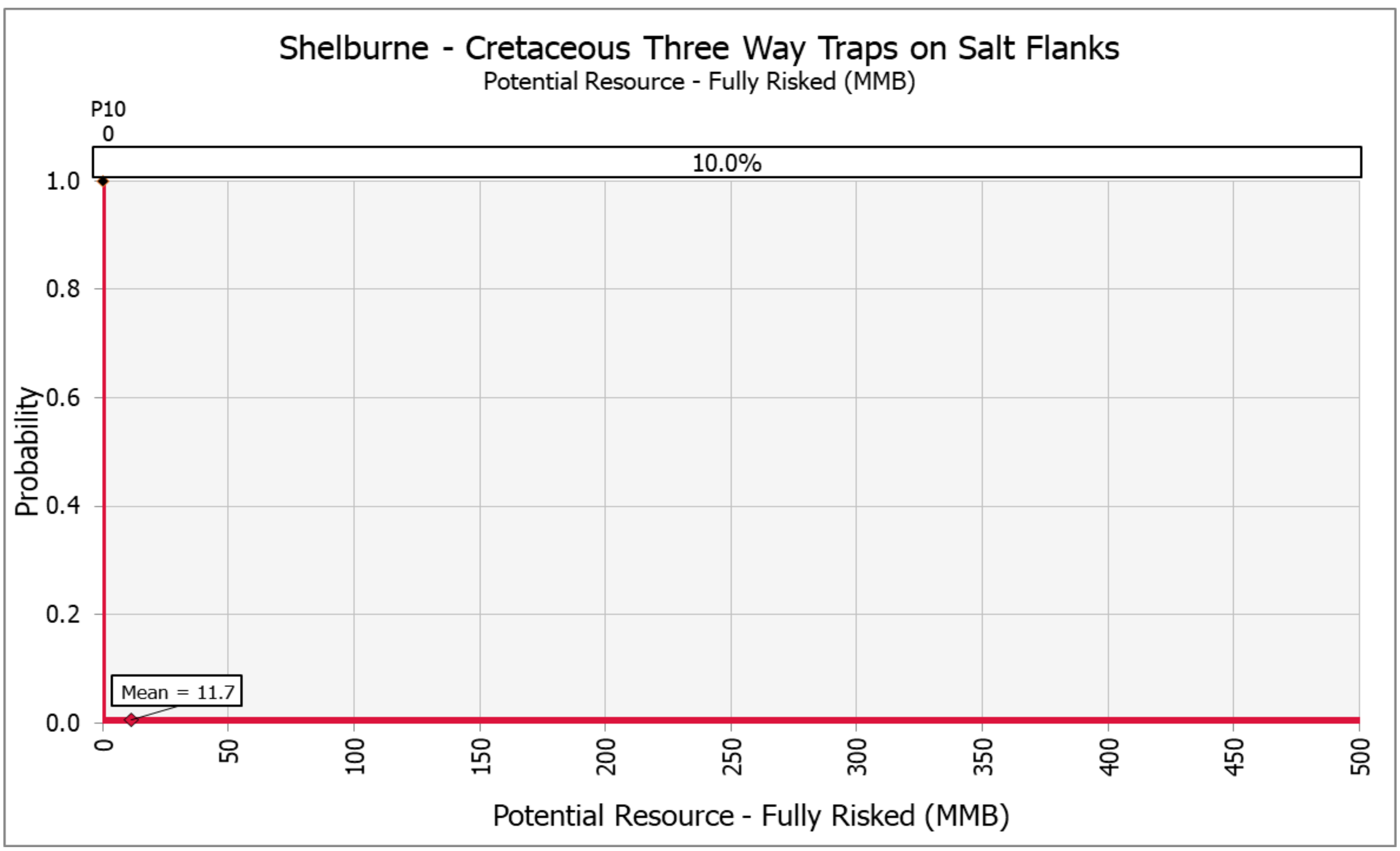

| | | Shelburne - Chalk Play - T50 closures | | | | | |
|---|---|---|---|---|---|---|---|
| | | Natural Gas | | Natural Gas Liquids | | Oil Equivalent | |
| | | BCF | $10^9$ $m^3$ | MMB | $10^6$ $m^3$ | MMBOE | $10^6$ $m^3$ |
| In-Place Unrisked | P90 | 28,958 | 820 | 158.1 | 25.14 | 9,511 | 1,512 |
| | P50 | 49,336 | 1,397 | 291.5 | 46.3 | 16,355 | 2,600 |
| | P10 | 79,429 | 2,249 | 497 | 79.0 | 26,455 | 4,206 |
| | Mean | 52,114 | 1,476 | 312.7 | 49.7 | 17,319 | 2,753 |
| In-Place Fully Risked | P90 | - | - | - | - | - | - |
| | P50 | - | - | - | - | - | - |
| | P10 | - | - | - | - | - | - |
| | Mean | 2,076 | 58.8 | 12.4 | 1.97 | 692 | 110 |
| Recoverable Unrisked | P90 | 6,274 | 178 | 34.3 | 5.46 | 2,021 | 321 |
| | P50 | 12,558 | 356 | 73.7 | 11.7 | 3,792 | 603 |
| | P10 | 23,347 | 661 | 144 | 22.9 | 6,539 | 1,040 |
| | Mean | 13,908 | 394 | 83.6 | 13.3 | 4,085 | 649 |
| Recoverable Fully Risked | P90 | - | - | - | - | - | - |
| | P50 | - | - | - | - | - | - |
| | P10 | - | - | - | - | - | - |
| | Mean | 561 | 15.9 | 3.36 | 0.534 | 165 | 26.2 |

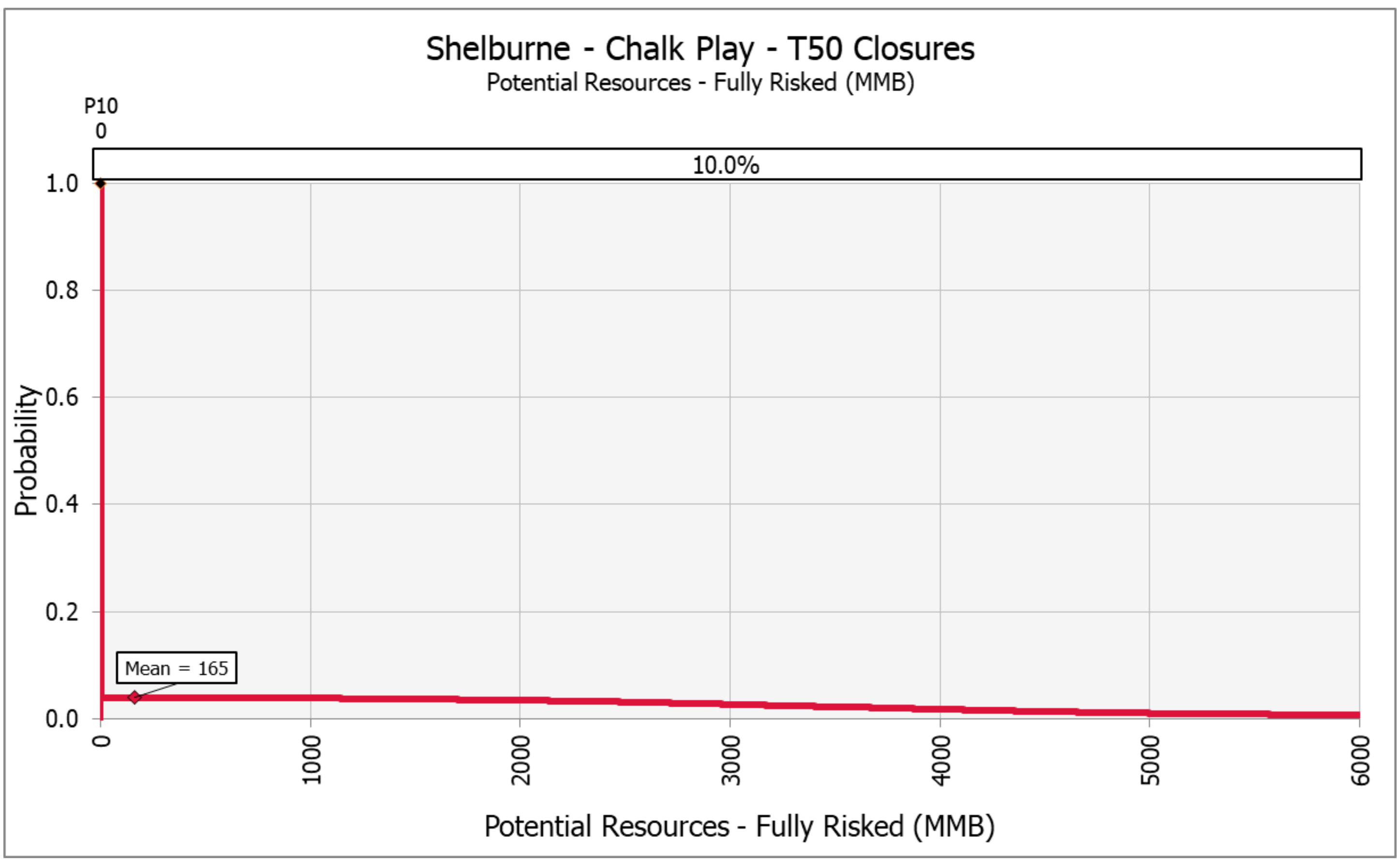

Appendix 4 – **D. Abenaki-Sable Corridor**

| | | Abenaki-Sable Pre-salt rotated fault blocks | | | | | |
|---|---|---|---|---|---|---|---|
| | | Natural Gas | | Natural Gas Liquids | | Oil Equivalent | |
| | | BCF | $10^9$ $m^3$ | MMB | $10^6$ $m^3$ | MMBOE | $10^6$ $m^3$ |
| In-Place Unrisked | P90 | 2,727 | 77.2 | 24.6 | 3.92 | 1,558 | 248 |
| | P50 | 4,387 | 124 | 43.2 | 6.86 | 2,574 | 409 |
| | P10 | 6,984 | 198 | 73.1 | 11.6 | 4,206 | 669 |
| | Mean | 4,651 | 132 | 46.5 | 7.40 | 2,752 | 438 |
| In-Place Fully Risked | P90 | - | - | - | - | - | - |
| | P50 | - | - | - | - | - | - |
| | P10 | - | - | - | - | - | - |
| | Mean | 13.2 | 0.374 | 0.122 | 0.019 | 7.66 | 1.22 |
| Recoverable Unrisked | P90 | 2,031 | 57.5 | 18.4 | 2.92 | 749 | 119 |
| | P50 | 3,277 | 92.8 | 32.3 | 5.14 | 1,227 | 195 |
| | P10 | 5,247 | 149 | 55.1 | 8.75 | 1,973 | 314 |
| | Mean | 3,487 | 98.8 | 34.9 | 5.55 | 1,302 | 207 |
| Recoverable Fully Risked | P90 | - | - | - | - | - | - |
| | P50 | - | - | - | - | - | - |
| | P10 | - | - | - | - | - | - |
| | Mean | 10.1 | 0.285 | 0.093 | 0.015 | 3.72 | 0.592 |

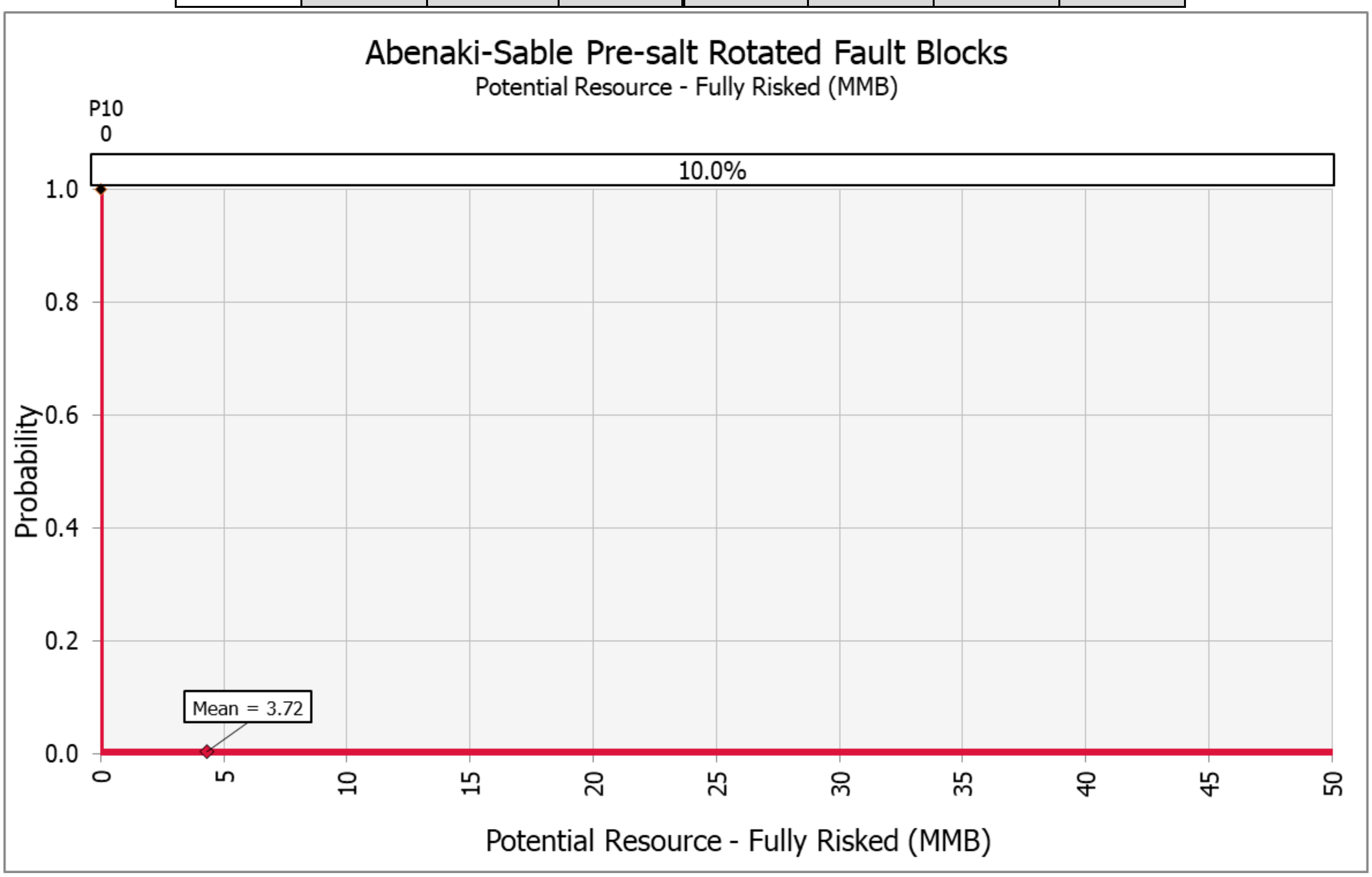

| | | Abenaki-Sable Missisauga Listric Fault Rollovers - Shelf | | | | | |
|---|---|---|---|---|---|---|---|
| | | Natural Gas | | Natural Gas Liquids | | Oil Equivalent | |
| | | BCF | $10^9$ $m^3$ | MMB | $10^6$ $m^3$ | MMBOE | $10^6$ $m^3$ |
| In-Place Unrisked | P90 | 16,410 | 465 | 154 | 24.4 | 4,481 | 712 |
| | P50 | 31,719 | 898 | 309 | 49.1 | 8,616 | 1,370 |
| | P10 | 54,638 | 1,547 | 568 | 90.4 | 14,825 | 2,357 |
| | Mean | 33,962 | 962 | 339 | 54.0 | 9,240 | 1,469 |
| In-Place Fully Risked | P90 | - | - | - | - | - | - |
| | P50 | - | - | - | - | - | - |
| | P10 | 39,174 | 1,109 | 396 | 63.0 | 10,659 | 1,695 |
| | Mean | 10,669 | 302 | 107 | 17.0 | 2,899 | 461 |
| Recoverable Unrisked | P90 | 12,289 | 348 | 115 | 18.3 | 2,762 | 439 |
| | P50 | 23,827 | 675 | 231 | 36.8 | 5,334 | 848 |
| | P10 | 40,851 | 1,157 | 426 | 67.7 | 9,135 | 1,452 |
| | Mean | 25,472 | 721 | 255 | 40.5 | 5,712 | 908 |
| Recoverable Fully Risked | P90 | - | - | - | - | - | - |
| | P50 | - | - | - | - | - | - |
| | P10 | 29,484 | 835 | 297 | 47.3 | 6,598 | 1,049 |
| | Mean | 8,004 | 227 | 80.0 | 12.7 | 1,794 | 285 |

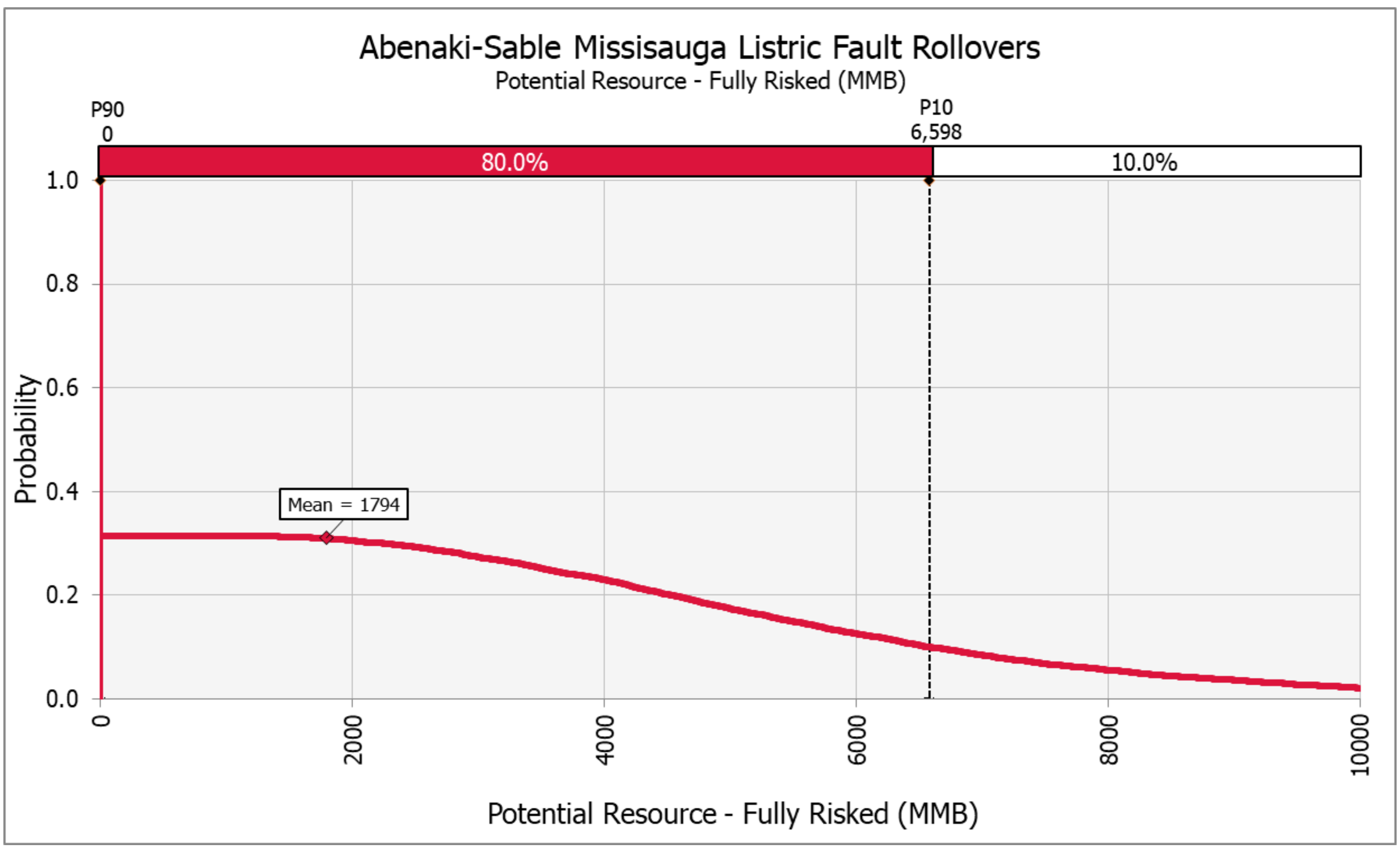

| | | Abenaki-Sable Logan Canyon Listric Fault Rollovers - Shelf | | | | | |
|---|---|---|---|---|---|---|---|
| | | Natural Gas | | Natural Gas Liquids | | Oil Equivalent | |
| | | BCF | $10^9$ $m^3$ | MMB | $10^6$ $m^3$ | MMBOE | $10^6$ $m^3$ |
| In-Place Unrisked | P90 | 9,351 | 265 | 87.5 | 13.9 | 2,839 | 451 |
| | P50 | 17,329 | 491 | 169 | 26.8 | 5,140 | 817 |
| | P10 | 29,139 | 825 | 302 | 48.1 | 8,526 | 1,355 |
| | Mean | 18,464 | 523 | 185 | 29.4 | 5,462 | 868 |
| In-Place Fully Risked | P90 | - | - | - | - | - | - |
| | P50 | - | - | - | - | - | - |
| | P10 | 17,549 | 497 | 173 | 27.4 | 5,197 | 826 |
| | Mean | 3,743 | 106 | 37.6 | 5.98 | 1,105 | 176 |
| Recoverable Unrisked | P90 | 7,011 | 199 | 65.4 | 10.4 | 1,675 | 266 |
| | P50 | 12,934 | 366 | 126 | 20.1 | 3,059 | 486 |
| | P10 | 21,832 | 618 | 227 | 36.1 | 5,093 | 810 |
| | Mean | 13,851 | 392 | 139 | 22.0 | 3,260 | 518 |
| Recoverable Fully Risked | P90 | - | - | - | - | - | - |
| | P50 | - | - | - | - | - | - |
| | P10 | 13,158 | 373 | 129 | 20.5 | 3,091 | 491 |
| | Mean | 2,805 | 79.4 | 28.2 | 4.48 | 660 | 105 |

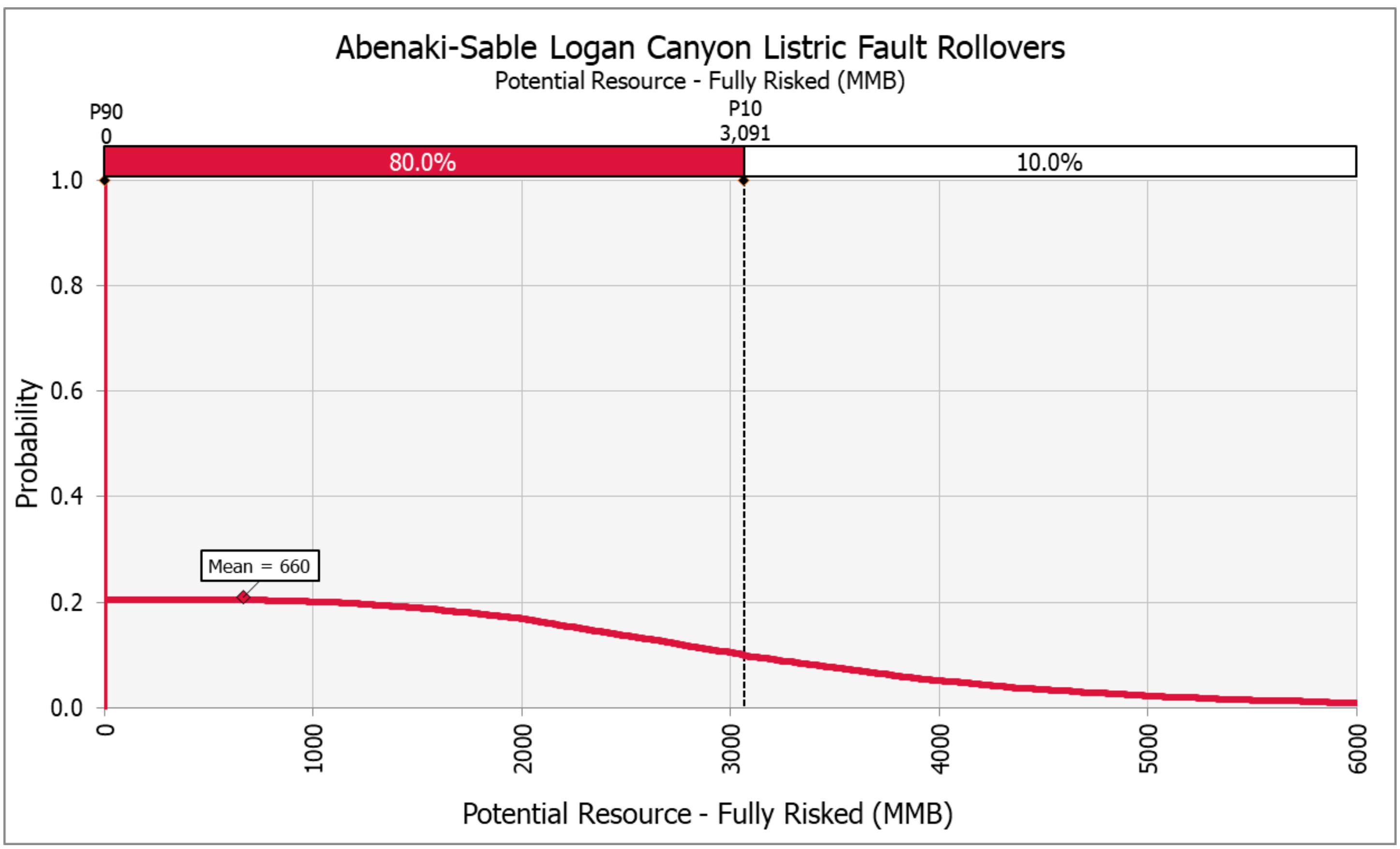

| | | Abenaki-Sable Porous Carbonate Bank Edge | | | | | |
|---|---|---|---|---|---|---|---|
| | | Natural Gas | | Natural Gas Liquids | | Oil Equivalent | |
| | | BCF | $10^9$ $m^3$ | MMB | $10^6$ $m^3$ | MMBOE | $10^6$ $m^3$ |
| In-Place Unrisked | P90 | 1,479 | 41.9 | 5.52 | 0.877 | 854 | 136 |
| | P50 | 3,311 | 93.7 | 12.9 | 2.05 | 1,946 | 309 |
| | P10 | 6,450 | 183 | 26.7 | 4.24 | 3,815 | 607 |
| | Mean | 3,694 | 105 | 14.8 | 2.35 | 2,188 | 348 |
| In-Place Fully Risked | P90 | - | - | - | - | - | - |
| | P50 | - | - | - | - | - | - |
| | P10 | 3,911 | 111 | 15.6 | 2.47 | 2,316 | 368 |
| | Mean | 958 | 27.1 | 3.85 | 0.612 | 567 | 90.1 |
| Recoverable Unrisked | P90 | 339 | 9.6 | 1.28 | 0.203 | 270 | 43.0 |
| | P50 | 821 | 23.2 | 3.24 | 0.514 | 623 | 99.0 |
| | P10 | 1,859 | 52.7 | 7.56 | 1.20 | 1,273 | 202 |
| | Mean | 984 | 27.9 | 3.94 | 0.626 | 712 | 113 |
| Recoverable Fully Risked | P90 | - | - | - | - | - | - |
| | P50 | - | - | - | - | - | - |
| | P10 | 1,013 | 28.7 | 4.03 | 0.641 | 752 | 120 |
| | Mean | 258 | 7.29 | 1.04 | 0.165 | 185 | 29.5 |

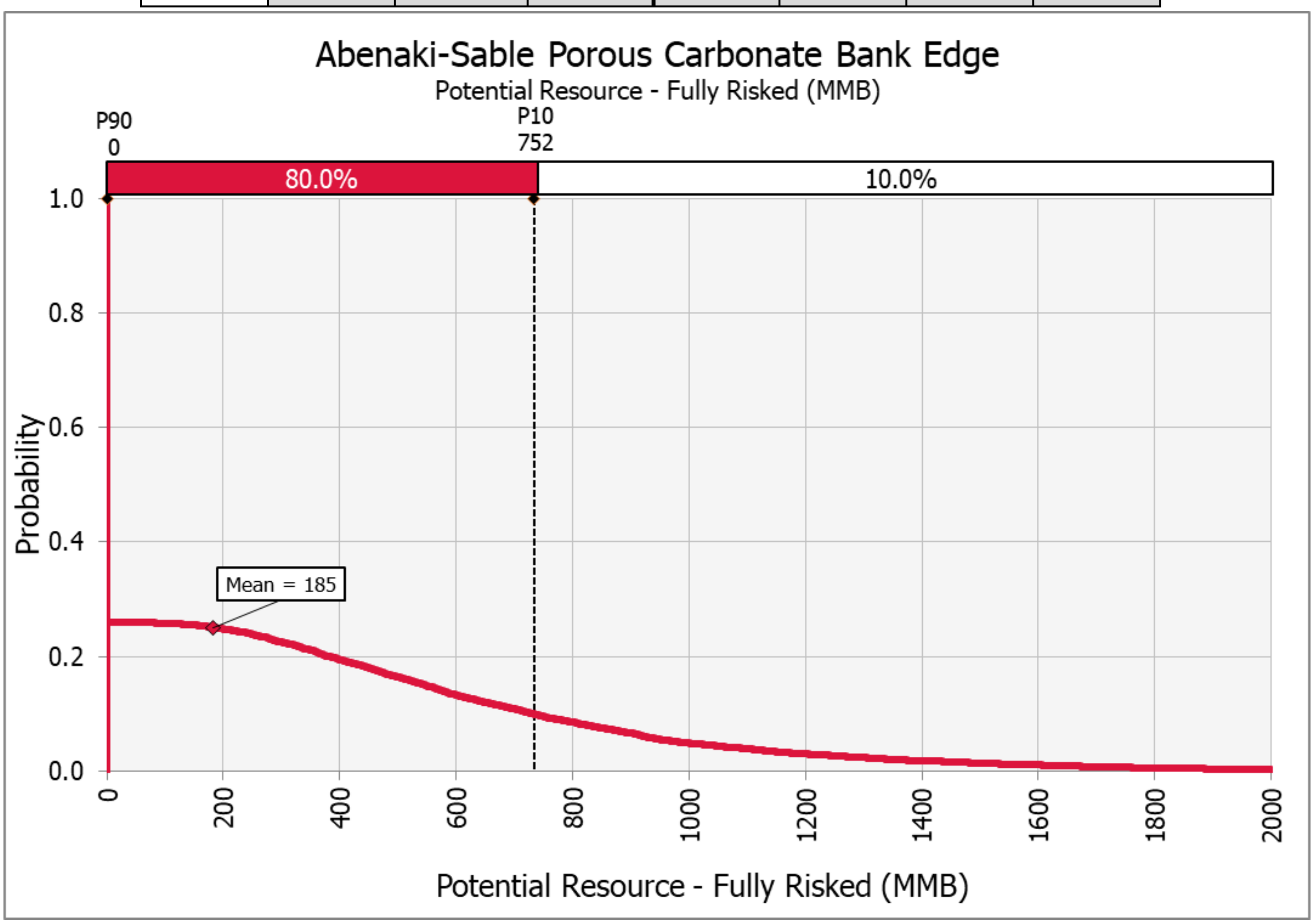

| | | Abenaki-Sable Cretaceous Stratigraphic Onlap | | | | | |
|---|---|---|---|---|---|---|---|
| | | Natural Gas | | Natural Gas Liquids | | Oil Equivalent | |
| | | BCF | $10^9$ $m^3$ | MMB | $10^6$ $m^3$ | MMBOE | $10^6$ $m^3$ |
| In-Place Unrisked | P90 | 991 | 28.1 | 9.28 | 1.476 | 181 | 28.8 |
| | P50 | 2,008 | 56.9 | 19.6 | 3.12 | 367 | 58.4 |
| | P10 | 3,651 | 103 | 37.6 | 5.98 | 665 | 106 |
| | Mean | 2,208 | 62.5 | 22.1 | 3.51 | 403 | 64.0 |
| In-Place Fully Risked | P90 | - | - | - | - | - | - |
| | P50 | - | - | - | - | - | - |
| | P10 | - | - | - | - | - | - |
| | Mean | 65.5 | 1.86 | 0.656 | 0.104 | 12.0 | 1.90 |
| Recoverable Unrisked | P90 | 741 | 21.0 | 6.91 | 1.10 | 135 | 21.5 |
| | P50 | 1,506 | 42.7 | 14.7 | 2.34 | 275 | 43.7 |
| | P10 | 2,751 | 77.9 | 28.3 | 4.50 | 502 | 79.8 |
| | Mean | 1,656 | 46.9 | 16.5 | 2.63 | 302 | 48.0 |
| Recoverable Fully Risked | P90 | - | - | - | - | - | - |
| | P50 | - | - | - | - | - | - |
| | P10 | - | - | - | - | - | - |
| | Mean | 49.3 | 1.40 | 0.493 | 0.078 | 8.99 | 1.43 |

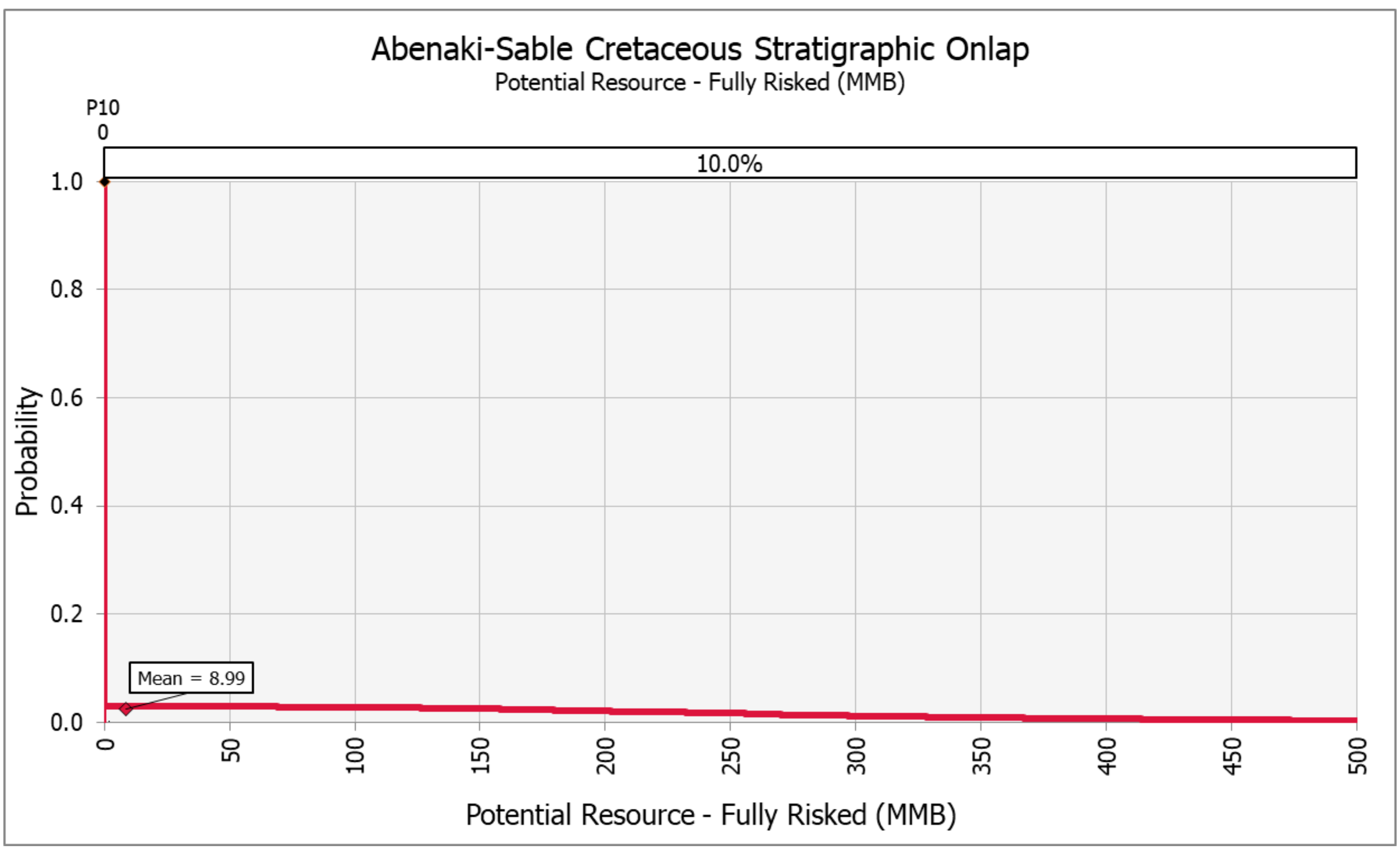

| | | Abenaki-Sable Sub-Salt Canopy Cut-off (Shelf) | | | | | |
|---|---|---|---|---|---|---|---|
| | | Natural Gas | | Natural Gas Liquids | | Oil Equivalent | |
| | | BCF | $10^9$ $m^3$ | MMB | $10^6$ $m^3$ | MMBOE | $10^6$ $m^3$ |
| In-Place Unrisked | P90 | 1,478 | 41.9 | 13.3 | 2.114 | 270 | 42.9 |
| | P50 | 2,403 | 68.1 | 23.6 | 3.75 | 438 | 69.7 |
| | P10 | 3,880 | 110 | 40.4 | 6.43 | 708 | 113 |
| | Mean | 2,558 | 72.4 | 25.6 | 4.07 | 467 | 74.2 |
| In-Place Fully Risked | P90 | - | - | - | - | - | - |
| | P50 | - | - | - | - | - | - |
| | P10 | - | - | - | - | - | - |
| | Mean | 88.6 | 2.51 | 0.883 | 0.140 | 16.2 | 2.57 |
| Recoverable Unrisked | P90 | 870 | 24.6 | 7.94 | 1.26 | 159 | 25.3 |
| | P50 | 1,434 | 40.6 | 14.2 | 2.25 | 262 | 41.6 |
| | P10 | 2,338 | 66.2 | 24.4 | 3.87 | 427 | 67.8 |
| | Mean | 1,535 | 43.5 | 15.3 | 2.44 | 280 | 44.5 |
| Recoverable Fully Risked | P90 | - | - | - | - | - | - |
| | P50 | - | - | - | - | - | - |
| | P10 | - | - | - | - | - | - |
| | Mean | 53.2 | 1.507 | 0.530 | 0.084 | 9.71 | 1.54 |

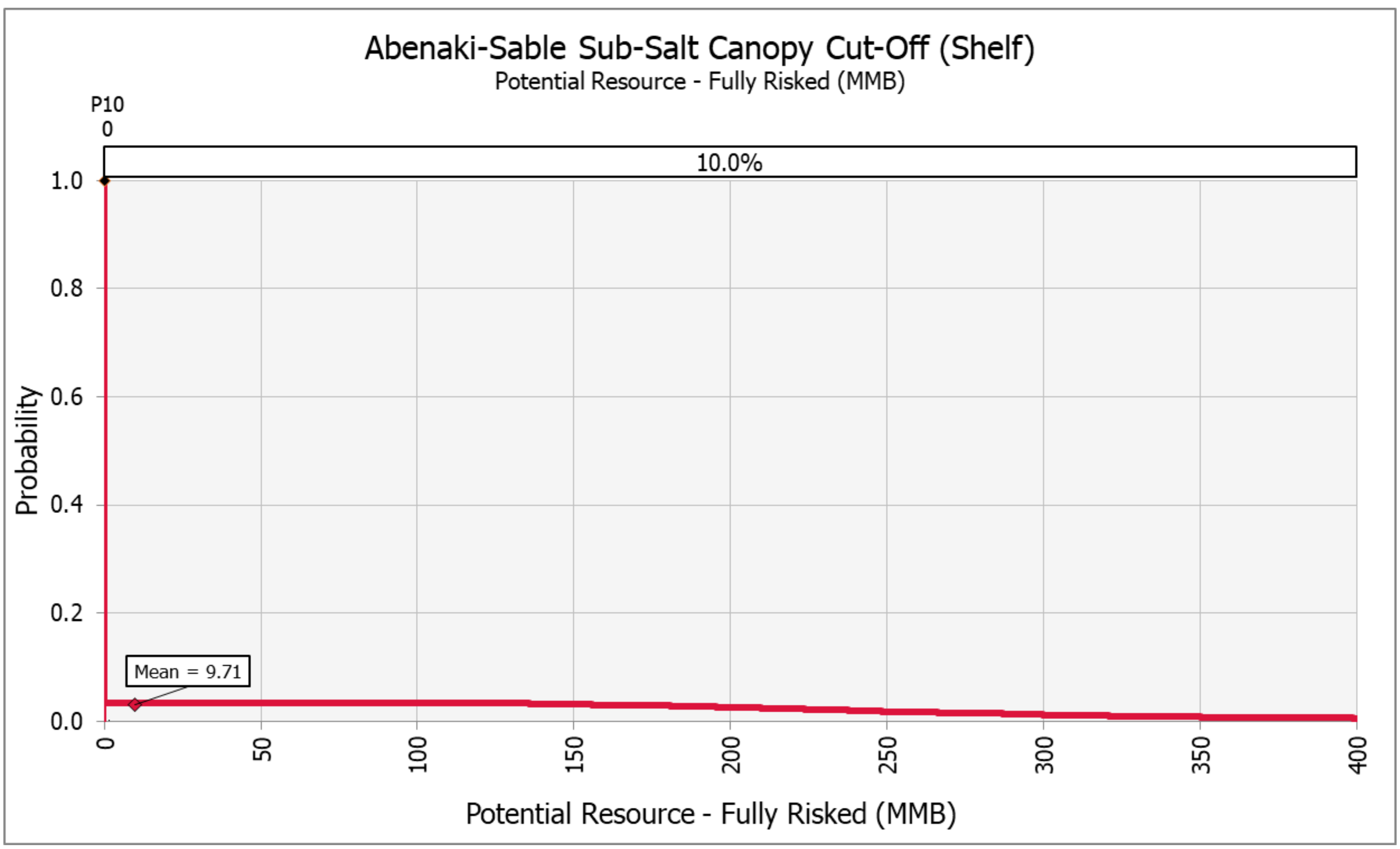

| | | Abenaki-Sable Sub-Salt Canopy Cut-off (Slope) | | | | | |
|---|---|---|---|---|---|---|---|
| | | Natural Gas | | Natural Gas Liquids | | Oil Equivalent | |
| | | BCF | $10^9$ $m^3$ | MMB | $10^6$ $m^3$ | MMBOE | $10^6$ $m^3$ |
| In-Place Unrisked | P90 | 34,246 | 970 | 316 | 50.2 | 6,241 | 992 |
| | P50 | 62,614 | 1,773 | 615 | 97.8 | 11,422 | 1,816 |
| | P10 | 108,189 | 3,064 | 1,129 | 180 | 19,721 | 3,135 |
| | Mean | 67,557 | 1,913 | 676 | 108 | 12,324 | 1,959 |
| In-Place Fully Risked | P90 | - | - | - | - | - | - |
| | P50 | - | - | - | - | - | - |
| | P10 | - | - | - | - | - | - |
| | Mean | 5,031 | 142.5 | 50.266 | 7.99 | 918 | 146 |
| Recoverable Unrisked | P90 | 25,634 | 725.9 | 236 | 37.5 | 4,664 | 742 |
| | P50 | 47,040 | 1,332.0 | 458 | 72.9 | 8,579 | 1,364 |
| | P10 | 81,089 | 2,296.2 | 846 | 134 | 14,823 | 2,357 |
| | Mean | 50,676 | 1,435.0 | 507 | 80.6 | 9,244 | 1,470 |
| Recoverable Fully Risked | P90 | - | - | - | - | - | - |
| | P50 | - | - | - | - | - | - |
| | P10 | - | - | - | - | - | - |
| | Mean | 3,763 | 107 | 37.6 | 5.98 | 686 | 109 |

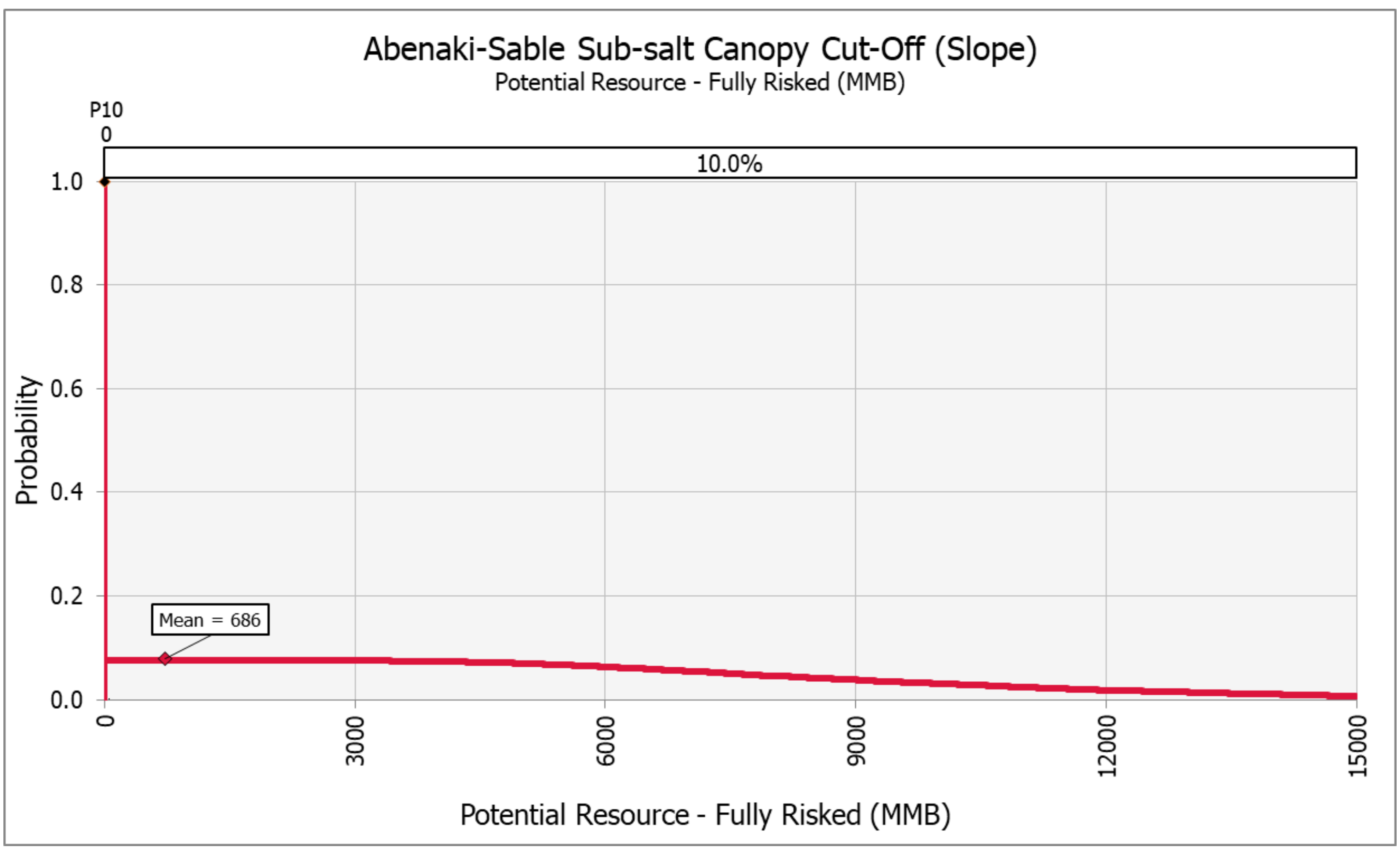

| | | Abenaki-Sable Jurassic Turtles & Folds (primary salt) | | | | | |
|---|---|---|---|---|---|---|---|
| | | Natural Gas | | Natural Gas Liquids | | Oil Equivalent | |
| | | BCF | $10^9$ $m^3$ | MMB | $10^6$ $m^3$ | MMBOE | $10^6$ $m^3$ |
| In-Place Unrisked | P90 | 11,333 | 321 | 102 | 16.2 | 2,067 | 329 |
| | P50 | 18,639 | 528 | 183 | 29.1 | 3,398 | 540 |
| | P10 | 29,076 | 823 | 309 | 49.1 | 5,310 | 844 |
| | Mean | 19,551 | 554 | 196 | 31.1 | 3,567 | 567 |
| In-Place Fully Risked | P90 | - | - | - | - | - | - |
| | P50 | - | - | - | - | - | - |
| | P10 | - | - | - | - | - | - |
| | Mean | 1,024 | 29.0 | 10.2 | 1.62 | 187 | 29.7 |
| Recoverable Unrisked | P90 | 6,746 | 191 | 60.6 | 9.64 | 1,227 | 195 |
| | P50 | 11,157 | 316 | 109 | 17.4 | 2,034 | 323 |
| | P10 | 17,550 | 497 | 186 | 29.6 | 3,203 | 509 |
| | Mean | 11,732 | 332 | 118 | 18.7 | 2,140 | 340 |
| Recoverable Fully Risked | P90 | - | - | - | - | - | - |
| | P50 | - | - | - | - | - | - |
| | P10 | - | - | - | - | - | - |
| | Mean | 615 | 17.4 | 6.12 | 0.972 | 112 | 17.8 |

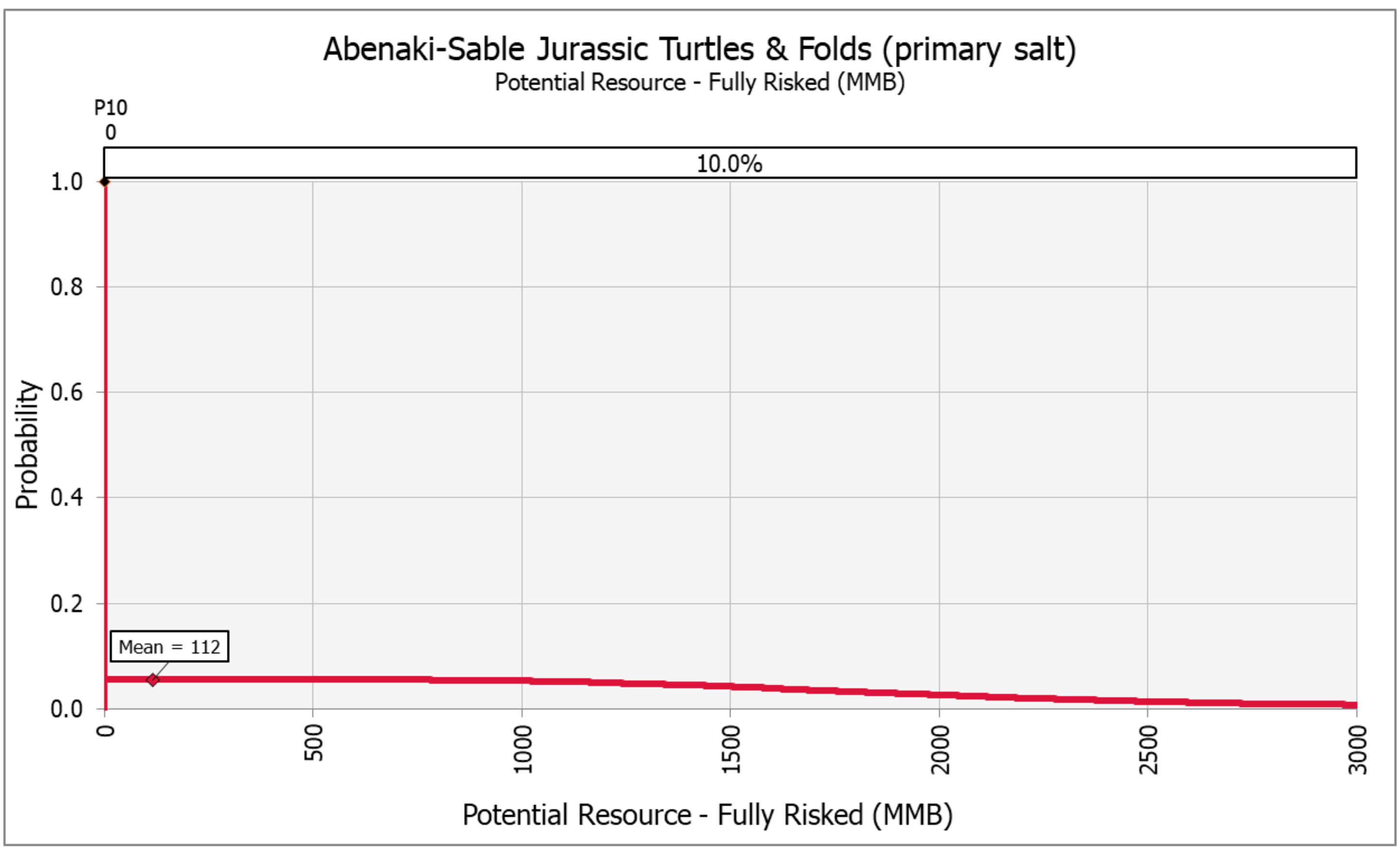

| | | Abenaki-Sable Cretaceous Turtles & Folds (primary salt) | | | | | |
|---|---|---|---|---|---|---|---|
| | | Natural Gas | | Natural Gas Liquids | | Oil Equivalent | |
| | | BCF | $10^9$ $m^3$ | MMB | $10^6$ $m^3$ | MMBOE | $10^6$ $m^3$ |
| In-Place Unrisked | P90 | 24,342 | 689 | 222 | 35.3 | 4,441 | 706 |
| | P50 | 43,152 | 1,222 | 422 | 67.1 | 7,863 | 1,250 |
| | P10 | 70,762 | 2,004 | 743 | 118.2 | 12,936 | 2,057 |
| | Mean | 45,764 | 1,296 | 458 | 72.8 | 8,348 | 1,327 |
| In-Place Fully Risked | P90 | - | - | - | - | - | - |
| | P50 | - | - | - | - | - | - |
| | P10 | 36,795 | 1,042 | 358 | 57.0 | 6,754 | 1,074 |
| | Mean | 7,093 | 201 | 70.8 | 11.3 | 1,294 | 206 |
| Recoverable Unrisked | P90 | 18,137 | 514 | 165 | 26.3 | 3,306 | 526 |
| | P50 | 32,269 | 914 | 316 | 50.2 | 5,885 | 936 |
| | P10 | 53,506 | 1,515 | 558 | 88.8 | 9,744 | 1,549 |
| | Mean | 34,320 | 972 | 343 | 54.6 | 6,261 | 995 |
| Recoverable Fully Risked | P90 | - | - | - | - | - | - |
| | P50 | - | - | - | - | - | - |
| | P10 | 27,397 | 776 | 265 | 42.1 | 5,018 | 798 |
| | Mean | 5,331 | 151 | 53.2 | 8.46 | 972 | 155 |

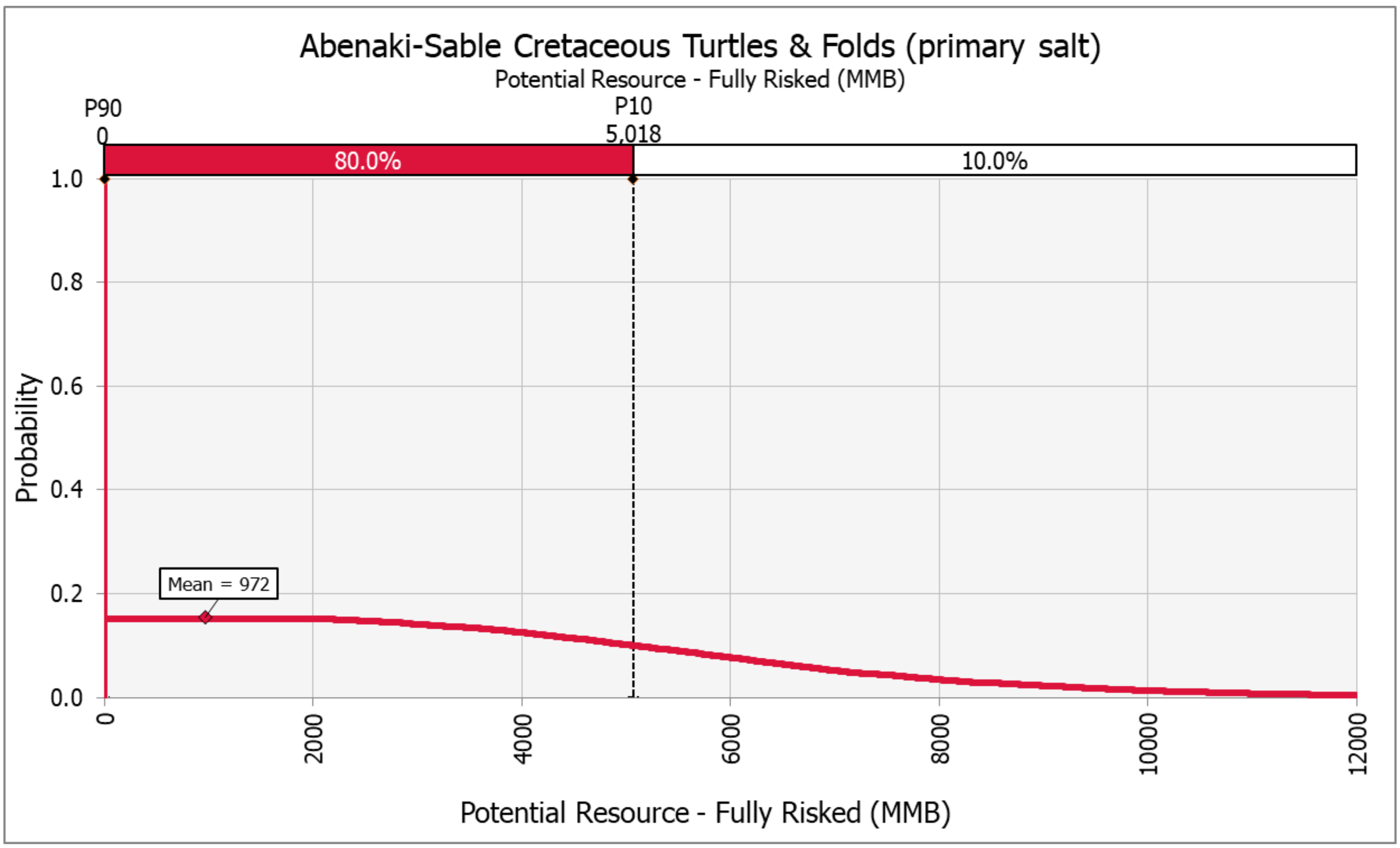

| | | Abenaki-Sable Cret Supra-Canopy Turtles & Folds (Sable) | | | | | |
|---|---|---|---|---|---|---|---|
| | | Natural Gas | | Natural Gas Liquids | | Oil Equivalent | |
| | | BCF | $10^9$ $m^3$ | MMB | $10^6$ $m^3$ | MMBOE | $10^6$ $m^3$ |
| In-Place Unrisked | P90 | 29,021 | 822 | 269 | 42.7 | 5,306 | 844 |
| | P50 | 52,597 | 1,489 | 513 | 81.5 | 9,596 | 1,526 |
| | P10 | 85,898 | 2,432 | 899 | 143 | 15,703 | 2,497 |
| | Mean | 55,413 | 1,569 | 554 | 88.1 | 10,108 | 1,607 |
| In-Place Fully Risked | P90 | - | - | - | - | - | - |
| | P50 | - | - | - | - | - | - |
| | P10 | 32,992 | 934 | 308 | 48.9 | 6,007 | 955 |
| | Mean | 6,587 | 187 | 65.8 | 10.5 | 1,202 | 191 |
| Recoverable Unrisked | P90 | 21,631 | 613 | 201 | 31.9 | 3,943 | 627 |
| | P50 | 39,260 | 1,112 | 383 | 60.9 | 7,162 | 1,139 |
| | P10 | 64,805 | 1,835 | 676 | 108 | 11,821 | 1,879 |
| | Mean | 41,564 | 1,177 | 416 | 66.1 | 7,582 | 1,205 |
| Recoverable Fully Risked | P90 | - | - | - | - | - | - |
| | P50 | - | - | - | - | - | - |
| | P10 | 24,707 | 700 | 228 | 36.3 | 4,496 | 715 |
| | Mean | 4,936 | 140 | 49.3 | 7.84 | 900 | 143 |

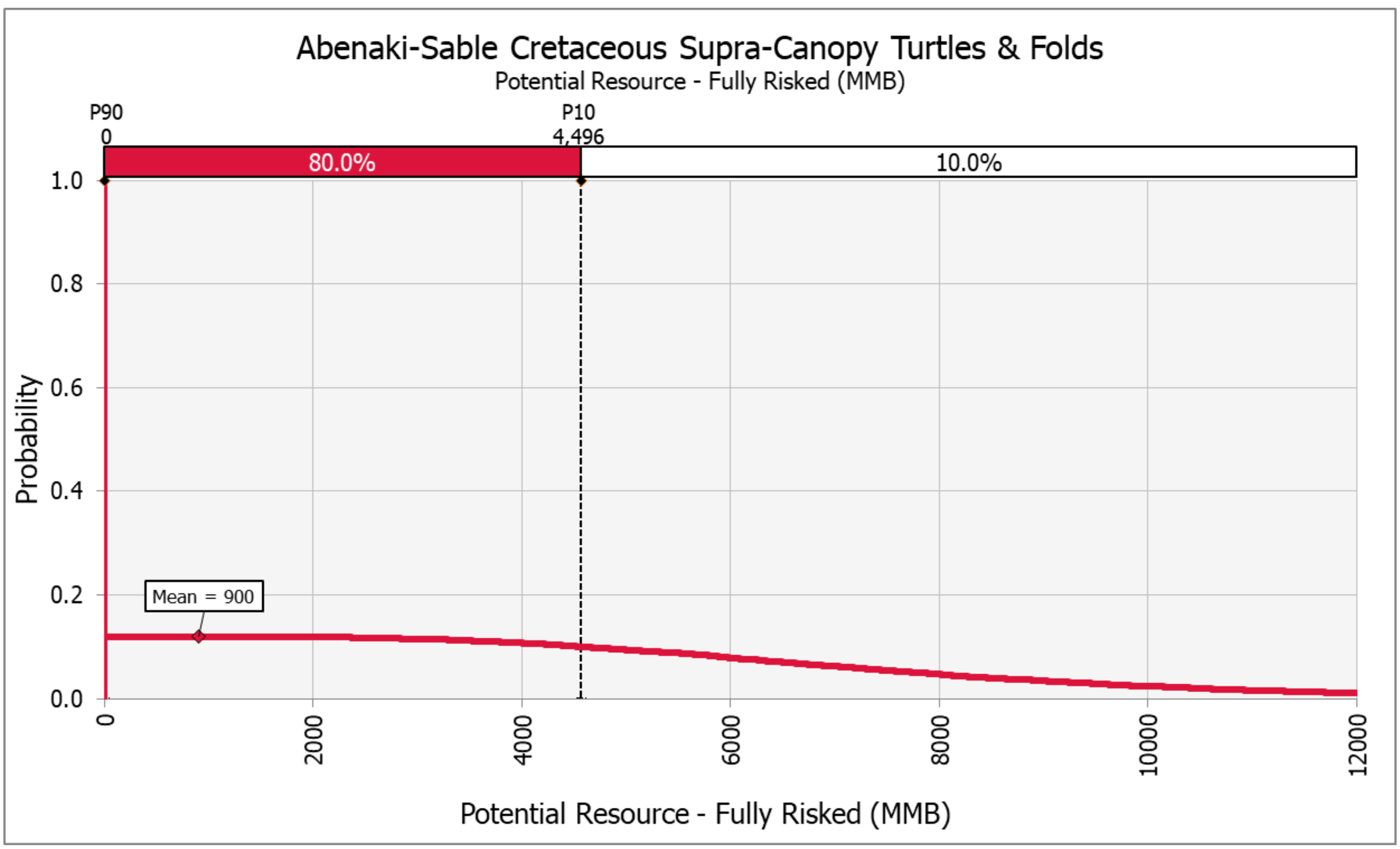

| | | Abenaki-Sable Cretaceous Three Way Traps on Salt Flanks | | | | | |
|---|---|---|---|---|---|---|---|
| | | Natural Gas | | Natural Gas Liquids | | Oil Equivalent | |
| | | BCF | $10^9$ $m^3$ | MMB | $10^6$ $m^3$ | MMBOE | $10^6$ $m^3$ |
| In-Place Unrisked | P90 | 7,936 | 225 | 72.5 | 11.5 | 1,446 | 230 |
| | P50 | 13,521 | 383 | 132 | 21.0 | 2,463 | 392 |
| | P10 | 21,757 | 616 | 229 | 36.3 | 3,977 | 632 |
| | Mean | 14,305 | 405 | 143 | 22.7 | 2,609 | 415 |
| In-Place Fully Risked | P90 | - | - | - | - | - | - |
| | P50 | - | - | - | - | - | - |
| | P10 | - | - | - | - | - | - |
| | Mean | 364 | 10.3 | 3.67 | 0.584 | 66.4 | 10.5 |
| Recoverable Unrisked | P90 | 5,940 | 168 | 54.4 | 8.64 | 1,084 | 172 |
| | P50 | 10,108 | 286 | 98.6 | 15.7 | 1,844 | 293 |
| | P10 | 16,326 | 462 | 172 | 27.3 | 2,987 | 475 |
| | Mean | 10,726 | 304 | 107 | 17.0 | 1,957 | 311 |
| Recoverable Fully Risked | P90 | - | - | - | - | - | - |
| | P50 | - | - | - | - | - | - |
| | P10 | - | - | - | - | - | - |
| | Mean | 273 | 7.73 | 2.76 | 0.438 | 49.8 | 7.92 |

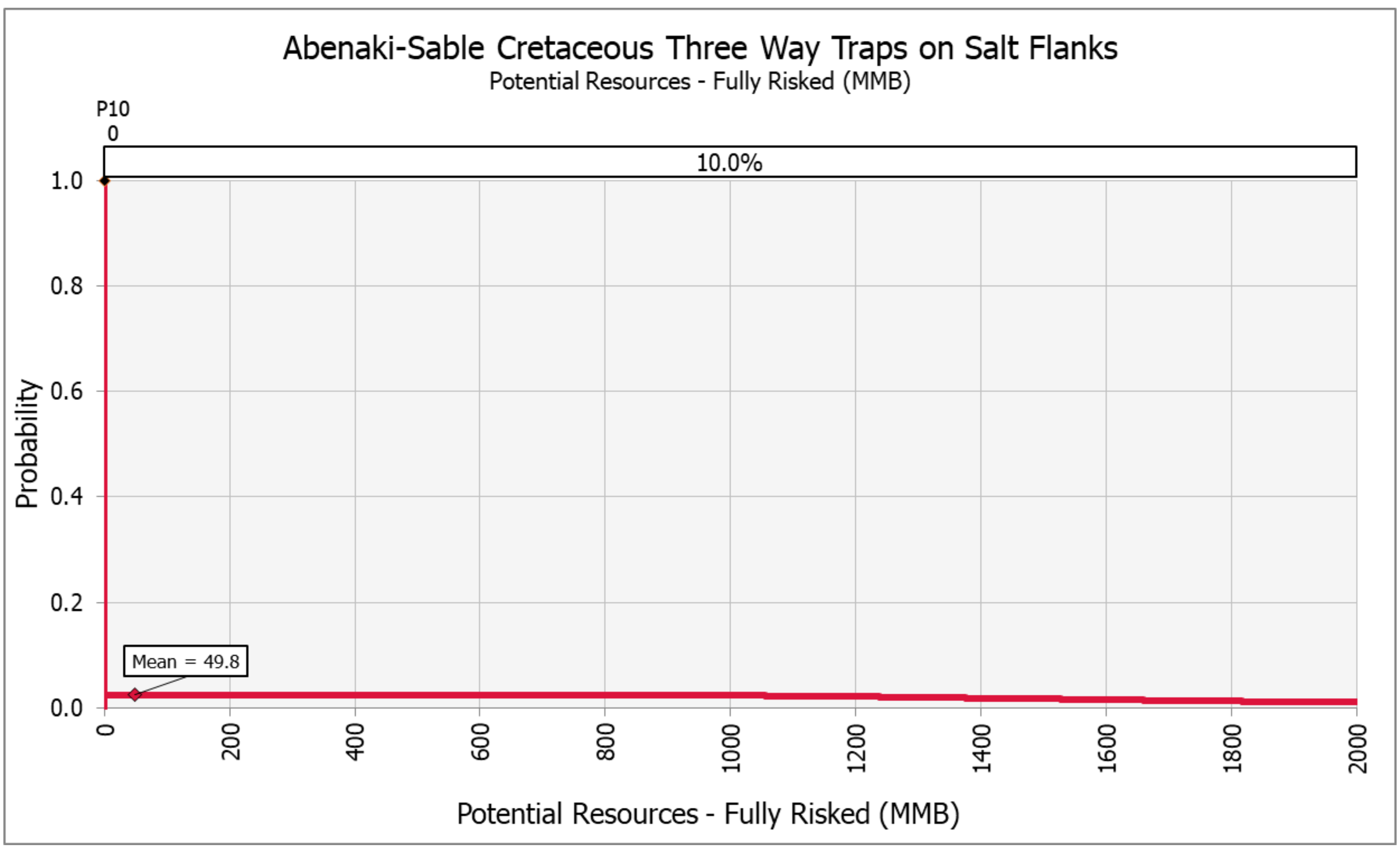

| | | Abenaki-Sable Chalk Play - T50 closures | | | | | |
|---|---|---|---|---|---|---|---|
| | | Natural Gas | | Natural Gas Liquids | | Oil Equivalent | |
| | | BCF | $10^9$ $m^3$ | MMB | $10^6$ $m^3$ | MMBOE | $10^6$ $m^3$ |
| In-Place Unrisked | P90 | 26,246 | 743 | 141 | 22.3 | 4,689 | 746 |
| | P50 | 39,567 | 1,120 | 233 | 37.0 | 7,059 | 1,122 |
| | P10 | 57,620 | 1,632 | 368 | 58.5 | 10,273 | 1,633 |
| | Mean | 40,918 | 1,159 | 245 | 39.0 | 7,300 | 1,161 |
| In-Place Fully Risked | P90 | - | - | - | - | - | - |
| | P50 | - | - | - | - | - | - |
| | P10 | - | - | - | - | - | - |
| | Mean | 3,269 | 92.6 | 19.8 | 3.15 | 583 | 92.8 |
| Recoverable Unrisked | P90 | 5,509 | 156 | 30.7 | 4.88 | 983 | 156 |
| | P50 | 10,038 | 284 | 58.6 | 9.32 | 1,792 | 285 |
| | P10 | 17,544 | 497 | 109 | 17.3 | 3,127 | 497 |
| | Mean | 10,914 | 309 | 65.4 | 10.4 | 1,947 | 310 |
| Recoverable Fully Risked | P90 | - | - | - | - | - | - |
| | P50 | - | - | - | - | - | - |
| | P10 | - | - | - | - | - | - |
| | Mean | 879 | 24.9 | 5.30 | 0.843 | 157 | 24.9 |

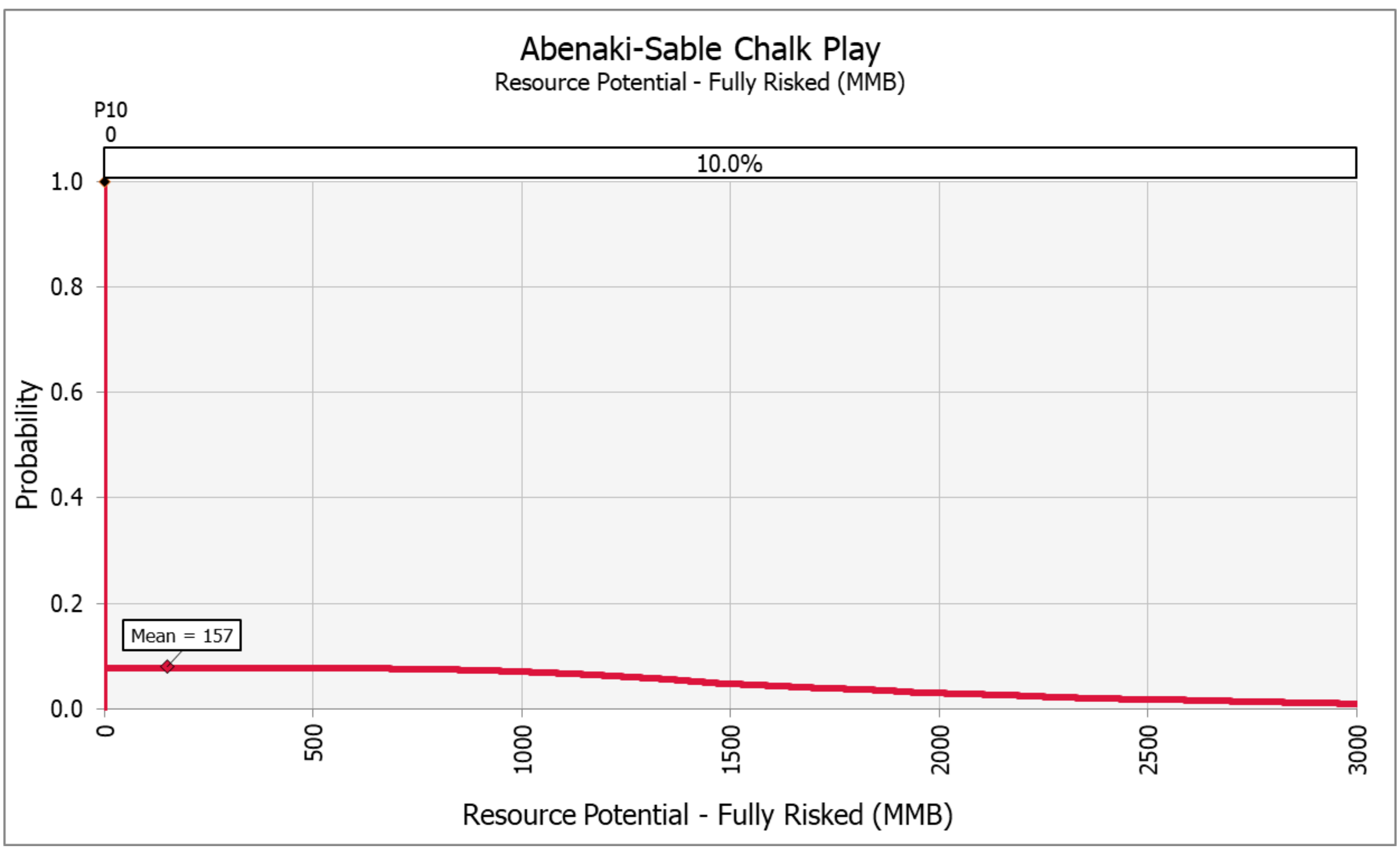

Appendix 5 – **E. Huron Corridor**

| | | Huron - Mic Mac Listric Fault Rollovers - Shelf | | | | | |
|---|---|---|---|---|---|---|---|
| | | Natural Gas | | Natural Gas Liquids | | Oil Equivalent | |
| | | BCF | $10^9$ $m^3$ | MMB | $10^6$ $m^3$ | MMBOE | $10^6$ $m^3$ |
| In-Place Unrisked | P90 | 4,560 | 129 | 40.9 | 6.50 | 831 | 132 |
| | P50 | 6,892 | 195 | 68.1 | 10.8 | 1,259 | 200 |
| | P10 | 10,345 | 293 | 109 | 17.4 | 1,889 | 300 |
| | Mean | 7,222 | 204 | 72.2 | 11.5 | 1,317 | 209 |
| In-Place Fully Risked | P90 | - | - | - | - | - | - |
| | P50 | - | - | - | - | - | - |
| | P10 | - | - | - | - | - | - |
| | Mean | 374 | 10.6 | 3.74 | 0.595 | 68.3 | 10.9 |
| Recoverable Unrisked | P90 | 2,706 | 76.6 | 24.4 | 3.87 | 493 | 78 |
| | P50 | 4,134 | 117 | 40.6 | 6.45 | 754 | 120 |
| | P10 | 6,242 | 177 | 65.7 | 10.4 | 1,138 | 181 |
| | Mean | 4,333 | 123 | 43.3 | 6.88 | 790 | 126 |
| Recoverable Fully Risked | P90 | - | - | - | - | - | - |
| | P50 | - | - | - | - | - | - |
| | P10 | - | - | - | - | - | - |
| | Mean | 224 | 6.35 | 2.24 | 0.356 | 40.9 | 6.50 |

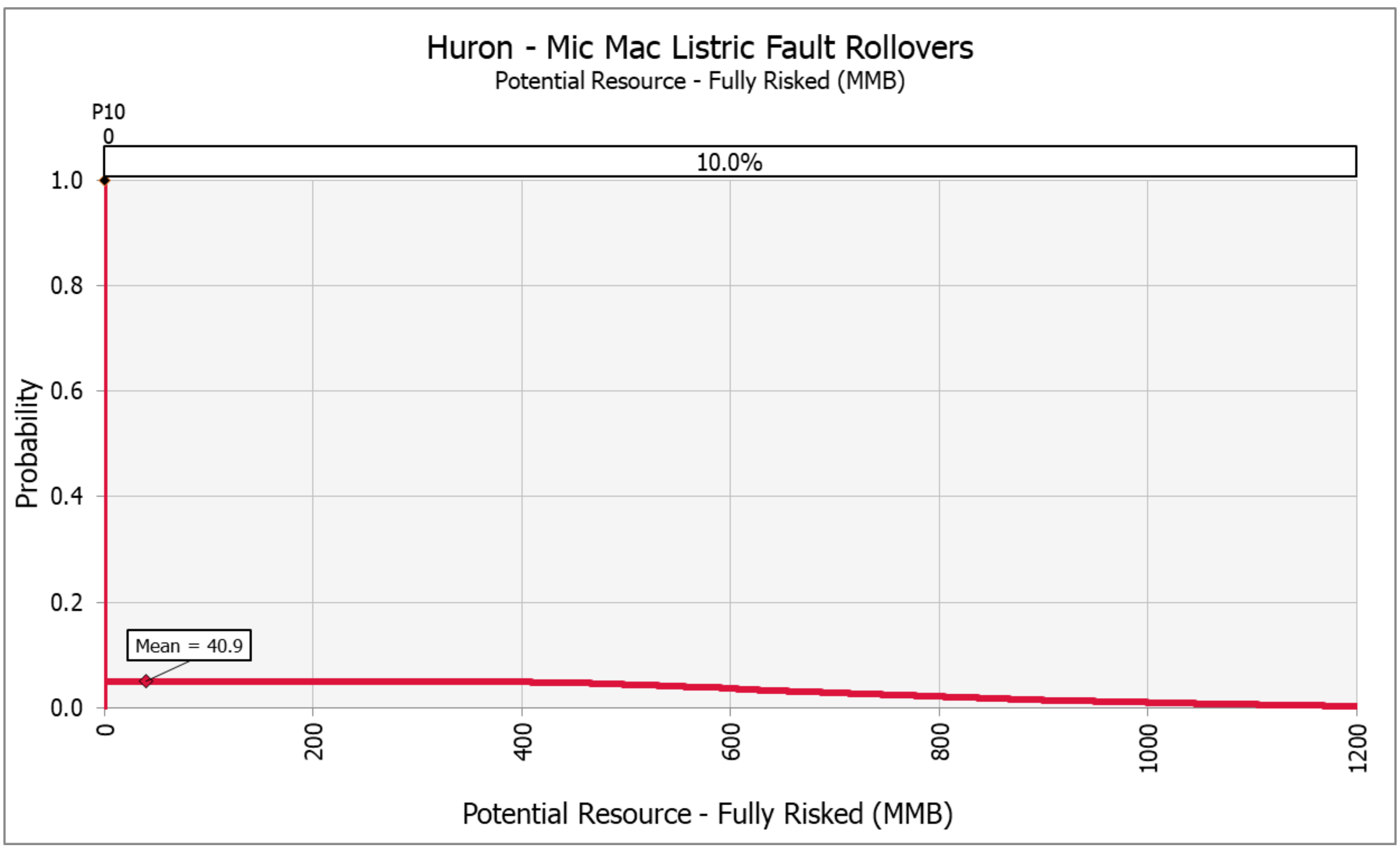

| | | Huron - Missisauga Listric Fault Rollovers - Shelf | | | | | |
|---|---|---|---|---|---|---|---|
| | | Natural Gas | | Natural Gas Liquids | | Oil Equivalent | |
| | | BCF | $10^9$ $m^3$ | MMB | $10^6$ $m^3$ | MMBOE | $10^6$ $m^3$ |
| In-Place Unrisked | P90 | 11,809 | 334 | 107 | 17.0 | 2,157 | 343 |
| | P50 | 18,950 | 537 | 186 | 29.5 | 3,458 | 550 |
| | P10 | 29,768 | 843 | 315 | 50.1 | 5,441 | 865 |
| | Mean | 20,066 | 568 | 201 | 31.9 | 3,660 | 582 |
| In-Place Fully Risked | P90 | - | - | - | - | - | - |
| | P50 | - | - | - | - | - | - |
| | P10 | 20,335 | 576 | 203 | 32.3 | 3,709 | 590 |
| | Mean | 4,852 | 137 | 48.7 | 7.75 | 885 | 141 |
| Recoverable Unrisked | P90 | 8,828 | 250 | 79.6 | 12.7 | 1,612 | 256 |
| | P50 | 14,192 | 402 | 139 | 22.1 | 2,589 | 412 |
| | P10 | 22,472 | 636 | 236 | 37.5 | 4,106 | 653 |
| | Mean | 15,051 | 426 | 150 | 23.9 | 2,745 | 436 |
| Recoverable Fully Risked | P90 | - | - | - | - | - | - |
| | P50 | - | - | - | - | - | - |
| | P10 | 15,233 | 431 | 153 | 24.3 | 2,780 | 442 |
| | Mean | 3,637 | 103 | 36.5 | 5.81 | 664 | 106 |

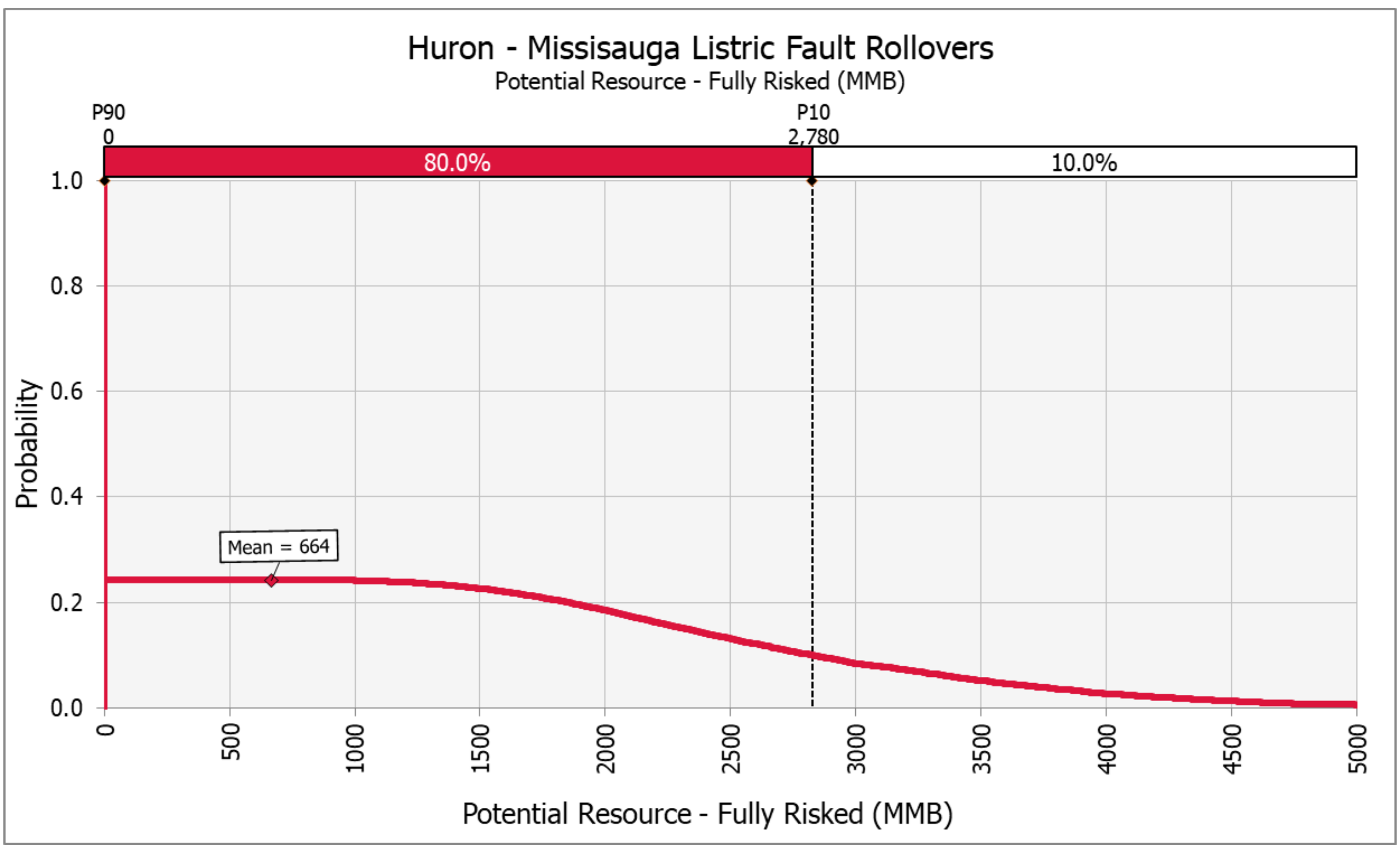

| | | Huron - Logan Canyon Listric Fault Rollovers - Shelf | | | | | |
|---|---|---|---|---|---|---|---|
| | | Natural Gas | | Natural Gas Liquids | | Oil Equivalent | |
| | | BCF | $10^9$ $m^3$ | MMB | $10^6$ $m^3$ | MMBOE | $10^6$ $m^3$ |
| In-Place Unrisked | P90 | 11,484 | 325 | 104 | 16.5 | 2,094 | 333 |
| | P50 | 18,857 | 534 | 186 | 29.6 | 3,441 | 547 |
| | P10 | 30,060 | 851 | 316 | 50.3 | 5,467 | 869 |
| | Mean | 19,954 | 565 | 200 | 31.7 | 3,640 | 579 |
| In-Place Fully Risked | P90 | - | - | - | - | - | - |
| | P50 | - | - | - | - | - | - |
| | P10 | - | - | - | - | - | - |
| | Mean | 1,546 | 43.8 | 15.3 | 2.44 | 282 | 44.8 |
| Recoverable Unrisked | P90 | 8,573 | 243 | 77.1 | 12.3 | 1,562 | 248 |
| | P50 | 14,128 | 400 | 140 | 22.2 | 2,580 | 410 |
| | P10 | 22,539 | 638 | 237 | 37.7 | 4,112 | 654 |
| | Mean | 14,968 | 424 | 150 | 23.8 | 2,730 | 434 |
| Recoverable Fully Risked | P90 | - | - | - | - | - | - |
| | P50 | - | - | - | - | - | - |
| | P10 | - | - | - | - | - | - |
| | Mean | 1,160 | 32.8 | 11.5 | 1.83 | 211 | 33.6 |

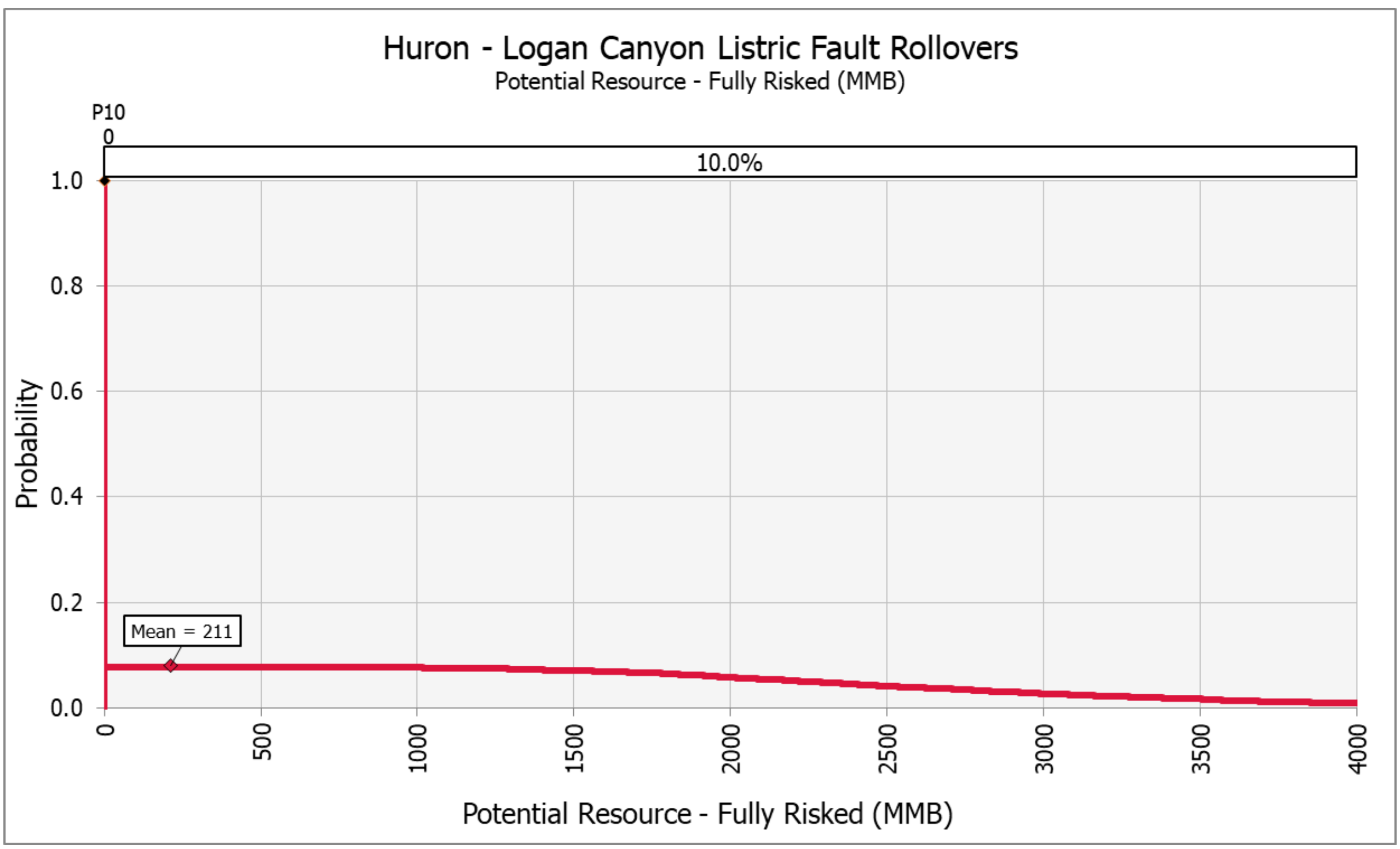

| | | Huron - Upper Slope Folds - Jurassic | | | | | |
|---|---|---|---|---|---|---|---|
| | | Natural Gas | | Natural Gas Liquids | | Oil Equivalent | |
| | | BCF | $10^9$ $m^3$ | MMB | $10^6$ $m^3$ | MMBOE | $10^6$ $m^3$ |
| In-Place Unrisked | P90 | 12,183 | 345 | 111 | 17.7 | 2,224 | 354 |
| | P50 | 20,023 | 567 | 196 | 31.1 | 3,648 | 580 |
| | P10 | 31,503 | 892 | 330 | 52.5 | 5,760 | 916 |
| | Mean | 21,060 | 596 | 211 | 33.5 | 3,842 | 611 |
| In-Place Fully Risked | P90 | - | - | - | - | - | - |
| | P50 | - | - | - | - | - | - |
| | P10 | - | - | - | - | - | - |
| | Mean | 1,608 | 45.5 | 16.0 | 2.546 | 293.3 | 46.6 |
| Recoverable Unrisked | P90 | 7,283 | 206 | 66.4 | 10.6 | 1,330 | 211 |
| | P50 | 11,969 | 339 | 117 | 18.5 | 2,183 | 347 |
| | P10 | 18,967 | 537 | 198 | 31.5 | 3,459 | 550 |
| | Mean | 12,627 | 358 | 126 | 20.1 | 2,303 | 366 |
| Recoverable Fully Risked | P90 | - | - | - | - | - | - |
| | P50 | - | - | - | - | - | - |
| | P10 | - | - | - | - | - | - |
| | Mean | 965 | 27.3 | 9.61 | 1.53 | 176 | 28.0 |

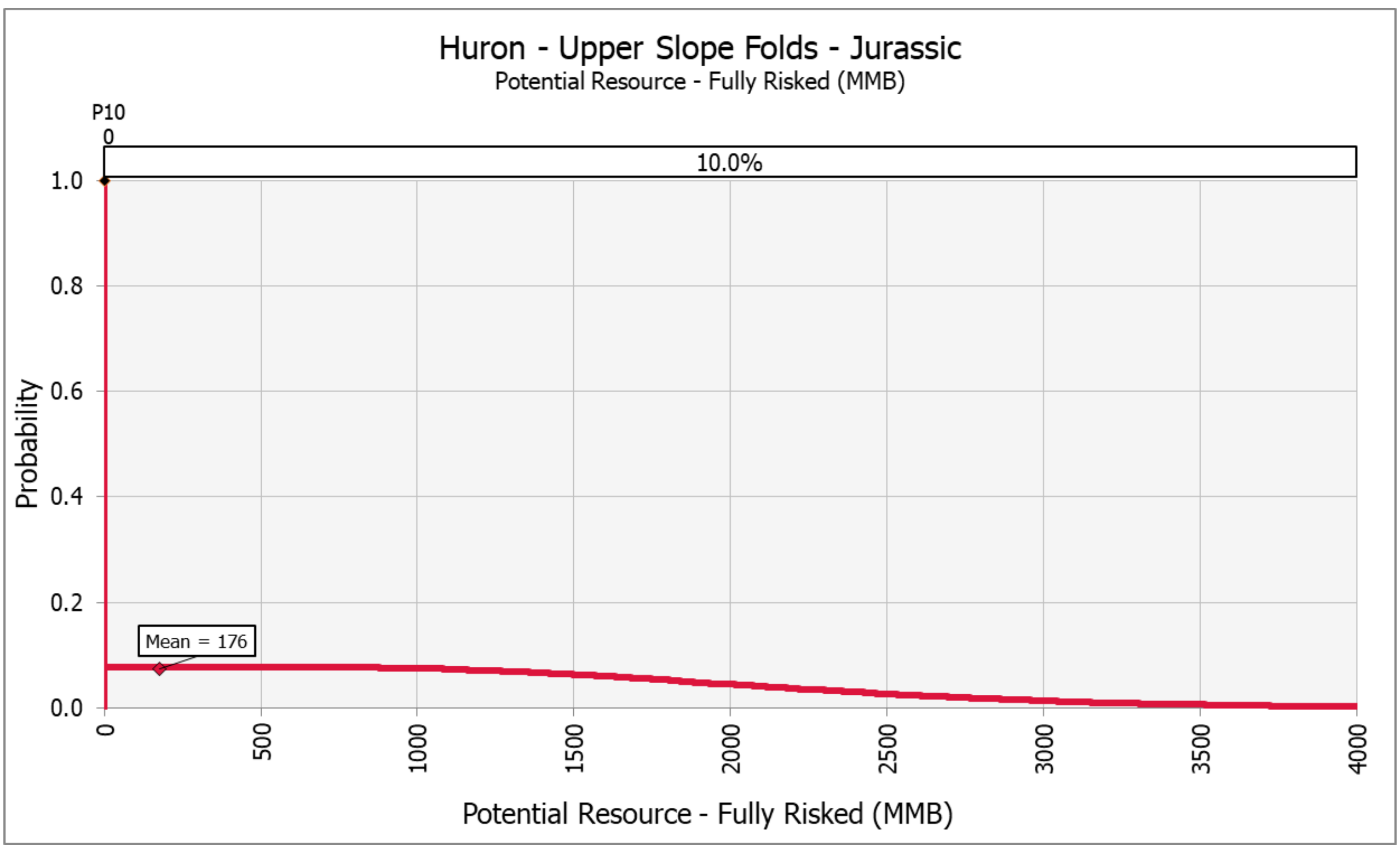

| | | Huron - Upper Slope Folds - Cretaceous (Stonehouse) | | | | | |
|---|---|---|---|---|---|---|---|
| | | Natural Gas | | Natural Gas Liquids | | Oil Equivalent | |
| | | BCF | $10^9$ $m^3$ | MMB | $10^6$ $m^3$ | MMBOE | $10^6$ $m^3$ |
| In-Place Unrisked | P90 | 25,281 | 716 | 230 | 36.6 | 4,608 | 733 |
| | P50 | 42,679 | 1,209 | 417 | 66.3 | 7,783 | 1,237 |
| | P10 | 69,752 | 1,975 | 727 | 115.6 | 12,727 | 2,023 |
| | Mean | 45,471 | 1,288 | 455 | 72.3 | 8,294 | 1,319 |
| In-Place Fully Risked | P90 | - | - | - | - | - | - |
| | P50 | - | - | - | - | - | - |
| | P10 | 40,462 | 1,146 | 394 | 62.6 | 7,376 | 1,173 |
| | Mean | 8,462 | 240 | 84.5 | 13.44 | 1,543 | 245 |
| Recoverable Unrisked | P90 | 18,851 | 534 | 172.2 | 27.4 | 3,439 | 547 |
| | P50 | 31,912 | 904 | 313 | 49.8 | 5,826 | 926 |
| | P10 | 52,513 | 1,487 | 546 | 86.9 | 9,587 | 1,524 |
| | Mean | 34,109 | 966 | 341 | 54.2 | 6,222 | 989 |
| Recoverable Fully Risked | P90 | - | - | - | - | - | - |
| | P50 | - | - | - | - | - | - |
| | P10 | 30,253 | 857 | 297 | 47.1 | 5,512 | 876 |
| | Mean | 6,355 | 180 | 63.5 | 10.1 | 1,159 | 184 |

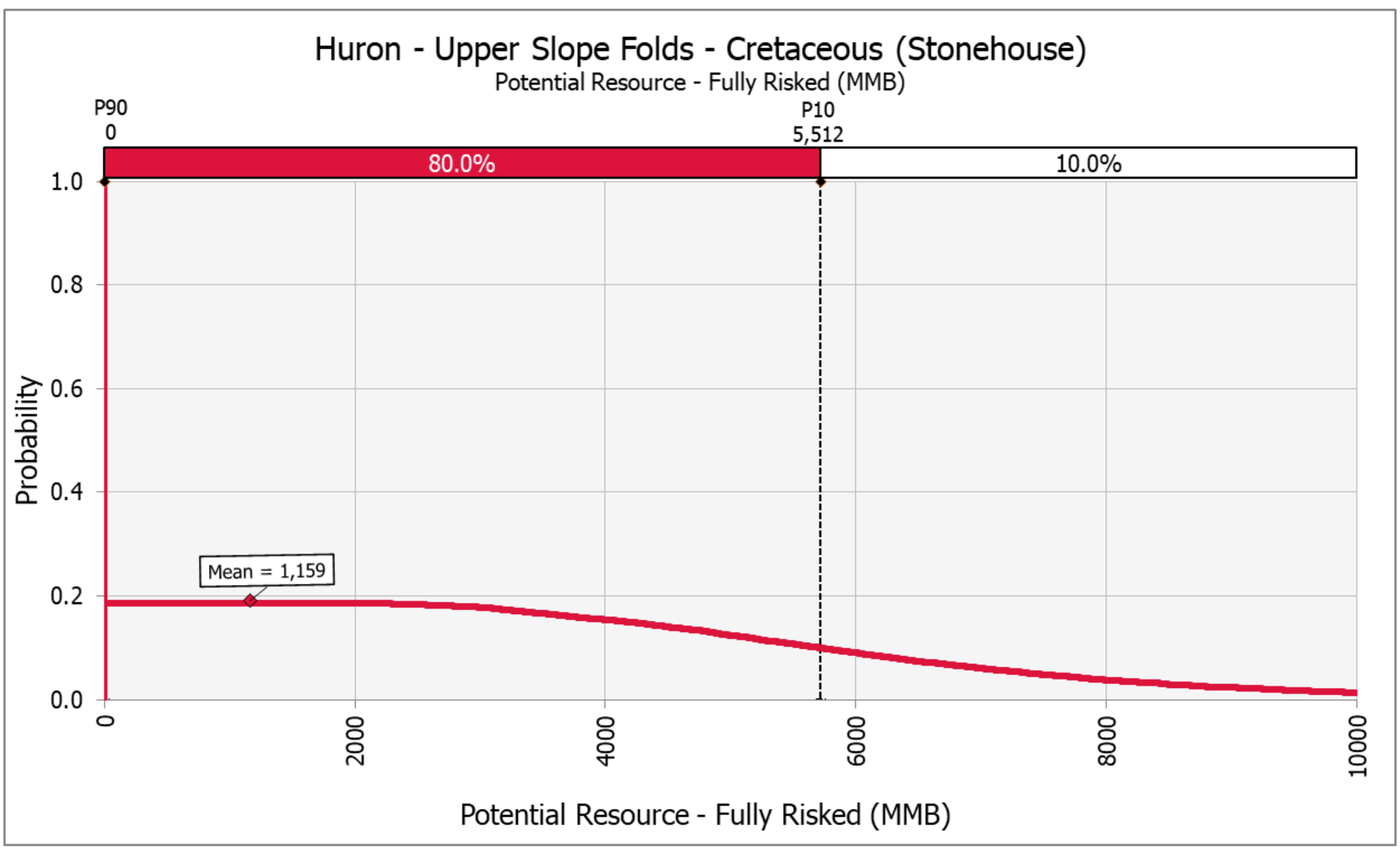

| | | Huron - Jurassic Supra-Canopy Turtles & Folds | | | | | |
|---|---|---|---|---|---|---|---|
| | | Natural Gas | | Natural Gas Liquids | | Oil Equivalent | |
| | | BCF | $10^9$ $m^3$ | MMB | $10^6$ $m^3$ | MMBOE | $10^6$ $m^3$ |
| In-Place Unrisked | P90 | 9,972 | 282 | 91.6 | 14.6 | 1,819 | 289 |
| | P50 | 16,280 | 461 | 160.0 | 25.4 | 2,969 | 472 |
| | P10 | 25,860 | 732 | 269 | 42.8 | 4,711 | 749 |
| | Mean | 17,231 | 488 | 172 | 27.3 | 3,143 | 500 |
| In-Place Fully Risked | P90 | - | - | - | - | - | - |
| | P50 | - | - | - | - | - | - |
| | P10 | - | - | - | - | - | - |
| | Mean | 1,434 | 40.6 | 14.3 | 2.27 | 261 | 41.6 |
| Recoverable Unrisked | P90 | 5,949 | 168 | 54.3 | 8.63 | 1,086 | 173 |
| | P50 | 9,753 | 276 | 95.6 | 15.2 | 1,779 | 283 |
| | P10 | 15,510 | 439 | 162 | 25.8 | 2,830 | 450 |
| | Mean | 10,336 | 293 | 103 | 16.4 | 1,885 | 300 |
| Recoverable Fully Risked | P90 | - | - | - | - | - | - |
| | P50 | - | - | - | - | - | - |
| | P10 | - | - | - | - | - | - |
| | Mean | 857 | 24.3 | 8.55 | 1.36 | 156 | 24.9 |

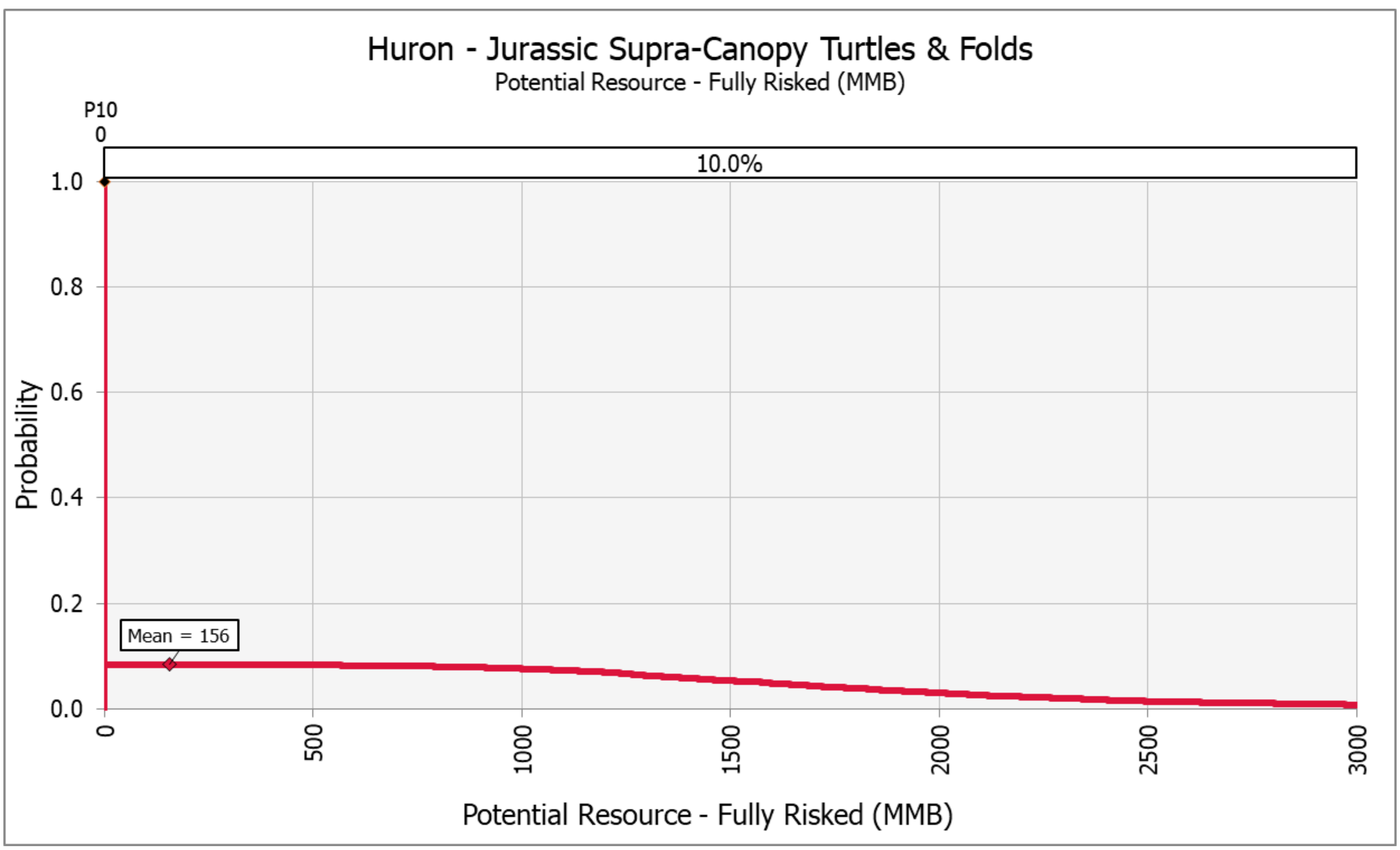

| | | Huron - Cretaceous Supra-Canopy | | | | | |
|---|---|---|---|---|---|---|---|
| | | Natural Gas | | Natural Gas Liquids | | Oil Equivalent | |
| | | BCF | $10^9$ $m^3$ | MMB | $10^6$ $m^3$ | MMBOE | $10^6$ $m^3$ |
| In-Place Unrisked | P90 | 5,773 | 163 | 52.5 | 8.35 | 1,053 | 167 |
| | P50 | 9,644 | 273 | 94.4 | 15.0 | 1,759 | 280 |
| | P10 | 15,574 | 441 | 163 | 26.0 | 2,840 | 451 |
| | Mean | 10,263 | 291 | 103 | 16.3 | 1,872 | 298 |
| In-Place Fully Risked | P90 | - | - | - | - | - | - |
| | P50 | - | - | - | - | - | - |
| | P10 | - | - | - | - | - | - |
| | Mean | 868 | 24.6 | 8.78 | 1.40 | 158.4 | 25.2 |
| Recoverable Unrisked | P90 | 4,278 | 121 | 39.1 | 6.22 | 781 | 124 |
| | P50 | 7,240 | 205 | 70.7 | 11.2 | 1,320 | 210 |
| | P10 | 11,703 | 331 | 123 | 19.6 | 2,137 | 340 |
| | Mean | 7,700 | 218 | 77.1 | 12.3 | 1,405 | 223 |
| Recoverable Fully Risked | P90 | - | - | - | - | - | - |
| | P50 | - | - | - | - | - | - |
| | P10 | - | - | - | - | - | - |
| | Mean | 652 | 18.5 | 6.60 | 1.05 | 119 | 18.9 |

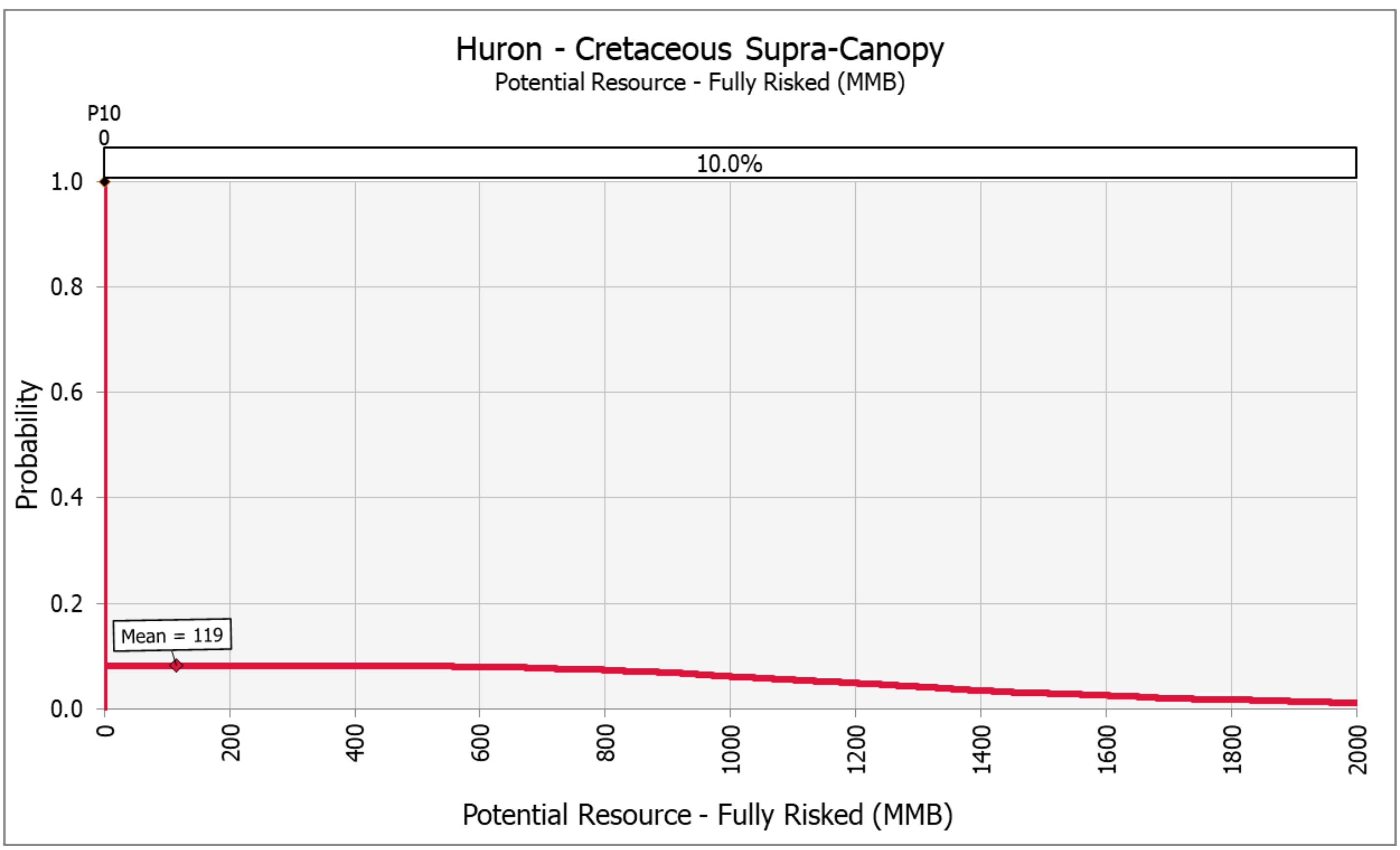

| | | Huron - Cretaceous Salt-Cored-Folds - Banquereau Fold-Belt | | | | | |
|---|---|---|---|---|---|---|---|
| | | Natural Gas | | Natural Gas Liquids | | Oil Equivalent | |
| | | BCF | $10^9$ $m^3$ | MMB | $10^6$ $m^3$ | MMBOE | $10^6$ $m^3$ |
| In-Place Unrisked | P90 | 23,528 | 666 | 217 | 34.4 | 7,494 | 1,191 |
| | P50 | 39,827 | 1,128 | 388 | 61.6 | 12,617 | 2,006 |
| | P10 | 64,040 | 1,813 | 674 | 107 | 20,429 | 3,248 |
| | Mean | 42,215 | 1,195 | 422 | 67.1 | 13,426 | 2,135 |
| In-Place Fully Risked | P90 | - | - | - | - | - | - |
| | P50 | - | - | - | - | - | - |
| | P10 | 26,765 | 758 | 249 | 39.5 | 8,295 | 1,319 |
| | Mean | 5,012 | 142 | 50.6 | 8.04 | 1,590 | 253 |
| Recoverable Unrisked | P90 | 17,517 | 496 | 162 | 25.8 | 4,337 | 690 |
| | P50 | 29,821 | 844 | 291 | 46.2 | 7,321 | 1,164 |
| | P10 | 48,054 | 1,361 | 508 | 80.7 | 11,848 | 1,884 |
| | Mean | 31,657 | 896 | 317 | 50.3 | 7,778 | 1,237 |
| Recoverable Fully Risked | P90 | - | - | - | - | - | - |
| | P50 | - | - | - | - | - | - |
| | P10 | 19,759 | 560 | 186 | 29.6 | 4,923 | 783 |
| | Mean | 3,763 | 107 | 38.0 | 6.04 | 923 | 147 |

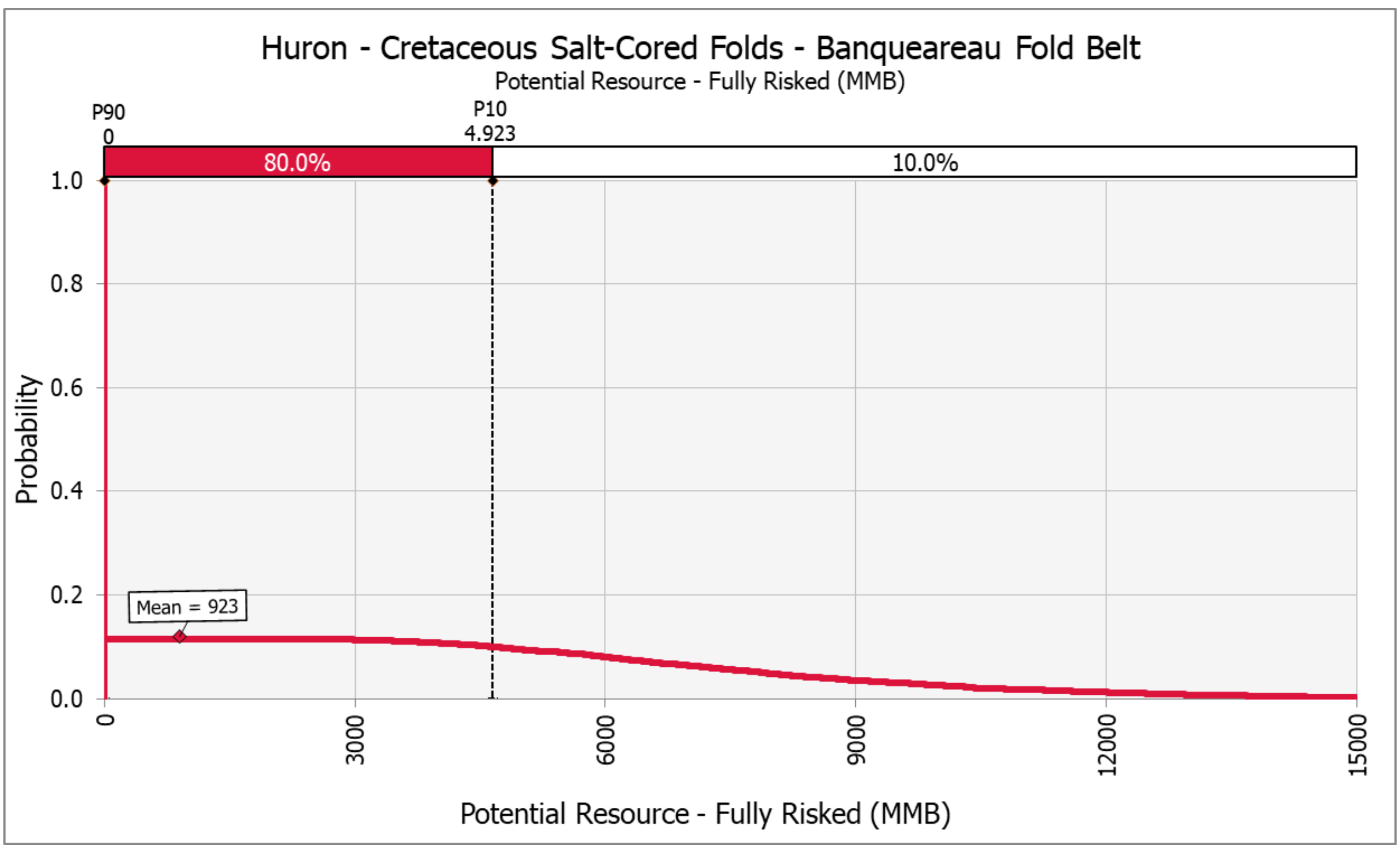

| | | Huron - Sub-Salt Canopy Cut-off (West Laurentian) | | | | | |
|---|---|---|---|---|---|---|---|
| | | Natural Gas | | Natural Gas Liquids | | Oil Equivalent | |
| | | BCF | $10^9$ $m^3$ | MMB | $10^6$ $m^3$ | MMBOE | $10^6$ $m^3$ |
| In-Place Unrisked | P90 | 3,176 | 90 | 29.1 | 4.62 | 577 | 91.8 |
| | P50 | 5,891 | 167 | 57.4 | 9.12 | 1,075 | 171 |
| | P10 | 10,112 | 286 | 106 | 16.8 | 1,843 | 293 |
| | Mean | 6,348 | 180 | 63.5 | 10.1 | 1,158 | 184 |
| In-Place Fully Risked | P90 | - | - | - | - | - | - |
| | P50 | - | - | - | - | - | - |
| | P10 | - | - | - | - | - | - |
| | Mean | 219 | 6.21 | 2.21 | 0.351 | 40.0 | 6.36 |
| Recoverable Unrisked | P90 | 2,368 | 67.0 | 21.8 | 3.46 | 432 | 68.7 |
| | P50 | 4,417 | 125 | 43.0 | 6.83 | 804 | 128 |
| | P10 | 7,553 | 214 | 79.2 | 12.6 | 1,378 | 219 |
| | Mean | 4,760 | 135 | 47.6 | 7.58 | 868 | 138 |
| Recoverable Fully Risked | P90 | - | - | - | - | - | - |
| | P50 | - | - | - | - | - | - |
| | P10 | - | - | - | - | - | - |
| | Mean | 165 | 4.67 | 1.66 | 0.264 | 30.1 | 4.79 |

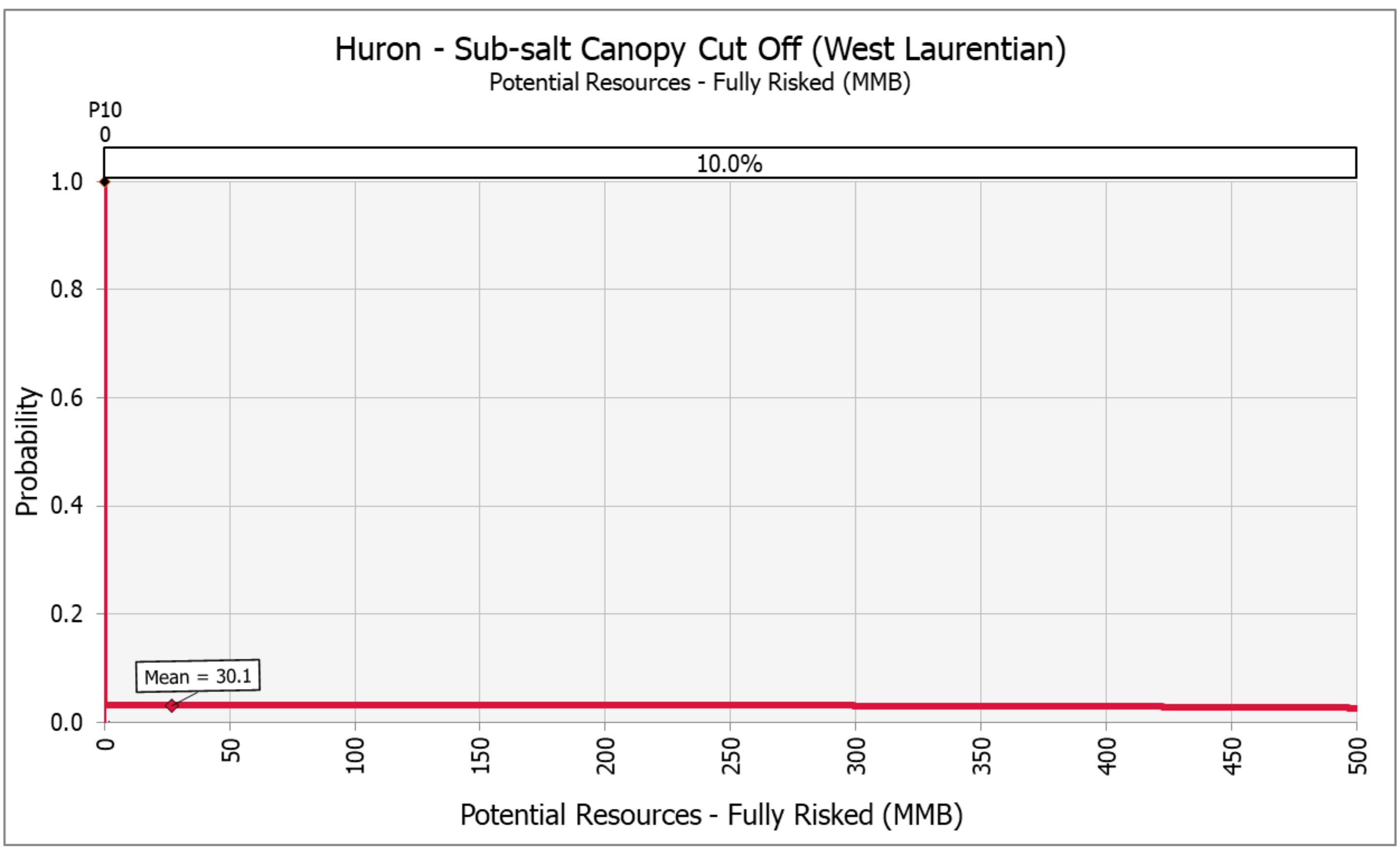

| | | Huron - Cretaceous Stratigraphic Onlap (seaward of BSW) | | | | | |
|---|---|---|---|---|---|---|---|
| | | Natural Gas | | Natural Gas Liquids | | Oil Equivalent | |
| | | BCF | $10^9$ $m^3$ | MMB | $10^6$ $m^3$ | MMBOE | $10^6$ $m^3$ |
| In-Place Unrisked | P90 | 4,206 | 119 | 38.5 | 6.12 | 1,331 | 212 |
| | P50 | 7,554 | 214 | 74.3 | 11.8 | 2,442 | 388 |
| | P10 | 13,087 | 371 | 136 | 21.6 | 4,233 | 673 |
| | Mean | 8,210 | 232 | 82.1 | 13.0 | 2,647 | 421 |
| In-Place Fully Risked | P90 | - | - | - | - | - | - |
| | P50 | - | - | - | - | - | - |
| | P10 | - | - | - | - | - | - |
| | Mean | 337 | 9.54 | 3.35 | 0.533 | 109.5 | 17.4 |
| Recoverable Unrisked | P90 | 3,149 | 89.2 | 28.9 | 4.59 | 776 | 123 |
| | P50 | 5,654 | 160 | 55.5 | 8.82 | 1,403 | 223 |
| | P10 | 9,817 | 278 | 102 | 16.2 | 2,428 | 386 |
| | Mean | 6,156 | 174 | 61.5 | 9.78 | 1,525 | 242 |
| Recoverable Fully Risked | P90 | - | - | - | - | - | - |
| | P50 | - | - | - | - | - | - |
| | P10 | - | - | - | - | - | - |
| | Mean | 253 | 7.16 | 2.51 | 0.400 | 63.0 | 10.0 |

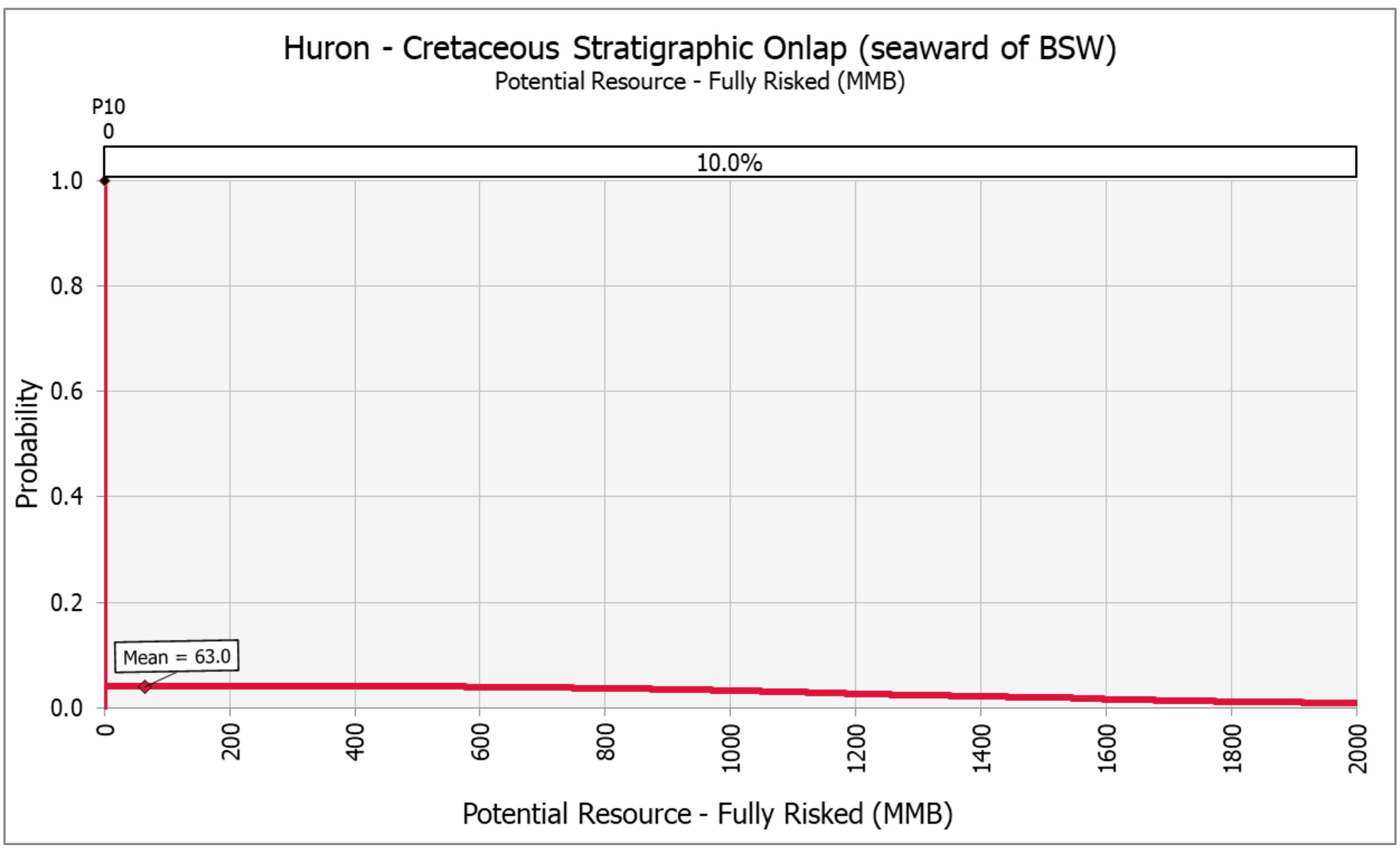

| | | Huron - Cretaceous Three-way Closures on Diapir Flanks | | | | | |
|---|---|---|---|---|---|---|---|
| | | Natural Gas | | Natural Gas Liquids | | Oil Equivalent | |
| | | BCF | $10^9$ $m^3$ | MMB | $10^6$ $m^3$ | MMBOE | $10^6$ $m^3$ |
| In-Place Unrisked | P90 | 10,683 | 303 | 97.7 | 15.5 | 3,475 | 553 |
| | P50 | 18,715 | 530 | 182 | 28.9 | 6,069 | 965 |
| | P10 | 29,674 | 840 | 309 | 49.2 | 9,742 | 1,549 |
| | Mean | 19,579 | 554 | 195 | 31.1 | 6,400 | 1,018 |
| In-Place Fully Risked | P90 | - | - | - | - | - | - |
| | P50 | - | - | - | - | - | - |
| | P10 | - | - | - | - | - | - |
| | Mean | 769 | 21.8 | 7.78 | 1.24 | 251 | 40.0 |
| Recoverable Unrisked | P90 | 7,934 | 225 | 73.1 | 11.6 | 1,996 | 317 |
| | P50 | 13,987 | 396 | 136 | 21.7 | 3,480 | 553 |
| | P10 | 22,297 | 631 | 231 | 36.8 | 5,587 | 888 |
| | Mean | 14,681 | 416 | 147 | 23.3 | 3,668 | 583 |
| Recoverable Fully Risked | P90 | - | - | - | - | - | - |
| | P50 | - | - | - | - | - | - |
| | P10 | - | - | - | - | - | - |
| | Mean | 579 | 16.4 | 5.86 | 0.932 | 145 | 23.0 |

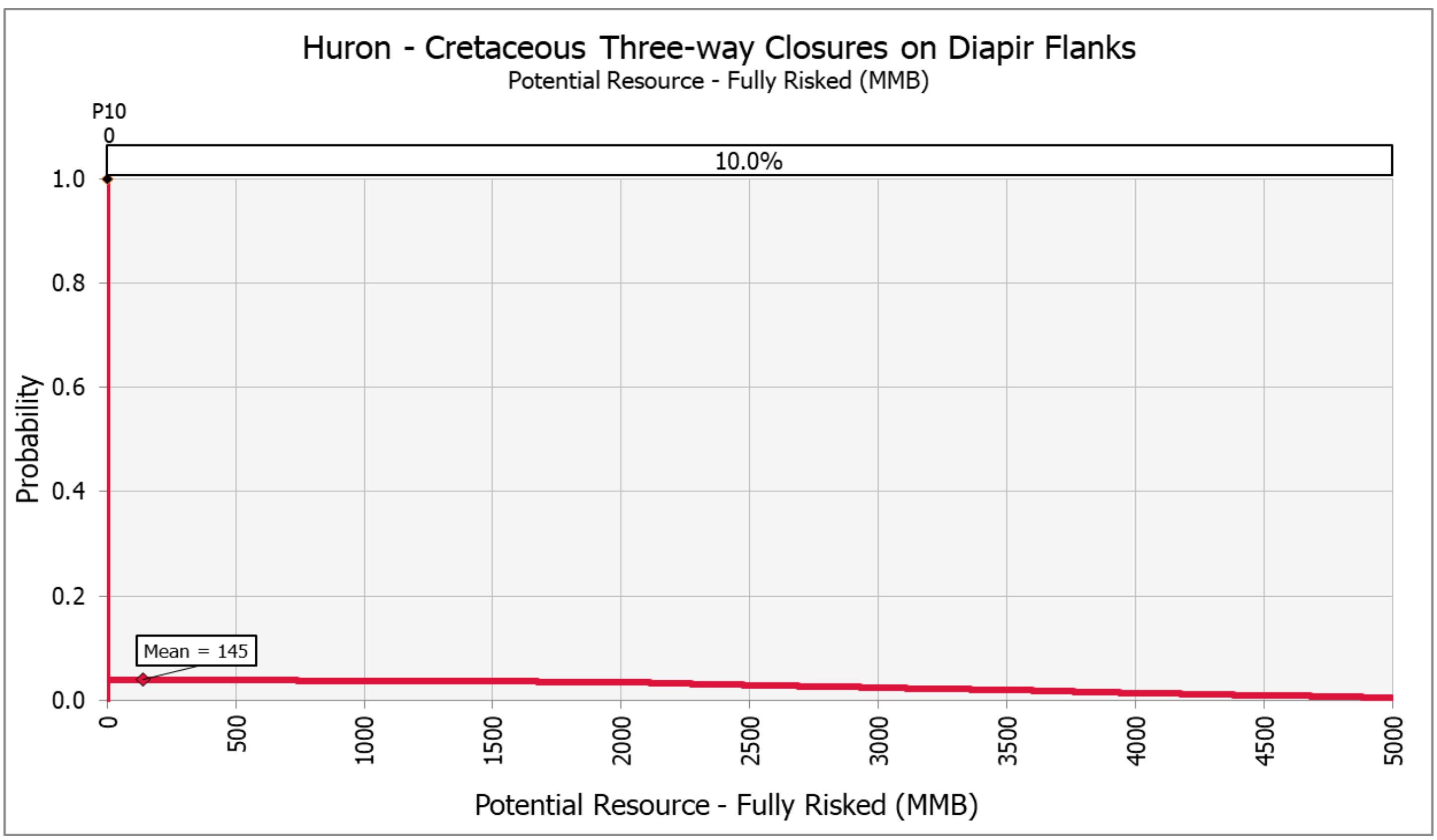

## Appendix 6 – **F. Sydney Basin**

| | | Sydney Basin - Horton Fault Blocks | | | | | |
|---|---|---|---|---|---|---|---|
| | | Natural Gas | | Natural Gas Liquids | | Oil Equivalent | |
| | | BCF | $10^9$ $m^3$ | MMB | $10^6$ $m^3$ | MMBOE | $10^6$ $m^3$ |
| In-Place Unrisked | P90 | 10,127 | 287 | 94.3 | 15.0 | 12,853 | 2,044 |
| | P50 | 18,252 | 517 | 178 | 28.3 | 23,411 | 3,722 |
| | P10 | 30,952 | 876 | 324 | 51.5 | 39,477 | 6,276 |
| | Mean | 19,601 | 555 | 196 | 31.2 | 25,026 | 3,979 |
| In-Place Fully Risked | P90 | - | - | - | - | - | - |
| | P50 | - | - | - | - | - | - |
| | P10 | - | - | - | - | - | - |
| | Mean | 611 | 17.3 | 6.08 | 0.967 | 776 | 123 |
| Recoverable Unrisked | P90 | 2,908 | 82.3 | 27.3 | 4.33 | 2,700 | 429 |
| | P50 | 6,117 | 173 | 59.6 | 9.48 | 5,105 | 812 |
| | P10 | 11,680 | 331 | 123 | 19.5 | 8,959 | 1,424 |
| | Mean | 6,870 | 195 | 68.8 | 10.9 | 5,542 | 881 |
| Recoverable Fully Risked | P90 | - | - | - | - | - | - |
| | P50 | - | - | - | - | - | - |
| | P10 | - | - | - | - | - | - |
| | Mean | 222 | 6.28 | 2.21 | 0.352 | 172 | 27.3 |

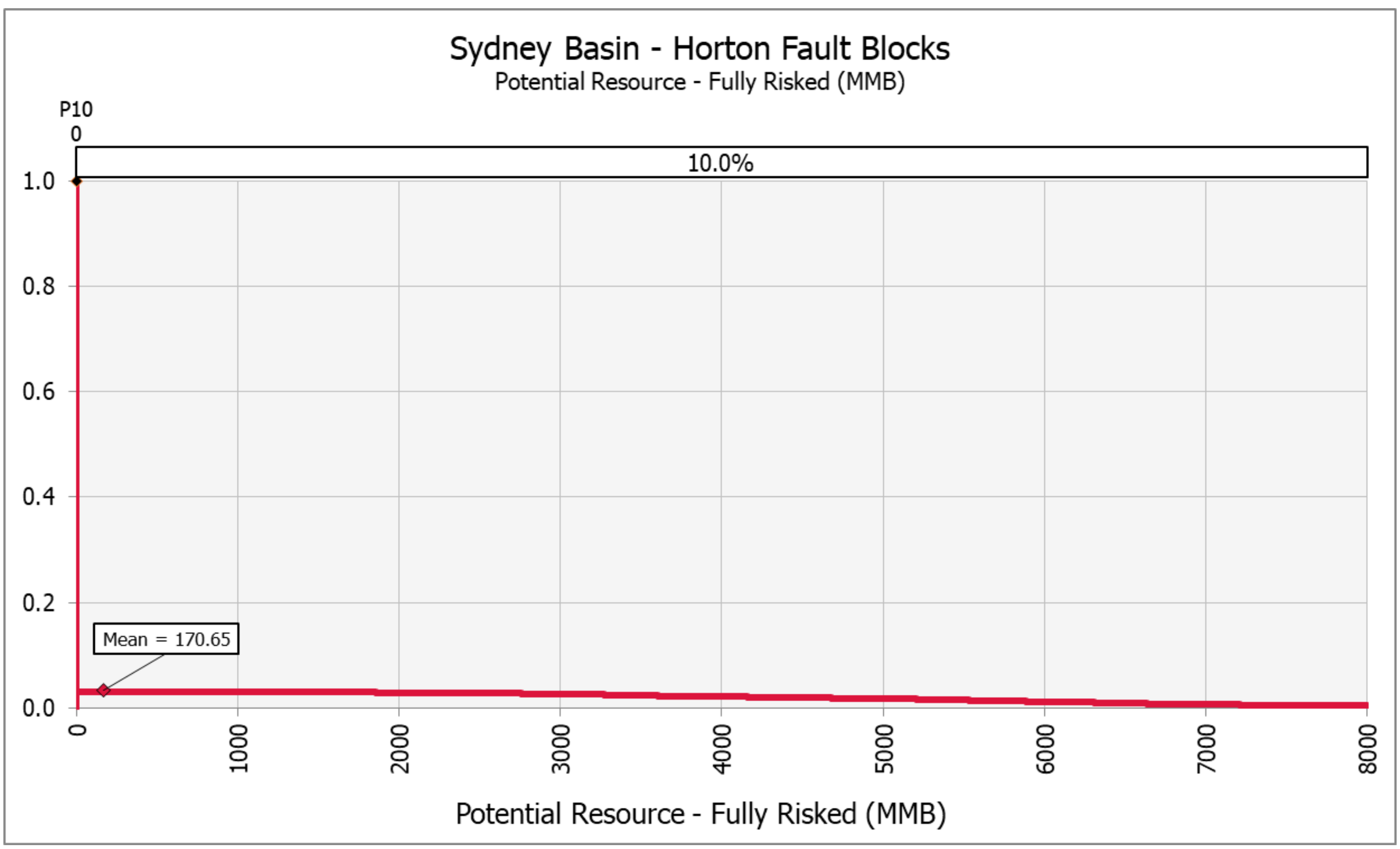

| | | Sydney Basin - Carboniferous Inversion Folds | | | | | |
|---|---|---|---|---|---|---|---|
| | | Natural Gas | | Natural Gas Liquids | | Oil Equivalent | |
| | | BCF | $10^9$ m$^3$ | MMB | $10^6$ m$^3$ | MMBOE | $10^6$ m$^3$ |
| In-Place Unrisked | P90 | 2,008 | 56.9 | 18.4 | 2.93 | 3,490 | 555 |
| | P50 | 3,612 | 102 | 35.3 | 5.61 | 6,221 | 989 |
| | P10 | 6,180 | 175 | 64.2 | 10.2 | 10,655 | 1,694 |
| | Mean | 3,901 | 110 | 39.0 | 6.20 | 6,714 | 1,067 |
| In-Place Fully Risked | P90 | - | - | - | - | - | - |
| | P50 | - | - | - | - | - | - |
| | P10 | - | - | - | - | - | - |
| | Mean | 313 | 8.87 | 3.14 | 0.500 | 540 | 85.8 |
| Recoverable Unrisked | P90 | 583 | 16.5 | 5.41 | 0.861 | 711 | 113 |
| | P50 | 1,219 | 34.5 | 12.0 | 1.90 | 1,320 | 210 |
| | P10 | 2,359 | 66.8 | 24.1 | 3.84 | 2,363 | 376 |
| | Mean | 1,366 | 38.7 | 13.7 | 2.17 | 1,450 | 231 |
| Recoverable Fully Risked | P90 | - | - | - | - | - | - |
| | P50 | - | - | - | - | - | - |
| | P10 | - | - | - | - | - | - |
| | Mean | 110 | 3.12 | 1.11 | 0.176 | 117 | 18.6 |

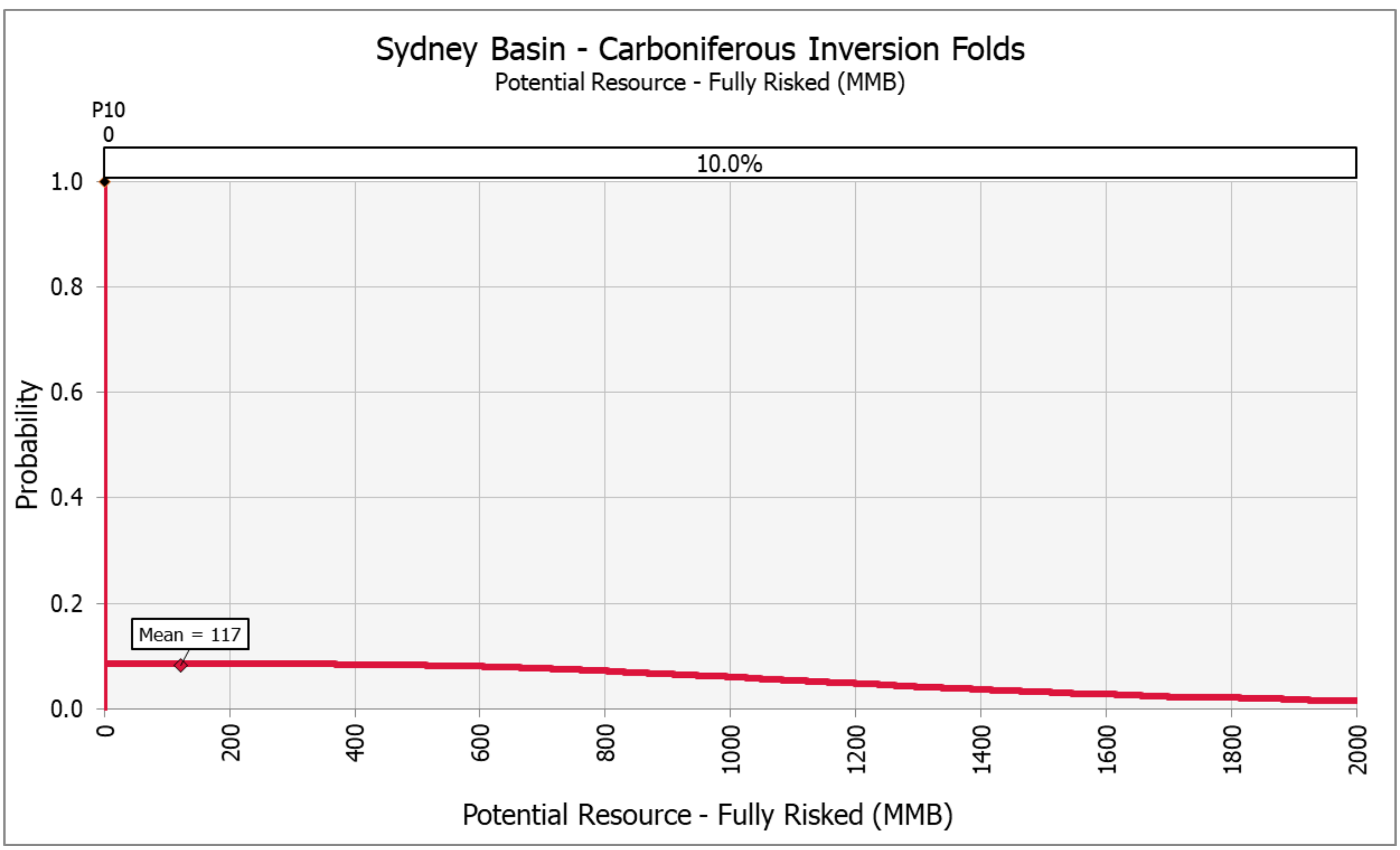

| | | Sydney Basin - Windsor Reefs | | | | | |
|---|---|---|---|---|---|---|---|
| | | Natural Gas | | Natural Gas Liquids | | Oil Equivalent | |
| | | BCF | $10^9$ $m^3$ | MMB | $10^6$ $m^3$ | MMBOE | $10^6$ $m^3$ |
| **In-Place Unrisked** | **P90** | 4,798 | 136 | 18.0 | 2.87 | 6,229 | 990 |
| | **P50** | 10,695 | 303 | 41.9 | 6.67 | 13,811 | 2,196 |
| | **P10** | 23,021 | 652 | 94.1 | 15.0 | 29,672 | 4,717 |
| | **Mean** | 12,569 | 356 | 50.2 | 7.99 | 16,234 | 2,581 |
| **In-Place Fully Risked** | **P90** | - | - | - | - | - | - |
| | **P50** | - | - | - | - | - | - |
| | **P10** | - | - | - | - | - | - |
| | **Mean** | 264 | 7.46 | 1.05 | 0.166 | 333 | 53.0 |
| **Recoverable Unrisked** | **P90** | 1,090 | 30.9 | 4.06 | 0.645 | 1,238 | 197 |
| | **P50** | 2,696 | 76.3 | 10.5 | 1.68 | 2,866 | 456 |
| | **P10** | 6,474 | 183 | 26.2 | 4.17 | 6,224 | 990 |
| | **Mean** | 3,356 | 95.0 | 13.4 | 2.13 | 3,392 | 539 |
| **Recoverable Fully Risked** | **P90** | - | - | - | - | - | - |
| | **P50** | - | - | - | - | - | - |
| | **P10** | - | - | - | - | - | - |
| | **Mean** | 69.6 | 1.97 | 0.274 | 0.044 | 70.0 | 11.1 |